Integration of Insulin Sensitivity in Adipose Tissue and Skeletal Muscle, and the Role of Exercise on Muscle Lipid Regulation

by

Michael Wesley Schleh

A dissertation submitted in partial fulfillment
of the requirements for the degree of
Doctor of Philosophy
(Movement Science)
in the University of Michigan
2022

Doctoral Committee:

Professor Jeffrey Horowitz, Chair
Professor Gregory Cartee
Associate Professor Jacob Haus
Professor Ormond MacDougald

Michael W. Schleh

mschleh@umich.edu

ORCID iD: 0000-0001-9969-6316

DEDICATION

This dissertation is dedicated to my parents and wife Emily, for your patience and constant support

ACKNOWLEDGEMENTS

To those I have had the pleasure to cross paths on my journey, I want to thank each of you for lending the energy to help me grow as a colleague, scholar, and a friend. I am fortunate to reach a defining point in my career training in an environment filled with motivational colleagues and mentors, and I thank all who were not mentioned here.

First I owe the most honorable thank you to my primary advisor Jeff Horowitz. Your hard work and dedication is inspiring, and you motivate everyone around you to work to the highest of their capabilities. Thank you for your patience, and allowing me to use my strengths, while pushing me to think critically and thoroughly through the toughest questions and obstacles during my PhD training. Neither of us were prepared to work together through a pandemic, and your support pushed me through this tough process that I could not have done without your guidance. You will always be a mentor and one that I will continue to look up wherever I end up.

I would like to extend my thanks to my advisory committee, who are all exceptionally wise mentors, and all lead research teams that have largely influenced my training at Michigan. Thank you Greg Cartee for providing wise and thoughtful guidance. Although we did not communicate most often, I appreciated all your guidance and discussion when it came my way. To Jake Haus, I appreciated working closely with you and your lab upon arrival to Michigan. I appreciated all your guidance and discussion both personally and professionally. Thank you Ormond MacDougald, who leads a rich scientific training environment, which has both prepared and inspired me to progress to my next position in postdoctoral training. Some of my greatest memories at Michigan have been with your lab during meetings and journal clubs, and inviting me to your home and at Lake Walloon with your family.

I am extremely grateful for every member of the Substrate Metabolism Lab who has been involved in one way or another in all three research projects. Thanks to Ben Ryan and Alison Ludzki for your constant dedication and involvement in my studies during the beginning of training. Thanks to Cheehoon Ahn for being instrumental to almost every aspect of all three of my dissertation studies, and being there for constant discussion, plus always giving time and effort

to improve the lab's mission. Thanks to Pallavi Varsheny for putting up with me while sharing an office and being a great friend. Lastly, thanks to Suzette Howton and Thomas Rhode for clinical and technical support.

Thanks to all members of the Human Bioenergetics Lab for being great friends and colleagues. Thanks to Tori and Edwin Miranda for being exceptional scientists and friends. To Corey Mazo and James Shadiow for sharing great conversation about sports, science, dogs, and everyday life. I will miss working closely with you all, and planning the next trip to the dog park.

Thanks to MacDougald lab members. Even though I was not directly involved in your lab, you all provided thoughtful guidance, support, and happy hours throughout a critical time in my training and development. Thanks to the core members of the lab: Becky Schill, Ken Lewis, Hiro Mori, Ziru Li, Steven Romanelli, and Devika Bagchi for the great times, and all you do to support scientists around you too.

Thank you to my previous colleagues that have also contributed to my development and training prior to coming to Michigan. Thank you to my previous colleagues from the Gatorade Sports Science Institute: Melissa Anderson, Tim Roberts, and Kortney Dalrymple for teaching me how to be a professional. Thank you to my mentors and colleagues from the University of Montana: Chuck Dumke, John Quindry, Brent Ruby, Brandon Gruver, Alice Reid, and Laura Porsche.

Thank you to my lovely and inspiring wife Emily Schleh. We have come so far since the beginning, and I look forward to the journey we have ahead. Thank you for all your support during this time, and always motiving me to always give my best. We truly make each other better people. I am fortunate we have each other to travel, grow our family together, and the many more great things we have to come.

Thank you to my family who has always provided support and enthusiasm throughout my PhD and professional career. To my sister Carly Schleh who has always had my back, and my parents John and Sharon Schleh, who have always been supportive for my adventures and encouraging me to pursue whatever I am passionate about. Thank you for being there every step of the way. It has been a ride!

TABLE OF CONTENTS

LIST OF TABLES

LIST OF FIGURES

LIST OF APPENDICES

ABSTRACT

Obesity is a major public health problem, and a leading risk factor for cardio-metabolic disorders, including insulin resistance, which underlies many obesity-related diseases. Although most adults with obesity are insulin resistant, some are relatively insulin sensitive, with minimal obesity-related disease risk-factors. Mounting evidence suggests that differences in the regulation of fatty acid (FA) release from abdominal subcutaneous adipose tissue (aSAT), as well as alterations in the regulation muscle lipids may be important contributors to the variability in insulin sensitivity in this population. Additionally, although some of the important health benefits of exercise, including enhanced insulin sensitivity, have been attributed to changes in muscle lipid metabolism, the effects of exercise muscle lipid regulation remain unclear. The overall aims of this dissertation were to examine the integrated relationship between skeletal muscle insulin sensitivity with aSAT morphology and metabolism, as well as to assess the effects of exercise on muscle lipid regulation. In Project 1, we found that in a cohort of 66 adults with obesity, insulin-mediated suppression of FA rate of appearance in the circulation (FA Ra suppression) was the strongest predictor of insulin-mediated glucose uptake ($r=0.51$, $p<0.01$). Importantly, proteomics analysis revealed that fibrotic content in aSAT may be an important contributor in determining the FA release in response to insulin. We also found those with low FA Ra suppression had a relatively high concentration of long-chain acylcarnitines ($p=0.02$) and triacylglycerol ($p<0.01$) in skeletal muscle, suggesting that persistent elevations in FA availability in those with low FA suppression in response to insulin may unfavorably impact muscle lipid profile. Project 2 expanded on these findings from Project 1 by demonstrating insulin resistance was accompanied by increased accumulation of large-sized lipid droplets (LD) in close proximity to the plasma membrane of the myocyte, which may contribute to insulin resistance. In Project 2 we also found that our insulin resistant cohort exhibited blunted interaction between the insulin receptor and key regulatory proteins (cluster of differentiation factor 36 [CD36] and Fyn), which was accompanied by impaired insulin signaling downstream of the insulin receptor. In Project 3, we examined the effect of 12 weeks of exercise training (comparing high-intensity interval training [HIIT] and moderate-intensity continuous

training [MICT]) on changes in the size and number of LDs in skeletal, as well as their distribution in either the intramyofibrillar (IMF) or subsarcolemmal (SS) regions of the myocyte. Training (both HIIT and MICT) increased intramyocellular lipid content ($p<0.01$), and this expansion in muscle lipid content was attributed to an increased number of LD per μm^2 ($p<0.01$) specifically within the IMF region of the myocyte. Findings from Project 3 also suggest that selective LD degradation ("lipophagy") may be upregulated the day after a session of exercise, but this response appeared to be transient because our measure of lipophagy was no longer elevated when measured 4 days after a session of exercise. Interestingly, despite the robust difference in exercise stimulus between MICT and HIIT, the effects of these exercise programs on intramyocellular LDs were remarkably similar. Overall, findings from my dissertation sheds light on an important cross-talk between adipose tissue and skeletal muscle, by which FA release from adipose tissue can alter muscle lipid regulation, as well as impair insulin sensitivity, and exercise can modify how (and where) muscle lipids are stored.

Chapter I

Statement of the Problem

Obesity prevalence in the United States has been increasing at an alarming rate, with over 40% of the population now considered obese (1-3). Obesity is a major modifiable risk factor for cardio-metabolic diseases, including coronary heart disease (4) and type 2 diabetes mellitus [T2DM] (5). Obesity is caused by a multitude of factors largely attributed to lifestyle and genetic influences, contributing to annual direct medical costs of over $300 billion for treating obesity-related diseases in the United States (6, 7), and over $2,500 per individual with obesity (8). Insulin resistance (i.e., impaired response to a physiological dose of insulin) is very common in obesity, and is known to underlie many of the aforementioned obesity-related diseases (9, 10) as well as many other obesity-related health complications, such as, chronically elevated hepatic glucose production, excessive lipolytic rates from abdominal subcutaneous adipose tissue (aSAT), and impaired skeletal muscle glucose uptake (11-15). Although the vast majority of obese adults are insulin resistant, there remain some obese adults who appear to be largely 'protected' from developing insulin resistance. Epidemiological studies suggest that approximately 10-30% of obese adults may be classified as 'metabolically healthy', with lower cardiometabolic disease risk (16-20). Therefore, along with advancing knowledge about factors underlying metabolic abnormalities in the large proportion of obese adults who are unhealthy, expanding our understanding about factors that help 'protect' those obese adults from developing insulin resistance will provide novel insight towards future therapies aimed to limit metabolic complications caused by excess weight gain.

Adipose tissue, once considered a relatively benign tissue of energy storage, is now known to be a key factor regulating whole-body metabolism and metabolic health (21, 22). Limitations in the capacity for aSAT to 'expand' and store lipid in a state of chronic nutrient excess (i.e., obesity), often results in an excessive release of fatty acid (FA) from aSAT into the systemic

circulation (23), which is an important factor underlying obesity-related insulin resistance (24-29). The high systemic FA availability and resultant uptake into metabolically impactful tissues such as skeletal muscle and liver can lead to a relatively large accumulation of fat in these tissues (ectopic lipid deposition), which is a key contributor to the development of insulin resistance (27, 30-37). Although chronically elevated FA mobilization rates into the circulation are very common in obesity, rates of lipolysis and/or FA release from aSAT can vary considerably among obese individuals (24, 26, 38). Recent data from our lab demonstrated that obese participants who maintained relatively low basal rates of FA mobilization (i.e., had enhanced capacity to store and sequester FAs in aSAT) were 'protected' from insulin resistance, and maintained normal insulin-mediated glucose uptake in skeletal muscle (26). However, the factors responsible for these subjects' enhanced ability to sequester more FAs in aSAT were not completely resolved (26). The robust suppression of FA mobilization by insulin has also been found to be a strong predictor of sensitivity to insulin-mediated glucose uptake in skeletal muscle (24, 29, 39). Additionally, aSAT structure and regulation of FA release and storage are important features underlying variability in the rates of lipolysis and FA mobilization from aSAT (40-44). In my dissertation, I hypothesized differences in aSAT structure (e.g., fat cell size and fibrosis) can play a key role underlying the inter-individual variation in FA release into the circulation from adults with obesity – and thereby may be an important determinant in maintaining whole-body insulin sensitivity and metabolic health. In addition, differences in the release of bioactive hormones/peptides from aSAT [e.g., adiponectin, leptin] (45, 46), as well as circulating FA released from aSAT (47) may also contribute to the propensity for dysfunctional aSAT that can lead to whole-body insulin resistance. Skeletal muscle is the primary site of insulin-mediated glucose uptake (48), and excessive FA uptake into muscle (released from aSAT) can result in an overabundance of cytosolic lipid intermediates (e.g. diacylglycerol, ceramides, and acylcarnitines) known to diminish insulin action (49-52). However, the impact by which high FA release from aSAT modifies skeletal muscle lipid composition and morphology (e.g., unsaturation and acyl-chain length) are still incomplete.

The first project of my dissertation aimed to identify clinical and subclinical factors that may be 'protecting' some obese adults from developing insulin resistance. Multivariate analysis (net elastic regression) determined a cluster of factors best 'predicting' insulin-mediated glucose uptake from a cohort of obese adults with generally homogenous body composition, but wide-ranging insulin sensitivity. Histological/morphological assessments (e.g., cell-size,

capillarization, fibrosis) on aSAT samples were performed, and untargeted proteomic analysis was completed from a sub-cohort of adults with High FA Ra suppression and Low FA Ra suppression (*abbreviated HS and LS in Chapter III*), to identify the proteomic differences that may be mediating aSAT dysfunction. Lastly, untargeted skeletal muscle lipidomic analysis was completed to identify both specific lipid species, as well as lipid class morphology (unsaturation and acyl-chain length) that may be modified by high rates of FA uptake into skeletal muscle, and also modify insulin-mediated glucose uptake in skeletal muscle. Findings from this project provide novel information towards the effect of aSAT metabolic health mediating skeletal muscle lipid composition, and thus, insulin-mediated glucose uptake. Identifying factors that may 'protect' the relatively few obese adults from developing insulin resistance will be important to better understand how to treat those who are insulin resistant (and metabolically 'unhealthy'). ***The specific aims for project 1 of my dissertation were:*** *1) to assess the relationship between key clinical/subclinical factors and insulin-mediated glucose uptake in a homogeneous cohort of adults with obesity. 2) Compare aSAT morphology and proteomic profile between adults with High aSAT insulin sensitivity vs. Low aSAT insulin sensitivity using untargeted proteomic analysis. 3) To identify the association between aSAT insulin sensitivity and insulin-mediated glucose uptake on; i) individual lipid species abundance, and ii) lipid morphology (i.e., acyl-chain length and unsaturation) in skeletal muscle.*

Because skeletal muscle is responsible for ~85% insulin-stimulated glucose uptake (48), understanding specific signaling mechanisms underlying impaired insulin-mediated glucose uptake in skeletal muscle has very high clinical impact. Signaling events initiated after insulin binds to its receptor at the skeletal muscle membrane are largely relayed by a series of intracellular phosphorylation/dephosphorylation events that ultimately trigger the translocation of the primary glucose transporter, GLUT4, from the cytosol to the plasma membrane, thereby allowing more glucose uptake into the cell (53). Importantly, signaling events regulating GLUT4 translocation include; 1) insulin-mediated tyrosine phosphorylation of the insulin receptor, 2) activation of downstream proteins [e.g., IRS-1, PI3K recruitment, protein kinase B (Akt), Akt Substrate of 160 KDa (AS160/TBC1D4)], and 3) GLUT4 translocation to the plasma membrane. In insulin resistant individuals, the phosphorylation/activation of some of these signaling proteins have been found to be diminished in response to insulin compared with those who are insulin sensitive (50, 54-59). Recently, *in vitro* findings from Samovski et al. demonstrated that the physical association

between the fatty acid transporter, CD36, the insulin receptor, and the src family kinase protein Fyn kinase, modified insulin receptor tyrosine phosphorylation and insulin signaling in cultured myotubes (60). Importantly, in this study, exposure to high FA availability (specifically saturated FA) diminished Fyn recruitment to CD36, and diminished insulin receptor tyrosine phosphorylation, as well as phosphorylation downstream of the insulin receptor to Akt (60). Therefore, this physical and functional relationship between CD36 and the insulin receptor may represent an important, yet not well-appreciated mechanism underlying insulin resistance. In Project 2 of my dissertation, the co-localization between CD36, Fyn kinase, and the insulin receptor was measured in skeletal muscle samples from obese adults with wide-ranging insulin sensitivity, and we assessed how this interaction may modify insulin-mediated phosphorylation of the insulin receptor, downstream phosphorylation to Akt, and its distal substrates (e.g. GSK, FOXO1, and AS160).

Lipid accumulation into skeletal muscle accumulates as a consequence of greater FA availability and is associated with the development of insulin resistance (52, 61, 62), and impaired insulin signaling (63, 64). Importantly, the localization of these intramyocellular lipids, and whether they are distributed towards the cell membrane or within the cytosol, are implicated to associate with insulin resistance (65, 66). Additionally, the characteristics regarding *how* lipids are stored as intramyocellular lipid droplets (LD) are speculated to contribute to the development of insulin resistance, if these intramyocellular LDs are improperly stored (67). The mechanistic link between where these lipids are located - whether around the periphery (i.e., subsarcolemmal [SS] region) or towards the center of the muscle fiber (i.e., intramyofibrillar [IMF] region), are similarly proposed to modify key insulin signaling steps when inadequately stored within the cell (68-70). In Project 2 of my dissertation, I compared intramyocellular LD characteristics with regards to their individual size, distribution (within the SS and IMF region), and abundance between type I and type II muscle fibers from sub-cohorts of adults with HIGH insulin sensitivity vs. LOW insulin sensitivity (*abbreviated HIGH and LOW in chapter IV*). The overall aim of this portion of my dissertation was to identify mechanisms by which FA availability and intramyocellular LD storage modifies insulin-mediated phosphorylation/activation of specific metabolic pathways known to affect insulin-mediated glucose uptake. Findings from this study will improve our understanding regarding why some adults with obesity do not develop robust insulin resistance. ***The specific aims for project 2 of my dissertation were:*** *1) Compare basal-*

and insulin-mediated interaction between CD36 and Fyn kinase with insulin receptor β, and insulin-stimulated signaling events proximal and distal to Akt in skeletal muscle from a cohort of adults with HIGH vs. LOW insulin sensitivity. 2) Compare intramyocellular LD characteristics and distribution within skeletal muscle from a cohort of adults with HIGH vs. LOW insulin sensitivity.

Exercise is often prescribed as a first-line approach to treat obesity-related complications including insulin resistance (71-74). The insulin-sensitizing effects of exercise have been attributed in part to changes in skeletal muscle lipid metabolism, and changes in both the abundance and composition of specific muscle lipid species (75). Exercise has been found to re-distribute the intramyocellular lipid pool by 'partitioning' lipids to be esterified as inert triacylglycerol within LDs, and away from accumulating as lipid intermediates (e.g., diacylglycerol, ceramide, acylcarnitine) known to impair insulin signaling (75, 76). Additionally, lipids localized to the muscle membrane are proposed to contribute to insulin resistance, as opposed to cytosolic lipid accumulation (65, 69, 77). Therefore, understanding the effects of exercise on the size and distribution of LDs within the myocyte, as well as their relative abundance in different muscle fiber-types (type I vs type II) may offer insights to the protective effects of exercise on lipid-induced insulin resistance (69, 78-80). This is important because intramyocellular LDs in the SS region (below the surface of the membrane) have been found to be associated with insulin resistance and/or T2DM (68-70, 77, 81). Additionally, the intensity of exercise may also play an important role in the regulating the abundance and localization of intramyocellular LDs, especially between muscle fiber types, because high-intensity exercise recruits Type II muscle fibers to a greater extent than moderate-intensity exercise (82).

Intramyocellular LD dynamics are complex, and are constantly cycling through processes between their biosynthesis in the endoplasmic reticulum (83) and their degradation by the lysosome (84, 85). The effects of exercise on the regulation of LD turnover within the myocyte is largely unexplored. Therefore, identifying the effects of exercise on LD synthesis and degradation may shed new light on the role for exercise to remodel and redistribute LDs to an insulin sensitizing phenotype. Project 3 of my dissertation identified the effects of exercise training (both high-intensity interval training and more conventional, moderate-intensity continuous training) on intramyocellular LD density, LD size, distribution (SS versus IMF), and abundance between type I and type II muscle fibers. Additionally, this project explored the effects of exercise on the LD

'life cycle' (i.e., LD turnover), by measuring LD co-localization with organelles associated with LD biogenesis (endoplasmic reticulum) and chaperone-mediated degradation (autophagasome). ***The specific aims for project 3 of my dissertation were***: *1) Determine the effects of 12 weeks high-intensity interval training (HIIT) and moderate-intensity continuous training (MICT) on total lipid content, LD distribution within the myocyte, and LD abundance between type I and type II skeletal muscle fibers in adults with obesity. 2) Determine the effects of 12-weeks HIIT and MICT on LD co-localization with the endoplasmic reticulum (index of LD biogenesis), and LD co-localization with the autophagasome (index of LD degradation/recycling) in skeletal muscle of adults with obesity.*

To summarize, the studies outlined in my dissertation proposal addressed the following aims:

PROJECT 1

Specific Aim 1: To assess the relationship between key clinical/subclinical factors and insulin-mediated glucose uptake in a homogeneous cohort of adults with obesity.

Specific Aim 2: Compare aSAT morphology and proteomic profile between adults with High aSAT insulin sensitivity versus Low aSAT insulin sensitivity using untargeted proteomic analysis.

Specific Aim 3: To identify the association between aSAT insulin sensitivity and insulin-mediated glucose uptake on; i) individual lipid species abundance, and ii) lipid morphology (i.e., acyl-chain length and unsaturation) in skeletal muscle.

PROJECT 2

Specific Aim 1: Compare basal- and insulin-mediated interaction between CD36 and Fyn kinase with insulin receptor β, and insulin-stimulated signaling events proximal and distal to Akt in skeletal muscle from a cohort of adults with HIGH versus LOW insulin sensitivity.

Specific Aim 2: Compare intramyocellular LD characteristics and distribution within skeletal muscle from a cohort of adults with HIGH versus LOW insulin sensitivity.

PROJECT 3

Specific Aim 1: Determine the effects of 12 weeks high-intensity interval training (HIIT) and moderate-intensity continuous training (MICT) on total lipid content, LD distribution within the myocyte, and LD abundance between type I and type II skeletal muscle fibers in adults with obesity.

Specific Aim 2: Determine the effects of 12-weeks HIIT and MICT on LD co-localization with the endoplasmic reticulum (index of LD biogenesis), and LD co-localization with the autophagasome (index of LD degradation/recycling) in skeletal muscle of adults with obesity.

There is a growing prevalence of obesity, and obesity-related conditions such as T2DM. These clinical and translational approaches from my dissertation were able to: 1) identify factors in aSAT that may help 'protect' adults with obesity from excessive lipid accumulation in skeletal muscle, and developing insulin resistance, 2) explore novel signaling mechanisms that may be impairing insulin-mediated glucose uptake in skeletal muscle of insulin resistant adults, and 3) identify the effect of acute exercise and exercise training adaptations aimed to benefit intramyocellular LD storage and distribution. Together, these integrative studies have improved our understanding about obesity-induced insulin resistance, and proposed a role for exercise to modify intramyocellular LD storage and regulation - in effort to identify how exercise limits lipid-induced insulin resistance in humans.

REFERENCES

1. Flegal KM, Kruszon-Moran D, Carroll MD, Fryar CD, and Ogden CL. Trends in Obesity Among Adults in the United States, 2005 to 2014. *JAMA.* 2016;315(21):2284-91.
2. Flegal KM, Carroll MD, Kuczmarski RJ, and Johnson CL. Overweight and obesity in the United States: prevalence and trends, 1960–1994. *International Journal of Obesity.* 1998;22(1):39-47.
3. Hales CM, Carroll MD, Fryar CD, and Ogden CL. Prevalence of obesity and severe obesity among adults: United States, 2017–2018. 2020.
4. Eckel RH, and Krauss RM. American Heart Association Call to Action: Obesity as a Major Risk Factor for Coronary Heart Disease. 1998;97(21):2099-100.
5. Nguyen NT, Nguyen X-MT, Lane J, and Wang P. Relationship between obesity and diabetes in a US adult population: findings from the National Health and Nutrition Examination Survey, 1999-2006. *Obes Surg.* 2011;21(3):351-5.
6. Biener A, Cawley J, and Meyerhoefer C. The Impact of Obesity on Medical Care Costs and Labor Market Outcomes in the US. *Clinical Chemistry.* 2018;64(1):108-17.
7. Biener A, Cawley J, and Meyerhoefer C. The High and Rising Costs of Obesity to the US Health Care System. *Journal of general internal medicine.* 2017;32(Suppl 1):6-8.
8. Cawley J, Biener A, Meyerhoefer C, Ding Y, Zvenyach T, Smolarz BG, et al. Direct medical costs of obesity in the United States and the most populous states. *Journal of Managed Care & Specialty Pharmacy.* 2021;27(3):354-66.
9. Warram JH, Martin BC, Krolewski AS, Soeldner JS, and Kahn CR. Slow glucose removal rate and hyperinsulinemia precede the development of type II diabetes in the offspring of diabetic parents. *Annals of internal medicine.* 1990;113(12):909-15.
10. Després JP, Lamarche B, Mauriège P, Cantin B, Dagenais GR, Moorjani S, et al. Hyperinsulinemia as an independent risk factor for ischemic heart disease. *The New England journal of medicine.* 1996;334(15):952-7.
11. Petersen MC, and Shulman GI. Mechanisms of Insulin Action and Insulin Resistance. *Physiol Rev.* 2018;98(4):2133-223.
12. Shulman GI. Cellular mechanisms of insulin resistance. *J Clin Invest.* 2000;106(2):171-6.
13. Shulman GI. Ectopic Fat in Insulin Resistance, Dyslipidemia, and Cardiometabolic Disease. *New England Journal of Medicine.* 2014;371(12):1131-41.
14. DeFronzo RA. From the Triumvirate to the Ominous Octet: A New Paradigm for the Treatment of Type 2 Diabetes Mellitus. *Diabetes.* 2009;58(4):773.
15. Samuel VT, and Shulman GI. The pathogenesis of insulin resistance: integrating signaling pathways and substrate flux. *J Clin Invest.* 2016;126(1):12-22.
16. Smith GI, Mittendorfer B, and Klein S. Metabolically healthy obesity: facts and fantasies. *J Clin Invest.* 2019;129(10):3978-89.

17. Wildman RP, Muntner P, Reynolds K, McGinn AP, Rajpathak S, Wylie-Rosett J, et al. The Obese Without Cardiometabolic Risk Factor Clustering and the Normal Weight With Cardiometabolic Risk Factor Clustering: Prevalence and Correlates of 2 Phenotypes Among the US Population (NHANES 1999-2004). *Archives of Internal Medicine.* 2008;168(15):1617-24.

18. Dvorak RV, DeNino WF, Ades PA, and Poehlman ET. Phenotypic characteristics associated with insulin resistance in metabolically obese but normal-weight young women. *Diabetes.* 1999;48(11):2210-4.

19. Stefan N, Kantartzis K, Machann J, Schick F, Thamer C, Rittig K, et al. Identification and characterization of metabolically benign obesity in humans. *Arch Intern Med.* 2008;168(15):1609-16.

20. Calori G, Lattuada G, Piemonti L, Garancini MP, Ragogna F, Villa M, et al. Prevalence, metabolic features, and prognosis of metabolically healthy obese Italian individuals: the Cremona Study. *Diabetes Care.* 2011;34(1):210-5.

21. Zhang Y, Proenca R, Maffei M, Barone M, Leopold L, and Friedman JM. Positional cloning of the mouse obese gene and its human homologue. *Nature.* 1994;372(6505):425-32.

22. Rosen ED, and Spiegelman BM. Adipocytes as regulators of energy balance and glucose homeostasis. *Nature.* 2006;444(7121):847-53.

23. Virtue S, and Vidal-Puig A. Adipose tissue expandability, lipotoxicity and the Metabolic Syndrome — An allostatic perspective. *Biochimica et Biophysica Acta (BBA) - Molecular and Cell Biology of Lipids.* 2010;1801(3):338-49.

24. Magkos F, Fabbrini E, Conte C, Patterson BW, and Klein S. Relationship between Adipose Tissue Lipolytic Activity and Skeletal Muscle Insulin Resistance in Nondiabetic Women. *The Journal of Clinical Endocrinology & Metabolism.* 2012;97(7):E1219-E23.

25. Horowitz JF, Coppack SW, Paramore D, Cryer PE, Zhao G, and Klein S. Effect of short-term fasting on lipid kinetics in lean and obese women. *The American journal of physiology.* 1999;276(2):E278-84.

26. Van Pelt DW, Guth LM, Wang AY, and Horowitz JF. Factors regulating subcutaneous adipose tissue storage, fibrosis, and inflammation may underlie low fatty acid mobilization in insulin-sensitive obese adults. 2017;313(4):E429-E39.

27. Kelley DE, Mokan M, Simoneau JA, and Mandarino LJ. Interaction between glucose and free fatty acid metabolism in human skeletal muscle. *J Clin Invest.* 1993;92(1):91-8.

28. Boden G. Role of fatty acids in the pathogenesis of insulin resistance and NIDDM. *Diabetes.* 1997;46(1):3-10.

29. Koh H-CE, van Vliet S, Pietka TA, Meyer GA, Razani B, Laforest R, et al. Subcutaneous adipose tissue metabolic function and insulin sensitivity in people with obesity. *Diabetes.* 2021:db210160.

30. Santomauro AT, Boden G, Silva ME, Rocha DM, Santos RF, Ursich MJ, et al. Overnight lowering of free fatty acids with Acipimox improves insulin resistance and glucose tolerance in obese diabetic and nondiabetic subjects. *Diabetes.* 1999;48(9):1836-41.

31. Schenk S, Harber MP, Shrivastava CR, Burant CF, and Horowitz JF. Improved insulin sensitivity after weight loss and exercise training is mediated by a reduction in plasma fatty acid mobilization, not enhanced oxidative capacity. 2009;587(20):4949-61.

32. Thiébaud D, DeFronzo RA, Jacot E, Golay A, Acheson K, Maeder E, et al. Effect of long chain triglyceride infusion on glucose metabolism in man. *Metabolism.* 1982;31(11):1128-36.

33. Dresner A, Laurent D, Marcucci M, Griffin ME, Dufour S, Cline GW, et al. Effects of free fatty acids on glucose transport and IRS-1-associated phosphatidylinositol 3-kinase activity. *J Clin Invest.* 1999;103(2):253-9.

34. Wolfe BM, Klein S, Peters EJ, Schmidt BF, and Wolfe RR. Effect of elevated free fatty acids on glucose oxidation in normal humans. *Metabolism.* 1988;37(4):323-9.

35. Roden M, Krssak M, Stingl H, Gruber S, Hofer A, Fürnsinn C, et al. Rapid impairment of skeletal muscle glucose transport/phosphorylation by free fatty acids in humans. *Diabetes.* 1999;48(2):358-64.

36. Turner N, Kowalski GM, Leslie SJ, Risis S, Yang C, Lee-Young RS, et al. Distinct patterns of tissue-specific lipid accumulation during the induction of insulin resistance in mice by high-fat feeding. *Diabetologia.* 2013;56(7):1638-48.

37. Montgomery MK, Nardo WD, and Watt MJ. Impact of Lipotoxicity on Tissue "Cross Talk" and Metabolic Regulation. 2019;34(2):134-49.

38. Van Pelt DW, Newsom SA, Schenk S, and Horowitz JF. Relatively low endogenous fatty acid mobilization and uptake helps preserve insulin sensitivity in obese women. *Int J Obes (Lond).* 2015;39(1):149-55.

39. Groop LC, Bonadonna RC, DelPrato S, Ratheiser K, Zyck K, Ferrannini E, et al. Glucose and free fatty acid metabolism in non-insulin-dependent diabetes mellitus. Evidence for multiple sites of insulin resistance. *J Clin Invest.* 1989;84(1):205-13.

40. Guilherme A, Virbasius JV, Puri V, and Czech MP. Adipocyte dysfunctions linking obesity to insulin resistance and type 2 diabetes. *Nature Reviews Molecular Cell Biology.* 2008;9(5):367-77.

41. McQuaid SE, Hodson L, Neville MJ, Dennis AL, Cheeseman J, Humphreys SM, et al. Downregulation of adipose tissue fatty acid trafficking in obesity: a driver for ectopic fat deposition? *Diabetes.* 2011;60(1):47-55.

42. Corvera S, and Gealekman O. Adipose tissue angiogenesis: impact on obesity and type-2 diabetes. *Biochimica et biophysica acta.* 2014;1842(3):463-72.

43. Khan T, Muise ES, Iyengar P, Wang ZV, Chandalia M, Abate N, et al. Metabolic Dysregulation and Adipose Tissue Fibrosis: Role of Collagen VI. 2009;29(6):1575-91.

44. Morigny P, Houssier M, Mouisel E, and Langin D. Adipocyte lipolysis and insulin resistance. *Biochimie.* 2016;125:259-66.

45. Tschritter O, Fritsche A, Thamer C, Haap M, Shirkavand F, Rahe S, et al. Plasma adiponectin concentrations predict insulin sensitivity of both glucose and lipid metabolism. *Diabetes.* 2003;52(2):239-43.

46. Kim J-Y, van de Wall E, Laplante M, Azzara A, Trujillo ME, Hofmann SM, et al. Obesity-associated improvements in metabolic profile through expansion of adipose tissue. *J Clin Invest.* 2007;117(9):2621-37.

47. Palomer X, Pizarro-Delgado J, Barroso E, and Vázquez-Carrera M. Palmitic and Oleic Acid: The Yin and Yang of Fatty Acids in Type 2 Diabetes Mellitus. *Trends in Endocrinology & Metabolism.* 2018;29(3):178-90.

48. DeFronzo RA, Jacot E, Jequier E, Maeder E, Wahren J, and Felber JP. The Effect of Insulin on the Disposal of Intravenous Glucose: Results from Indirect Calorimetry and Hepatic and Femoral Venous Catheterization. 1981;30(12):1000-7.

49. Itani SI, Zhou Q, Pories WJ, MacDonald KG, and Dohm GL. Involvement of protein kinase C in human skeletal muscle insulin resistance and obesity. *Diabetes.* 2000;49(8):1353-8.

50. Adams JM, Pratipanawatr T, Berria R, Wang E, DeFronzo RA, Sullards MC, et al. Ceramide Content Is Increased in Skeletal Muscle From Obese Insulin-Resistant Humans. 2004;53(1):25-31.

51. Koves TR, Ussher JR, Noland RC, Slentz D, Mosedale M, Ilkayeva O, et al. Mitochondrial Overload and Incomplete Fatty Acid Oxidation Contribute to Skeletal Muscle Insulin Resistance. *Cell Metabolism.* 2008;7(1):45-56.

52. Perseghin G, Scifo P, De Cobelli F, Pagliato E, Battezzati A, Arcelloni C, et al. Intramyocellular triglyceride content is a determinant of in vivo insulin resistance in humans: a 1H-13C nuclear magnetic resonance spectroscopy assessment in offspring of type 2 diabetic parents. 1999;48(8):1600-6.

53. Cohen P. The origins of protein phosphorylation. *Nature Cell Biology.* 2002;4(5):E127-E30.

54. Karlsson HK, Zierath JR, Kane S, Krook A, Lienhard GE, and Wallberg-Henriksson H. Insulin-stimulated phosphorylation of the Akt substrate AS160 is impaired in skeletal muscle of type 2 diabetic subjects. *Diabetes.* 2005;54(6):1692-7.

55. Middelbeek RJW, Chambers MA, Tantiwong P, Treebak JT, An D, Hirshman MF, et al. Insulin stimulation regulates AS160 and TBC1D1 phosphorylation sites in human skeletal muscle. *Nutrition & Diabetes.* 2013;3(6):e74-e.

56. Tonks KT, Ng Y, Miller S, Coster ACF, Samocha-Bonet D, Iseli TJ, et al. Impaired Akt phosphorylation in insulin-resistant human muscle is accompanied by selective and heterogeneous downstream defects. *Diabetologia.* 2013;56(4):875-85.

57. Pratipanawatr W, Pratipanawatr T, Cusi K, Berria R, Adams JM, Jenkinson CP, et al. Skeletal muscle insulin resistance in normoglycemic subjects with a strong family history of type 2 diabetes is associated with decreased insulin-stimulated insulin receptor substrate-1 tyrosine phosphorylation. *Diabetes.* 2001;50(11):2572-8.

58. Storgaard H, Song XM, Jensen CB, Madsbad S, Björnholm M, Vaag A, et al. Insulin signal transduction in skeletal muscle from glucose-intolerant relatives of type 2 diabetic patients [corrected]. *Diabetes.* 2001;50(12):2770-8.

59. Vind BF, Pehmøller C, Treebak JT, Birk JB, Hey-Mogensen M, Beck-Nielsen H, et al. Impaired insulin-induced site-specific phosphorylation of TBC1 domain family, member

4 (TBC1D4) in skeletal muscle of type 2 diabetes patients is restored by endurance exercise-training. *Diabetologia.* 2011;54(1):157-67.

60. Samovski D, Dhule P, Pietka T, Jacome-Sosa M, Penrose E, Son N-H, et al. Regulation of Insulin Receptor Pathway and Glucose Metabolism by CD36 Signaling. 2018;67(7):1272-84.

61. Krssak M, Falk Petersen K, Dresner A, DiPietro L, Vogel SM, Rothman DL, et al. Intramyocellular lipid concentrations are correlated with insulin sensitivity in humans: a 1H NMR spectroscopy study. *Diabetologia.* 1999;42(1):113-6.

62. Pan DA, Lillioja S, Kriketos AD, Milner MR, Baur LA, Bogardus C, et al. Skeletal muscle triglyceride levels are inversely related to insulin action. *Diabetes.* 1997;46(6):983-8.

63. Roden M, Price TB, Perseghin G, Petersen KF, Rothman DL, Cline GW, et al. Mechanism of free fatty acid-induced insulin resistance in humans. *J Clin Invest.* 1996;97(12):2859-65.

64. Yu C, Chen Y, Cline GW, Zhang D, Zong H, Wang Y, et al. Mechanism by which fatty acids inhibit insulin activation of insulin receptor substrate-1 (IRS-1)-associated phosphatidylinositol 3-kinase activity in muscle. *The Journal of biological chemistry.* 2002;277(52):50230-6.

65. Perreault L, Newsom SA, Strauss A, Kerege A, Kahn DE, Harrison KA, et al. Intracellular localization of diacylglycerols and sphingolipids influences insulin sensitivity and mitochondrial function in human skeletal muscle. *JCI Insight.* 2018;3(3):e96805.

66. Kahn D, Perreault L, Macias E, Zarini S, Newsom SA, Strauss A, et al. Subcellular localisation and composition of intramuscular triacylglycerol influence insulin sensitivity in humans. *Diabetologia.* 2020.

67. Gemmink A, Goodpaster BH, Schrauwen P, and Hesselink MKC. Intramyocellular lipid droplets and insulin sensitivity, the human perspective. *Biochimica et Biophysica Acta (BBA) - Molecular and Cell Biology of Lipids.* 2017;1862(10, Part B):1242-9.

68. Nielsen J, Mogensen M, Vind BF, Sahlin K, Højlund K, Schrøder HD, et al. Increased subsarcolemmal lipids in type 2 diabetes: effect of training on localization of lipids, mitochondria, and glycogen in sedentary human skeletal muscle. *Am J Physiol Endocrinol Metab.* 2010;298(3):E706-13.

69. Daemen S, Gemmink A, Brouwers B, Meex RCR, Huntjens PR, Schaart G, et al. Distinct lipid droplet characteristics and distribution unmask the apparent contradiction of the athlete's paradox. *Molecular Metabolism.* 2018;17:71-81.

70. Chee C, Shannon CE, Burns A, Selby AL, Wilkinson D, Smith K, et al. Relative Contribution of Intramyocellular Lipid to Whole-Body Fat Oxidation Is Reduced With Age but Subsarcolemmal Lipid Accumulation and Insulin Resistance Are Only Associated With Overweight Individuals. *Diabetes.* 2016;65(4):840-50.

71. Colberg SR, Sigal RJ, Yardley JE, Riddell MC, Dunstan DW, Dempsey PC, et al. Physical Activity/Exercise and Diabetes: A Position Statement of the American Diabetes Association. *Diabetes Care.* 2016;39(11):2065.

72. Garber CE, Blissmer B, Deschenes MR, Franklin BA, Lamonte MJ, Lee IM, et al. American College of Sports Medicine position stand. Quantity and quality of exercise for developing and maintaining cardiorespiratory, musculoskeletal, and neuromotor fitness in apparently healthy adults: guidance for prescribing exercise. *Medicine and science in sports and exercise.* 2011;43(7):1334-59.

73. Bray GA, Frühbeck G, Ryan DH, and Wilding JPH. Management of obesity. *The Lancet.* 2016;387(10031):1947-56.

74. Pedersen BK, and Saltin B. Exercise as medicine - evidence for prescribing exercise as therapy in 26 different chronic diseases. *Scandinavian journal of medicine & science in sports.* 2015;25 Suppl 3:1-72.

75. Schenk S, and Horowitz JF. Acute exercise increases triglyceride synthesis in skeletal muscle and prevents fatty acid–induced insulin resistance. *J Clin Invest.* 2007;117(6):1690-8.

76. Dubé JJ, Amati F, Stefanovic-Racic M, Toledo FG, Sauers SE, and Goodpaster BH. Exercise-induced alterations in intramyocellular lipids and insulin resistance: the athlete's paradox revisited. *Am J Physiol Endocrinol Metab.* 2008;294(5):E882-8.

77. Nielsen J, Christensen AE, Nellemann B, and Christensen B. Lipid droplet size and location in human skeletal muscle fibers are associated with insulin sensitivity. 2017;313(6):E721-E30.

78. Gemmink A, Daemen S, Brouwers B, Huntjens PR, Schaart G, Moonen-Kornips E, et al. Dissociation of intramyocellular lipid storage and insulin resistance in trained athletes and type 2 diabetes patients; involvement of perilipin 5? *J Physiol.* 2018;596(5):857-68.

79. Zacharewicz E, Hesselink MKC, and Schrauwen P. Exercise counteracts lipotoxicity by improving lipid turnover and lipid droplet quality. *Journal of internal medicine.* 2018;284(5):505-18.

80. Seibert JT, Najt CP, Heden TD, Mashek DG, and Chow LS. Muscle Lipid Droplets: Cellular Signaling to Exercise Physiology and Beyond. *Trends in Endocrinology & Metabolism.* 2020.

81. Koh H-CE, Ørtenblad N, Winding KM, Hellsten Y, Mortensen SP, and Nielsen J. High-intensity interval, but not endurance, training induces muscle fiber type-specific subsarcolemmal lipid droplet size reduction in type 2 diabetic patients. 2018;315(5):E872-E84.

82. Gibala MJ, Little JP, MacDonald MJ, and Hawley JA. Physiological adaptations to low-volume, high-intensity interval training in health and disease. 2012;590(5):1077-84.

83. Olzmann JA, and Carvalho P. Dynamics and functions of lipid droplets. *Nature reviews Molecular cell biology.* 2019;20(3):137-55.

84. Liu K, and Czaja MJ. Regulation of lipid stores and metabolism by lipophagy. *Cell Death & Differentiation.* 2013;20(1):3-11.

85. Rambold AS, Cohen S, and Lippincott-Schwartz J. Fatty acid trafficking in starved cells: regulation by lipid droplet lipolysis, autophagy, and mitochondrial fusion dynamics. *Developmental cell.* 2015;32(6):678-92.

Chapter II

Review of Literature

INTRODUCTION

Obesity is a major health problem and has been increasing in prevalence, with more than 40% of the United States now classified as obese (1). Obesity is a major risk factor for cardiovascular disease (2, 3), type 2 diabetes mellitus [T2DM] (4), and several cancers (5-7). Alarmingly, its complications are also major predisposing factors for SARS-CoV-2 hospitalization and intensive care unit admissions (8, 9). Due to the multitude of conditions by which obesity is a risk factor and its high prevalence in the United States, the annual direct costs for treating obesity-related complications has surpassed $300 billion (10), and this expense equates to almost 8% of total United States healthcare expenditures (10, 11). Lifestyle and weight loss interventions (i.e., increased physical activity and dietary interventions) have been found to be effective strategies for preventing T2DM (12), and were even found more effective than current anti-diabetic medications at preventing T2DM onset (13). Unfortunately, successful long-term weight loss maintenance is rather poor. For example, it has been reported one in six adults from the National Health and Nutrition Examination Survey (NHANES; > 14,000 participants) were unable to maintain 10% weight loss one year after completing their respective programs (14). With the increased prevalence of obesity and poor weight management outcomes in United States, further research is needed to identify specific mechanisms underlying; 1) the metabolic implications of obesity, 2) how metabolic health is improved following lifestyle interventions, and 3) beneficial effects of exercise in obese adults. Importantly, mechanistic findings from these studies will be crucial towards developing treatments necessary to mitigate the negative metabolic health outcomes caused by obesity.

Obesity is associated with a cluster of metabolic abnormalities, many of which are linked to insulin resistance. Insulin resistance is characterized by a suppressed response to the glucose lowering, and anti-lipolytic effect of insulin [Figure II-1A] (15). Consequently, in insulin resistant individuals, a greater amount of insulin is necessary to; 1) decrease lipolytic rate from adipose

tissue, 2) decrease hepatic glucose output from the liver, 3) increase protein synthesis, and 4) increase glucose uptake into skeletal muscle (Figure II-1B). In fact, many obese insulin resistant individuals do not develop hyperglycemia due to a compensatory increase in insulin secretion from the pancreas (15, 16). The pathology of insulin resistance cannot be isolated to one specific tissue or mechanism, but rather it is associated with a cluster of derangements. Determining mechanisms of insulin resistance in metabolically active tissues such as adipose, skeletal muscle, and liver is tremendously important for the treatment and/or protection against metabolic dysregulation in obese adults.

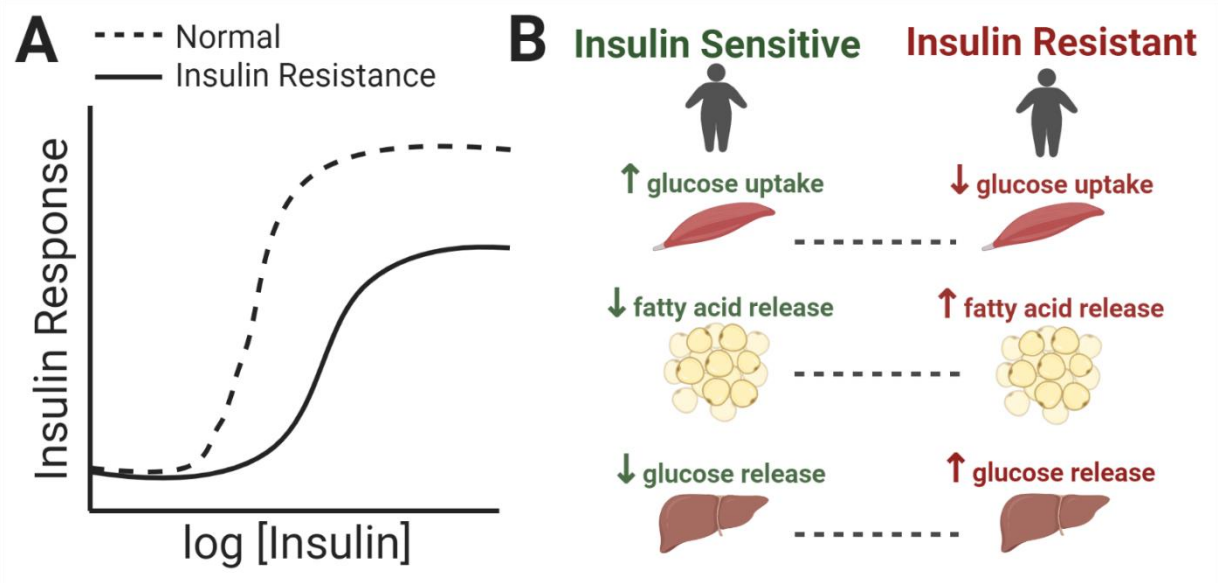

Figure II-1: Theoretical model for obesity-induced insulin resistance.

A) A downward shift in the insulin dose-response curve is associated with obesity-induced insulin resistance (i.e., post-receptor insulin resistance), and B) Metabolic response to a physiological dose of insulin in insulin sensitive versus insulin resistant individuals.

Although the majority of obese adults develop insulin resistance, not all obese adults develop insulin resistance or cardiometabolic disease risk associated with obesity. In fact, there is a significant proportion (~10-30%) of obese adults classified as 'metabolically healthy', and maintain insulin sensitivity similar to lean and healthy adults, despite carrying excessive fat mass (17-23). Therefore, emphasis aimed to identify clinical and subclinical factors within the aforementioned target tissues (specifically adipose tissue & skeletal muscle) that are *protecting*

obese adults from developing insulin resistance will be invaluable to identify the underlying progression of insulin resistance caused by obesity. In **SECTION I** of my review of the literature, I will focus on insulin action with respect to glucose transport and fatty acid lipolysis/fatty acid metabolism in skeletal muscle and adipose tissue respectively. Additionally, I will introduce the potential by which mass-spectrometry based proteomics characterizes insulin action and signal transduction *on a global scale*. In **SECTION II**, I will review mechanisms by which obesity largely contributes to the development of insulin resistance. More specifically, I will review the impact excessive fatty acid mobilization rates from white adipose tissue on insulin-stimulated glucose uptake in skeletal muscle. Additionally, I will also introduce a unique mechanism by which the well-known fatty acid translocase, CD36, may play a role in regulating insulin action in skeletal muscle at the insulin receptor, and how the interaction is perturbed by high fatty acid mobilization in obesity. In **SECTION III**, I will review factors in adipose tissue that may help 'protect' obese adults from developing insulin resistance. More specifically, I will review hypothesized factors by which 'metabolically healthy' obese adults maintain low fatty acid mobilization rates from adipose tissue, and have limited 'lipid overflow' into non-adipose tissues such as skeletal muscle and liver (i.e., ectopic lipid deposition). **SECTION IV** will review mechanisms by which exercise improves insulin sensitivity in obese adults. Specifically focusing on fatty acid metabolism and storage after both acute exercise and chronic exercise training. Our lab's working model details that even a single exercise session promotes stimuli central towards reversing obesity-induced insulin resistance by promoting triglyceride synthesis in skeletal muscle, which 'partitions' lipids towards inert triglyceride storage and away from harmful lipid intermediates (24). Additionally, I will review mechanisms by which exercise regulates the localization and structural organization of intramyocellular lipid droplets [LDs] (19), a key organelle associated with inert triglyceride storage in skeletal muscle.

I - Mechanisms of Insulin Action in Skeletal Muscle and Adipose Tissue

Insulin is a critical hormone regulating glucose and fatty acid dynamics, and central to controlling glucose uptake in skeletal muscle and fatty acid release from adipose tissue. In skeletal muscle, insulin regulates glucose homeostasis by; 1) increasing glucose uptake by GLUT4 exocytosis from the cytosol to the cell membrane, and 2) increasing glucose storage by activating glycogen synthase [Figure II-2] (25-27). Importantly, glucose transport into the cell has been

found to be the rate limiting step for glucose disposal (28, 29), suggesting mechanisms regulating insulin-stimulated GLUT4 translocation to the membrane are important to alleviate impairments in glucose control associated with insulin resistance. Insulin-stimulated glucose uptake is initiated through binding insulin to the insulin receptor (IR) - a tyrosine kinase protein located at the cell membrane. Upon binding, a conformational change in the IR causes the two transmembrane β subunits to move together, causing intracellular tyrosine autophosphorylation (30). Once the IR is phosphorylated, insulin receptor substrates (IRS-1 & IRS-2) are recruited to the IR, interacting at the phosphotyrosine binding domain (31, 32). In skeletal muscle, IRS-1 is the primary insulin receptor substrate (33). Tyrosine phosphorylation of IRS-1 then recruits phosphatidylinositol 3-kinase (PI3K) to the cell membrane (34), where PI3K contains a regulatory p85 subunit and catalytic p110 subunit (32). PI3K then catalyzes the reaction of phosphatidylinositol-3,4,5-trisphosphate (PIP_3) from phosphatidylinositol-4,5-bisphosphate [PIP_2] (35). Then, PIP_3 recruits phosphoinositide-dependent protein kinase-1 (PDK1), which phosphorylates Protein Kinase B (Akt), and Akt becomes phosphorylated by PDK1 at Thr ^{308} (32). Additionally, Akt is phosphorylated at Ser^{473} by mTORC2 (36). When Akt becomes activated, Akt substrate of 160kDa (AS160/TBC1D4) is then phosphorylated at Thr^{642}, releasing AS160 inhibition of Rab-GTPase activity, and promoting GLUT4 release from GLUT4 storage vesicles into the cell membrane. Rab8A, Rab10, and Rab13 are some examples of Rab GTPases influencing GLUT4 translocation (37, 38). In more simple terms, AS160 phosphorylation by Akt can be thought of as 'releasing the brakes' on GLUT 4 translocation (39). However, the signaling mechanisms described above are not the sole substrates of insulin action, and is important to note Akt is central to many metabolic functions, and activates several regulatory protein substrates (TSC2, PRAS40, GSK3 β, SREBP, TBC1D1, PDE3B, FOXO, and many more) (40). Regulation of these Akt substrates will be discussed later in SECTION I.

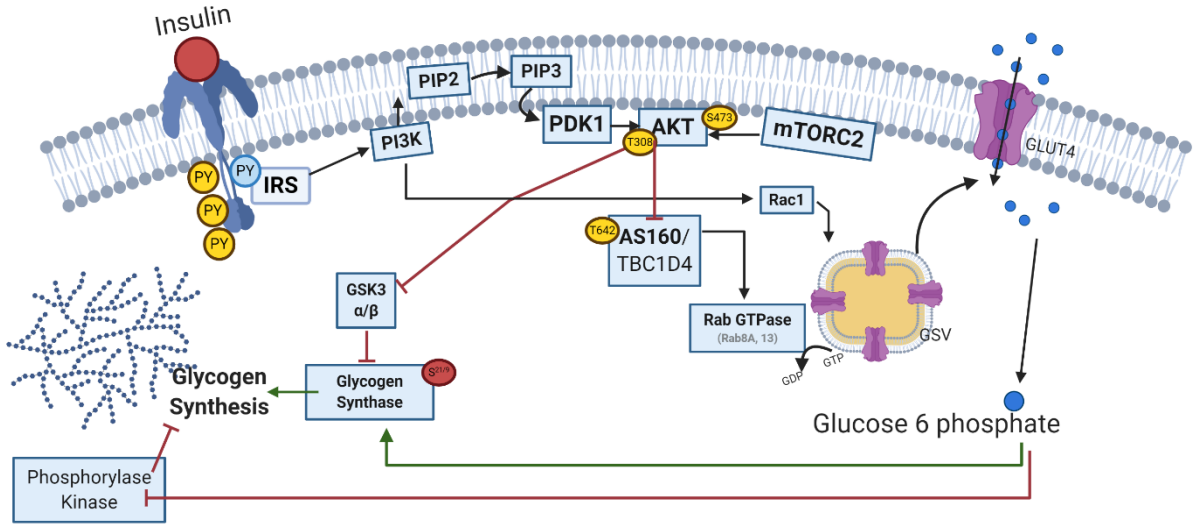

Figure II-2: Insulin promotes glucose uptake by GLUT4 translocation.

One major pathway by which insulin controls metabolism is to regulate glucose uptake. Insulin signaling can be separated into proximal segments that are activated from the insulin receptor, insulin receptor substrate (IRS), phosphoinositide 3-kinase (PI3K) and Akt. The distal segments to Akt related to GLUT4 translocation includes phosphorylation of Akt substrate of 160 KDa (AS160) to inhibit the Rab GTPase influence of AS160 on GLUT4 storage vesicles, promoting GLUT4 translocation.

Insulin acts on adipocytes to suppress fatty acid release into the circulation (lipolysis), and promotes lipid and glucose uptake (Figure II-3). Lipolysis is the release (i.e., hydrolysis) of fatty acids stored as triacylglycerol (TAG), thus, promoting TAG storage. Therefore, insulin limits fatty acid release into the circulation when present in high abundance (i.e., positive energy balance). Lipolysis is largely activated by β-adrenergic signaling, in which catecholamine binding to β-adrenergic receptor activates G-protein coupled receptors to activate adenylyl cyclase, and then adenylyl cyclase activates cyclic AMP (cAMP), which subsequently activates protein kinase A (PKA). Activated PKA then phosphorylates hormone sensitive lipase (HSL) at Ser^{563}, Ser^{659}, Ser^{660} (41). The most commonly described phosphorylation site from PKA is on HSL at Ser^{660}. Phosphorylated HSL then translocates from the cytosol to the LD membrane, where HSL hydrolyses diacylglycerol [DAG] to monoacyclglycerol. PKA also activate proteins responsible for the initial step of TAG hydrolysis, by phosphorylating PLIN to recruit comparative gene identification-58 (CGI58 [ABHD5]) and activate adipose triglyceride lipase (ATGL) at Ser^{406} (42). ATGL is responsible for TAG hydrolysis to DAG (43), and is negatively regulated by G(0)/G(S) switch 2 [G0S2] (44). Insulin-stimulated lipolysis suppression involves the reversal of β-

adrenergic stimulation, preventing PKA activation by cAMP (45, 46). Insulin largely suppresses lipolysis through phosphodiesterase 3B (PDE3B), which degrades cAMP and limits PKA phosphorylation on both HSL and PLIN (47). The mechanism by which insulin activates PDE3B at Ser^{273} have proposed to be through Akt (48), while others have suggested Akt is not required for insulin-stimulated lipolysis suppression (49).

Insulin-stimulated glucose uptake in adipose tissue is only a minor proportion of whole-body glucose uptake [<5%] (50). Insulin-stimulated glucose entry into adipose tissue is regulated by GLUT4 translocation, and glucose is largely converted to fatty acids through lipogenesis, which is activated by carbohydrate response elements, and regulated by acetyl-CoA carboxylase (51). Therefore, glucose is largely stored as TAG in the adipocyte as opposed to glycogen in skeletal muscle, but the contribution of glucose to de novo lipogenesis is still minimal in human adipose tissue. Although adipose tissue and skeletal muscle provide key roles in glucose and fatty acid regulation, it is important to note that insulin action is not exclusive to these two tissues, and other notable tissues include; 1) liver regulation of glucose output (52, 53), 2) brain regulation of food intake and neural regulation of adipose tissue lipolysis (54, 55), and 3) vascular regulation of insulin delivery (56). Therefore, our current understanding of the pathogenesis of insulin resistance (and selective insulin resistance) in all metabolic tissues are still very limited. A full elucidation of insulin-signaling mechanisms from multiple tissues will be required, each with their own unique metabolic function and insulin action.

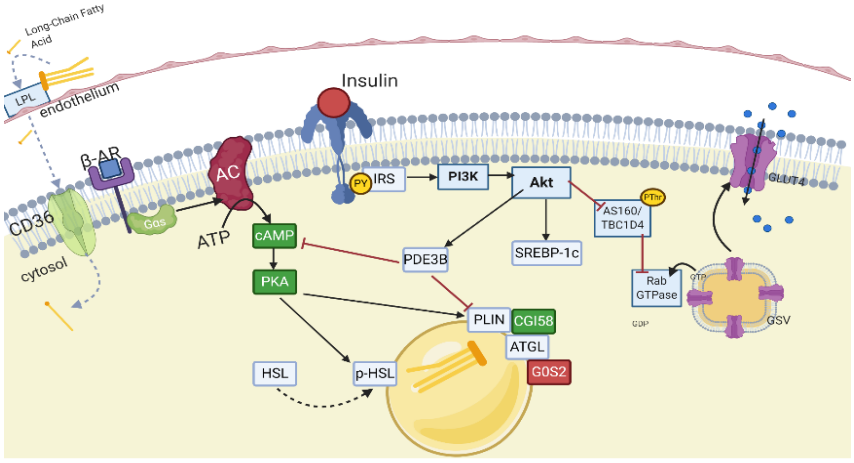

Figure II-3: Insulin regulation of lipolysis in adipose tissue

Insulin is a potent inhibitor of lipolysis in adipose tissue. Insulin signaling is propagated through proximal components to activate Phosphodiesterase 3B (PDE3B), which inhibits adenylyl cyclase activation of cyclic AMP (cAMP), and further inhibiting protein kinase A (PKA) activation. Thus, limiting HSL influence on lipolysis.

Mechanisms of Insulin Action and Regulation beyond Akt.

Protein phosphorylation is central to signal transduction and cellular function, and the most widely profiled posttranslational modification (PTM) signaled by insulin (57, 58). Phosphorylation involves the transfer of γ-phosphate from ATP, and is regulated by kinase/phosphatase influence onto serine, threonine, and tyrosine residues of substrate proteins (57). For many metabolic studies, the measurement of phosphorylation-dependent signaling events have involved targeted approaches with antibodies of known phosphorylation sites and functions (e.g., immunoblotting methods). By using targeted approaches, these studies have advanced our understanding in cell signaling tremendously, and have successfully identified defects in key insulin-stimulated signaling events in skeletal muscle associated with insulin resistance/T2DM such as; 1) lower PI3K activation (59, 60), 2) lower Akt activation (61), and 3) lower GLUT4 abundance at the plasma membrane (62). Although Akt is central to many cellular metabolic processes and insulin-mediated Akt activation is attenuated in the insulin resistant state, it has been found to regulate over 100 substrates from a variety of other functions such as protein/lipid kinases, transcription factors, regulators of small G proteins and vesicle trafficking, metabolic enzymes, E3 ubiquitin ligases, and cell cycle regulation (40). Additionally, Humphrey et al., found over 50% of the insulin-regulated phosphoproteome is signaled through Akt in adipocytes (63), suggesting potential to define influential Akt substrates and signaling networks underlying impaired glucose uptake beyond the canonical PI3K-Akt pathways.

Mass-spectrometry (MS) based phosphoproteomic studies in metabolism have developed the coverage to introduce large scale and highly interconnected signaling networks in response to stimuli far from a traditional 'linear' view of signal transduction (64-66). MS-based phosphoproteomics have the potential to profile and analytically define *systems-wide interpretations* of conditions or response to a stimuli that are used to identify; 1) pathway enrichment, 2) novel regulatory kinases (67), and 3) protein-protein interaction networks (68), which may be underlying insulin resistance. Therefore, performing these large-scale analyses under various biological conditions will broaden our understanding of signaling throughout the proteome via phosphorylation, and reveal the scale and convergence of multiple signaling pathways (e.g., Akt and mTOR pathway convergence) occurring in response to stimuli and/or underlying disease (69). Since phosphorylation is a major regulator of insulin action in all tissues, and alterations in signaling activity are likely underlying impaired insulin action in the respective

tissue. A *global* investigation using MS-based phosphoproteomics to determine signaling impairments are highly desirable and will fill a paucity of systems-wide data underlying insulin resistance *in vivo*.

Although MS-based phosphoproteomics provide a 'systems-wide' analysis of protein activity, a major challenge lies in defining how key signaling kinase/phosphatase activity onto a substrate regulates the cellular fate in the cell. Key regulatory kinases have complex behavior, and are typically phosphorylated at multiple sites to 'fine-tune' signal transduction. At the simplest form of signal transduction, the regulation of protein activity by a single phosphorylation site can be interpreted as the sum of kinase and phosphatase activity to regulate phosphorylation, and thus, substrate activity (Figure II-4A). However, the activation/deactivation of specific proteins is not simple, and is influenced by several factors such as nutrient availability, cytokines, hormones, growth factors, and neural inputs to regulate information sent through the cell to control cellular function (69, 70). In order to regulate signal transduction, multiple sites can be controlled simultaneously on the same protein. For example, Humphrey et al., demonstrated 5,011 proteins were phosphorylated at 23,589 phosphorylation sites when insulin-stimulated in 3T3-L1 adipocytes (63). This study is one example suggesting several sites of phosphorylation along the thousands of phosphorylated proteins are regulating their function, many of which are still unknown (63, 69). If protein function were indeed regulated at multiple sites, it would seem ideal to analyze several sites along the target protein to prevent dependence of a single site as the sole regulator of cellular fate of the cell. For this reason, the concept of 'multiple-site phosphorylation' has been introduced to address these complexities. One example of multiple-site phosphorylation is 'priming', in which phosphorylation of one site increases (or decreases) its affinity for other sites to become phosphorylated (Figure II-4B). This example of priming allows the protein to work in a hierarchical manner, in which phosphorylation of one regulatory site initiates a conformational change in the target protein to increase phosphorylation from other kinases at different sites within the protein to control its end-effect (71). In the context of glucose control and insulin action, a classic example of priming is the regulation of glycogen synthase by glycogen synthase kinase 3β (GSK3β), in which the priming phosphorylation of glycogen synthase by casein kinase II at Ser^{656} is necessary for GSK3β to phosphorylate its substrate (glycogen synthase). Once glycogen synthase is phosphorylated at Ser^{656}, GSK3β progressively phosphorylates glycogen

synthase at Ser^{652}, Ser^{648}, Ser^{644}, and Ser^{640} (+4) in succession to modulate glycogen synthase activity (71).

Key regulatory proteins can also function as 'signal integrators' in metabolism, in which they are targeted by multiple kinases by independent pathways to control the activation of the specific end-effect (Figure II-4C). One example of signal integration in glucose metabolism is the phosphorylation convergence on AS160 at Thr^{642} and Ser^{588} from Akt, AMPK (72), and PKC (73) to regulate GLUT4 translocation. This form of signal integration is an important effect in the context of metabolic control initiated from independent signals. In this case, describing how the function of a signal integrator such as AS160 contributes to greater insulin-stimulated glucose uptake after exercise by convergence from multiple kinases (Akt and AMPK). Other examples of signal integration proteins in metabolism that are regulated by multiple pathways includes Akt, AMPK, TSC, PFK, SREBP, and FOXO (70).

Protein activity and cellular function can also be regulated by key 'signal processors', in which proteins can converge contrasting stimuli (activation & inhibition signals) onto signaling kinases to regulate cellular function (Figure II-4D). As opposed to signal integration - where the summation of like stimuli influence protein action, signal processors receive information from two contrasting stimuli to regulate downstream cellular response (Figure II-4D). A well-known example of a signal processor regulating cellular function lies in autophagy regulation, by which AMPK and mTOR independently regulate Unc-51 Like Autophagy Activating Kinase 1 (ULK1) to signal ATG1, which is responsible for initiating autophagy (74). AMPK promotes autophagy as it is a key nutrient sensor of energy deficit, and mTOR is on the contrary, inhibiting autophagy to promote cell growth when in positive energy balance. ULK1 in this event functions as a signal processor, and is regulated by AMPK at Ser^{317} & Ser^{777}, and from mTOR at Ser^{757} to either promote or conserve autophagy respectively (74). Other key examples of signal processors regulating metabolism and glucose uptake includes the phosphorylation of p70S6K (activated by mTORC1), which phosphorylates IRS1, leading to inhibition of Akt at Thr^{308}, an example of a classic feedback inhibition (75). Although MS-based phosphoproteomics cannot directly assess the function of the three previously mentioned mechanisms regulating signal transduction (priming, signal integration, and signal processing), these data have potential use towards hypothesizing future functional studies in response to a given stimulus underlying a disease and/or condition. Importantly, MS-based phosphoproteomics will continue to be an indispensable

resource to produce signaling roadmaps and networks unique to specific tissue underlying impaired metabolic function.

Regulation of protein activity is also regulated by a balance between both kinase and phosphatase activity. Most research in the context of insulin signaling has emphasized the impact of altered kinase activity as a focus of insulin resistance However, the balance between kinase and phosphatase activity is essential to control insulin-mediated effects, and the influence of phosphatases on protein dephosphorylation should not be ignored. In the context of dephosphorylation and insulin signaling, protein phosphatase 1B (PTP1B) was found to directly interacts IRS-1, and has been found that hyperglycemia can impair insulin-stimulated IRS-1 activation through overexpression of PTP1B (76). Another relevant phosphatase is protein phosphatase 2A (PP2A), which negatively regulates insulin action by dephosphorylating Akt (77). Perhaps understanding feedback signals (e.g., fatty acids and cytokines) regulating phosphatase activity will be important towards identifying the underlying mechanisms of impaired insulin-mediated glucose uptake. In summary, Project 2 of my dissertation will use the previously mentioned information from SECTION I to identify the effect of altered protein activation/inactivation among canonical proteins with Akt/PI3K signaling on insulin resistance. Beyond the analysis of targeted proteins associated with insulin signaling, Project 2 will also complete untargeted phosphoproteomics to identify novel proteins and networks perturbed under insulin resistance.

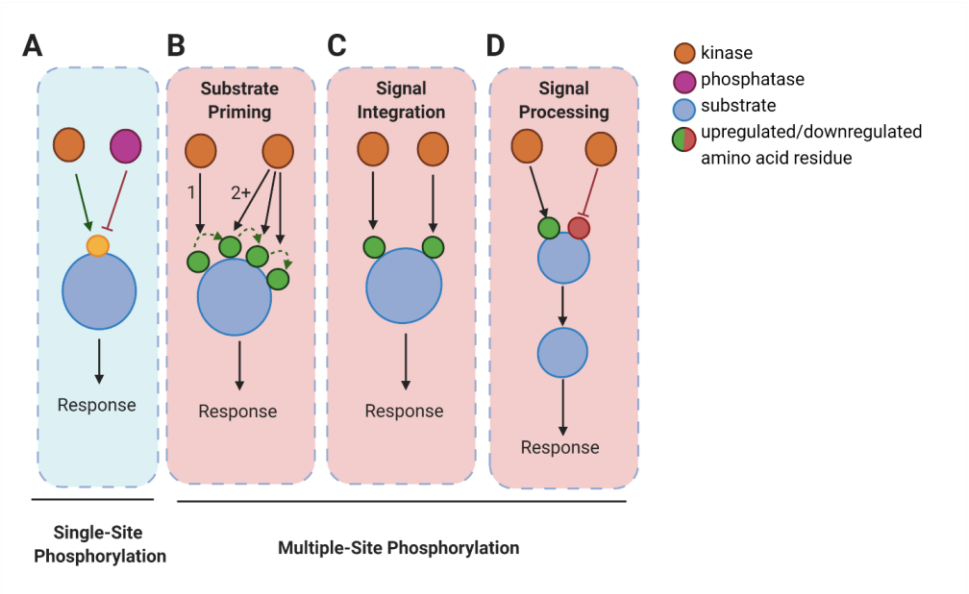

Figure II-4: Regulation of kinase-substrate activity by multiple site phosphorylation.

II - Excessive Fatty Acid Mobilization Impairs Insulin-Stimulated Glucose Uptake.

Obesity is a major risk factor for insulin resistance, and greater mobilization of fatty acids into the circulation than essential is a key factor underlying insulin resistance (53, 78). The consequential effect of high rates systemic fatty acid mobilization leads to greater lipid uptake into insulin sensitive and metabolically active tissues (Figure II-5). Therefore, the accumulation of lipid byproducts in these tissues then interferes with insulin response in metabolically important tissues such as muscle and liver (78). Skeletal muscle is important for glucose uptake and storage, as it accounts for ~85% of insulin-stimulated glucose uptake, and a key mediator of insulin resistance commonly found in obesity and T2DM (79). Additionally, the liver is an important organ in the context of glucose control, as it plays a critical role in glucose storage and production, both of which become impaired when faced with an overabundance**.** This section will largely focus on factors mediating lipid-induced resistance caused by obesity in skeletal muscle.

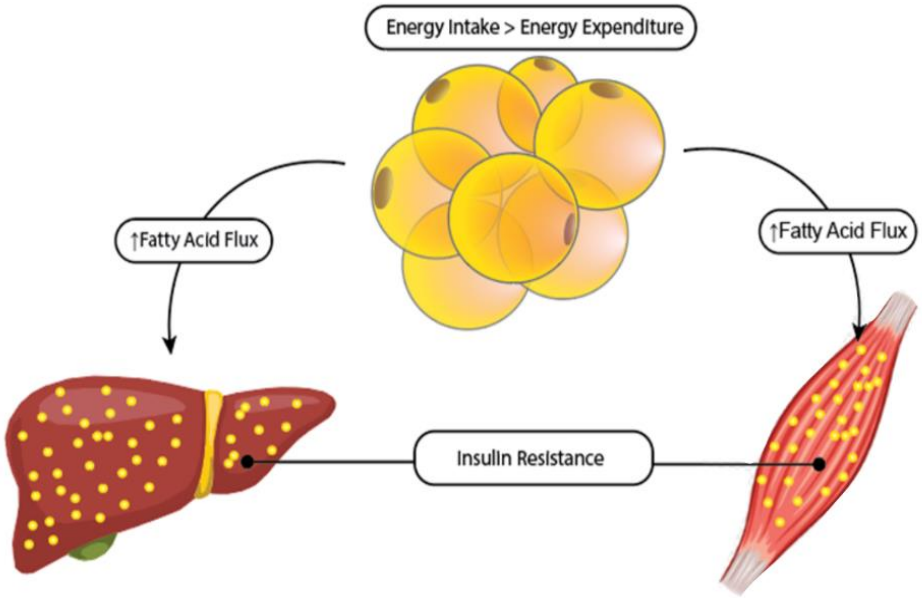

Figure II-5: Contribution of adipose tissue to ectopic lipid deposition in obesity.

Obesity is a key factor leading to greater fatty acid mobilization from adipose tissue, resulting in the ectopic deposition of lipids in liver and skeletal muscle, mediating insulin resistance. Redrawn from Shulman, 2014 (78).

Mechanisms by which fatty acids 'compete' with glucose oxidation were first proposed by Randle and colleagues in the 1960s, and coined the 'glucose-fatty acid cycle' in skeletal and cardiac muscle [Figure II-6A] (80). The working model by which the glucose-fatty acid cycle impairs glucose uptake proposed that greater fatty acid availability increases fat oxidation and diminishes glucose oxidation and uptake, which is regulated by high $[\frac{\text{acetyl}-\text{CoA}}{\text{CoA}}]$ and $[\frac{\text{NADH}}{\text{NAD+}}]$ in the mitochondria. The greater accumulation of these metabolites (acetyl-CoA and NADH) occurs as a results greater fat oxidation caused by excessive fatty acid availability, in which the metabolites allosterically inhibits pyruvate dehydrogenase (PDH) to prevent acetyl-CoA overabundance from entering the mitochondria via glycolysis. Additionally, greater Krebs cycle flux increases citrate concentration and inhibits phosphofructokinase (PFK) activity - a key rate-limiting enzyme in glycolysis. PFK inhibition will then increase cellular levels of glucose 6-phosphate, inhibiting hexokinase activity and diminishing glucose transported into the cell from the bloodstream to enter glycolysis. Although the mechanisms outlined by Randle are convincing, recent studies have challenged this theory. These studies contradicting the Randle Cycle reported glucose oxidation and uptake were not impaired as a product of allosteric modifications along key glycolytic enzymes, but rather inhibition of proximal insulin signaling proteins that affect glucose uptake into the cell, thus preventing GLUT4 translocation (29, 81-84). Studies challenging the Randle Cycle (largely by Shulman and colleagues) used magnetic resonance spectroscopy measures in skeletal muscle coupled with glucose tracers, and found labeled glucose and glucose-6-phosphate are decreased in skeletal muscle following an overnight lipid infusions (82, 83), concluding a more proximal and direct mechanism signaled by fatty acids are impairing insulin-stimulated glucose uptake. These findings then expanded to several lipid species and intermediates such as TAG, DAG, ceramide, and acylcarnitines as key lipids mediators of insulin signaling in response to obesity (Figure II-6B).

DAG is an intermediate of many lipid biosynthetic pathways, and DAG accumulation in skeletal muscle has been found to impair insulin signaling through activation of novel PKCs (53). The relationship between obesity-induced insulin resistance and DAG were found from studies showing DAG abundance increased upon lipid infusion (82, 83), and directly associated with insulin resistance in obese and diabetic populations (81, 85, 86). The transient increase in DAG was found to directly impair insulin signaling in skeletal muscle by phosphorylating PKCθ at Ser^{1101}, where it translocates to the cell membrane. Then, activated PKCθ phosphorylates IRS1 at

Ser^{307} and Ser^{1101} (decreasing IRS1 activity), and limited PI3K recruitment to the membrane upon insulin-stimulation (87-89). The relationship within the DAG-PKCθ axis has been confirmed in rodent studies, in which mice lacking PKCθ were protected from insulin resistance following lipid infusions, and mice containing IRS1 $Ser^{302,\ 307,\ and\ 612}$→Ala mutations were also protected from insulin resistance (90, 91). Similar to skeletal muscle, liver PKCε phosphorylation is activated by DAG, and limits IRS-1 activity by phosphorylating the insulin receptor at Thr^{1160}, inhibiting IRS-1 from binding to the insulin receptor along the phosphotyrosine binding domain. (52). To demonstrate this relationship in rodents, PKCε knockout mice were protected from insulin resistance following three days high-fat feeding (92). To provide further support for the relationship between DAG and impaired insulin signaling, mice overexpressing skeletal muscle diacylglycerol acyltransferase-1 (DGAT1 - the enzyme responsible for glycerolipid synthesis of DAG to TAG), increased not only TAG concentration, but improved insulin sensitivity due to attenuations in DAG in skeletal muscle causing by 'partitioning' of lipid intermediates (93). Although the impact of DAG as a lipid intermediate impairing insulin signaling has been heavily studied, other clinical studies did not found DAG accumulation to associate with insulin resistance in obese adults (94, 95). The impact of DAG localization, chain-length, and saturation are also unique to their influence on insulin response, and have been found to play an important role as both spatial- and species-specific mediators related to insulin signaling (96, 97). In which saturated DAG localized to the sarcolemma were associated with insulin resistance compared to cytosolic DAG abundance. Although DAG is the primary glycerolipid preceding TAG in glycerolipid synthesis, the accumulation of TAG in skeletal muscle has been largely associated as an 'inert' lipid store largely accumulating in LDs (98). Some studies have linked intramyocellular triglycerides (IMTG) abundance (99-101) and saturation state (102, 103) to associate with insulin resistance and/or T2DM, while others do not support IMTG as a direct cause to insulin resistance (104). Recently, the localization of IMTG in the subsarcolemmal region of skeletal muscle was found to be associated with insulin resistance (105), and are consistent to findings regarding DAG localized to sarcolemma were also negatively impacting insulin signaling (96, 97). Therefore, the location of glycerolipids in the myocyte may be an equally important factor negatively affecting insulin signaling due to its location near the membrane and insulin receptor, and will be more advantageous to measure by region compared to whole-cell abundance. Although the impact of DAG on PKC isoforms have been well-studied, future studies are warranted to understand the

relationship between DAG and non-PKC targets, localization, and species-specific (chain length/unsaturation) on insulin sensitivity.

Ceramides are bioactive lipid intermediates that play a crucial role in cell signaling, and are intermediates to the formation of sphingolipids, which are largely present in cell membranes and lipid bilayers. Ceramide accumulation has also been implicated in the impairment of insulin action in obesity similar to DAG [Figure II-6B] (106, 107). Adams et al. (2004) reported total skeletal muscle ceramide abundance was nearly 2-fold greater in insulin-resistant obese adults, and this effect was accompanied by a significant reduction in levels of Akt phosphorylation at Ser^{473} (108). In agreement with the previous studies, ceramides were found to increase protein phosphatase-2A (PP2A) activity - a key phosphatase of Akt, which resulted in lower Akt activation (109). Ceramides were also found to recruit atypical PKCζ, which inactivates Akt by diminishing its cell-surface recruitment and phosphorylation (110). Unlike the mechanisms associated with DAG, ceramides did not influence IRS-1 activation, suggesting an independent role separate from DAG promoting insulin resistance (110). Importantly, the therapeutic effect of reducing ceramide content has been found with exercise and weight loss, suggesting its role as a key mediator of obesity-induced insulin resistance (111). At the individual lipid species level, skeletal muscle C18:0 ceramides negatively associated with insulin sensitivity, and C18:0 abundance decreased following a single bout of exercise (112). Therefore, suggesting an insulin-sensitizing effect from reducing C18:0 following an acute exercise session may be underlying both insulin resistance and explain the beneficial effects of acute exercise. Beyond PKCζ and PP2A as ceramide substrates causing insulin resistance, ceramides in skeletal muscle and circulation positively associated with inflammation and TNFα activation, suggesting an inflammatory response promoting whole body insulin resistance (113-115). Although the impact of ceramide appears to be an attractive target for insulin resistance therapies, its impact on insulin sensitivity in skeletal muscle has been challenged, where other clinical studies found no relationship between ceramide content and insulin sensitivity (116-118). Similar to studies in DAG, more specific mechanistic studies will be needed to bring forward specific effects of ceramide accumulation on insulin action, as several correlative relationships found in clinical trials cannot determine if this lipid species directly cause of insulin resistance.

Acylcarnitines and long-chain acyl-CoA accumulation in skeletal muscle represents a separate mechanism from the previously mentioned (DAG-PKC and Ceramide-Akt), by which

lipid delivery to the mitochondria is unable to be matched by oxidation or TAG synthesis, resulting in acylcarnitine accumulation and impaired insulin signaling (119-121). The link between the increased abundance of these polar lipids have been found to be associated with a perturbed (or *incomplete*) fat oxidation, in which greater rates of fatty acids enter β-oxidation and outpace TCA cycle activity, resulting in an overabundance of acyl-CoA unable to be metabolized completely to acetyl-CoA (119). This notion of 'incomplete' fatty acid metabolism has been translated to other studies stating obese and/or insulin resistant adults have intrinsic deficiencies resulting in dysfunctional mitochondrial fat oxidation (122-124). Several mechanisms associated with these lipid-derived metabolites on insulin resistance have been postulated, such as; 1) increased mitochondrial-derived oxidative stress (125, 126), 2) increased redox balance (125, 127), 3) endoplasmic reticulum (ER) stress (128, 129), and 4) upregulation of pro-inflammatory transcription factors linked to insulin resistance JNK, IKK-β, NF-κB, and PKC translation (121, 130). Additionally, acylcarnitine chain-length may also be associated with insulin resistance, as HFD Zucker rats showed excessive accumulation of long-chain acylcarnitine [>10C] (119). In humans, long-chain acylcarnitine accumulation has also been implicated to associate with insulin resistance, in which insulin resistant men had greater acylcarnitine accumulation as opposed to more insulin sensitive women (131). However, this notion has been challenged, where others have suggest acylcarnitine is simply a byproduct of inability to adapt to increasing fatty acid supply, and not dysfunction in the mitochondria per se (132). The insulin-sensitizing effects of exercise have also been shown to occur by decreasing acylcarnitine accumulation, where exercise reverses the over accumulation of acyl-CoA and acylcarnitine caused by increasing TCA flux for energy production (133). It is still unclear if acylcarnitines directly affects insulin signaling, as individuals with mutations in long chain acyl-CoA dehydrogenase have elevated acylcarnitines, yet normal glucose tolerance (134). Whether acylcarnitines and/or long chain acyl-CoA directly impairs insulin signaling is still questioned, as the accumulation of these lipids may simply be an 'index' of energy surplus derived from adipose tissue, and their direct effect on insulin signaling is still unclear.

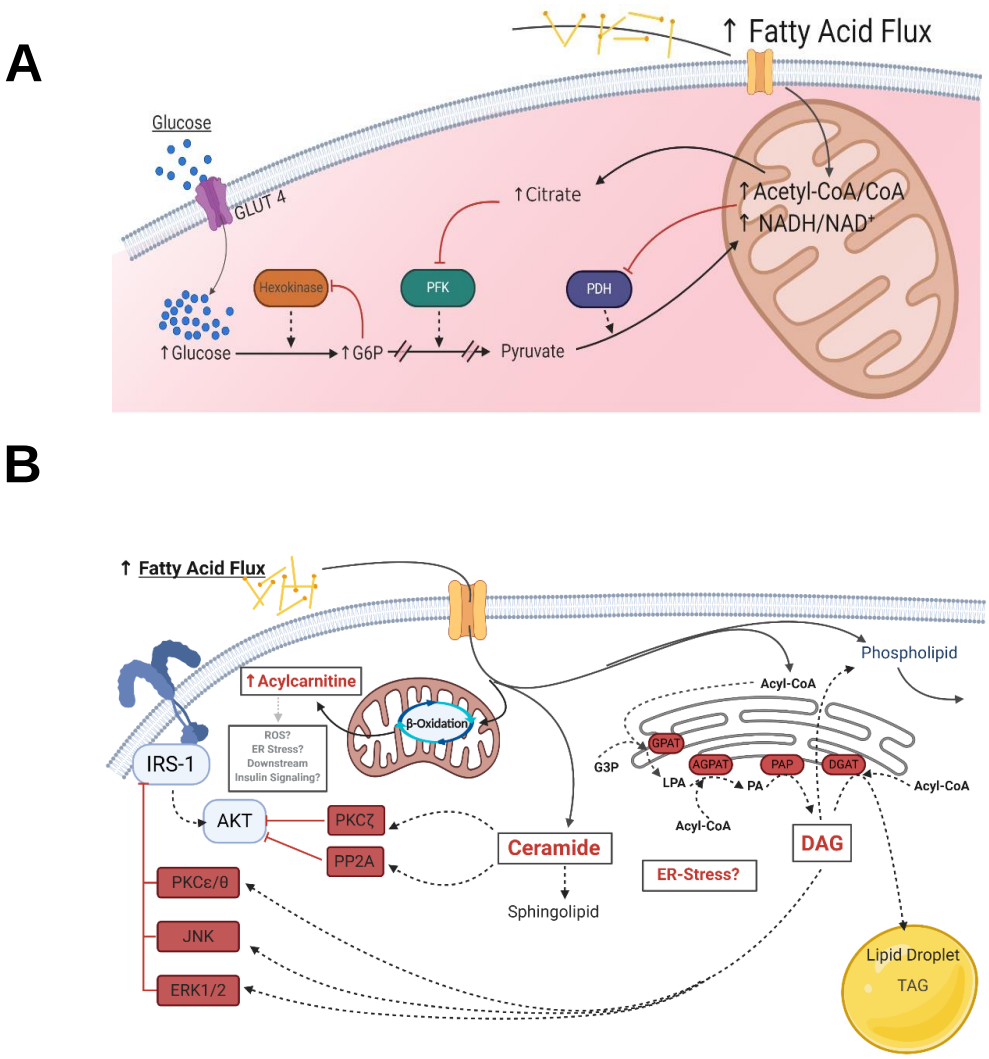

Figure II-6: Proposed mechanisms by which lipid accumulation in skeletal muscle negatively affects insulin sensitivity.

A) The glucose-fatty acid cycle (Randle Cycle) impairs glucose oxidation by direct competition with fatty acids. B) Pathways by which lipid-induced insulin resistance is caused by DAG, ceramide, and acylcarnitine accumulation.

A Unique Relationship between CD36 and Insulin-Stimulated Glucose Uptake

Fatty acid translocase, commonly known as CD36, is a well-known membrane glycoprotein associated with long-chain fatty acid transport into the cell, aimed to increase fatty acid availability and oxidation (135, 136). CD36 is translocated from the cytosol to the plasma membrane in

response to both insulin and muscle contraction to increase fatty acid transport and energy availability (137, 138). The physiological importance of this protein in skeletal muscle was first found in mice containing either CD36 overexpression or CD36 deletion. Mice overexpressing CD36 had greater fatty acid oxidation during contraction presumably due to greater translocation capacity compared to wild-type mice. Conversely, mice depleted of CD36 impaired fatty acid uptake and oxidation due to impaired transport capacity (139). However, our understanding about the role of CD36 has expanded beyond fatty acid transport, and is also found to be a key protein regulating both fatty acid and glucose metabolism (136, 140-142). In a series of unique *in vitro* studies, Samovski et al. found CD36 not only be a key regulator of fatty acid uptake, but also regulates glucose metabolism through insulin action in skeletal muscle (141). Particularly, the authors showed skeletal muscle specific CD36 knockout mice had lower insulin-stimulated glucose uptake compared to wild-type mice. Furthermore, using an in vitro model of skeletal muscle myocytes, CD36 knockout myocytes had lower insulin-stimulated IR phosphorylation at Tyr^{100}, lower recruitment of p85 (regulatory subunit of PI3K) to the insulin receptor, and lower AKT phosphorylation at Ser^{473}. However, when these myocytes were cultured in high saturated fatty acid media, palmitic acid (C16:0) decreased glucose uptake, and lower glucose uptake was explained by Fyn kinase dissociation from CD36 (Figure II-7A, II-7B). The interaction between CD36, IR, and Fyn kinase are attractive, as humans with genetic CD36 variations are also associated high HOMA-IR (insulin resistance) and T2DM (143). Perhaps in the context of obesity, these studies represent an important, yet unacknowledged mechanism underlying insulin resistance caused by excessive fatty acid availability in skeletal muscle. This relationship demonstrated previously brings forward an exciting new theory into new and novel relationships associated with insulin signaling through the insulin receptor in skeletal muscle. Importantly, it is very clear high lipolytic rates are strongly associated with impaired insulin mediated glucose uptake in vivo, and the signal regulated by CD36 appears to be an attractive model in to address *in vivo*. In summary, to address the topics reviewed in this section, Project 1 and 2 aimed to identify the association between lipolytic control from adipose tissue, skeletal muscle lipid profile, and insulin-mediated glucose uptake from skeletal muscle in insulin resistant and insulin sensitive obese adults. Additionally, mechanisms regulating insulin signaling through CD36 interaction with Fyn and IR were identified from both basal and insulin-mediated muscle samples from obese subjects with wide-ranging insulin sensitivity and rates of lipolysis.

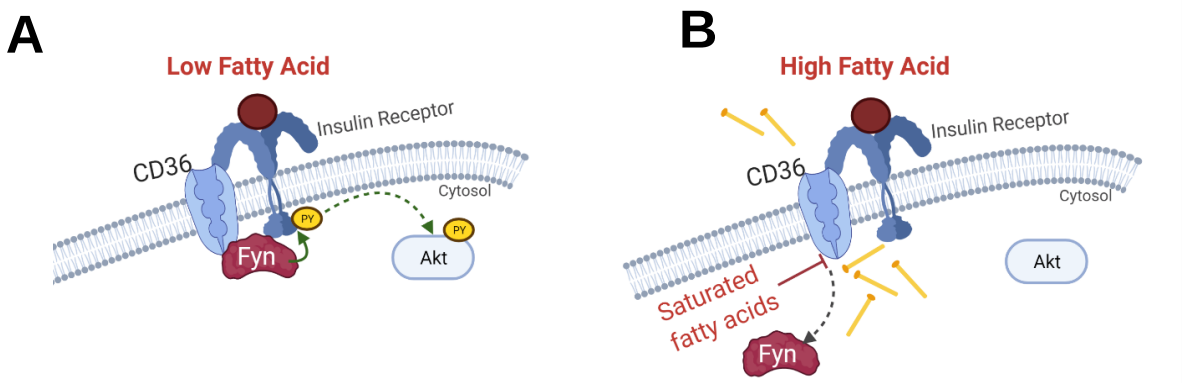

Figure II-7: Proposed mechanism by which CD36 regulates insulin action in skeletal muscle

A) Response to low fatty acid availability. B) Response to high fatty acid availability **(141).**

III - Factors Protecting Obese Adults from Developing Insulin Resistance – An Adipose-Centric View

Adipose tissue was once considered a passive tissue of energy storage, but is now known to be a central regulator in whole-body energy homeostasis and metabolism (144, 145). Adipose tissue is the central organ for lipid storage, and responds to energy surplus via; 1) adipose expansion (hypertrophy) - permitting lipid uptake and storage into preexisting adipocytes, and 2) preadipocyte proliferation (hyperplasia) - converting dedicated precursor cells into new adipocytes (i.e., adipogenesis) (146, 147). Unfortunately, hypertrophic adipocytes are normal in obesity, and the point when adipocytes expand to their 'threshold' (via hypertrophy) is when greater rates of fatty acid mobilization and ectopic lipid accumulation likely occurs due to limited expansion capability. (148, 149). However, adipose tissue may expand in a 'healthy' context, and it is speculated having a high adipogenic capacity to accommodate hypertrophic expansion may increase the potential by which more lipid can be stored in adipocytes without excessive flux into the circulation. Structural features in adipose tissue have been considered as one of the underlying factors associated with 'healthy' adipose tissue expansion, and a mechanism by which obese adults are protected from developing insulin resistance caused by high rates of fatty acid mobilization. These structural features associated with healthy adipose tissue include; 1) greater oxygen demand/delivery capacity (angiogenesis) (150), 2) extracellular matrix (ECM) remodeling to increase adipose plasticity and limit fibrosis (151), and 3) proliferation of new adipocytes into

more abundant (smaller-sized) adipocytes (146, 147). Additionally, the inflammatory environment in adipose tissue may also influence metabolic health in obese adults by regulating the secretion of pro-inflammatory cytokines (e.g., IL-1β, TNF-α, IL-6) (152), which have lipolytic influence on the adipose tissue (153). This section will review adipose storage capacity, and mechanisms by which 'healthy' adipose tissue maintains lipid influx and storage, preventing ectopic lipid storage and poor metabolic health outcomes due to maintenance of low fatty acid mobilization (Figure II-8).

In obesity, ectopic lipid accumulation stems from an imbalance between fatty acids released from adipose tissue over its storage capacity. The metabolic regulation of fatty acid hydrolysis from lipids stored as triglycerides in adipose tissue is through lipolysis (as described in SECTION I). The importance of limiting lipolysis was shown by Santomauro et al., who found a single overnight acipimox administration (a potent antilipolytic drug) lowered plasma fatty acids ~60%, but importantly, acipimox administration improved insulin sensitivity using both hyperinsulinemic-euglycemic clamp and oral glucose tolerance test (154). As explained previously, lipolysis involves the coordination between HSL and ATGL activation to regulate TAG hydrolysis from lipid droplets, and is heavily regulated by β-adrenergic signaling (pro-lipolytic), and insulin (anti-lipolytic). Our lab found maintaining lower rates of basal fatty acid mobilization from adipose tissue are 'protective' against insulin resistance in obese adults, and lower fatty acid mobilization rates were associated with lower HSL activation at Ser^{660} and p44/42 MAPK activation at Thr^{202}/Tyr^{204} in adipose tissue (155). Alternatively, reduced ability to suppress the anti-lipolytic effect of insulin may have a profound effect on fatty acid mobilization throughout the entire day. This relationship between insulin sensitivity in adipose tissue and insulin-mediated glucose uptake in skeletal muscle has been well documented (156), and lipolytic rate is typically greater in T2DM compared with obese nondiabetics (157). Additionally, adipose tissue insulin resistance (measured by fasting plasma free fatty acid and fasting insulin) directly associated along the glucose tolerance spectrum (from groups of normal glucose tolerance, impaired glucose tolerance, and T2DM) determined by oral glucose tolerance test (158). However, in human clinical studies it is difficult to conclude if adipose tissue insulin resistance precedes impairments in insulin-mediated glucose uptake in skeletal muscle, or if insulin resistance in skeletal muscle and adipose tissue are occurring in parallel.

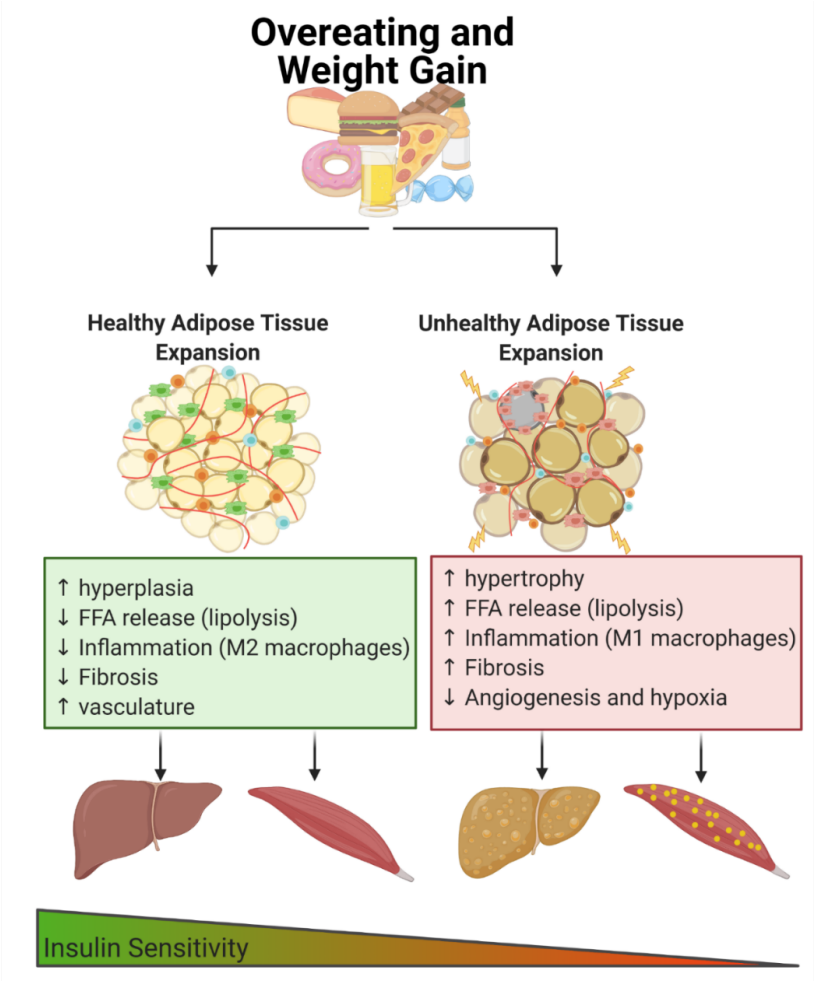

Figure II-8: Factors associated with 'metabolically healthy' adipose tissue expansion.

Healthy adipose expansion is associated with an anti-inflammatory, lower fibrosis development in the extracellular matrix, and adequate vascularization supports the metabolic needs of the cell. Redrawn from Kusminski et al. (159).

The influence of subcutaneous versus visceral adipose tissue depots on metabolic health in humans has been of interest due to the association between visceral fat mass and insulin resistance (160). Visceral adipose tissue has generally been associated with insulin resistance due to its lipolytic influence, however, only a small portion of circulating fatty acids stem from visceral adipose tissue, and the majority originating from subcutaneous tissue (161). Nielsen et al., found about 90% of circulating fatty acids are released from subcutaneous adipose tissue, and of these circulating fatty acids derived from subcutaneous adipose tissue, ~70% are derived from the abdominal region (161). These data demonstrate the contributing importance of subcutaneous

adipose tissue in the control of fatty acid mobilization, and the influence of subcutaneous adipose tissue controlling lipid deposition in non-adipose organs (skeletal muscle and liver). Therefore, excess visceral adiposity likely represents a marker of the relative inability for subcutaneous adipose tissue to act as an 'energy sink' when in energy surplus, and not considerably contributing to fatty acid induced insulin resistance.

Enhanced capacity for triglyceride synthesis (i.e., esterification) in adipose tissue may also contribute to attenuating fatty acid mobilization, which may help protect against insulin resistance. Human studies using deuterated water to track long-term turnover and storage of TAG found that net TAG synthesis and storage are significantly greater in insulin sensitive compared to insulin resistant obese adults (162). Therefore, increasing the capacity to store TAG in adipocytes likely prevents excessive fatty acids from entering the circulation and transported into non-adipose tissues. The regulation of triglyceride storage in adipose tissue is dependent on fatty acid transport into the cell (via fatty-acid translocase/CD36), and esterification enzymes glycerol-3-phosphate acyltransferase (GPAT) and diacylglycerol acyltransferase (DGAT). GPAT 1/2 (localized to mitochondria) and GPAT 3/4 (localized to ER) catalyze the first step in triglyceride synthesis, by synthesizing acyl-CoA to the glycerol-3-phosphate backbone (163, 164). In addition, DGAT 1/2 controls the final step in triglyceride synthesis by esterifying fatty acyl-CoA & DAG to TAG (98, 165). Our lab recently found GPAT1 protein abundance was greater in adults with lower fatty acid mobilization rates, suggesting a greater ability to esterify fatty acids into triglyceride and protect from excessive release (166). However, GPAT activity was not measured. Overall, it is important to consider how the rates of lipolysis, fatty acid transport, and esterification impact the rate of fatty acid mobilization from adipose tissue, and the subsequent influence on insulin resistance in skeletal muscle.

'Healthy' adipose tissue expansion should accommodate excessive lipid supply into adipocytes without adverse inflammatory and/or lipolytic consequence. One way to expand the adipose tissue pool is by differentiating new adipocytes derived from adipocyte precursors. Adipogenesis is the process involving the differentiation of adipose precursor cells (i.e., preadipocytes), and adipogenesis is proposed to be important at maintaining metabolic health of the adipocyte. As adipocytes expand (hypertrophy) during period of weight gain, the increased mechanical and hypoxic stress at the adipocyte contributes to elevated lipolysis (148), inflammation, and ECM deposition with the adipose depot (167). Alternatively, enhanced capacity

to make new fats cells through adipogenesis will be important to alleviate the burden caused by abnormally hypertrophic adipocytes. In addition, clinical studies suggest small adipocytes (although a surrogate measure of adipogenesis) may prevent insulin resistance (168-170), and lowered T2D incidence (171).

The commitment of adipogenesis occurs when precursor cells (expressing platelet-derived growth factor α [PDGFRα]) are restricted to the adipocyte lineage and unable to form into other cells (e.g., myoblasts, osteoblasts, and fibroblasts). The most prominent nuclear receptor regulating adipogenesis is peroxisome proliferator-activated receptor gamma [PPARγ] (172). The importance of this nuclear receptor on metabolic health has been demonstrated in humans containing PPARγ mutations, who have lower body fat, but are insulin resistant due to impaired proliferation of new fat cells (173). Downstream of PPARγ, is the activation of CCAAT/enhancer-binding protein α (C/EBPα), in which the interaction between these two proteins are important for committing to differentiated adipocytes (174). Additionally, extracellular signals have been reported to activate preadipocyte differentiation such as insulin, glucocorticoids, bone morphogenetic proteins (BMPs) (147), and can be suppressed through WNT (175) and Hedgehog (176) signaling ligands. The prominence of single-cell RNA sequencing has also suggested stromal cells containing $CD142^{+}$ sub-populations within this fraction, appear to exert anti-adipogenic effects on cells within the same adipose depot (177). Attempts to connect adipogenesis in clinic studies have been sparse and contain mixed results and interpretations. McLaughlin et al. found insulin resistant obese adults to have a greater proportion of small adipose cells (20-50 μm), and decreased expression of adipogenic genes (PPARγ1, PPARγ2, GLUT4). Their data suggested that an inability to recruit populations of mature adipocytes (>50 μm, that appear larger and differentiated) were underlying the development of insulin resistance in obese adults (168). Additionally, metabolically healthy obese women had greater proportion of preadipocytes (identified as CD34+), which suggests a greater differentiation potential was underlying the progression of metabolic syndrome (178). The previously mentioned studies have attempted to profile adipogenesis capacity by indirect measurements from adipose tissue (such as static protein and gene expression). However, studies directly measuring adipogenesis by the deuterated water ($_2H_2O$) incorporation into adipose tissue DNA (4 weeks after ingestion) found no difference between insulin resistant and insulin sensitive adults (162). Using the same $_2H_2O$ labeling technique, White et al. challenged the 'adipose tissue expandability' hypothesis by completing

$_2H_2O$ labeling for 8 weeks, and found new adipocyte formation was negatively associated with insulin sensitivity (179). Therefore, these data suggested a higher abundance of small adipocytes (newly formed in the insulin resistant population) was still associated with a decreased capacity to store lipid as opposed to subjects who had fewer adipocytes proliferating into adipocytes, but were larger with greater storage capacity. Despite mixed results, it is still intriguing to consider adipose tissue expandability through adipogenesis as a key factor protecting obese adults from metabolic dysregulation. However, clinical studies linking the formation of new adipocytes to metabolic health are still unresolved.

In obesity, there is a connection between white adipose tissue fibrosis and insulin resistance. Minimizing fibrosis in the adipose tissue is thought to allow for more effective adipocyte expansion when in energy surplus (159, 180, 181). To maintain healthy adipose tissue expansion, remodeling of the extracellular matrix (ECM) must occur to accommodate nutrient excess by improving expansion capacity. However, obesity is also associated with chronic low-grade inflammation, in which ECM accumulation and fibrosis occurs, and represents a physical constraint to adipose tissue expansion (182, 183). The ECM is composed of collagens (I, III, IV, V, and VI) and adhesion proteins (fibronectin, elastin, laminin, integrin and proteoglycan) necessary for tissue structure, cell adhesion, differentiation, and signal transduction processes (184). With respect to adipose tissue plasticity and expansion, collagen VI abundance has been profiled to directly associate with insulin resistance due to ECM fibrosis, and inability to expand adipocytes, which postulates the potential for lower collagen VI abundance as a protective factor against insulin resistance in obese adults. The relationship between collagen VI and insulin resistance has been demonstrated in collagen VI-null ob/ob mice, where adipose tissue mass expansion was not inhibited in these mice, allowing lipid to accumulate in adipose tissue without restriction (185). Importantly, this increased adiposity was associated with lower local inflammation and insulin resistance compared to collagen VI–expressing ob/ob mice (185). Data from our lab also found collagen VI mRNA abundance directly correlated with basal rate of lipolysis (155), and others have also reported associations between collagen VI abundance and inflammation/macrophage activation (186, 187). Interestingly, modifiers of ECM formation may underlie fibrosis in adipose tissue. The balance between matrix metalloproteinases (MMPs), a collagenase responsible for degrading ECM collagens, and tissue inhibitor of metalloproteinase (TIMP) may be critical regulators underlying ECM formation in obese adipose tissue as well (188).

However, in human adipose tissue, MMP9 was positively associated with insulin resistance and BMI, but MMP-9 accumulation in insulin resistant adults was speculated to be an effect of greater inflammation in adipose tissue, as MMP-9 is also abundant in macrophages (189, 190). Therefore, to interpret the adipose tissue specific effect of MMPs on fibrosis, it is warranted to separate the mature adipocyte and stromal vascular fraction. It is important to note adipose tissue inflammation also promotes ECM formation, and the specific signals affecting adipose tissue progenitor cell differentiation towards a fibrogenic cell program is still poorly understood (181). Whether ECM is a direct contributor to the development of insulin resistance, or secondary to inflammatory and/or mechanical stress in adipocytes remains questioned. Therefore, assessing both inflammatory and ECM mediators of fibrosis in conjunction will be fundamental to developing treatment for obesity-related conditions.

Obesity is often associated with chronic low-grade inflammation, consisting of macrophage infiltration and immune cell activation, which produce and secretes pro-inflammatory cytokines to affect both local and systemic metabolism (152, 191-193). Understanding the influence of immune cells in adipose tissue are very important, as macrophages are the most abundant immune cell in adipose tissue, consisting of ~40% of the entire cell population within the stromal vascular fraction in obese adults (152). Inflammatory triggers associated with obesity are still incomplete, however, obesity-induced adipose tissue remodeling likely initiates pro-inflammatory responses from intrinsic signals [e.g., adipocyte death, hypoxia, and mechanical stress] (194). The macrophage profile switch in obesity is associated with a transition from an anti-inflammatory (M2) to pro-inflammatory (M1) profile (152, 195), resulting in over-accumulation of local and systemic cytokines such as TNFα, IL-6, IL-8, IL-1β, C-reactive protein, and monocyte chemoattractant protein-1 (MCP-1) (196). Additionally, excessive accumulation of the aforementioned cytokines have also been shown to impair both systemic and local insulin signaling by activating toll-like receptors, inhibitor of κB kinases (IKKBs), nuclear factor κB (NF-κB), and c-JUN N-terminal kinases (JNK) pathways (197). Of the pro-inflammatory cytokines, TNFα has been linked to systemic insulin resistance, and is upregulated in obesity, where it is secreted from pro-inflammatory macrophages originating in adipose tissue (198). Importantly, TNFα impairs local and systemic insulin signaling by phosphorylating IRS1 in the adipocyte, suggesting a role to impair lipolysis suppression in the fed state, and insulin signaling in non-adipose tissues (191). In studies assessing inflammatory differences in insulin sensitive versus

insulin resistant obese adults, the insulin sensitive obese adults had lower abundance of thrombospondine-1, pro-inflammatory mediator of TGF-β1 (199, 200), and $CD4^+$ T cells (Th17 and Th22), known to produce pro-inflammatory cytokines in adipose tissue (201). Greater expression of inflammation-related genes (e.g., CD68, EMR1, IL8, IL6 and MCP/CCL2) were also reported in insulin resistant compared to insulin sensitive obese adults (202). However, it is important to note complete removal of inflammation is also deleterious to metabolic health, and inflammation should be considered as an adaptive response to promote safe nutrient and lipid storage (203, 204). Understanding mechanisms responsible for adipose tissue inflammation in obesity has important therapeutic potential, and minimizing chronic low-grade inflammation is likely a factor by which obese adults are 'protected' from insulin resistance.

Adipose tissue is also recognized as an active endocrine organ, secreting a number of adipocyte-derived secretory factors (i.e., adipokines) altering metabolic function in other organs. The most abundant secreted factor, adiponectin (Acrp30), is of potential interest as a factor 'protecting' obese adults from insulin resistance, as it has been directly associated with insulin sensitivity in obese men and women (205), and more abundant in the circulation of metabolically healthy obese adults (206-208). Many mechanisms of action by adiponectin have been proposed, but not confirmed. The insulin sensitizing mechanism of adiponectin has been found in transgenic adiponectin overexpressing ob/ob mice that remained glucose tolerant despite dramatic weight gain. Holland et al. found ceramidase enzyme activity is increased by adiponectin, converting ceramides to sphingosine-1-phosphate at a greater rate, and away from the harmful effects of ceramide on insulin signaling (209). Recently, Li et al. showed 2 weeks adiponectin treatment increased insulin-stimulated glucose uptake in mice by lowering ectopic lipid deposition, and thus, membrane-associated DAG, which diminished PKCθ and PKCε activity in skeletal muscle (210). Many other studies identifying the therapeutic effect of adiponectin have found this adipokine to increase β-oxidation and suppress lipid accumulation in liver (211), suppress of gluconeogenesis (212), stimulate AMPK activity (213), and even promote adipogenesis (214). If adiponectin functions in paracrine fashion, then perhaps its release from adipose tissue signals its native tissue to upregulate lipid storage, as it is inversely associated with fat mass. In the case of 'metabolically healthy' obesity, adiponectin secretion may promote fatty acid transport and synthesis back into adipose tissue of healthy obese adults, while metabolically unhealthy adults who have expanded their adipose tissue storage capacity signal for limited adiponectin release, diminishing fatty acid

uptake into adipose tissue, and cause further ectopic lipid deposition (210). The previously mentioned preclinical and in vitro models show adiponectin potential as a therapeutic target against obesity-induced insulin resistance despite the absence of a clear clinical model for adiponectin's action *in vivo*. In summary, Project 1 of my dissertation identified specific factors from adipose tissue (listed in SECTION III) that may be differing between insulin resistant and insulin sensitive obese adults. Adipose tissue samples from two groups of varying insulin resistant versus metabolically healthy cohorts were compared by us histological, and untargeted proteomics to speculate underlying factors that may be associated with high lipolytic rate in obese adults, and thus, insulin resistance.

IV - Exercise Protects Against Lipid-Induced Insulin Resistance – Role of Lipid Storage

Exercise is often prescribed as a first-line approach for treating obesity-related complications including insulin resistance (215-218), and the beneficial effects of metabolic fitness are associated with lower incidence of cardiovascular disease (219), and T2DM (220). Notably, lifestyle interventions involving both exercise and weight loss have been found to be very successful at preventing T2DM onset for at-risk adults, and were even more effective than the most commonly prescribed anti-diabetic medication (12, 13). However, research demonstrating the profound impact of exercise training on insulin sensitivity remains equivocal, as the effect of weight loss and timing from the most recent exercise session obscures our ability to assess the direct effect of exercise training on metabolic health independent from the most recent exercise session (221, 222). Therefore, the effect of exercise independent of weight loss, and the timing of exercise with respect to the acute effects (transient) compared with long-term effect stemming from the adaptive response to training are not completely understood. Although the effect of exercise on metabolic health is well known, its impact on insulin sensitivity are likely transient, persisting only ~24-72 hours after an exercise session (223-228). Project 3 of my dissertation identified the effect of exercise training and timing on skeletal muscle metabolism in the context of lipid handling into intramyocellular LDs. Additionally, because the timing of exercise plays an influential role in insulin sensitivity, I will review the acute (post-exercise) effects and chronic (training) effects of exercise on intramyocellular triglyceride (IMTG) regulation within LDs.

Fatty acids are largely stored as IMTG in skeletal muscle, and are an important energy source during exercise (229-231). Therefore, after a moderate/vigorous exercise session (<80% VO_{2max}) there is often a transient reduction in intramyocellular lipid (IMCL) abundance (which are largely stored as IMTG), ranging from ~20-70% decrease after a bout of exercise (232-234). IMTG are stored within LDs in skeletal muscle, where the distribution of LDs and properties (i.e., size, and protein composition) within skeletal muscle may be important in the regulation of lipolysis and fatty acid availability for mitochondrial respiration during exercise, and may prevent from lipotoxicity in muscle. To support the notion LD distribution may remodel to promote fatty acid availability for subsequent exercise bouts, our lab found even a single exercise session stimulates IMTG synthesis after an overnight lipid infusion, which in turn is an important mediator against the lipotoxic accumulation of lipid intermediates such as DAG and ceramide (24). Importantly, properties of the LD in skeletal muscle includes; 1) LD membrane composition, 2) LD size, 3) LD density, and 4) LD localization to metabolically impactful organelles such as the membrane and mitochondria (Figure II-9A and II-9B). These LD characteristics may play a unique role not only regulating fatty acid availability and oxidation during exercise, but as an underlying factor to prevent insulin resistance by improving the capacity for inert IMTG storage. Fortunately, advancements in microscopy enable more in-depth assessments of the previously described factors (LD size and location) within the myocyte (235). The adaptive restructuring of LDs after a session of exercise to improve fatty acid availability may be a protective mechanism by which exercise training protects against insulin resistance in obese adults (236, 237).

The assembly of LDs are initiated in endoplasmic reticulum (ER), in which several steps occur to synthesize TAG and sterol esters (e.g., cholesterol esters) into the LD organelle [Figure II-10] (165). The first step of TAG synthesis is the esterification of acyl-CoA to glycerol-3-phosphate regulated by GPAT family of proteins, and diacylglycerol acyltransferases regulated by DGAT 1/2. When neutral TAG are esterified, they are dispersed between the leaflets of the ER bilayer. As neutral lipid continues to accumulate, a neutral lipid lens is formed, causing LD budding from the ER bilayer towards the cytosol. As LD growth continues, the ER membrane supplies the growth of the phospholipid monolayer (largely composed phosphatidylcholine and phosphatidylethanolamine). Additionally, LD membrane proteins that are assembled in the ER become localized to the LD, which includes enzymes to support TAG biosynthesis (GPAT4 and

DGAT2), and proteins to translocate LDs to support metabolic function of organelles within the cell (165).

Of the proteins that coat LD membranes, perilipins have been the most commonly characterized LD membrane protein (238) – with PLIN2 and PLIN5 the most abundant within skeletal muscle (239, 240). These PLIN proteins may be an important determinant of fuel utilization in the myocyte. Whytock et al. demonstrated PLIN5+ LDs were lower after exercise due to a preferential co-localization between PLIN5 and HSL to increase lipolytic activity during exercise (241). Additionally, other studies found an acute exercise session increased contact between LD and mitochondria, and speculated to increase contact sent from signals initiated by mitochondrial respiration (242, 243). Interestingly, the relationship between LD-mitochondrial contacts have been found to demonstrate not only a relationship by which fatty acid utilization from the LD is improved. Also, LD-mitochondrial contact has been shown to promote LD-expansion in vitro (244). Although the mechanism between LD-mitochondrial contact to promote LD expansion is still unclear, it is speculative to consider a potential relationship by which LD expansion occurs post-exercise by a mitochondrial contact site. With response to the localization of LDs after an acute exercise session, some studies found a single exercise session decreased LD abundance in the intramyofibrillar region (IMF: towards the middle of the myocyte), but not the subsarcolemmal region (SS: around the periphery) (245, 246).

LD remodeling after exercise training stems from the summation of repeated exercise bouts, and LDs in skeletal muscle are thought to expand in effort to enhance fatty acid turnover and oxidation. As noted above, the day after each exercise session, there is often a greater flux of fatty acids towards IMTG storage, resulting in expanded IMTG pool following exercise. In fact, IMCL expansion occurs in as little as 2 weeks of exercise training, contributing as an early response, perhaps as an adaptation to accommodate the energy demand during prolonged exercise (232). Interestingly, IMTG are also commonly found to be elevated in insulin resistant obese adults and T2DM adults. The observation that IMTG are also high in insulin sensitive athletes has been described as the 'athlete's paradox'. Exercise training has been found to increase total LD volume by increasing LD number (# LDs per μm^2) as opposed to size of LDs per se (242, 247, 248). The increase in LD number (and not size) may be adaptive response to increase LD surface area to volume ratio, allowing for rapid mobilization and turnover of fatty acids stored as IMTG in LDs (242, 247, 248). Aerobic training was found to increase IMF LD number (249), and reduce

SS LDs (236, 250). The localization of LDs may therefore explain the divergence in insulin sensitivity in athletes versus T2DM adults despite having similar IMTG abundance. The relationship between LD localization and insulin sensitivity are unique, as studies measuring the relationship between the LD environment and insulin sensitivity found a greater proportion of LDs in the SS region of Type II fibers in T2DM adults (250), and SS LD accumulation was also associated with insulin resistance (237, 245, 251). For clinical relevance, Koh et al. found 11 weeks high-intensity interval training (HIIT) decreased SS LD abundance and not IMF LD abundance (250). This relationship is important to note as IMF mitochondria were previously found to associate with a more oxidative mitochondria as opposed to SS mitochondria (249). Additionally, the redistribution of lipids from the SS to the IMF regions may be an underlying factor for greater fat oxidation potential following exercise training, and shunting of LDs away from the membrane where key insulin signaling proteins (e.g., insulin receptor) are located.

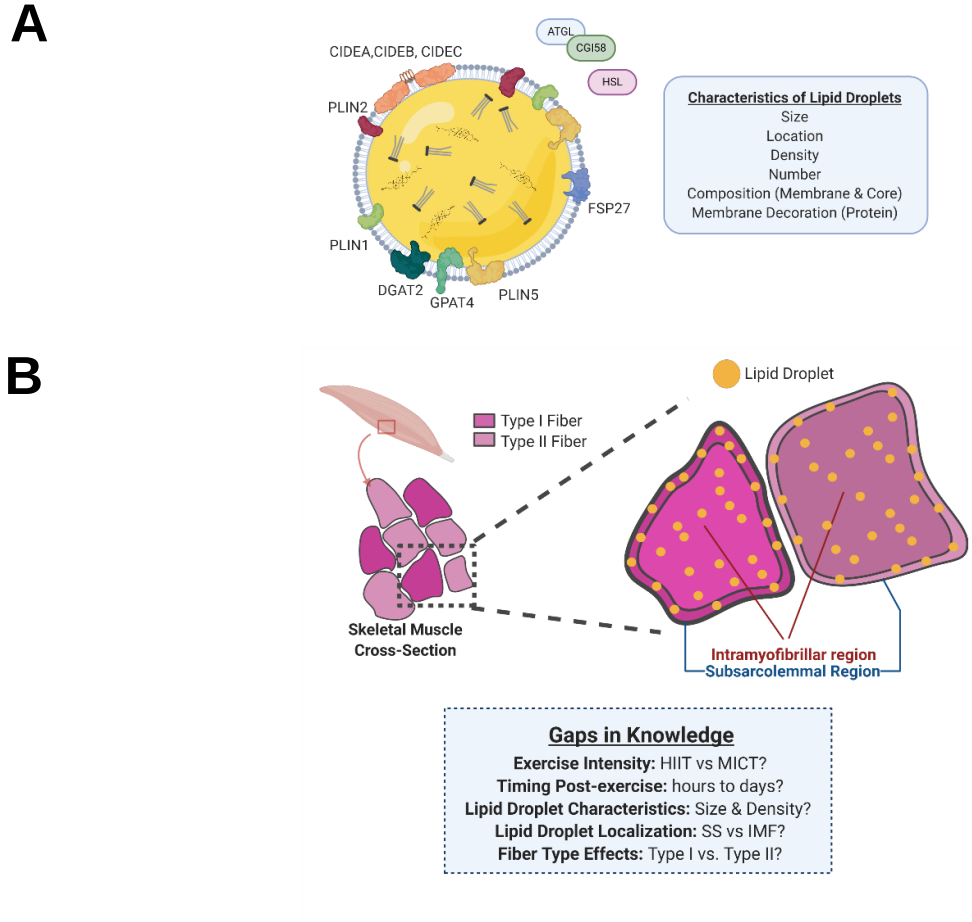

Figure II-9: Lipid droplet organization and distribution within skeletal muscle.

A) Characteristics of LDs. LDs are stored as TAG rich organelles ranging in size from ~0.2-1.4 μm^2, and contain a hydrophobic core surrounded by a phospholipid monolayer comprising hundreds of proteins regulating structure and function **(98)**. B) Representation of skeletal muscle LD distribution and gaps in knowledge pertaining to exercise intensity and timing on lipid droplet distribution.

LD size and number are regulated by both TAG synthesis (anabolism) and degradation (catabolism). As described previously, the synthesis of TAG into LDs are largely governed by GPAT and DGAT proteins. However, the LD pool is dynamic – and the LD pool turns over via cycling through processes of synthesis and degradation. Contrary to LD synthesis, and when in a state of energy deficit, lipolysis occurs to provide mitochondria fatty acid substrates for β-oxidation through lipolytic mechanisms regulated by ATGL and HSL (described in SECTION I). However, a relatively unexplored mechanism of LD degradation in skeletal muscle is through the autophagic degradation of intracellular LDs (lipophagy), and a less-appreciated means that may regulate energy balance in the cell through bulk transport of fatty acids, and also LD remodeling

(252, 253). LDs break down by 'lipophagy' as an adaptive mechanism to increase nutrient availability for the next bout of nutrient deficiency (253). There are many possible mechanisms by which nutrient deprivation can increase lipophagy, and has been thought to be regulated by AMPK and mTOR balance through their independent regulation on autophagy-related proteins (254). Lysosomes, once thought to be an organelle responsible degrading and recycling cellular waste from organelles, also has implications to secrete essential proteins and lipids to other regions of the cell, influencing signaling and energy metabolism (255). Lysosome mediated lipophagy was first introduced in 2009 in hepatocytes (256). The first study elucidating the regulation of lipophagy was by Singh et al., who found; i) inhibition of autophagy increased hepatic triglyceride and LD content, and lowered triglyceride breakdown, ii) LD structural proteins co-localize with a key regulator of chaperone-mediated autophagy – light chain protein 3 (LC3), 3) intracellular lipid accumulation decreased autophagy (lower LD-LAMP1 co-localization), and 4) LDs directly fuse with LC3+ autophagasomes (256). Other studies have revealed LC3 and LAMP2 (lysosomal marker) are important regulators in lipophagy by demonstrating the following; 1) LC3 directly interacts with ATGL at the LD (257), and 2) removing lysosomal-associated membrane protein 2 (LAMP2A, an important regulator mediator in autophagy at the lysosome) leads to LD accumulation (258). It is well-known autophagy is regulated by the Atg class of proteins (Atg1, Atg5, and Atg7), which are downstream of key metabolic sensors mTOR and AMPK. Therefore, it is hypothetical these regulatory proteins are responsible for lipophagy in some extent, given their influence in metabolism and energy balance. It has not been tested if exercise increases mechanisms for lipid breakdown and re-distribution through lipophagy, but plausible due to the energy deficit and glycogen depletion caused from each exercise bout. The molecular mechanisms by which lipophagy is regulated is far from understood, and major questions have not been answered such as lipid recruitment, signals promoting lipophagy, and the benefits of bulk fatty acid appearance via lipophagy as opposed to controlled mechanisms lipolysis. However, it is attractive to consider LD remodeling following an exercise bout may produce favorable insulin responsiveness, in which lipophagy is an underlying factor to aid in LD redistribution. In summary, Project 3 of my dissertation tested; 1) The effect of exercise training (both acute and chronic effects) on LD characteristics (LD size and number), LD distribution (IMF versus SS), and fiber-type specific abundance, and 2) the effect of exercise training (both acute and chronic

effects) on LD biogenesis by co-localization with the ER and LD degradation by co-localization with the autophagasome.

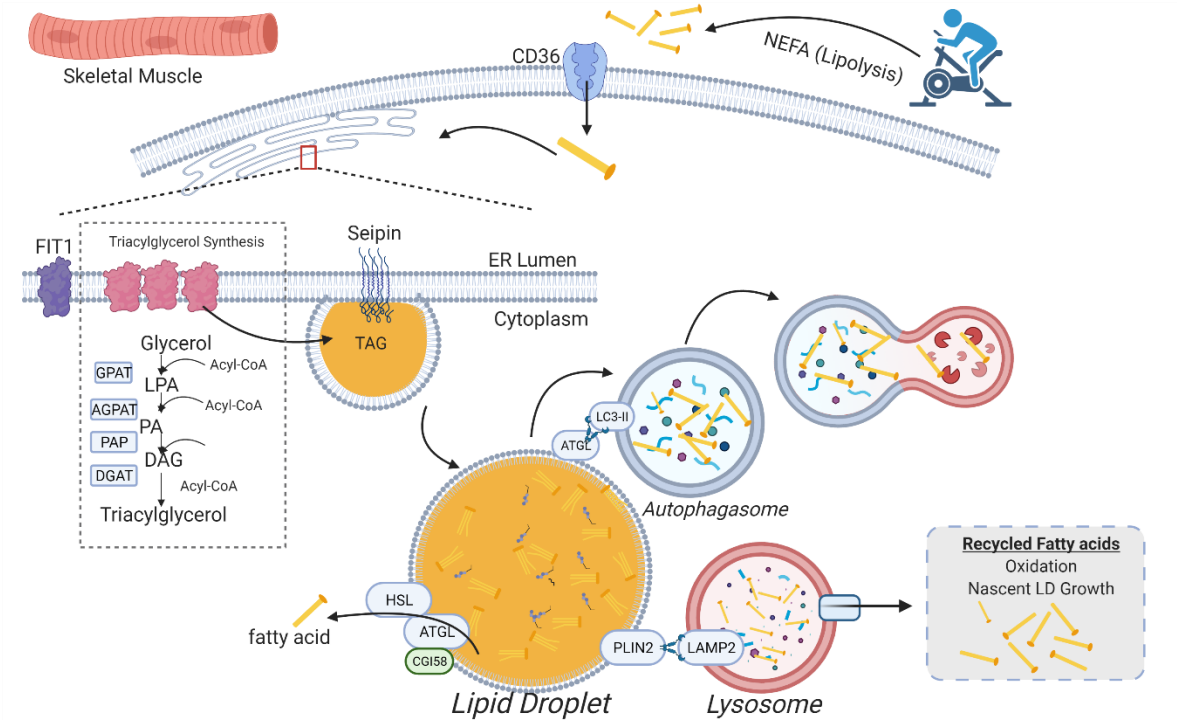

Figure II-10: Overview of lipid droplet biogenesis and degradation by autophagy.

De novo LD biogenesis ocurrs at the endoplasmic reticulum, while degradation by chaperone mediated autophagy ('lipophagy') occurs by lysosomal degradation. Lipophagy has been speculated to occur by interaction with the autophagasome marker, LC3, and ATGL, as well as PLIN2 directly interaction with the lysosome (LAMP2).

SUMMARY

Adipose tissue expands with weight gain by increasing TAG storage within adipocytes. However, the capacity for adipose tissue to store TAG are often exceeded, contributing to free fatty acid spillover, and ectopic lipid deposition. As a result of inadequate fatty acid storage in adipose tissue, the accumulation of these ectopic lipids are associated with insulin resistance and cardio-metabolic disease.

Upon obesity, adipose tissue must remodel in effort to sustain TAG storage. The specific factors associated with adipose tissue remodeling is dependent upon increasing the number of adipocytes (adipogenesis), improving blood flow (angiogenesis), limit ECM fibrosis in effort to promote adequate expansion, and limiting excess immune cell infiltration. The consequence of impaired adipose tissue remodeling results in greater fatty acid availability to ectopic tissues such as skeletal muscle, and causes lipid infiltration known to modify insulin signaling and glucose uptake into skeletal muscle.

Each exercise session triggers and adaptive response modify lipid handling in the myocyte in effort to increase fatty acid availability for mitochondrial respiration. Fortunately, the insulin sensitizing effect of exercise may be attributing to modifications in lipid storage within LDs, and limit the influence of cellular lipotoxicity in the myocyte. To this end, exercise is likely a beneficial prescription to improve metabolic health for those who are insulin resistant as a result of improper adipose tissue remodeling.

REFERENCES

1. Hales CM, Carroll MD, Fryar CD, and Ogden CL. Prevalence of obesity and severe obesity among adults: United States, 2017–2018. 2020.
2. Poirier P, Giles TD, Bray GA, Hong Y, Stern JS, Pi-Sunyer FX, et al. Obesity and cardiovascular disease: pathophysiology, evaluation, and effect of weight loss: an update of the 1997 American Heart Association Scientific Statement on Obesity and Heart Disease from the Obesity Committee of the Council on Nutrition, Physical Activity, and Metabolism. *Circulation.* 2006;113(6):898-918.
3. Eckel RH, and Krauss RM. American Heart Association Call to Action: Obesity as a Major Risk Factor for Coronary Heart Disease. 1998;97(21):2099-100.
4. Nguyen NT, Nguyen X-MT, Lane J, and Wang P. Relationship between obesity and diabetes in a US adult population: findings from the National Health and Nutrition Examination Survey, 1999-2006. *Obes Surg.* 2011;21(3):351-5.
5. Bhaskaran K, Douglas I, Forbes H, dos-Santos-Silva I, Leon DA, and Smeeth L. Body-mass index and risk of 22 specific cancers: a population-based cohort study of 5·24 million UK adults. *The Lancet.* 2014;384(9945):755-65.
6. López-Suárez A. Burden of cancer attributable to obesity, type 2 diabetes and associated risk factors. *Metabolism.* 2019;92:136-46.
7. Lega IC, and Lipscombe LL. Review: Diabetes, Obesity, and Cancer—Pathophysiology and Clinical Implications. *Endocrine Reviews.* 2019;41(1):33-52.
8. Kang Z, Luo S, Gui Y, Zhou H, Zhang Z, Tian C, et al. Obesity is a potential risk factor contributing to clinical manifestations of COVID-19. *International Journal of Obesity.* 2020.
9. Simonnet A, Chetboun M, Poissy J, Raverdy V, Noulette J, Duhamel A, et al. High Prevalence of Obesity in Severe Acute Respiratory Syndrome Coronavirus-2 (SARS-CoV-2) Requiring Invasive Mechanical Ventilation. 2020;28(7):1195-9.
10. Biener A, Cawley J, and Meyerhoefer C. The Impact of Obesity on Medical Care Costs and Labor Market Outcomes in the US. *Clinical Chemistry.* 2018;64(1):108-17.
11. Dee A, Kearns K, O'Neill C, Sharp L, Staines A, O'Dwyer V, et al. The direct and indirect costs of both overweight and obesity: a systematic review. *BMC research notes.* 2014;7:242.
12. Lindström J, Louheranta A, Mannelin M, Rastas M, Salminen V, Eriksson J, et al. The Finnish Diabetes Prevention Study (DPS). *Lifestyle intervention and 3-year results on diet and physical activity.* 2003;26(12):3230-6.
13. Knowler W, Barrett-Connor E, Fowler S, Hamman R, Lachin J, Walker E, et al. Reduction in the Incidence of Type 2 Diabetes with Lifestyle Intervention or Metformin. 2002;346(6):393-403.
14. Kraschnewski JL, Boan J, Esposito J, Sherwood NE, Lehman EB, Kephart DK, et al. Long-term weight loss maintenance in the United States. *Int J Obes (Lond).* 2010;34(11):1644-54.

15. Reaven GM. Banting lecture 1988. Role of insulin resistance in human disease. *Diabetes.* 1988;37(12):1595-607.

16. Kahn SE, Hull RL, and Utzschneider KM. Mechanisms linking obesity to insulin resistance and type 2 diabetes. *Nature.* 2006;444(7121):840-6.

17. Smith GI, Mittendorfer B, and Klein S. Metabolically healthy obesity: facts and fantasies. *J Clin Invest.* 2019;129(10):3978-89.

18. Hamer M, and Stamatakis E. Metabolically healthy obesity and risk of all-cause and cardiovascular disease mortality. *The Journal of clinical endocrinology and metabolism.* 2012;97(7):2482-8.

19. Wildman RP, Muntner P, Reynolds K, McGinn AP, Rajpathak S, Wylie-Rosett J, et al. The Obese Without Cardiometabolic Risk Factor Clustering and the Normal Weight With Cardiometabolic Risk Factor Clustering: Prevalence and Correlates of 2 Phenotypes Among the US Population (NHANES 1999-2004). *Archives of Internal Medicine.* 2008;168(15):1617-24.

20. Abbasi F, Brown BW, Lamendola C, McLaughlin T, and Reaven GM. Relationship between obesity, insulin resistance, and coronary heart disease risk. *Journal of the American College of Cardiology.* 2002;40(5):937-43.

21. Calori G, Lattuada G, Piemonti L, Garancini MP, Ragogna F, Villa M, et al. Prevalence, metabolic features, and prognosis of metabolically healthy obese Italian individuals: the Cremona Study. *Diabetes Care.* 2011;34(1):210-5.

22. Stefan N, Kantartzis K, Machann J, Schick F, Thamer C, Rittig K, et al. Identification and characterization of metabolically benign obesity in humans. *Arch Intern Med.* 2008;168(15):1609-16.

23. Dvorak RV, DeNino WF, Ades PA, and Poehlman ET. Phenotypic characteristics associated with insulin resistance in metabolically obese but normal-weight young women. *Diabetes.* 1999;48(11):2210-4.

24. Schenk S, and Horowitz JF. Acute exercise increases triglyceride synthesis in skeletal muscle and prevents fatty acid–induced insulin resistance. *J Clin Invest.* 2007;117(6):1690-8.

25. Karnieli E, Zarnowski MJ, Hissin PJ, Simpson IA, Salans LB, and Cushman SW. Insulin-stimulated translocation of glucose transport systems in the isolated rat adipose cell. Time course, reversal, insulin concentration dependency, and relationship to glucose transport activity. *The Journal of biological chemistry.* 1981;256(10):4772-7.

26. Klip A, Ramlal T, Young DA, and Holloszy JO. Insulin-induced translocation of glucose transporters in rat hindlimb muscles. *FEBS letters.* 1987;224(1):224-30.

27. James DE, Brown R, Navarro J, and Pilch PF. Insulin-regulatable tissues express a unique insulin-sensitive glucose transport protein. *Nature.* 1988;333(6169):183-5.

28. Ren JM, Marshall BA, Gulve EA, Gao J, Johnson DW, Holloszy JO, et al. Evidence from transgenic mice that glucose transport is rate-limiting for glycogen deposition and glycolysis in skeletal muscle. *The Journal of biological chemistry.* 1993;268(22):16113-5.

29. Song JD, Alves TC, Befroy DE, Perry RJ, Mason GF, Zhang X-M, et al. Dissociation of Muscle Insulin Resistance from Alterations in Mitochondrial Substrate Preference. *Cell Metabolism.* 2020;32(5):726-35.e5.

30. Lee J, Pilch PF, Shoelson SE, and Scarlata SF. Conformational Changes of the Insulin Receptor upon Insulin Binding and Activation As Monitored by Fluorescence Spectroscopy. *Biochemistry.* 1997;36(9):2701-8.

31. Cohen P. The twentieth century struggle to decipher insulin signalling. *Nature Reviews Molecular Cell Biology.* 2006;7(11):867-73.

32. Taniguchi CM, Emanuelli B, and Kahn CR. Critical nodes in signalling pathways: insights into insulin action. *Nature Reviews Molecular Cell Biology.* 2006;7(2):85-96.

33. Huang C, Thirone AC, Huang X, and Klip A. Differential contribution of insulin receptor substrates 1 versus 2 to insulin signaling and glucose uptake in l6 myotubes. *The Journal of biological chemistry.* 2005;280(19):19426-35.

34. Esposito DL, Li Y, Cama A, and Quon MJ. Tyr(612) and Tyr(632) in human insulin receptor substrate-1 are important for full activation of insulin-stimulated phosphatidylinositol 3-kinase activity and translocation of GLUT4 in adipose cells. *Endocrinology.* 2001;142(7):2833-40.

35. Rameh LE, and Cantley LC. The role of phosphoinositide 3-kinase lipid products in cell function. *The Journal of biological chemistry.* 1999;274(13):8347-50.

36. Guertin DA, Stevens DM, Thoreen CC, Burds AA, Kalaany NY, Moffat J, et al. Ablation in mice of the mTORC components raptor, rictor, or mLST8 reveals that mTORC2 is required for signaling to Akt-FOXO and PKCalpha, but not S6K1. *Developmental cell.* 2006;11(6):859-71.

37. Leto D, and Saltiel AR. Regulation of glucose transport by insulin: traffic control of GLUT4. *Nature Reviews Molecular Cell Biology.* 2012;13(6):383-96.

38. Sun Y, Bilan PJ, Liu Z, and Klip A. Rab8A and Rab13 are activated by insulin and regulate GLUT4 translocation in muscle cells. 2010;107(46):19909-14.

39. Klip A, Sun Y, Chiu TT, and Foley KP. Signal transduction meets vesicle traffic: the software and hardware of GLUT4 translocation. 2014;306(10):C879-C86.

40. Manning BD, and Toker A. AKT/PKB Signaling: Navigating the Network. *Cell.* 2017;169(3):381-405.

41. Holm C. Molecular mechanisms regulating hormone-sensitive lipase and lipolysis. *Biochemical Society Transactions.* 2003;31(6):1120-4.

42. Granneman JG, Moore H-PH, Krishnamoorthy R, and Rathod M. Perilipin controls lipolysis by regulating the interactions of AB-hydrolase containing 5 (Abhd5) and adipose triglyceride lipase (Atgl). *The Journal of biological chemistry.* 2009;284(50):34538-44.

43. Zimmermann R, Strauss JG, Haemmerle G, Schoiswohl G, Birner-Gruenberger R, Riederer M, et al. Fat Mobilization in Adipose Tissue Is Promoted by Adipose Triglyceride Lipase. *Science.* 2004;306(5700):1383.

44. Yang X, Lu X, Lombès M, Rha GB, Chi YI, Guerin TM, et al. The G(0)/G(1) switch gene 2 regulates adipose lipolysis through association with adipose triglyceride lipase. *Cell Metab.* 2010;11(3):194-205.

45. Duncan RE, Ahmadian M, Jaworski K, Sarkadi-Nagy E, and Sul HS. Regulation of Lipolysis in Adipocytes. 2007;27(1):79-101.

46. Jaworski K, Sarkadi-Nagy E, Duncan RE, Ahmadian M, and Sul HS. Regulation of Triglyceride Metabolism.IV. Hormonal regulation of lipolysis in adipose tissue. 2007;293(1):G1-G4.

47. Choi YH, Park S, Hockman S, Zmuda-Trzebiatowska E, Svennelid F, Haluzik M, et al. Alterations in regulation of energy homeostasis in cyclic nucleotide phosphodiesterase 3B-null mice. *J Clin Invest.* 2006;116(12):3240-51.

48. Kitamura T, Kitamura Y, Kuroda S, Hino Y, Ando M, Kotani K, et al. Insulin-induced phosphorylation and activation of cyclic nucleotide phosphodiesterase 3B by the serine-threonine kinase Akt. *Mol Cell Biol.* 1999;19(9):6286-96.

49. DiPilato LM, Ahmad F, Harms M, Seale P, Manganiello V, and Birnbaum MJ. The Role of PDE3B Phosphorylation in the Inhibition of Lipolysis by Insulin. *Mol Cell Biol.* 2015;35(16):2752-60.

50. DeFronzo RA, Jacot E, Jequier E, Maeder E, Wahren J, and Felber JP. The Effect of Insulin on the Disposal of Intravenous Glucose: Results from Indirect Calorimetry and Hepatic and Femoral Venous Catheterization. 1981;30(12):1000-7.

51. Herman MA, Peroni OD, Villoria J, Schön MR, Abumrad NA, Blüher M, et al. A novel ChREBP isoform in adipose tissue regulates systemic glucose metabolism. *Nature.* 2012;484(7394):333-8.

52. Samuel VT, Liu Z-X, Qu X, Elder BD, Bilz S, Befroy D, et al. Mechanism of Hepatic Insulin Resistance in Non-alcoholic Fatty Liver Disease. 2004;279(31):32345-53.

53. Samuel VT, and Shulman GI. The pathogenesis of insulin resistance: integrating signaling pathways and substrate flux. *J Clin Invest.* 2016;126(1):12-22.

54. Chen W, Balland E, and Cowley MA. Hypothalamic Insulin Resistance in Obesity: Effects on Glucose Homeostasis. *Neuroendocrinology.* 2017;104(4):364-81.

55. Vogt MC, and Brüning JC. CNS insulin signaling in the control of energy homeostasis and glucose metabolism - from embryo to old age. *Trends in endocrinology and metabolism: TEM.* 2013;24(2):76-84.

56. Wasserman DH, Wang TJ, and Brown NJ. The Vasculature in Prediabetes. 2018;122(8):1135-50.

57. Cohen P. The origins of protein phosphorylation. *Nature Cell Biology.* 2002;4(5):E127-E30.

58. Hunter T. Protein kinases and phosphatases: The Yin and Yang of protein phosphorylation and signaling. *Cell.* 1995;80(2):225-36.

59. Cusi K, Maezono K, Osman A, Pendergrass M, Patti ME, Pratipanawatr T, et al. Insulin resistance differentially affects the PI 3-kinase- and MAP kinase-mediated signaling in human muscle. *J Clin Invest.* 2000;105(3):311-20.

60. Kruszynska YT, Worrall DS, Ofrecio J, Frias JP, Macaraeg G, and Olefsky JM. Fatty Acid-Induced Insulin Resistance: Decreased Muscle PI3K Activation But Unchanged Akt Phosphorylation. *The Journal of Clinical Endocrinology & Metabolism.* 2002;87(1):226-34.

61. Tonks KT, Ng Y, Miller S, Coster ACF, Samocha-Bonet D, Iseli TJ, et al. Impaired Akt phosphorylation in insulin-resistant human muscle is accompanied by selective and heterogeneous downstream defects. *Diabetologia.* 2013;56(4):875-85.

62. Zierath JR, He L, Gumà A, Odegoard Wahlström E, Klip A, and Wallberg-Henriksson H. Insulin action on glucose transport and plasma membrane GLUT4 content in skeletal muscle from patients with NIDDM. *Diabetologia.* 1996;39(10):1180-9.

63. Humphrey Sean J, Yang G, Yang P, Fazakerley Daniel J, Stöckli J, Yang Jean Y, et al. Dynamic Adipocyte Phosphoproteome Reveals that Akt Directly Regulates mTORC2. *Cell Metabolism.* 2013;17(6):1009-20.

64. Olsen JV, Blagoev B, Gnad F, Macek B, Kumar C, Mortensen P, et al. Global, in vivo, and site-specific phosphorylation dynamics in signaling networks. *Cell.* 2006;127(3):635-48.

65. Olsen JV, and Mann M. Status of large-scale analysis of post-translational modifications by mass spectrometry. *Molecular & cellular proteomics : MCP.* 2013;12(12):3444-52.

66. Sharma K, D'Souza Rochelle CJ, Tyanova S, Schaab C, Wiśniewski Jacek R, Cox J, et al. Ultradeep Human Phosphoproteome Reveals a Distinct Regulatory Nature of Tyr and Ser/Thr-Based Signaling. *Cell Reports.* 2014;8(5):1583-94.

67. Hornbeck PV, Kornhauser JM, Tkachev S, Zhang B, Skrzypek E, Murray B, et al. PhosphoSitePlus: a comprehensive resource for investigating the structure and function of experimentally determined post-translational modifications in man and mouse. *Nucleic acids research.* 2012;40(Database issue):D261-70.

68. Rudolph JD, de Graauw M, van de Water B, Geiger T, and Sharan R. Elucidation of Signaling Pathways from Large-Scale Phosphoproteomic Data Using Protein Interaction Networks. *Cell Systems.* 2016;3(6):585-93.e3.

69. Needham EJ, Parker BL, Burykin T, James DE, and Humphrey SJ. Illuminating the dark phosphoproteome. 2019;12(565):eaau8645.

70. Humphrey SJ, James DE, and Mann M. Protein Phosphorylation: A Major Switch Mechanism for Metabolic Regulation. *Trends in Endocrinology & Metabolism.* 2015;26(12):676-87.

71. Dajani R, Fraser E, Roe SM, Young N, Good V, Dale TC, et al. Crystal structure of glycogen synthase kinase 3 beta: structural basis for phosphate-primed substrate specificity and autoinhibition. *Cell.* 2001;105(6):721-32.

72. Treebak JT, Taylor EB, Witczak CA, An D, Toyoda T, Koh HJ, et al. Identification of a novel phosphorylation site on TBC1D4 regulated by AMP-activated protein kinase in skeletal muscle. *American journal of physiology Cell physiology.* 2010;298(2):C377-85.

73. Thong FS, Bilan PJ, and Klip A. The Rab GTPase-activating protein AS160 integrates Akt, protein kinase C, and AMP-activated protein kinase signals regulating GLUT4 traffic. *Diabetes.* 2007;56(2):414-23.

74. Kim J, Kundu M, Viollet B, and Guan K-L. AMPK and mTOR regulate autophagy through direct phosphorylation of Ulk1. *Nature Cell Biology.* 2011;13(2):132-41.

75. Um SH, Frigerio F, Watanabe M, Picard F, Joaquin M, Sticker M, et al. Absence of S6K1 protects against age- and diet-induced obesity while enhancing insulin sensitivity. *Nature.* 2004;431(7005):200-5.

76. Maegawa H, Ide R, Hasegawa M, Ugi S, Egawa K, Iwanishi M, et al. Thiazolidine derivatives ameliorate high glucose-induced insulin resistance via the normalization of protein-tyrosine phosphatase activities. *The Journal of biological chemistry.* 1995;270(13):7724-30.

77. Ugi S, Imamura T, Maegawa H, Egawa K, Yoshizaki T, Shi K, et al. Protein Phosphatase 2A Negatively Regulates Insulin's Metabolic Signaling Pathway by Inhibiting Akt (Protein Kinase B) Activity in 3T3-L1 Adipocytes. 2004;24(19):8778-89.

78. Shulman GI. Ectopic Fat in Insulin Resistance, Dyslipidemia, and Cardiometabolic Disease. *New England Journal of Medicine.* 2014;371(12):1131-41.

79. DeFronzo RA, and Tripathy D. Skeletal Muscle Insulin Resistance Is the Primary Defect in Type 2 Diabetes. 2009;32(suppl 2):S157-S63.

80. Randle PJ, Garland PB, Hales CN, and Newsholme EA. The glucose fatty-acid cycle. Its role in insulin sensitivity and the metabolic disturbances of diabetes mellitus. *Lancet (London, England).* 1963;1(7285):785-9.

81. Shulman GI. Cellular mechanisms of insulin resistance. *J Clin Invest.* 2000;106(2):171-6.

82. Roden M, Price TB, Perseghin G, Petersen KF, Rothman DL, Cline GW, et al. Mechanism of free fatty acid-induced insulin resistance in humans. *J Clin Invest.* 1996;97(12):2859-65.

83. Dresner A, Laurent D, Marcucci M, Griffin ME, Dufour S, Cline GW, et al. Effects of free fatty acids on glucose transport and IRS-1-associated phosphatidylinositol 3-kinase activity. *J Clin Invest.* 1999;103(2):253-9.

84. Griffin ME, Marcucci MJ, Cline GW, Bell K, Barucci N, Lee D, et al. Free fatty acid-induced insulin resistance is associated with activation of protein kinase C theta and alterations in the insulin signaling cascade. *Diabetes.* 1999;48(6):1270-4.

85. Heydrick SJ, Ruderman NB, Kurowski TG, Adams HB, and Chen KS. Enhanced Stimulation of Diacylglycerol and Lipid Synthesis by Insulin in Denervated Muscle: Altered Protein Kinase C Activity and Possible Link to Insulin Resistance. 1991;40(12):1707-11.

86. Yu C, Chen Y, Cline GW, Zhang D, Zong H, Wang Y, et al. Mechanism by which fatty acids inhibit insulin activation of insulin receptor substrate-1 (IRS-1)-associated phosphatidylinositol 3-kinase activity in muscle. *The Journal of biological chemistry.* 2002;277(52):50230-6.

87. Schmitz-Peiffer C, Browne CL, Oakes ND, Watkinson A, Chisholm DJ, Kraegen EW, et al. Alterations in the Expression and Cellular Localization of Protein Kinase C Isozymes ε and θ Are Associated With Insulin Resistance in Skeletal Muscle of the High-Fat–Fed Rat. 1997;46(2):169-78.

88. Kellerer M, Mushack J, Seffer E, Mischak H, Ullrich A, and Häring HU. Protein kinase C isoforms α, δ and θ require insulin receptor substrate-1 to inhibit the tyrosine kinase activity of the insulin receptor in human kidney embryonic cells (HEK 293 cells). *Diabetologia.* 1998;41(7):833-8.

89. Morino K, Petersen KF, and Shulman GI. Molecular Mechanisms of Insulin Resistance in Humans and Their Potential Links With Mitochondrial Dysfunction. 2006;55(Supplement 2):S9-S15.

90. Kim JK, Fillmore JJ, Sunshine MJ, Albrecht B, Higashimori T, Kim D-W, et al. PKC-θ knockout mice are protected from fat-induced insulin resistance. *J Clin Invest.* 2004;114(6):823-7.

91. Morino K, Neschen S, Bilz S, Sono S, Tsirigotis D, Reznick RM, et al. Muscle-Specific IRS-1 Ser→Ala Transgenic Mice Are Protected From Fat-Induced Insulin Resistance in Skeletal Muscle. 2008;57(10):2644-51.

92. Samuel VT, Liu ZX, Wang A, Beddow SA, Geisler JG, Kahn M, et al. Inhibition of protein kinase Cepsilon prevents hepatic insulin resistance in nonalcoholic fatty liver disease. *J Clin Invest.* 2007;117(3):739-45.

93. Liu L, Zhang Y, Chen N, Shi X, Tsang B, and Yu Y-H. Upregulation of myocellular DGAT1 augments triglyceride synthesis in skeletal muscle and protects against fat-induced insulin resistance. *J Clin Invest.* 2007;117(6):1679-89.

94. Coen PM, Hames KC, Leachman EM, DeLany JP, Ritov VB, Menshikova EV, et al. Reduced skeletal muscle oxidative capacity and elevated ceramide but not diacylglycerol content in severe obesity. *Obesity (Silver Spring, Md).* 2013;21(11):2362-71.

95. Zhang C, Klett EL, and Coleman RA. Lipid signals and insulin resistance. *Clin Lipidol.* 2013;8(6):659-67.

96. Bergman BC, Hunerdosse DM, Kerege A, Playdon MC, and Perreault L. Localisation and composition of skeletal muscle diacylglycerol predicts insulin resistance in humans. *Diabetologia.* 2012;55(4):1140-50.

97. Perreault L, Newsom SA, Strauss A, Kerege A, Kahn DE, Harrison KA, et al. Intracellular localization of diacylglycerols and sphingolipids influences insulin sensitivity and mitochondrial function in human skeletal muscle. *JCI Insight.* 2018;3(3):e96805.

98. Walther TC, and Farese RV, Jr. Lipid droplets and cellular lipid metabolism. *Annual review of biochemistry.* 2012;81:687-714.

99. Pan DA, Lillioja S, Kriketos AD, Milner MR, Baur LA, Bogardus C, et al. Skeletal muscle triglyceride levels are inversely related to insulin action. *Diabetes.* 1997;46(6):983-8.

100. Perseghin G, Scifo P, De Cobelli F, Pagliato E, Battezzati A, Arcelloni C, et al. Intramyocellular triglyceride content is a determinant of in vivo insulin resistance in

humans: a 1H-13C nuclear magnetic resonance spectroscopy assessment in offspring of type 2 diabetic parents. 1999;48(8):1600-6.

101. Phillips DI, Caddy S, Ilic V, Fielding BA, Frayn KN, Borthwick AC, et al. Intramuscular triglyceride and muscle insulin sensitivity: evidence for a relationship in nondiabetic subjects. *Metabolism.* 1996;45(8):947-50.

102. Manco M, Mingrone G, Greco AV, Capristo E, Gniuli D, De Gaetano A, et al. Insulin resistance directly correlates with increased saturated fatty acids in skeletal muscle triglycerides. *Metabolism.* 2000;49(2):220-4.

103. Savage DB, Watson L, Carr K, Adams C, Brage S, Chatterjee KK, et al. Accumulation of saturated intramyocellular lipid is associated with insulin resistance. *Journal of lipid research.* 2019;60(7):1323-32.

104. Bergman BC, and Goodpaster BH. Exercise and Muscle Lipid Content, Composition, and Localization: Influence on Muscle Insulin Sensitivity. 2020;69(5):848-58.

105. Kahn D, Perreault L, Macias E, Zarini S, Newsom SA, Strauss A, et al. Subcellular localisation and composition of intramuscular triacylglycerol influence insulin sensitivity in humans. *Diabetologia.* 2020.

106. Holland WL, Brozinick JT, Wang L-P, Hawkins ED, Sargent KM, Liu Y, et al. Inhibition of Ceramide Synthesis Ameliorates Glucocorticoid-, Saturated-Fat-, and Obesity-Induced Insulin Resistance. *Cell Metabolism.* 2007;5(3):167-79.

107. Chavez Jose A, and Summers Scott A. A Ceramide-Centric View of Insulin Resistance. *Cell Metabolism.* 2012;15(5):585-94.

108. Adams JM, Pratipanawatr T, Berria R, Wang E, DeFronzo RA, Sullards MC, et al. Ceramide Content Is Increased in Skeletal Muscle From Obese Insulin-Resistant Humans. 2004;53(1):25-31.

109. Dobrowsky RT, Kamibayashi C, Mumby MC, and Hannun YA. Ceramide activates heterotrimeric protein phosphatase 2A. *The Journal of biological chemistry.* 1993;268(21):15523-30.

110. Powell DJ, Turban S, Gray A, Hajduch E, and Hundal HS. Intracellular ceramide synthesis and protein kinase Czeta activation play an essential role in palmitate-induced insulin resistance in rat L6 skeletal muscle cells. *The Biochemical journal.* 2004;382(Pt 2):619-29.

111. Amati F, Dubé JJ, Alvarez-Carnero E, Edreira MM, Chomentowski P, Coen PM, et al. Skeletal Muscle Triglycerides, Diacylglycerols, and Ceramides in Insulin Resistance. *Another Paradox in Endurance-Trained Athletes?* 2011;60(10):2588-97.

112. Bergman BC, Brozinick JT, Strauss A, Bacon S, Kerege A, Bui HH, et al. Muscle sphingolipids during rest and exercise: a C18:0 signature for insulin resistance in humans. *Diabetologia.* 2016;59(4):785-98.

113. Holland WL, Bikman BT, Wang L-P, Yuguang G, Sargent KM, Bulchand S, et al. Lipid-induced insulin resistance mediated by the proinflammatory receptor TLR4 requires saturated fatty acid–induced ceramide biosynthesis in mice. *J Clin Invest.* 2011;121(5):1858-70.

114. Haus JM, Kashyap SR, Kasumov T, Zhang R, Kelly KR, DeFronzo RA, et al. Plasma Ceramides Are Elevated in Obese Subjects With Type 2 Diabetes and Correlate With the Severity of Insulin Resistance. 2009;58(2):337-43.

115. Boon J, Hoy AJ, Stark R, Brown RD, Meex RC, Henstridge DC, et al. Ceramides Contained in LDL Are Elevated in Type 2 Diabetes and Promote Inflammation and Skeletal Muscle Insulin Resistance. 2013;62(2):401-10.

116. Skovbro M, Baranowski M, Skov-Jensen C, Flint A, Dela F, Gorski J, et al. Human skeletal muscle ceramide content is not a major factor in muscle insulin sensitivity. *Diabetologia.* 2008;51(7):1253-60.

117. Itani SI, Ruderman NB, Schmieder F, and Boden G. Lipid-Induced Insulin Resistance in Human Muscle Is Associated With Changes in Diacylglycerol, Protein Kinase C, and IκB-α. 2002;51(7):2005-11.

118. Petersen MC, and Jurczak MJ. CrossTalk opposing view: Intramyocellular ceramide accumulation does not modulate insulin resistance. 2016;594(12):3171-4.

119. Koves TR, Ussher JR, Noland RC, Slentz D, Mosedale M, Ilkayeva O, et al. Mitochondrial Overload and Incomplete Fatty Acid Oxidation Contribute to Skeletal Muscle Insulin Resistance. *Cell Metabolism.* 2008;7(1):45-56.

120. Ellis BA, Poynten A, Lowy AJ, Furler SM, Chisholm DJ, Kraegen EW, et al. Long-chain acyl-CoA esters as indicators of lipid metabolism and insulin sensitivity in rat and human muscle. 2000;279(3):E554-E60.

121. Muoio Deborah M, and Neufer PD. Lipid-Induced Mitochondrial Stress and Insulin Action in Muscle. *Cell Metabolism.* 2012;15(5):595-605.

122. Hulver MW, Berggren JR, Cortright RN, Dudek RW, Thompson RP, Pories WJ, et al. Skeletal muscle lipid metabolism with obesity. *Am J Physiol Endocrinol Metab.* 2003;284(4):E741-7.

123. Kim J-Y, Hickner RC, Cortright RL, Dohm GL, and Houmard JA. Lipid oxidation is reduced in obese human skeletal muscle. 2000;279(5):E1039-E44.

124. Kelley DE, He J, Menshikova EV, and Ritov VB. Dysfunction of Mitochondria in Human Skeletal Muscle in Type 2 Diabetes. *Diabetes.* 2002;51(10):2944.

125. Fisher-Wellman KH, and Neufer PD. Linking mitochondrial bioenergetics to insulin resistance via redox biology. *Trends in endocrinology and metabolism: TEM.* 2012;23(3):142-53.

126. Anderson EJ, Lustig ME, Boyle KE, Woodlief TL, Kane DA, Lin CT, et al. Mitochondrial H2O2 emission and cellular redox state link excess fat intake to insulin resistance in both rodents and humans. *J Clin Invest.* 2009;119(3):573-81.

127. Hoehn KL, Salmon AB, Hohnen-Behrens C, Turner N, Hoy AJ, Maghzal GJ, et al. Insulin resistance is a cellular antioxidant defense mechanism. 2009;106(42):17787-92.

128. Özcan U, Cao Q, Yilmaz E, Lee A-H, Iwakoshi NN, Özdelen E, et al. Endoplasmic Reticulum Stress Links Obesity, Insulin Action, and Type 2 Diabetes. 2004;306(5695):457-61.

129. Malhotra JD, and Kaufman RJ. Endoplasmic reticulum stress and oxidative stress: a vicious cycle or a double-edged sword? *Antioxidants & redox signaling.* 2007;9(12):2277-93.

130. Bloch-Damti A, and Bashan N. Proposed mechanisms for the induction of insulin resistance by oxidative stress. *Antioxidants & redox signaling.* 2005;7(11-12):1553-67.

131. Broussard JL, Perreault L, Macias E, Newsom SA, Harrison K, Bui HH, et al. Sex Differences in Insulin Sensitivity are Related to Muscle Tissue Acylcarnitine But Not Subcellular Lipid Distribution. *Obesity (Silver Spring, Md).* 2021;29(3):550-61.

132. Holloszy JO. "Deficiency" of Mitochondria in Muscle Does Not Cause Insulin Resistance. *Diabetes.* 2013;62(4):1036.

133. Koves TR, Li P, An J, Akimoto T, Slentz D, Ilkayeva O, et al. Peroxisome proliferator-activated receptor-gamma co-activator 1alpha-mediated metabolic remodeling of skeletal myocytes mimics exercise training and reverses lipid-induced mitochondrial inefficiency. *The Journal of biological chemistry.* 2005;280(39):33588-98.

134. Gillingham MB, Harding CO, Schoeller DA, Matern D, and Purnell JQ. Altered body composition and energy expenditure but normal glucose tolerance among humans with a long-chain fatty acid oxidation disorder. 2013;305(10):E1299-E308.

135. Abumrad NA, el-Maghrabi MR, Amri EZ, Lopez E, and Grimaldi PA. Cloning of a rat adipocyte membrane protein implicated in binding or transport of long-chain fatty acids that is induced during preadipocyte differentiation. Homology with human CD36. *The Journal of biological chemistry.* 1993;268(24):17665-8.

136. Pepino MY, Kuda O, Samovski D, and Abumrad NA. Structure-function of CD36 and importance of fatty acid signal transduction in fat metabolism. *Annual review of nutrition.* 2014;34:281-303.

137. Bradley NS, Snook LA, Jain SS, Heigenhauser GJF, Bonen A, and Spriet LL. Acute endurance exercise increases plasma membrane fatty acid transport proteins in rat and human skeletal muscle. 2012;302(2):E183-E9.

138. Luiken JJFP, Dyck DJ, Han X-X, Tandon NN, Arumugam Y, Glatz JFC, et al. Insulin induces the translocation of the fatty acid transporter FAT/CD36 to the plasma membrane. 2002;282(2):E491-E5.

139. Ibrahimi A, Bonen A, Blinn WD, Hajri T, Li X, Zhong K, et al. Muscle-specific overexpression of FAT/CD36 enhances fatty acid oxidation by contracting muscle, reduces plasma triglycerides and fatty acids, and increases plasma glucose and insulin. *The Journal of biological chemistry.* 1999;274(38):26761-6.

140. Samovski D, Sun J, Pietka T, Gross RW, Eckel RH, Su X, et al. Regulation of AMPK Activation by CD36 Links Fatty Acid Uptake to β-Oxidation. 2015;64(2):353-9.

141. Samovski D, Dhule P, Pietka T, Jacome-Sosa M, Penrose E, Son N-H, et al. Regulation of Insulin Receptor Pathway and Glucose Metabolism by CD36 Signaling. 2018;67(7):1272-84.

142. Sun S, Tan P, Huang X, Zhang W, Kong C, Ren F, et al. Ubiquitinated CD36 sustains insulin-stimulated Akt activation by stabilizing insulin receptor substrate 1 in myotubes. *Journal of Biological Chemistry.* 2018;293(7):2383-94.

143. Corpeleijn E, Van Der Kallen CJH, Kruijshoop M, Magagnin MGP, De Bruin TWA, Feskens EJM, et al. Direct association of a promoter polymorphism in the CD36/FAT fatty acid transporter gene with Type 2 diabetes mellitus and insulin resistance. 2006;23(8):907-11.

144. Zhang Y, Proenca R, Maffei M, Barone M, Leopold L, and Friedman JM. Positional cloning of the mouse obese gene and its human homologue. *Nature.* 1994;372(6505):425-32.

145. Rosen ED, and Spiegelman BM. Adipocytes as regulators of energy balance and glucose homeostasis. *Nature.* 2006;444(7121):847-53.

146. MacDougald OA, and Mandrup S. Adipogenesis: forces that tip the scales. *Trends in endocrinology and metabolism: TEM.* 2002;13(1):5-11.

147. Ghaben AL, and Scherer PE. Adipogenesis and metabolic health. *Nature Reviews Molecular Cell Biology.* 2019;20(4):242-58.

148. Laurencikiene J, Skurk T, Kulyté A, Hedén P, Åström G, Sjölin E, et al. Regulation of Lipolysis in Small and Large Fat Cells of the Same Subject. *The Journal of Clinical Endocrinology & Metabolism.* 2011;96(12):E2045-E9.

149. Mittendorfer B, Magkos F, Fabbrini E, Mohammed BS, and Klein S. Relationship between body fat mass and free fatty acid kinetics in men and women. *Obesity (Silver Spring, Md).* 2009;17(10):1872-7.

150. Corvera S, and Gealekman O. Adipose tissue angiogenesis: impact on obesity and type-2 diabetes. *Biochimica et biophysica acta.* 2014;1842(3):463-72.

151. Cao Y. Angiogenesis and vascular functions in modulation of obesity, adipose metabolism, and insulin sensitivity. *Cell Metab.* 2013;18(4):478-89.

152. Lumeng CN, Bodzin JL, and Saltiel AR. Obesity induces a phenotypic switch in adipose tissue macrophage polarization. *J Clin Invest.* 2007;117(1):175-84.

153. Langin D, and Arner P. Importance of TNFalpha and neutral lipases in human adipose tissue lipolysis. *Trends in endocrinology and metabolism: TEM.* 2006;17(8):314-20.

154. Santomauro AT, Boden G, Silva ME, Rocha DM, Santos RF, Ursich MJ, et al. Overnight lowering of free fatty acids with Acipimox improves insulin resistance and glucose tolerance in obese diabetic and nondiabetic subjects. *Diabetes.* 1999;48(9):1836-41.

155. Van Pelt DW, Guth LM, Wang AY, and Horowitz JF. Factors regulating subcutaneous adipose tissue storage, fibrosis, and inflammation may underlie low fatty acid mobilization in insulin-sensitive obese adults. 2017;313(4):E429-E39.

156. Magkos F, Fabbrini E, Conte C, Patterson BW, and Klein S. Relationship between Adipose Tissue Lipolytic Activity and Skeletal Muscle Insulin Resistance in Nondiabetic Women. *The Journal of Clinical Endocrinology & Metabolism.* 2012;97(7):E1219-E23.

157. Basu A, Basu R, Shah P, Vella A, Rizza RA, and Jensen MD. Systemic and regional free fatty acid metabolism in type 2 diabetes. 2001;280(6):E1000-E6.

158. Gastaldelli A, Gaggini M, and DeFronzo RA. Role of Adipose Tissue Insulin Resistance in the Natural History of Type 2 Diabetes: Results From the San Antonio Metabolism Study. 2017;66(4):815-22.

159. Kusminski CM, Bickel PE, and Scherer PE. Targeting adipose tissue in the treatment of obesity-associated diabetes. *Nature Reviews Drug Discovery.* 2016;15(9):639-60.

160. Ross R, Aru J, Freeman J, Hudson R, and Janssen I. Abdominal adiposity and insulin resistance in obese men. 2002;282(3):E657-E63.

161. Nielsen S, Guo Z, Johnson CM, Hensrud DD, and Jensen MD. Splanchnic lipolysis in human obesity. *J Clin Invest.* 2004;113(11):1582-8.

162. Allister CA, Liu LF, Lamendola CA, Craig CM, Cushman SW, Hellerstein MK, et al. In vivo 2H2O administration reveals impaired triglyceride storage in adipose tissue of insulin-resistant humans. *Journal of lipid research.* 2015;56(2):435-9.

163. Igal RA, Wang S, Gonzalez-Baró M, and Coleman RA. Mitochondrial Glycerol Phosphate Acyltransferase Directs the Incorporation of Exogenous Fatty Acids into Triacylglycerol. 2001;276(45):42205-12.

164. Cao J, Li JL, Li D, Tobin JF, and Gimeno RE. Molecular identification of microsomal acyl-CoA:glycerol-3-phosphate acyltransferase, a key enzyme in de novo triacylglycerol synthesis. *Proceedings of the National Academy of Sciences of the United States of America.* 2006;103(52):19695-700.

165. Olzmann JA, and Carvalho P. Dynamics and functions of lipid droplets. *Nature reviews Molecular cell biology.* 2019;20(3):137-55.

166. Pelt DWV, Guth LM, and Horowitz JF. Aerobic exercise elevates markers of angiogenesis and macrophage IL-6 gene expression in the subcutaneous adipose tissue of overweight-to-obese adults. 2017;123(5):1150-9.

167. Halberg N, Khan T, Trujillo ME, Wernstedt-Asterholm I, Attie AD, Sherwani S, et al. Hypoxia-inducible factor 1alpha induces fibrosis and insulin resistance in white adipose tissue. *Mol Cell Biol.* 2009;29(16):4467-83.

168. McLaughlin T, Sherman A, Tsao P, Gonzalez O, Yee G, Lamendola C, et al. Enhanced proportion of small adipose cells in insulin-resistant vs insulin-sensitive obese individuals implicates impaired adipogenesis. *Diabetologia.* 2007;50(8):1707-15.

169. Lundgren M, Svensson M, Lindmark S, Renström F, Ruge T, and Eriksson JW. Fat cell enlargement is an independent marker of insulin resistance and 'hyperleptinaemia'. *Diabetologia.* 2007;50(3):625-33.

170. Hammarstedt A, Graham TE, and Kahn BB. Adipose tissue dysregulation and reduced insulin sensitivity in non-obese individuals with enlarged abdominal adipose cells. *Diabetology & Metabolic Syndrome.* 2012;4(1):42.

171. Yang J, Eliasson B, Smith U, Cushman SW, and Sherman AS. The size of large adipose cells is a predictor of insulin resistance in first-degree relatives of type 2 diabetic patients. *Obesity (Silver Spring, Md).* 2012;20(5):932-8.

172. Tontonoz P, Hu E, and Spiegelman BM. Stimulation of adipogenesis in fibroblasts by PPAR gamma 2, a lipid-activated transcription factor. *Cell.* 1994;79(7):1147-56.

173. Barroso I, Gurnell M, Crowley VE, Agostini M, Schwabe JW, Soos MA, et al. Dominant negative mutations in human PPARgamma associated with severe insulin resistance, diabetes mellitus and hypertension. *Nature.* 1999;402(6764):880-3.

174. Wu Z, Rosen ED, Brun R, Hauser S, Adelmant G, Troy AE, et al. Cross-Regulation of C/EBPα and PPARγ Controls the Transcriptional Pathway of Adipogenesis and Insulin Sensitivity. *Molecular Cell.* 1999;3(2):151-8.

175. Ross SE, Hemati N, Longo KA, Bennett CN, Lucas PC, Erickson RL, et al. Inhibition of adipogenesis by Wnt signaling. *Science.* 2000;289(5481):950-3.

176. Suh JM, Gao X, McKay J, McKay R, Salo Z, and Graff JM. Hedgehog signaling plays a conserved role in inhibiting fat formation. *Cell Metab.* 2006;3(1):25-34.

177. Schwalie PC, Dong H, Zachara M, Russeil J, Alpern D, Akchiche N, et al. A stromal cell population that inhibits adipogenesis in mammalian fat depots. *Nature.* 2018;559(7712):103-8.

178. Park HT, Lee ES, Cheon YP, Lee DR, Yang KS, Kim YT, et al. The relationship between fat depot-specific preadipocyte differentiation and metabolic syndrome in obese women. *Clinical endocrinology.* 2012;76(1):59-66.

179. White UA, Fitch MD, Beyl RA, Hellerstein MK, and Ravussin E. Association of In Vivo Adipose Tissue Cellular Kinetics With Markers of Metabolic Health in Humans. *The Journal of clinical endocrinology and metabolism.* 2017;102(7):2171-8.

180. Sun K, Tordjman J, Clément K, and Scherer Philipp E. Fibrosis and Adipose Tissue Dysfunction. *Cell Metabolism.* 2013;18(4):470-7.

181. Marcelin G, Silveira ALM, Martins LB, Ferreira AVM, and Clément K. Deciphering the cellular interplays underlying obesity-induced adipose tissue fibrosis. *J Clin Invest.* 2019;129(10):4032-40.

182. Divoux A, Tordjman J, Lacasa D, Veyrie N, Hugol D, Aissat A, et al. Fibrosis in Human Adipose Tissue: Composition, Distribution, and Link With Lipid Metabolism and Fat Mass Loss. *Diabetes.* 2010;59(11):2817.

183. Henegar C, Tordjman J, Achard V, Lacasa D, Cremer I, Guerre-Millo M, et al. Adipose tissue transcriptomic signature highlights the pathological relevance of extracellular matrix in human obesity. *Genome Biology.* 2008;9(1):R14.

184. Williams AS, Kang L, and Wasserman DH. The extracellular matrix and insulin resistance. *Trends in Endocrinology & Metabolism.* 2015;26(7):357-66.

185. Khan T, Muise ES, Iyengar P, Wang ZV, Chandalia M, Abate N, et al. Metabolic Dysregulation and Adipose Tissue Fibrosis: Role of Collagen VI. 2009;29(6):1575-91.

186. Pasarica M, Gowronska-Kozak B, Burk D, Remedios I, Hymel D, Gimble J, et al. Adipose Tissue Collagen VI in Obesity. *The Journal of Clinical Endocrinology & Metabolism.* 2009;94(12):5155-62.

187. Spencer M, Yao-Borengasser A, Unal R, Rasouli N, Gurley CM, Zhu B, et al. Adipose tissue macrophages in insulin-resistant subjects are associated with collagen VI and fibrosis and demonstrate alternative activation. *Am J Physiol Endocrinol Metab.* 2010;299(6):E1016-27.

188. Chun T-H. Peri-adipocyte ECM remodeling in obesity and adipose tissue fibrosis. *Adipocyte.* 2012;1(2):89-95.

189. Tinahones FJ, Coín-Aragüez L, Mayas MD, Garcia-Fuentes E, Hurtado-Del-Pozo C, Vendrell J, et al. Obesity-associated insulin resistance is correlated to adipose tissue vascular endothelial growth factors and metalloproteinase levels. *BMC physiology.* 2012;12:4.

190. Unal R, Yao-Borengasser A, Varma V, Rasouli N, Labbate C, Kern PA, et al. Matrix Metalloproteinase-9 Is Increased in Obese Subjects and Decreases in Response to Pioglitazone. *The Journal of Clinical Endocrinology & Metabolism.* 2010;95(6):2993-3001.

191. Hotamisligil GS, Shargill NS, and Spiegelman BM. Adipose expression of tumor necrosis factor-alpha: direct role in obesity-linked insulin resistance. *Science.* 1993;259(5091):87.

192. Weisberg SP, McCann D, Desai M, Rosenbaum M, Leibel RL, and Ferrante AW, Jr. Obesity is associated with macrophage accumulation in adipose tissue. *J Clin Invest.* 2003;112(12):1796-808.

193. Xu H, Barnes GT, Yang Q, Tan G, Yang D, Chou CJ, et al. Chronic inflammation in fat plays a crucial role in the development of obesity-related insulin resistance. *J Clin Invest.* 2003;112(12):1821-30.

194. Reilly SM, and Saltiel AR. Adapting to obesity with adipose tissue inflammation. *Nature Reviews Endocrinology.* 2017;13(11):633-43.

195. Lee YS, Wollam J, and Olefsky JM. An Integrated View of Immunometabolism. *Cell.* 2018;172(1):22-40.

196. Jernås M, Palming J, Sjöholm K, Jennische E, Svensson PA, Gabrielsson BG, et al. Separation of human adipocytes by size: hypertrophic fat cells display distinct gene expression. *FASEB journal : official publication of the Federation of American Societies for Experimental Biology.* 2006;20(9):1540-2.

197. Shoelson SE, Herrero L, and Naaz A. Obesity, Inflammation, and Insulin Resistance. *Gastroenterology.* 2007;132(6):2169-80.

198. Hotamisligil GS, Shargill NS, and Spiegelman BM. Adipose expression of tumor necrosis factor-alpha: direct role in obesity-linked insulin resistance. *Science.* 1993;259(5091):87-91.

199. Varma V, Yao-Borengasser A, Bodles AM, Rasouli N, Phanavanh B, Nolen GT, et al. Thrombospondin-1 is an adipokine associated with obesity, adipose inflammation, and insulin resistance. *Diabetes.* 2008;57(2):432-9.

200. Crawford SE, Stellmach V, Murphy-Ullrich JE, Ribeiro SMF, Lawler J, Hynes RO, et al. Thrombospondin-1 Is a Major Activator of TGF-β1 In Vivo. *Cell.* 1998;93(7):1159-70.

201. Fabbrini E, Cella M, McCartney SA, Fuchs A, Abumrad NA, Pietka TA, et al. Association Between Specific Adipose Tissue CD4+ T-Cell Populations and Insulin Resistance in Obese Individuals. *Gastroenterology.* 2013;145(2):366-74.e3.

202. McLaughlin T, Deng A, Gonzales O, Aillaud M, Yee G, Lamendola C, et al. Insulin resistance is associated with a modest increase in inflammation in subcutaneous adipose tissue of moderately obese women. *Diabetologia.* 2008;51(12):2303-8.

203. Wernstedt Asterholm I, Tao C, Morley TS, Wang QA, Delgado-Lopez F, Wang ZV, et al. Adipocyte inflammation is essential for healthy adipose tissue expansion and remodeling. *Cell Metab.* 2014;20(1):103-18.

204. Zhu Q, An YA, Kim M, Zhang Z, Zhao S, Zhu Y, et al. Suppressing adipocyte inflammation promotes insulin resistance in mice. *Molecular metabolism.* 2020;39:101010-.

205. Tschritter O, Fritsche A, Thamer C, Haap M, Shirkavand F, Rahe S, et al. Plasma adiponectin concentrations predict insulin sensitivity of both glucose and lipid metabolism. *Diabetes.* 2003;52(2):239-43.

206. Aguilar-Salinas CA, García EG, Robles L, Riaño D, Ruiz-Gomez DG, García-Ulloa AC, et al. High adiponectin concentrations are associated with the metabolically healthy obese phenotype. *The Journal of clinical endocrinology and metabolism.* 2008;93(10):4075-9.

207. Ahl S, Guenther M, Zhao S, James R, Marks J, Szabo A, et al. Adiponectin Levels Differentiate Metabolically Healthy vs Unhealthy Among Obese and Nonobese White Individuals. *The Journal of Clinical Endocrinology & Metabolism.* 2015;100(11):4172-80.

208. Doumatey AP, Bentley AR, Zhou J, Huang H, Adeyemo A, and Rotimi CN. Paradoxical Hyperadiponectinemia is Associated With the Metabolically Healthy Obese (MHO) Phenotype in African Americans. *Journal of endocrinology and metabolism.* 2012;2(2):51-65.

209. Holland WL, Miller RA, Wang ZV, Sun K, Barth BM, Bui HH, et al. Receptor-mediated activation of ceramidase activity initiates the pleiotropic actions of adiponectin. *Nature Medicine.* 2011;17(1):55-63.

210. Li X, Zhang D, Vatner DF, Goedeke L, Hirabara SM, Zhang Y, et al. Mechanisms by which adiponectin reverses high fat diet-induced insulin resistance in mice. *Proceedings of the National Academy of Sciences.* 2020;117(51):32584.

211. Yamauchi T, Kamon J, Waki H, Terauchi Y, Kubota N, Hara K, et al. The fat-derived hormone adiponectin reverses insulin resistance associated with both lipoatrophy and obesity. *Nature Medicine.* 2001;7(8):941-6.

212. Miller RA, Chu Q, Le Lay J, Scherer PE, Ahima RS, Kaestner KH, et al. Adiponectin suppresses gluconeogenic gene expression in mouse hepatocytes independent of LKB1-AMPK signaling. *J Clin Invest.* 2011;121(6):2518-28.

213. Yamauchi T, Kamon J, Minokoshi Y, Ito Y, Waki H, Uchida S, et al. Adiponectin stimulates glucose utilization and fatty-acid oxidation by activating AMP-activated protein kinase. *Nature Medicine.* 2002;8(11):1288-95.

214. Fu Y, Luo N, Klein RL, and Garvey WT. Adiponectin promotes adipocyte differentiation, insulin sensitivity, and lipid accumulation. *Journal of lipid research.* 2005;46(7):1369-79.

215. Colberg SR, Sigal RJ, Yardley JE, Riddell MC, Dunstan DW, Dempsey PC, et al. Physical Activity/Exercise and Diabetes: A Position Statement of the American Diabetes Association. *Diabetes Care.* 2016;39(11):2065.

216. Garber CE, Blissmer B, Deschenes MR, Franklin BA, Lamonte MJ, Lee IM, et al. American College of Sports Medicine position stand. Quantity and quality of exercise for developing and maintaining cardiorespiratory, musculoskeletal, and neuromotor fitness in apparently healthy adults: guidance for prescribing exercise. *Medicine and science in sports and exercise.* 2011;43(7):1334-59.

217. Bray GA, Frühbeck G, Ryan DH, and Wilding JPH. Management of obesity. *The Lancet.* 2016;387(10031):1947-56.

218. Pedersen BK, and Saltin B. Exercise as medicine - evidence for prescribing exercise as therapy in 26 different chronic diseases. *Scandinavian journal of medicine & science in sports.* 2015;25 Suppl 3:1-72.

219. Blair SN, Kohl HW, III, Paffenbarger RS, Jr, Clark DG, Cooper KH, and Gibbons LW. Physical Fitness and All-Cause Mortality: A Prospective Study of Healthy Men and Women. *JAMA.* 1989;262(17):2395-401.

220. Wei M, Gibbons LW, Mitchell TL, Kampert JB, Lee CD, and Blair SN. The association between cardiorespiratory fitness and impaired fasting glucose and type 2 diabetes mellitus in men. *Annals of internal medicine.* 1999;130(2):89-96.

221. Fisher G, Brown AW, Bohan Brown MM, Alcorn A, Noles C, Winwood L, et al. High Intensity Interval- vs Moderate Intensity- Training for Improving Cardiometabolic Health in Overweight or Obese Males: A Randomized Controlled Trial. *PLoS One.* 2015;10(10):e0138853.

222. Schenk S, Harber MP, Shrivastava CR, Burant CF, and Horowitz JF. Improved insulin sensitivity after weight loss and exercise training is mediated by a reduction in plasma fatty acid mobilization, not enhanced oxidative capacity. 2009;587(20):4949-61.

223. Heath GW, Gavin JR, Hinderliter JM, Hagberg JM, Bloomfield SA, and Holloszy JO. Effects of exercise and lack of exercise on glucose tolerance and insulin sensitivity. *Journal of Applied Physiology.* 1983;55(2):512-7.

224. Mikines KJ, Sonne B, Farrell PA, Tronier B, and Galbo H. Effect of physical exercise on sensitivity and responsiveness to insulin in humans. 1988;254(3):E248-E59.

225. Richter EA, Mikines KJ, Galbo H, and Kiens B. Effect of exercise on insulin action in human skeletal muscle. 1989;66(2):876-85.

226. Newsom SA, Everett AC, Hinko A, and Horowitz JF. A Single Session of Low-Intensity Exercise Is Sufficient to Enhance Insulin Sensitivity Into the Next Day in Obese Adults. 2013;36(9):2516-22.

227. Ryan BJ, Schleh MW, Ahn C, Ludzki AC, Gillen JB, Varshney P, et al. Moderate-intensity exercise and high-intensity interval training affect insulin sensitivity similarly in obese adults. *The Journal of clinical endocrinology and metabolism.* 2020.

228. King DS, Dalsky GP, Clutter WE, Young DA, Staten MA, Cryer PE, et al. Effects of exercise and lack of exercise on insulin sensitivity and responsiveness. 1988;64(5):1942-6.

229. van Loon LJ, Greenhaff PL, Constantin-Teodosiu D, Saris WH, and Wagenmakers AJ. The effects of increasing exercise intensity on muscle fuel utilisation in humans. *J Physiol.* 2001;536(Pt 1):295-304.

230. Romijn JA, Coyle EF, Sidossis LS, Gastaldelli A, Horowitz JF, Endert E, et al. Regulation of endogenous fat and carbohydrate metabolism in relation to exercise intensity and duration. 1993;265(3):E380-E91.

231. Horowitz J. Fatty acid mobilization from adipose tissue during exercise. *Trends in endocrinology and metabolism: TEM.* 2003;14:386-92.

232. Schrauwen-Hinderling VB, Schrauwen P, Hesselink MK, van Engelshoven JM, Nicolay K, Saris WH, et al. The increase in intramyocellular lipid content is a very early response to training. *The Journal of clinical endocrinology and metabolism.* 2003;88(4):1610-6.

233. Shepherd SO, Cocks M, Tipton KD, Ranasinghe AM, Barker TA, Burniston JG, et al. Preferential utilization of perilipin 2-associated intramuscular triglycerides during 1 h of moderate-intensity endurance-type exercise. *Experimental physiology.* 2012;97(8):970-80.

234. van Loon LJ, Koopman R, Stegen JH, Wagenmakers AJ, Keizer HA, and Saris WH. Intramyocellular lipids form an important substrate source during moderate intensity exercise in endurance-trained males in a fasted state. *J Physiol.* 2003;553(Pt 2):611-25.

235. Daemen S, van Zandvoort MAMJ, Parekh SH, and Hesselink MKC. Microscopy tools for the investigation of intracellular lipid storage and dynamics. *Molecular Metabolism.* 2016;5(3):153-63.

236. Daemen S, Gemmink A, Brouwers B, Meex RCR, Huntjens PR, Schaart G, et al. Distinct lipid droplet characteristics and distribution unmask the apparent contradiction of the athlete's paradox. *Molecular Metabolism.* 2018;17:71-81.

237. Gemmink A, Daemen S, Brouwers B, Huntjens PR, Schaart G, Moonen-Kornips E, et al. Dissociation of intramyocellular lipid storage and insulin resistance in trained athletes and type 2 diabetes patients; involvement of perilipin 5? *J Physiol.* 2018;596(5):857-68.

238. McFarlan JT, Yoshida Y, Jain SS, Han XX, Snook LA, Lally J, et al. In vivo, fatty acid translocase (CD36) critically regulates skeletal muscle fuel selection, exercise performance, and training-induced adaptation of fatty acid oxidation. *The Journal of biological chemistry.* 2012;287(28):23502-16.

239. Mason RR, and Watt MJ. Unraveling the roles of PLIN5: linking cell biology to physiology. *Trends in Endocrinology & Metabolism.* 2015;26(3):144-52.

240. Bosma M, Hesselink MKC, Sparks LM, Timmers S, Ferraz MJ, Mattijssen F, et al. Perilipin 2 Improves Insulin Sensitivity in Skeletal Muscle Despite Elevated Intramuscular Lipid Levels. *Diabetes.* 2012;61(11):2679.

241. Whytock KL, Shepherd SO, Wagenmakers AJM, and Strauss JA. Hormone-sensitive lipase preferentially redistributes to lipid droplets associated with perilipin-5 in human skeletal muscle during moderate-intensity exercise. *J Physiol.* 2018;596(11):2077-90.

242. Tarnopolsky MA, Rennie CD, Robertshaw HA, Fedak-Tarnopolsky SN, Devries MC, and Hamadeh MJ. Influence of endurance exercise training and sex on intramyocellular lipid and mitochondrial ultrastructure, substrate use, and mitochondrial enzyme activity. *American journal of physiology Regulatory, integrative and comparative physiology.* 2007;292(3):R1271-8.

243. Devries MC, Lowther SA, Glover AW, Hamadeh MJ, and Tarnopolsky MA. IMCL area density, but not IMCL utilization, is higher in women during moderate-intensity endurance exercise, compared with men. *American journal of physiology Regulatory, integrative and comparative physiology.* 2007;293(6):R2336-42.

244. Benador IY, Veliova M, Mahdaviani K, Petcherski A, Wikstrom JD, Assali EA, et al. Mitochondria Bound to Lipid Droplets Have Unique Bioenergetics, Composition, and Dynamics that Support Lipid Droplet Expansion. *Cell Metab.* 2018;27(4):869-85.e6.

245. Chee C, Shannon CE, Burns A, Selby AL, Wilkinson D, Smith K, et al. Relative Contribution of Intramyocellular Lipid to Whole-Body Fat Oxidation Is Reduced With Age but Subsarcolemmal Lipid Accumulation and Insulin Resistance Are Only Associated With Overweight Individuals. *Diabetes.* 2016;65(4):840-50.

246. Koh H-CE, Nielsen J, Saltin B, Holmberg H-C, and Ørtenblad N. Pronounced limb and fibre type differences in subcellular lipid droplet content and distribution in elite skiers before and after exhaustive exercise. 2017;595(17):5781-95.

247. van Loon LJ, Koopman R, Manders R, van der Weegen W, van Kranenburg GP, and Keizer HA. Intramyocellular lipid content in type 2 diabetes patients compared with overweight sedentary men and highly trained endurance athletes. *Am J Physiol Endocrinol Metab.* 2004;287(3):E558-65.

248. Shepherd SO, Cocks M, Tipton KD, Ranasinghe AM, Barker TA, Burniston JG, et al. Sprint interval and traditional endurance training increase net intramuscular triglyceride breakdown and expression of perilipin 2 and 5. *J Physiol.* 2013;591(3):657-75.

249. Ferreira R, Vitorino R, Alves RM, Appell HJ, Powers SK, Duarte JA, et al. Subsarcolemmal and intermyofibrillar mitochondria proteome differences disclose functional specializations in skeletal muscle. *Proteomics.* 2010;10(17):3142-54.

250. Koh H-CE, Ørtenblad N, Winding KM, Hellsten Y, Mortensen SP, and Nielsen J. High-intensity interval, but not endurance, training induces muscle fiber type-specific subsarcolemmal lipid droplet size reduction in type 2 diabetic patients. 2018;315(5):E872-E84.

251. Nielsen J, Mogensen M, Vind BF, Sahlin K, Højlund K, Schrøder HD, et al. Increased subsarcolemmal lipids in type 2 diabetes: effect of training on localization of lipids, mitochondria, and glycogen in sedentary human skeletal muscle. *Am J Physiol Endocrinol Metab.* 2010;298(3):E706-13.

252. Liu K, and Czaja MJ. Regulation of lipid stores and metabolism by lipophagy. *Cell Death & Differentiation.* 2013;20(1):3-11.

253. Rambold AS, Cohen S, and Lippincott-Schwartz J. Fatty acid trafficking in starved cells: regulation by lipid droplet lipolysis, autophagy, and mitochondrial fusion dynamics. *Developmental cell.* 2015;32(6):678-92.

254. Mihaylova MM, and Shaw RJ. The AMPK signalling pathway coordinates cell growth, autophagy and metabolism. *Nature Cell Biology.* 2011;13(9):1016-23.

255. Settembre C, Fraldi A, Medina DL, and Ballabio A. Signals from the lysosome: a control centre for cellular clearance and energy metabolism. *Nature Reviews Molecular Cell Biology.* 2013;14(5):283-96.

256. Singh R, Kaushik S, Wang Y, Xiang Y, Novak I, Komatsu M, et al. Autophagy regulates lipid metabolism. *Nature.* 2009;458(7242):1131-5.

257. Martinez-Lopez N, Garcia-Macia M, Sahu S, Athonvarangkul D, Liebling E, Merlo P, et al. Autophagy in the CNS and Periphery Coordinate Lipophagy and Lipolysis in the Brown Adipose Tissue and Liver. *Cell Metabolism.* 2016;23(1):113-27.

258. Kaushik S, and Cuervo AM. AMPK-dependent phosphorylation of lipid droplet protein PLIN2 triggers its degradation by CMA. *Autophagy.* 2016;12(2):432-8.

Chapter III

Project 1

Assessment of Factors Underlying Whole-Body Insulin Resistance in Adults with Obesity.

ABSTRACT

Obesity is a major risk factor for many cardio-metabolic disorders, including insulin resistance. Although most adults with obesity are insulin resistant, some do remain relatively insulin sensitive. Factors underlying the variability in insulin sensitivity in adults with obesity are not completely clear. We hypothesize factors related to abdominal subcutaneous adipose tissue (aSAT) structure and metabolism may be important contributors. The primary aims of this study were to: 1) assess relationships between key clinical and subclinical factors with insulin-mediated glucose uptake in a relatively homogeneous cohort of adults with obesity, and 2) examine the potential contribution of adipocyte size and proteomic profile of aSAT to the rate of fatty acid (FA) mobilization into the systemic circulation. Sixty-six adults with obesity (BMI=34±3 kg/m^2) were assessed for insulin sensitivity (hyperinsulinemic-euglycemic clamp), and stable isotope dilution methods were used to quantify in vivo glucose, FA, and glycerol kinetics. We found insulin-mediated FA Ra suppression to be the strongest independent predictor of whole-body insulin sensitivity ($r=0.51$; $p<0.01$). Interestingly, FA Ra suppression was negatively correlated with lipid accumulation in both the liver and visceral adipose tissue. Proteomics analyses on aSAT samples from sub-cohorts of subjects with Low Fa Ra suppression (LS) versus High FA Ra suppression (HS; n=8 per group) revealed greater extracellular matrix (ECM) collagen proteins and TGFβ1 in LS versus HS. This finding suggests high aSAT fibrotic content may contribute to a reduced ability for insulin to suppress FA release. We also conducted lipidomics analyses in skeletal muscle samples and found an inverse correlation between FA Ra suppression and the acyl-chain length of acylcarnitine and triacylglycerol, suggesting regulation of FA release from aSAT in response to insulin may contribute to long-chain lipid accumulation in skeletal muscle. Overall, our findings support the notion that retaining the ability for insulin to markedly suppress FA release from aSAT has very favorable metabolic implications in skeletal muscle and liver. This may help explain why some adults with obesity remain 'protected' from developing skeletal muscle insulin resistance.

INTRODUCTION

Insulin resistance (i.e., a sub-optimal response to insulin's effect on glucose uptake) is a major factor underlying many obesity-related diseases (1). Although most adults with obesity are insulin resistant, it has been reported that as many as 30% of obese adults remain relatively insulin sensitive, with minimal metabolic health complications (2-4). Why some adults with obesity are profoundly resistant to insulin-mediated glucose uptake, while others are relatively insulin sensitive, remains elusive. Findings from our lab (5, 6) and others (7-9) suggest maintaining low fatty acid (FA) availability in the systemic circulation may help 'protect' some obese adults from developing insulin resistance. Importantly, the vast majority of the FA delivered into the systemic circulation are derived from abdominal subcutaneous adipose tissue (aSAT), rather than gluteal/femoral- or visceral adipose tissue (10). The rate of FA mobilization from aSAT into the systemic circulation is primarily determined by rate of triacylglycerol hydrolysis (i.e., lipolysis) and by the rate at which the FAs liberated by lipolysis are re-incorporated back into triacylglycerol within the adipocyte (i.e., re-esterification). While these processes are chiefly regulated by the activity of the lipase and acyltransferase enzymes that catalyze lipolysis and esterification, adipose tissue morphology (e.g., cell size, vascularization, fibrosis), as well as local and systemic inflammation may also impact FA release (11-13). Therefore, these factors within aSAT may play an important role in determining the magnitude of whole-body insulin resistance and overall metabolic health in adults with obesity.

The metabolic consequences of excessively high FA availability are due in large part to high rates for FA uptake and resultant 'ectopic' lipid accumulation in tissues such as skeletal muscle and liver (14, 15). High rates of FA uptake in the liver can greatly impair hepatic insulin sensitivity and can also lead to the development of chronic liver disorders such as nonalcoholic fatty liver disease (NAFLD) and nonalcoholic steatohepatitis (NASH). Because skeletal muscle is the primary site of insulin-mediated glucose uptake (16), preservation of insulin action in skeletal muscle is paramount for maintaining whole-body insulin sensitivity. Excessive FA uptake into skeletal muscle and the accumulation of lipid intermediates such as diacylglycerol (17), ceramide (18), and long-chain acyl-CoA (19) have been causally linked with impairing insulin signaling (20-22). In addition, the acyl-chain length (23, 24) and saturation state (25) of these and other lipid species have been suggested to impact skeletal muscle insulin signaling. Given the important repercussions stemming from a high FA uptake and lipid accumulation in skeletal

muscle and liver, an enhanced ability to store and sequester FA in aSAT should be metabolically favorable by excess FA availability that contributes to ectopic lipid deposition. However, the relationship between FA mobilization from aSAT and lipid accumulation in these tissues remains unresolved.

The primary aims of this study were to: 1) assess relationships between key clinical and subclinical factors with insulin-mediated glucose uptake in a relatively homogeneous cohort of adults with obesity, and 2) examine the potential contribution of adipocyte size, ECM collagen accumulation, and proteomic profile in aSAT to the rate of FA mobilization into the systemic circulation. We also sought to examine relationships between systemic FA mobilization and the accumulation of different lipid species within skeletal muscle, as well as hepatic lipid accumulation and function. We hypothesized that maintaining a relatively low rate of FA mobilization in the systemic circulation will be associated with enhanced insulin-mediated glucose uptake and lower ectopic lipid accumulation in liver and visceral adipose tissue. Furthermore, we hypothesized a relatively low rate of FA mobilization will be associated with lower ectopic lipid accumulation in the liver and skeletal muscle, with attenuated abundance of saturated- and long-chain muscle lipids, which in turn will also be associated with enhanced insulin sensitivity.

METHODS

Participants

Sixty-six men (n=20) and women (n=46) with obesity completed the study (BMI= 30-40 kg/m^2; Table III-1). All participants were 'inactive' and not engaged in any planned physical aerobic or resistance exercise, and weight stable (±2 kg) for the previous 6 months. Participants were not prescribed medications affecting glucose or lipid metabolism, have a history of heart disease, or smokers. All women were pre-menopausal with regularly occurring menses, and not pregnant, or lactating. The study protocol was approved by the University of Michigan Institutional Review Board, and registered at clinicaltrials.gov (NCT02717832 and NCT02706093). All participants were provided written informed consent before participation.

Body Composition, Visceral Fat Area, and Liver Fat.

Body composition was assessed by dual-energy X-ray absorptiometry (Lunar DPX DEXA Scanner, GE) at the Michigan Clinical Unit (MCRU). Visceral fat area (cm^2) and liver fat percentage was measured by magnetic resonance imaging (MRI: Ingenia 3T MR System, Phillips) at the University of Michigan Medicine's Department of Radiology.

Experimental Protocol

Participants received a standardized meal consisting of a dinner (30% daily energy expenditure; 55% carbohydrate, 30% fat, 15% protein) and snack (10% daily energy expenditure) the day before the study trial, and arrived to MCRU at 0700h the following morning (See Appendix A for study schematic). After 30min quiet rest, resting metabolic rate (RMR) and substrate oxidation (fat and carbohydrate) was measured via indirect calorimetry (Vmax Encore; CareFusion). At ~0800h, intravenous catheters were inserted into the hand vein for continuous blood sampling, and forearm vein for continuous isotope, insulin, and glucose infusion. At ~0900h, baseline blood samples were collected for background isotope labeling, followed by a primed continuous [6,6 $^2H_2$]glucose infusion (35 µmol/kg priming dose, and 0.41 µmol/kg/min continuous infusion; Cambridge Isotopes), and [$^2H_5$]glycerol (1.5 µmol/kg priming dose, and 0.1 µmol/kg/min continuous infusion; Cambridge). At ~0915h, skeletal muscle biopsies were collected from the vastus lateralis, and aSAT biopsies were collected by aspiration lateral to the umbilicus. For aSAT biopsies, one pass of intact tissue was collected with a Bergström needle, and immediately stored in ice-cold formalin, and paraffin embedded for cell size and histochemical analyses. Upon obtaining both skeletal muscle and aSAT biopsies, any visible connective tissue was removed, samples quickly rinsed in saline, blotted dry, and flash frozen in liquid nitrogen. At ~1000h, a continuous [1-^{13}C]palmitate bound to albumin infusion began to determine FA kinetics (0.04 µmol/kg/min continuous infusion; Cambridge). Three arterialized samples were collected (heated hand technique) at 1050h, 1055h, and 1100h to determine fasting glucose rate of appearance (Ra), FA Ra, and glycerol Ra into the circulation. At ~1100h, a 2h hyperinsulinemic-euglycemic clamp procedure began to determine insulin-mediated glucose uptake (index of whole-body insulin sensitivity; 40 mU/m^2/min) (26). Continuous blood glucose samples were obtained every 5min (StatStrip, Nova Biomedical, Waltham MA), and dextrose infusion rate was modified in attempt maintain baseline glucose concertation (~5 mM) at the end of the clamp procedure.

Five more blood samples were obtained during the last 20min of the clamp to determine insulin-mediated substrate kinetics.

Participant stratification into High versus Low FA Ra suppression sub-cohorts

For paired analyses, a sub-cohort of participants were stratified into High FA Ra suppression (HS) versus Low FA Ra suppression (LS) determined by the % change in FA Ra from baseline to hyperinsulinemia during the clamp (HS=85±2 %, LS=63±6 % FA Ra suppression; n=8 in each sub-cohort; Figure III-4A and III-4B). Importantly, participants selected for sub-cohort stratification were strictly matched for sex, body mass, and fat mass to avoid the confounding effect of body composition on metabolic health (Figure III-4C and Table III-1).

Analytical Procedures

Plasma glucose, glycerol, and FA kinetics.

The tracer-to-tracee ratio (TTR) to quantify glucose, glycerol, and palmitate kinetics were determined by gas-chromatography-mass spectrometry (GC/MS) using a Mass Selective Detector 5973 system (Agilent Technologies). For FA kinetics, proteins were precipitated by the addition of acetone to plasma, and hexane used to extract plasma lipids. FAs were converted to methyl esters with iodomethane, and isolated using solid phase extraction cartridges (Supelclean LC-Si Silica gel SPE tubes; 505048, Sigma-Aldrich). [1-^{13}C]palmitate TTR was determined from the average integrative abundance at the following mass-to-charge ratios (m/z) for methyl palmitate (270/271) and methyl ester palmitate (74/75) for both endogenous and isotope labeled palmitate respectively. Glucose TTR was selectively analyzed and peak abundances averaged at the following m/z for ion fragments (103/105, 115/117, 127/129, and 217/219) for endogenous and isotope labeled [6,6 $^{2}H_2$]glucose respectively. Glycerol TTR was selectively analyzed and averaged from m/z peak intensities at the following ion fragments (103/106, 116/120, and 145/148) for endogenous and isotope labeled [$^{2}H_5$]glycerol respectively.

Plasma metabolite, cytokine, and hormone concentration

Plasma glucose, non-esterified fatty acid (NEFA), triacylglycerol, high-density lipoproteins (HDL), and total cholesterol were measured in plasma from commercially available colorimetric assays. Plasma interleukin-6 (IL-6), C-reactive protein (CRP), leptin, total

adiponectin, and high molecular-weight (HMW) adiponectin were measured via enzyme-linked immunoassay (ELISA). Insulin was measured by radioimmunoassay. See Table III-3 for vendor information and details.

aSAT proteomics

Proteomic analysis from aSAT samples were completed by the Mass Spectrometry-Based Proteomics Resource Facility (Department of Pathology, University of Michigan). Liquid chromatography-mass spectrometry (LC-MS/MS) analysis was conducted using an RSLC Ultimate 3000 nano-ultra performance liquid chromatographer (Thermo-Fisher) and Orbitrap Fusion mass spectrometer (Thermo-Fisher). To prepare samples, ~125 mg aSAT from each subject was homogenized in 0.6 mL ice-cold lysis buffer (50mM Tris-HCl, 1mM EDTA, 0.5% SDS, 0.01% Triton X-100), 1% protease inhibitor cocktail (P8340, Sigma-Aldrich), and two steel ball bearings per sample. Samples were solubilized for 60min by inverted end-over-end rotation at 50rpm at 4°C, and centrifuged for ~3-5 cycles at 15,000g for 15min at 4°C, removing the lipid layer between cycles until lipid was not visible. Protein concentration was determined by bicinchoninic acid (BCA) assay method, and diluted in lysis buffer to 2µg/µL. See Appendix B for detailed protocols describing protein extraction, tandem mass tag (TMT) labeling procedure, and LC-MS/MS analysis and quantification.

Visceral and Liver fat.

Fat content from MRI images were captured by the Dixon method (27), and image acquisition was described previously from our lab (28). Visceral fat area was measured from 3, 5-mm axial slices between L2-L3 vertebral region, and liver fat percentage was measured from 3, 5-mm axials slices of the liver.

Skeletal muscle lipidomics

Untargeted lipidomic analysis (LC-MS) was completed by the Michigan Regional Comprehensive Metabolomics Resource Core (University of Michigan School of Medicine) using an ABSCIEX 5600 triple time-of-flight MS (SCIEX). Following homogenization, lipids were extracted by a modified Bligh-Dyer method using a 2:2:2 ratio volume of methanol:H2O:dichloromethane at room temperature after spiking internal standards (29). The organic layer was collected and dried under nitrogen, then the dried lipid extract reconstituted in

100 µL of Buffer B (10:85:5 acetonitrile/isopropanol/H2O) containing 10 mM ammonium acetate and subjected to LC-MS by electrospray ionization (LABSIEX 5600 TOF MS:SCIEX). Lipids were identified using LIPIDBLAST computer-generated tandem-MS library (30), and normalized to tissue wet weight.

Calculations

Fatty acid, glucose, and glycerol rate of appearance

Palmitate, glycerol, and glucose Ra were calculated from their respective TTR using the Steele equation for steady state conditions (31). Fatty acid Ra was determined by dividing palmitate Ra by the ratio of total palmitate (C16:0) to FAs within a standard (as shown previously by our lab; (5)).

Insulin-mediated glucose uptake and hepatic insulin sensitivity.

Insulin-mediated glucose uptake was determined by glucose infusion rate per kilogram fat free mass, and normalized to plasma insulin during the last 20 minutes of the hyperinsulinemic-euglycemic clamp when glucose concentrations were stable (nmol/kgFFM/min / (µU/mL)). Hepatic insulin sensitivity was determined by glucose Ra % suppression from basal to insulin-mediated conditions.

Resting metabolic rate and substrate oxidation

Resting Metabolic Rate (RMR: kcal/day) was calculated from the Weir equation (32). Fat oxidation (g/min) was calculated from VO_2 (L/min) and VCO_2 (L/min), and corrected for urinary nitrogen production by the equation detailed by Frayn (33).

aSAT cell size and fibrosis.

aSAT samples were fixed in 10% neutral buffer formalin at 4°C, and paraffin embedded in labeled histology cassettes and processed into a paraffin block. Mean adipocyte size was determined by NIH Image J using macro described by Parlee et al., (34). A lower threshold of 1000 μm^2 was set, and frequency distribution calculated from 30 bins per subject. Large and small adipocyte distributions were quantified by the highest and lowest quartiles from the entire study cohort (n=66). For fibrosis measurements, picrosirius red stained samples were measured as

described previously (35), and normalized to total tissue surface area measured from 10 random fields at 10x magnification for each sample, and quantified with NIH Image J (36).

Statistical Analysis

All measurements were tested for normality (shapiro-wilk test) and log transformed if normality was not achieved. For multivariate analysis, net elastic regression (LASSO) was used to identify clinical and subclinical factors best predicting insulin-mediated glucose uptake (nmol/kg FFM/min / (μU/mL)) using glmnet package in R (37). Univariate analysis correlating all measured variables and insulin-mediated glucose uptake independently was analyzed by Pearson's correlation coefficient, and adjusted for age and sex using the 'partial.r' function in the Psych package in R (38). Student's t-test compared metabolic outcomes in HS versus LS sub-cohorts. For proteomic analysis, differential expression was determined by LIMMA package in R (39). Proteins with $p<0.05$ and abundance ratio >1.5 between groups were considered differentially expressed. For lipidomic analysis, integrated abundance was log transformed. Lipids either negatively or positively associated with both insulin-mediated glucose uptake and FA Ra suppression were displayed based on significance ($p<0.05$), and adjusted for multiple comparisons (40). Hierarchical clustering for Spearman's coefficients correlating insulin-mediated glucose uptake and FA Ra suppression with lipid abundance were clustered by Euclidean distance measures by k-means clustering (k=5). β-coefficients for standardized abundance (z-score transformation) of individual lipid species with respect to acyl-chain length and unsaturation were correlated with standardized rates of insulin-mediated glucose uptake and FA Ra suppression (β_z). Then, correlations between β_z versus acyl-chain length, and β_z versus unsaturation were correlated by Pearson's coefficient. Data are displayed mean±SD. Statistical analysis was completed using R version 4.1.0 (41).

RESULTS

Study participants

Participant characteristics are presented in Table III-1. All participants were obese (BMI range = 30-40 kg/m^2, body fat= 43.5 ± 5.4 %), and did not present with fasting hyperglycemia (4.9 ± 0.5 mM). Despite being largely homogeneous for body composition and most other physical

and clinical measures, insulin-mediated glucose uptake varied widely among our participants (Figure III-1).

Clinical and subclinical factors associated with insulin-mediated glucose uptake.

Multiple linear regression analysis for our clinical outcomes indicated high HMW adiponectin, HDL, and total adiponectin all directly correlated with insulin-mediated glucose uptake (determined by non-zero coefficients; see Appendix C for full list of explanatory variables), while BMI, plasma triacylglycerol, visceral adipose tissue (VAT), and liver fat percentage all inversely correlated with insulin-mediated glucose uptake (Figure III-2A). Regression analysis for the subclinical factors (e.g., fat oxidation, lipolytic rate, FA kinetics, hepatic glucose production; see Appendix C for full list) indicated that insulin-mediated suppression of FA Ra ('FA Ra suppression' – expressed as percent change from basal), basal hepatic glucose production (i.e., glucose Ra), insulin-mediated suppression of hepatic glucose production, basal fat oxidation, and glycerol Ra during the insulin clamp were all directly correlated with insulin-mediated glucose uptake (Figure III-2B). In contrast, FA Ra during the insulin clamp inversely correlated with insulin-mediated glucose uptake (Figure III-2B). The subset factors from the LASSO regression were then analyzed by multiple linear regression with the following models: MODEL 1 = clinical factors models, and MODEL 2 = subclinical factors model. Both models significantly associated with insulin-mediated glucose uptake (MODEL 1: adjusted R^2=0.21, p<0.01; MODEL 2: adjusted R^2=0.55, p<0.01; Table III-2).

Univariate analysis demonstrated that insulin-mediated FA Ra suppression had the highest positive relationship with insulin-mediated glucose uptake (Figure III-2C and III-2D). In accordance with this, FA Ra measured at the end of the clamp period was negatively correlated with insulin-mediated glucose uptake (Figure III-2C and III-2E).

Adipocyte cell size

Mean adipocyte area inversely associated with both insulin-mediated glucose uptake (r=-0.29, p=0.035; Figure III-3A), and FA Ra suppression (r=-0.27, p=0.049; Figure III-3B). By stratifying the adipocyte area from aSAT samples from all subjects into quartiles, we defined adipocytes in quartile 1 (<3196μm^2) as 'small adipocytes' and those in quartile 4 (>6784μm^2) as 'large adipocytes' (Figure III-3C). Using these definitions, we found the proportion of small adipocytes did not associate with insulin-mediated glucose uptake (p=0.18; Figure III-3E) or FA

Ra suppression (p= 0.13; Figure III-3F). However, the proportion of large adipocytes tended to correlate inversely with insulin-mediated glucose uptake (r=-0.26, p=0.07; Figure III-3G), and was inversely correlated with FA Ra suppression (r=-0.28, p=0.04; Figure III-3H).

Sub-cohort stratification based of FA Ra suppression

Similar to the wide range of insulin-mediated glucose uptake rates among our participants, FA Ra suppression also varied widely (Figure III-4A). We stratified subjects into tertiles based on their FA Ra suppression to compare subjects with High Suppression (HS; range = 82.5-88.0% suppression) versus those with Low Suppression (LS; range = 50.7-68.5% suppression) sub-cohorts (Figure III-4A and III-4B). Importantly, subjects in the HS and LS sub-cohorts were tightly matched for fat mass, body fat %, and sex (Table III-1, Figure III-4C). There were no differences in basal FA Ra between sub-cohorts (Figure III-4D), so the difference in FA Ra suppression was truly a consequence of differences in the suppression in FA Ra in response to insulin (Figure III-4D). As anticipated, insulin-mediated glucose uptake was significantly greater in HS versus LS, and this was the case whether expressed normalized to plasma insulin concentration (Figure III-4E) or not (Figure III-4F). Glucose Ra suppression during the insulin clamp (a measure of hepatic insulin sensitivity) was also greater in HS versus LS (Figures III-4G and III-4H). Although there were no significant differences in liver fat or VAT area between the HS and LS (Figure III-4I and III-4J) sub-cohorts, when we examined this relationship across our entire cohort, we did find significant inverse correlations between liver fat and FA Ra suppression, as well as between VAT area and FA Ra suppression (both $p<0.01$; Figure III-4K and III-4L).

aSAT proteomics

Untargeted proteomic analysis identified 2,519 unique proteins (Figure III-5A). Of the proteins identified, 148 differentially expressed protein in HS versus LS. Of these differentially expressed proteins; 115 proteins were greater in LS versus HS, and 33 proteins greater in HS versus LS ($p<0.05$ & abundance ratio >1.5; Figure III-5B and III-5C).

Using the KEGG database (42), we found *ECM-receptor interaction* pathway (hsa04512) to present the highest significant enrichment in LS versus HS (FDR=$2.3e^{-4}$; Figure III-5D). Of these proteins within ECM-receptor expression pathway, COL1A1, COL3A1, COL23A1, GP1BA, SEPT5, ITGA2B, ITGB3, and THSB1 were all expressed greater in LS versus HS (Figure III-5E). In line with this finding in our HS and LS sub-cohorts, when examined across all subjects

in our study, we found an inverse correlation between picrosirius red staining (index of extracellular matrix fibrosis) and peripheral glucose disposal ($r=-0.37$, $p<0.01$; Appendix D). Although we found no significant differences between HS versus LS for each independent collagen VI isoform (COL6A1, COL6A2, COL6A3; Figure III-5E), the sum of all COLVI subunits (∑COL6A1, COL6A2, COL6A3) was greater in LS ($p=0.02$; Figure III-5F). This is important because excessive collagen VI accumulation in aSAT has been linked with impaired adipose tissue expansion, inflammation, and whole-body insulin resistance (43, 44). Additionally, transforming growth factor β1 (TGFβ1), which is a key mediator of fibrosis activated by inflammatory stimuli (45), was expressed greater in LS ($p=1.18e^{-6}$, abundance ratio=2.06; Figure III-5G).

Skeletal muscle lipidomics

High rates of FA flux from aSAT into the systemic circulation contributes to high rates of FA uptake in skeletal muscle, potentially accumulating bioactive lipid species that are linked with impaired insulin signaling in skeletal muscle. Our muscle lipidomics analysis revealed 21 specific lipid species that were significantly correlated with both insulin-mediated glucose uptake and FA Ra suppression (Figure III-6A and III-6B). The lipids that were positively correlated with both insulin-mediated glucose uptake and FA Ra suppression consisted primarily of phosphatidylcholine (PC) and phosphatidylethanolamine (PE) species – while the lipids inversely correlated with both insulin-mediated glucose uptake and FA Ra suppression included some triacylglycerol (TAG), PC, Plasmenyl-PE, and acylcarnitine (Figure III-6C).

To assess whether relationships existed between lipid composition (e.g., acyl-chain length) of some key muscle lipids and insulin-mediated glucose uptake or FA Ra suppression, we plotted the β-coefficient values for z-score transformed glucose $uptake_z$ and FA Ra $suppression_z$ versus the chain length of muscle fatty acids (Figures III-7A and III-7B), acylcarnitines (Figures III-7C and III-7D), diacylglycerol (DAG; Figures III-7E and III-7F) and TAG (Figure III-7G and III-7H). We found inverse correlations for insulin-mediated glucose $uptake_z$ and acyl-chain length of fatty acids ($p=0.038$; Figure III-7A) and acylcarnitine ($p<0.01$; Figure III-7C). We also found an inverse correlations between acylcarnitine chain-length and FA Ra $suppression_z$ ($r=-0.42$, $p=0.02$; Figure III-7D). DAG chain-length was not associated with either insulin-mediated glucose $uptake_z$ or FA Ra $suppression_z$ (Figures III-7E and III-7F). We also found significant inverse correlations between TAG chain length and glucose $uptake_z$ ($r=-0.40$, $p<0.01$; Figure III-7G), and FA Ra $suppression_z$ ($r=-0.51$, $p<0.01$; Figure III-7H). We performed the same analysis to examine

relationships between the degree of unsaturation (i.e., number of double-bonds) of these lipid species and both insulin-mediated glucose uptake and FA Ra suppression, and no significant relationships were present (Appendix E).

DISCUSSION

In agreement with previous work from our lab (5, 6) and others (7, 9, 22), we confirmed that whole body insulin-mediated glucose uptake varies greatly among a relatively homogeneous population of adults with obesity. In our aim to identify factors that may underlie this variability, one of the key findings from our study was the robust positive correlation observed between insulin-mediated suppression of FA released from aSAT ("FA Ra suppression") and insulin-mediated glucose uptake. Because the vast majority of insulin-mediated glucose uptake occurs in skeletal muscle (16) - we interpret this finding to suggest that the ability for insulin to potently suppress FA release from aSAT may be an important mediator to preserve muscle insulin sensitivity. Although our correlational analyses do not confirm causality, our findings are consistent with other studies (7-9), and also with previous findings demonstrating pharmacological reduction in systemic FA mobilization improved insulin-mediated glucose uptake (24, 46). From a clinical perspective, we interpret our findings to suggest enhanced suppression of FA release in response to insulin will markedly lower FA release from aSAT after meals and snacks – thereby maintaining systemic FA availability to relatively low levels throughout the day. In turn, this limits systemic FA availability for ectopic lipid accumulation in insulin responsive tissues, such as skeletal muscle and liver. Our current findings also expand on previous work suggesting aSAT morphology – such as smaller adipocyte size and lower ECM fibrosis may contribute to enhanced FA Ra suppression in response to insulin. Additionally, our novel findings suggest that high FA Ra suppression in response to insulin, thereby mitigating the excessive systemic FA availability that is very common in obesity (47), may alter lipid composition in skeletal muscle. Overall, findings from this study support an important tissue-specific *cross-talk* occurring between adipose tissue, skeletal muscle, and liver, by which the regulation of FA release from aSAT in response to insulin may have important implications on skeletal muscle and liver metabolism.

Excessive FA release from aSAT into the systemic circulation is known to be a key factor underlying many obesity-related cardiometabolic complications, including insulin resistance (20,

22, 46, 48). Because the vast majority of FA released into the circulation are derived from aSAT as opposed to VAT sources (10), the regulation of FA metabolism in aSAT is a major contributing factor for obesity-related complications. Our observation that of all parameters measured, insulin-mediated FA Ra suppression had the highest positive correlation with insulin-mediated glucose uptake supports the notion of important integrated effects of insulin on both aSAT and skeletal muscle, which is the primary site of insulin-mediated glucose uptake. Additionally, altered response for aSAT to effectively suppress FA release in response to insulin has high clinical relevance, because during waking hours most individuals are chronically 'under the influence' of insulin from their most recent meal or snack. Therefore, our findings suggest that adults with obesity who are more sensitive to suppress FA release from aSAT in response to insulin may be somewhat 'protected' from developing insulin resistance in skeletal muscle.

Insulin suppresses FA release from adipose tissue by both inhibiting lipolysis, and stimulating FA re-esterification for triacylglycerol synthesis (49), thereby preventing FA liberated by lipolysis to leave the adipocyte. Our glycerol Ra data (the gold-standard for measuring whole body lipolysis), indicates that differences in the magnitude of FA Ra suppression among our participants did not appear to be due to a differences in sensitivity to the anti-lipolytic effects of insulin. Instead, differences in the rate FA re-esterification back into triacylglycerol may help explain the variability in FA Ra suppression. This is consistent with earlier work demonstrating that the high rate of FA release from aSAT in response to insulin in obese compared with lean women was primarily dictated by the efficiency of FA re-esterification in response to insulin, and not to differences to the anti-lipolytic effect of insulin (50). Intracellular re-esterification of FA back into triacylglycerol is largely regulated by the acyltransferase proteins, glycerol 3-phosphate acyltransferase (GPAT) and diacylglycerol acyltransferase (DGAT), and enhanced sensitivity of these proteins in response to insulin may contribute to greater FA Ra suppression. Interestingly, while DGAT has been found to be acutely sensitive to insulin (51, 52), the effect of insulin on GPAT activity is less clear (53). In addition to the regulation of re-esterification, factors such as aSAT blood flow (54), as well as morphological features such as size (55, 56) and fibrosis (5) may also contribute to the variability in FA Ra suppression in response to insulin.

Much of the excess body fat mass in obesity is stored within hypertrophied adipocytes, and the abundance of large adipocytes has been found to be an important predictor of insulin resistance and type 2 diabetes (57). Fatty acid release from isolated adipocytes in vitro has been found to be

greater in large compared to small adipocytes (55, 56), which aligns with our finding that adipocyte area was inversely related to insulin-mediated FA Ra suppression. Adipocytes often expand during weight gain without a compensatory increase in vascularization (58), resulting in hypertrophic adipocytes with a low capillary density. A relatively low adipocyte capillary density can induce intracellular hypoxia, initiating a cascade of responses, including increased recruitment of pro-inflammatory macrophages to aSAT (59-61). Indeed, adipose tissue with hypertrophic adipocytes are often found to have elevated pro-inflammatory macrophage and a high abundance of inflammatory cytokines (62-64). The accumulation of pro-inflammatory cytokines (e.g., TNFα, IL6, and IL1β) have been reported to attenuate adipose tissue insulin signaling (65-67), and may contribute to lower FA Ra suppression in response to insulin. Additionally, lower capillary density in hypertrophied adipocytes, and a resultant compromise in microcirculation in the tissue, may lower insulin delivery, which could further blunt insulin-mediated FA Ra suppression in vivo.

Hypoxia and inflammation are also known to modify the fibrotic content and composition of adipose tissue ECM (12, 68, 69). The collagen-rich ECM network is essential for structural support of adipocytes, and physical interaction of the fibrotic ECM network within adipocytes can have important impact on insulin signaling (43, 70). Highly fibrotic adipose ECM can also pose a physical restriction for adipocyte expansion during episodes of weight gain, and the resulting mechanical stress within the adipocyte has been proposed to increase pro-inflammatory cytokine production (71). Conversely, removing this physical restriction in mice via genetic manipulation to lower collagen VI content was found to markedly reduce macrophage/inflammatory insult in adipose tissue and vastly improve overall metabolic profile (43). Experiments in preclinical models have also shown adipose tissue fibrosis to disrupt insulin signaling in the tissue (43, 70). In humans, the influence for ECM fibrosis to modify insulin signaling and/or delivery of insulin to the adipocyte has been speculated to modify FA mobilization, but to our knowledge has not been confirmed. In the current study, our observation that subjects with Low insulin-mediated FA Ra suppression (LS) had a greater collagen protein accumulation compared with subjects who demonstrated High FA Ra suppression (HS), supports the prospect that fibrotic adipose tissue ECM may negatively influence insulin-mediated lipid metabolism.

Interestingly, adipose tissue fibrosis appears to be both a cause and consequence of increased inflammatory stress within the tissue (12, 44, 68). TGFβ1 is a primary regulator of fibrosis development, and is derived as a result of pro-inflammatory stimuli (44, 72-74).

Activation of TGFβ1 is responsible for progenitor cell differentiation into myofibroblasts, and may contribute to increased progenitor cell differentiation away from adipogenesis toward myofibroblasts differentiation in the ECM (45, 72). Our finding that the greater collagen VI content in our LS versus HS subjects was accompanied by an elevated TGFβ1 abundance in the LS subjects aligns with its important role in fibrogenesis. Some of the increased inflammatory stimuli that may activate TGFβ1 in adipose tissue can stem from hypoxia induced by low tissue perfusion of hypertrophied adipocytes, as noted above. Additionally, local hypoxia may increase fibrosis independently of TGFβ1, through HIF1α-mediated activation of platelet-derived growth factor receptor β ($PDGFR\beta^{+}$) progenitor cells towards the myofibroblasts lineage (59, 69, 75). Together, hypoxia and inflammatory stimuli can promote adipose tissue ECM fibrosis, which may contribute to an impaired suppression of FA release from aSAT in response to insulin.

Perhaps the most important clinical implication of retaining the ability to effectively suppress FA release from aSAT in response to insulin is the potential to limit ectopic lipid accumulation in skeletal muscle, liver, and VAT. Chronically elevated FA delivery and uptake in the liver can result in hepatic steatosis and related disorders (e.g., nonalcoholic fatty liver disease [NAFLD], nonalcoholic steatohepatitis [NASH]), and can greatly impair hepatic glucose metabolism and liver function (76, 77). Importantly, our findings that hepatic insulin sensitivity was significantly greater in HS versus LS and that liver fat content was inversely correlated with FA Ra suppression across our full cohort support the favorable impact of enhanced insulin-mediated suppression of FA release from aSAT on liver metabolism. Additionally, although VAT is commonly linked to the etiology of many cardio-metabolic diseases, much of the fat stored in VAT are derived from FA released from aSAT (10). Our findings indicate that VAT lipid accumulation was inversely correlated with FA Ra suppression in response to insulin suggests the intriguing possibility that enhanced FA Ra suppression in response to insulin may help diminish VAT stores, thereby reducing the health risks associated with VAT.

The link between excessive FA uptake in skeletal muscle and insulin resistance has been largely attributed to an accumulation of lipid intermediates and metabolites, such as diacylglycerol (17) and ceramide (18), as well as long-chain acyl CoA (78). Although we did not find did not find diacylglycerol or ceramide to be associated with insulin-mediated glucose uptake in our participants, our findings that acyl-chain length of fatty acids, acylcarnitines, and triacylglycerol in skeletal muscle inversely related with insulin-mediated glucose uptake supports the role of

aberrant lipid metabolism interfering with insulin action in skeletal muscle. These findings are in general agreement with a previous study demonstrating that lowering 24h fatty acid availability with acipimox (a potent lipolytic inhibitor) decreased long-chain fatty acyl-CoA accumulation in skeletal muscle with an accompanying improvement in insulin sensitivity (24). An accumulation of long-chain lipids in skeletal muscle can be a consequence of 'incomplete' FA oxidation due to a high rate of fatty acid uptake and β-oxidation relative to flux through the tricarboxylic acid cycle (78), which is especially low when sedentary. High abundance of long-chain lipids such as acylcarnitines in skeletal muscle are proposed to promote insulin resistance by; 1) increased inflammatory environment (79-81), 2) mitochondrial-derived oxidative stress (82-84), and 3) ER stress (85, 86). Although TAG is a neutral lipid, we found long-chain triacylglycerol accumulation inversely related with whole-body insulin sensitivity, but the implications of this finding are not clear. Our finding that lipid species and composition within the PC and PE lipid classes were related to insulin sensitivity is consistent with previous work (87, 88). Skeletal muscle phospholipid profile (89, 90), as well as phospholipid classes have been found to play important roles in mitochondrial membrane fluidity and integrity (87, 91), which can impact insulin signaling. Overall, we contend the relatively low sensitivity for insulin-mediated FA Ra suppression, and a resultant elevation in FA availability throughout the day, will modify skeletal muscle lipid composition and contribute to insulin resistance.

An important limitation of this clinical study is high reliance correlational analyses, which obviously does not allow us to assign causation to the integrative interpretations of our findings. For example, we interpret our finding to suggest impaired suppression of FA released from aSAT in response to insulin may precede the insulin resistance for glucose metabolism in muscle and liver, but we acknowledge the limitation of this interpretations based on these correlational analyses. Additionally, although we address the potential role of hypoxia and inflammation on fibrogenesis in aSAT, this supposition was based on prior evidence (59, 61), and we do not provide direct data to support this notion. We also acknowledge several other systemic mechanisms may be contributing to low FA Ra suppression in response to insulin that include; 1) increased sympathetic tone (92), 2) alterations in cellular heterogeneity of adipocytes responsive to insulin (93), and/or 3) senescence of adipocytes (94) - all of which are recently implicated as possible underlying factors that were not tested in the current study. Lastly, although the subjects in our

LS and HS groups were matched for sex, we recognize sex differences may be an important contributing factor to differences observed.

In summary, our data indicate greater suppression of FA release from aSAT in response to insulin may help preserve insulin-mediated glucose uptake in some adults with obesity. Greater suppression of FA release from aSAT in response to insulin was also related to lower hepatic and VAT, and greater hepatic insulin sensitivity. Together, these findings support the prospect that sustaining the ability for insulin to potently suppress FA release from aSAT may be a very important factor to help maintain metabolic health in adults with obesity. Adipocyte size, aSAT inflammation, and fibrosis may be important mediators of the response to insulin in aSAT. These proposed effects in aSAT may contribute to lower insulin-mediated glucose uptake through the accumulation of long-chain fatty acids, acylcarnitine, and TAG lipids. Overall, our findings point to an important tissue-specific *cross-talk*, by which retaining insulin response to suppress FA release from aSAT may have very impactful metabolic implications in skeletal muscle and liver.

ACKNOWLEDGEMENTS

We thank the study participants for their efforts; Dr. Benjamin Carr, Dr. Jacob Haus, Jeffrey Wysocki, RN; the staff at the Michigan Clinical Research Unit; and all the members of the Substrate Metabolism Lab for study assistance. We would like to thank the Proteomics Resource Facility (PRF) at the University of Michigan, Department of Pathology, for conducting mass spectrometry experiments, and Michigan Regional Comprehensive Metabolomics Resource Core for conducting lipidomic analysis.

FIGURES

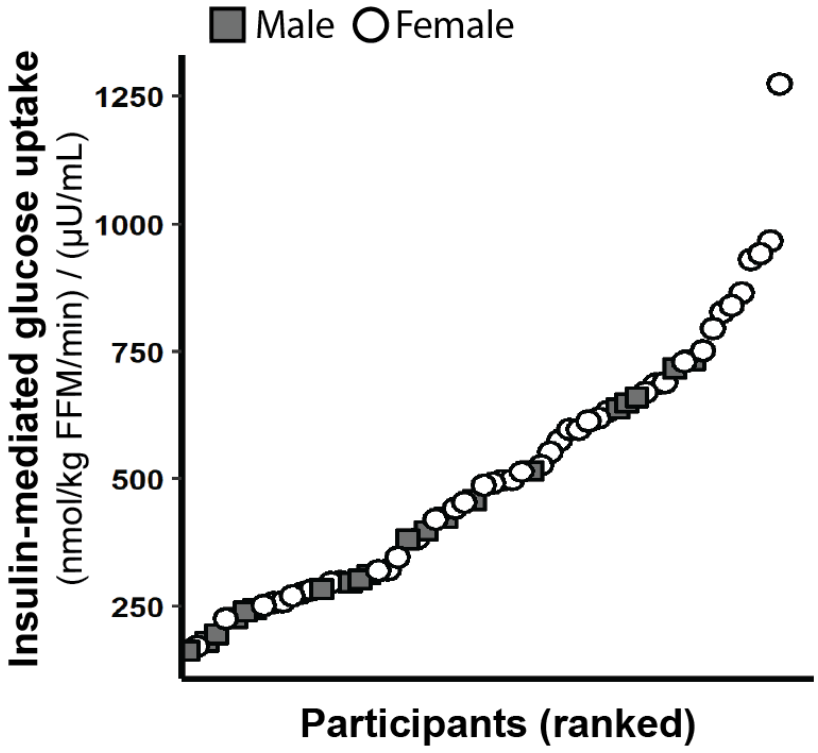

Figure III-1: Insulin-mediated glucose uptake variability across all participants (n=66).

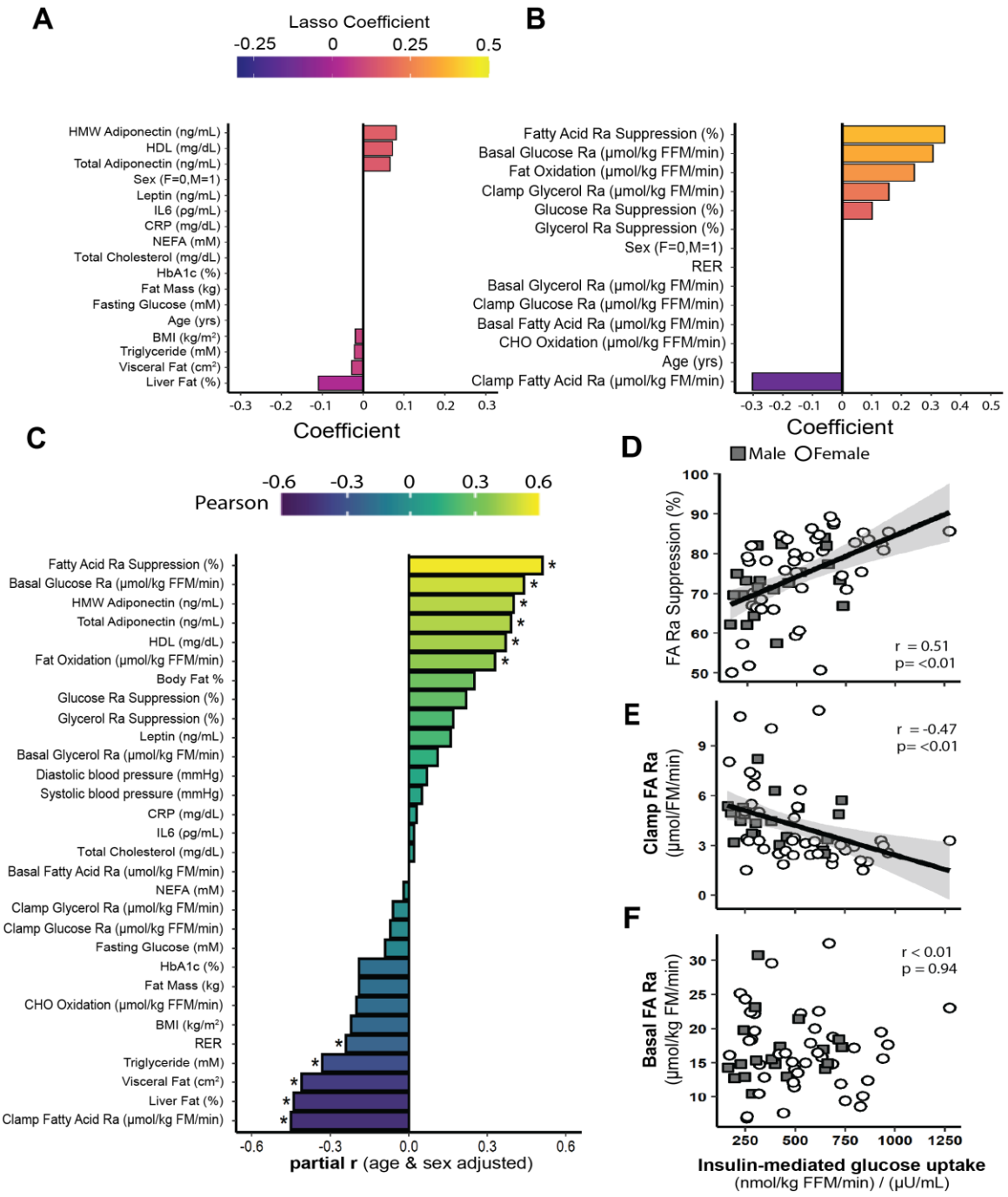

Figure III-2: Clinical and subclinical factors associated with insulin-mediated glucose uptake.

A) Lasso regression coefficients for clinical factors associated with insulin-mediated glucose uptake. B) Lasso regression coefficients for subclinical factors (i.e., substrate control and oxidation under fasting and hyperinsulinemia), and insulin-mediated glucose uptake. C) Independent correlation (Pearson's) for all individual factors associated with insulin-mediated glucose uptake, adjusted for age and sex (partial r). D-F) Relationships between insulin-mediated glucose uptake and FA Ra suppression (D), insulin-mediated FA Ra (clamp) (E), and basal FA Ra (F). * Significant correlation versus insulin-mediated glucose uptake (nmol/kg FFM/min) / (µU/mL)) ($p < 0.05$).

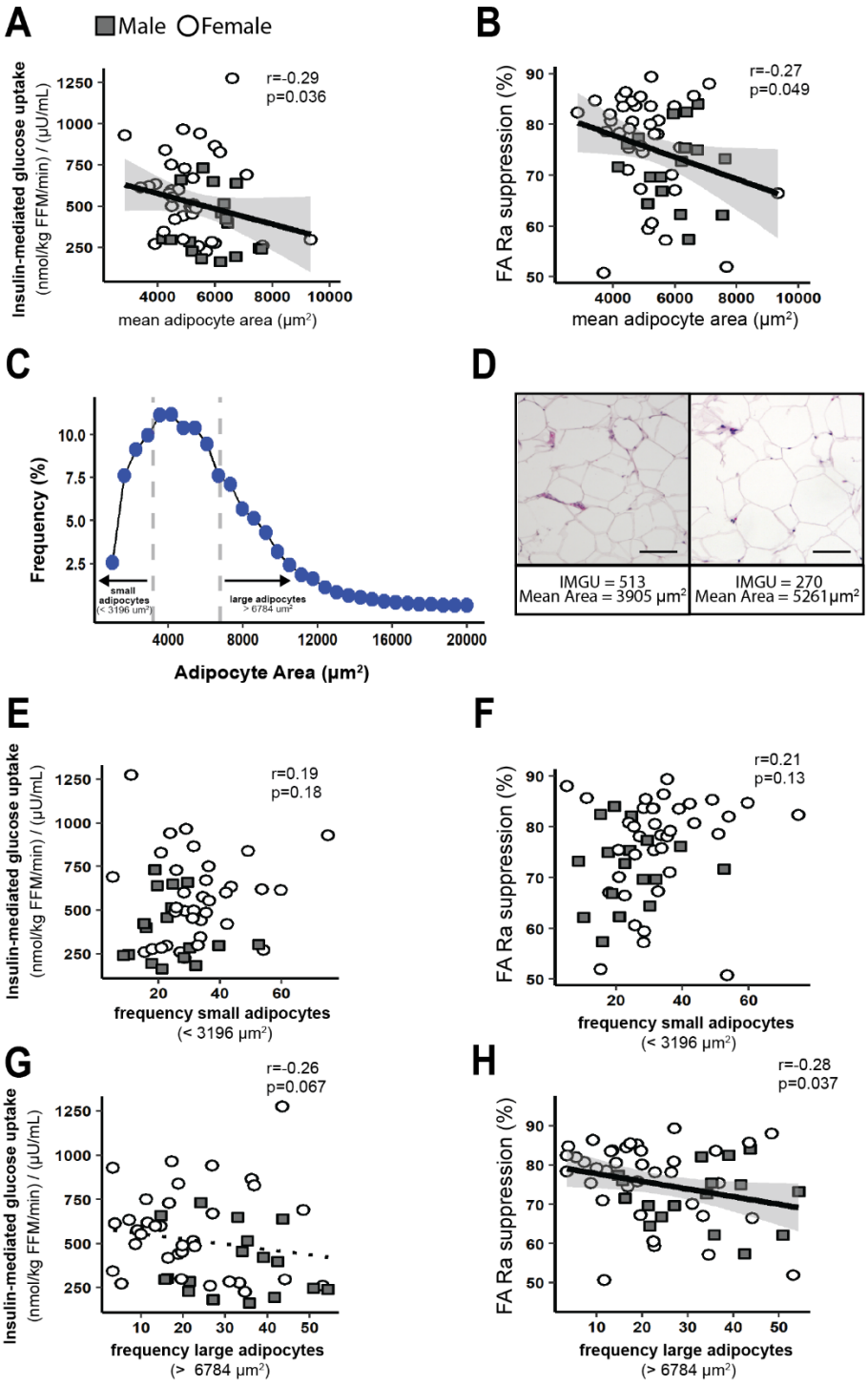

Figure III-3: Relationships between adipose tissue cell size and insulin sensitivity.

Association between mean adipocyte size and A) insulin-mediated glucose uptake, B) FA Ra suppression. C) Adipocyte cell size distribution from study cohort (bins=30). D) Representative image for a participant with high (513 nmol/kg FFM/min/insulin) and low (270 nmol/kg FFM/min/insulin) insulin-mediated glucose uptake, scale bar = 100μm. Association between the frequency of small adipocytes (1000-3196μm^2) and E) insulin-mediated glucose uptake, F) FA Ra suppression. Association between the frequency of large adipocytes (> 6784μm^2) and G) insulin-mediated glucose uptake, H) FA Ra suppression.

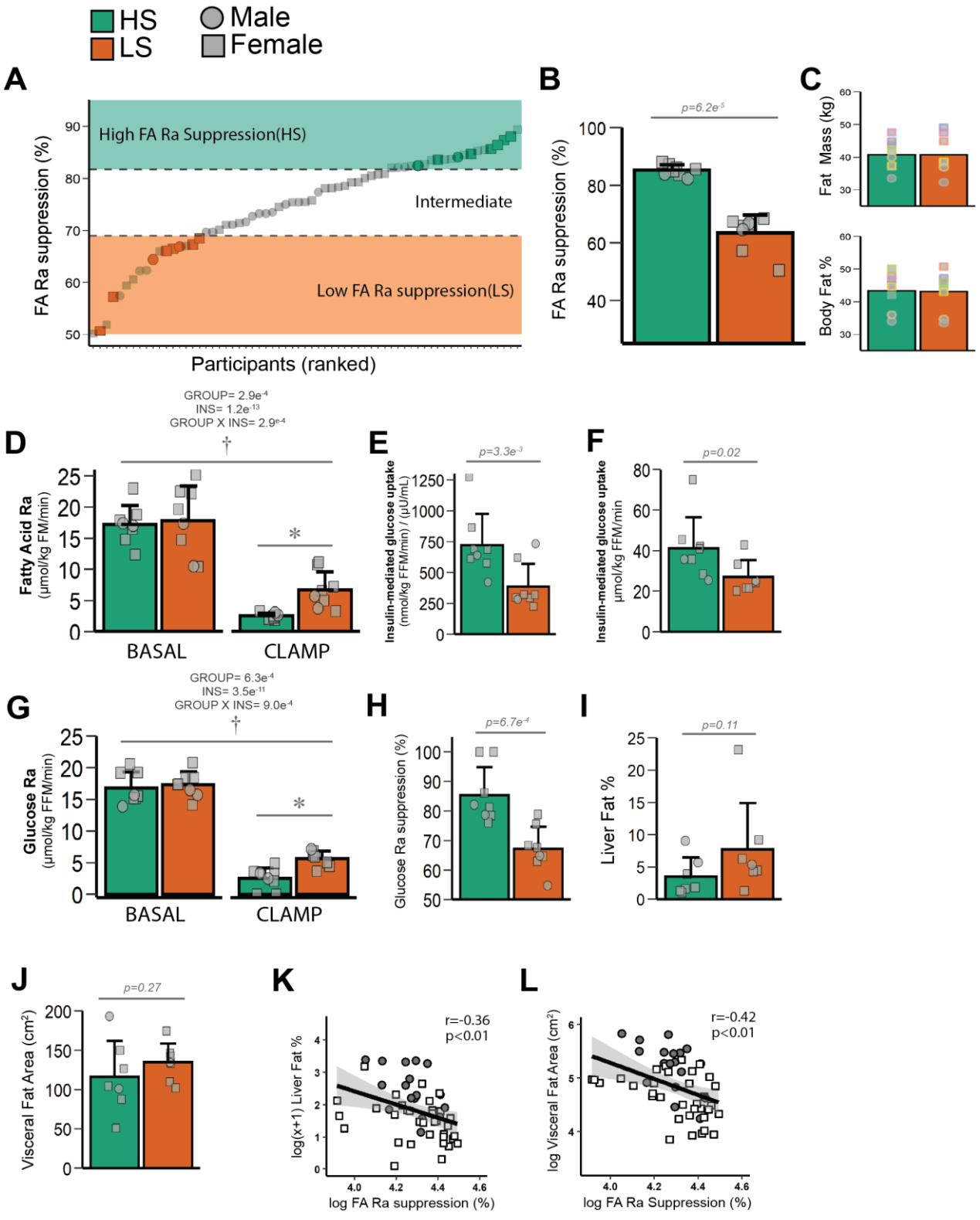
HS
LS
Male
Female
A
FA Ra suppression (%)
High FA Ra Suppression(HS)
Intermediate
Low FA Ra suppression(LS)
Participants (ranked)
B
p=6.2e-5
FA Ra suppression (%)
C
Fat Mass (kg)
Body Fat %
D
GROUP= 2.9e-4
INS= 1.2e-13
GROUP X INS= 2.9e-4
Fatty Acid Ra
(µmol/kg FFM/min)
BASAL
CLAMP
E
p=3.3e-3
Insulin-mediated glucose uptake
(nmol/kg FFM/min) / (µU/mL)
F
p=0.02
Insulin-mediated glucose uptake
µmol/kg FFM/min
G
GROUP= 6.3e-4
INS= 3.5e-11
GROUP X INS= 9.0e-4
Glucose Ra
(µmol/kg FFM/min)
BASAL
CLAMP
H
p=6.7e-4
Glucose Ra suppression (%)
I
p=0.11
Liver Fat %
J
p=0.27
Visceral Fat Area (cm²)
K
r=-0.36
p<0.01
log(x+1) Liver Fat %
log FA Ra suppression (%)
L
r=-0.42
p<0.01
log Visceral Fat Area (cm²)
log FA Ra Suppression (%)

Figure III-4: Comparison of insulin-mediated glucose uptake, hepatic insulin sensitivity, liver fat, and visceral fat area from a sub-cohort matched for body composition, and discordant FA Ra suppression.

A) Participants of discordant FA Ra suppression and well-matched for body composition and sex were paired into 'High Suppression' (HS) and 'Low suppression' (LS) sub-cohorts. B) FA Ra suppression between HS versus LS. C) Body composition (fat mass and body fat %) between groups. Colors for individual data indicates participant matching for body composition and sex. D) Fatty acid Ra measured under basal and during the hyperinsulinemic-euglycemic clamp. E-F) Measures of insulin-mediated glucose uptake normalized to insulin (nmol/kg FFM/min/insulin: E), and not normalized to insulin (µmol/kg FFM/min: F). G) Glucose Ra measured before and during hyperinsulinemic-euglycemic clamp. H) Hepatic insulin sensitivity measured as glucose Ra suppression during the hyperinsulinemic-euglycemic clamp. I-J) Liver fat % (I), and visceral fat area (cm^2) between groups (J). K) Association between liver fat % and FA Ra suppression for all study participants. L) Association between visceral fat area and FA Ra suppression for all study participants. Data are mean ± SD. * $p<0.05$ HS versus LS. † $p< 0.05$ basal versus clamp (insulin-stimulated) during hyperinsulinemic-euglycemic clamp.

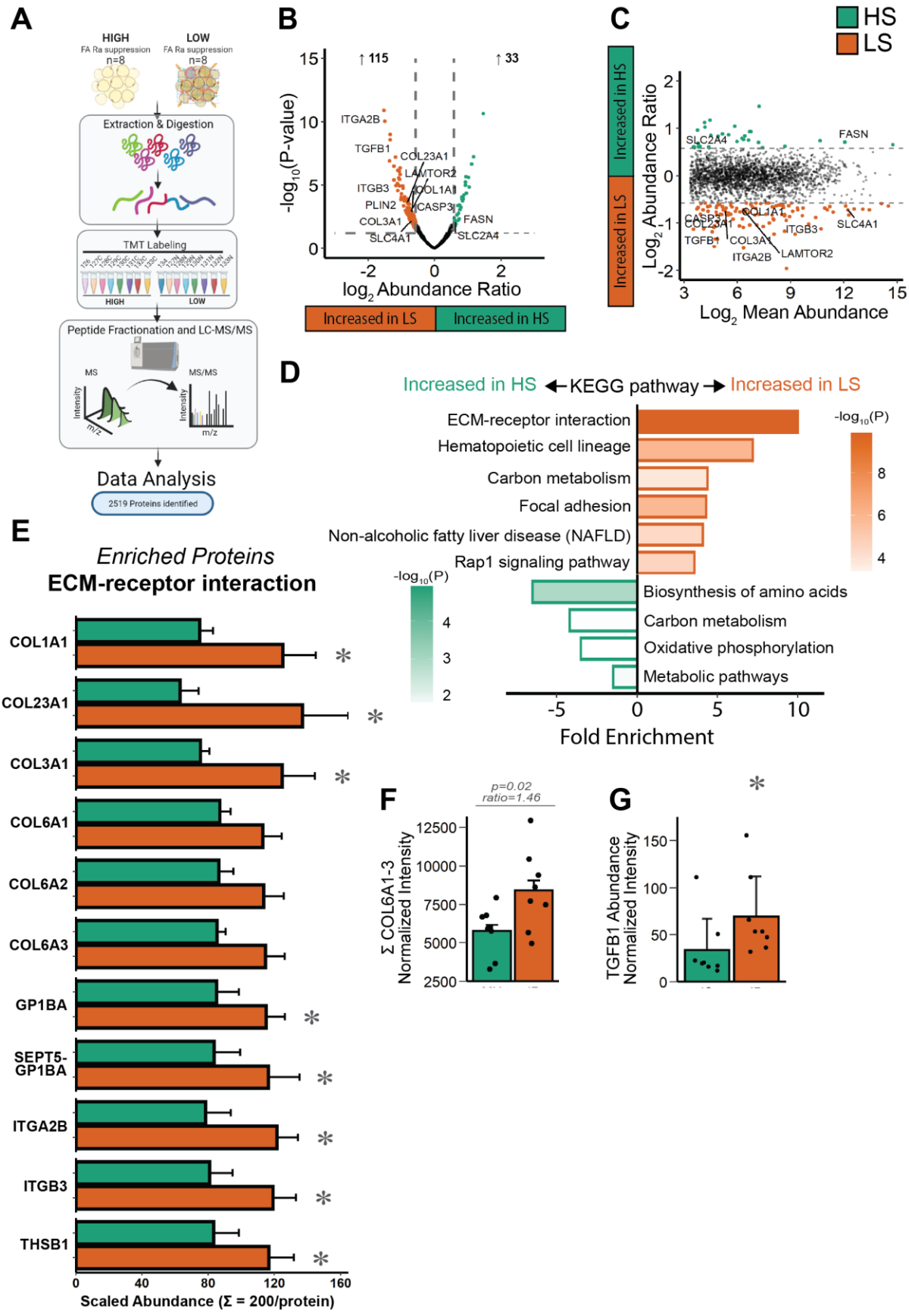
A
HIGH
FA Ra suppression
n=8
LOW
FA Ra suppression
n=8
Extraction & Digestion
TMT Labeling
HIGH
LOW
Peptide Fractionation and LC-MS/MS
MS
MS/MS
Intensity
m/z
Data Analysis
2519 Proteins identified
B
↑ 115
↑ 33
-log10(P-value)
ITGA2B
TGFB1
COL23A1
LAMTOR2
ITGB3
COL1A1
PLIN2
CASP3
COL3A1
FASN
SLC4A1
SLC2A4
log2 Abundance Ratio
Increased in LS
Increased in HS
C
HS
LS
Increased in HS
Increased in LS
Log2 Abundance Ratio
FASN
SLC2A4
CASP3
COL1A1
COL23A1
ITGB3
SLC4A1
TGFB1
COL3A1
ITGA2B
LAMTOR2
Log2 Mean Abundance
D
Increased in HS
KEGG pathway
Increased in LS
ECM-receptor interaction
Hematopoietic cell lineage
Carbon metabolism
Focal adhesion
Non-alcoholic fatty liver disease (NAFLD)
Rap1 signaling pathway
-log10(P)
Biosynthesis of amino acids
Carbon metabolism
Oxidative phosphorylation
Metabolic pathways
Fold Enrichment
E
Enriched Proteins
ECM-receptor interaction
COL1A1
COL23A1
COL3A1
COL6A1
COL6A2
COL6A3
GP1BA
SEPT5-GP1BA
ITGA2B
ITGB3
THSB1
Scaled Abundance (Σ = 200/protein)
F
p=0.02
ratio=1.46
Σ COL6A1-3 Normalized Intensity
G
TGFB1 Abundance Normalized Intensity

Figure III-5: Comparison of adipose tissue proteome in HS versus LS sub-cohorts.

A) Overview of proteomic workflow. B) Volcano plot showing differentially expressed proteins between groups ($p<0.05$, abundance ratio>1.5), and arrows indicating the number of proteins differentially expressed between groups. C) MA plots demonstrating differentially expressed proteins with respect to integrative abundance. D) Kyoto encyclopedia of genes and genomes (KEGG) pathway enrichment (top ten). E) Differentially expressed proteins from *ECM-receptor interaction* KEGG pathway (hsa04512). F) Protein expression for COL6A protein (∑COL6A1, COL6A2, COL6A3), and G) TGFβ1. Data are mean±SD. * $p<0.05$ and abundance ratio ≥1.5.

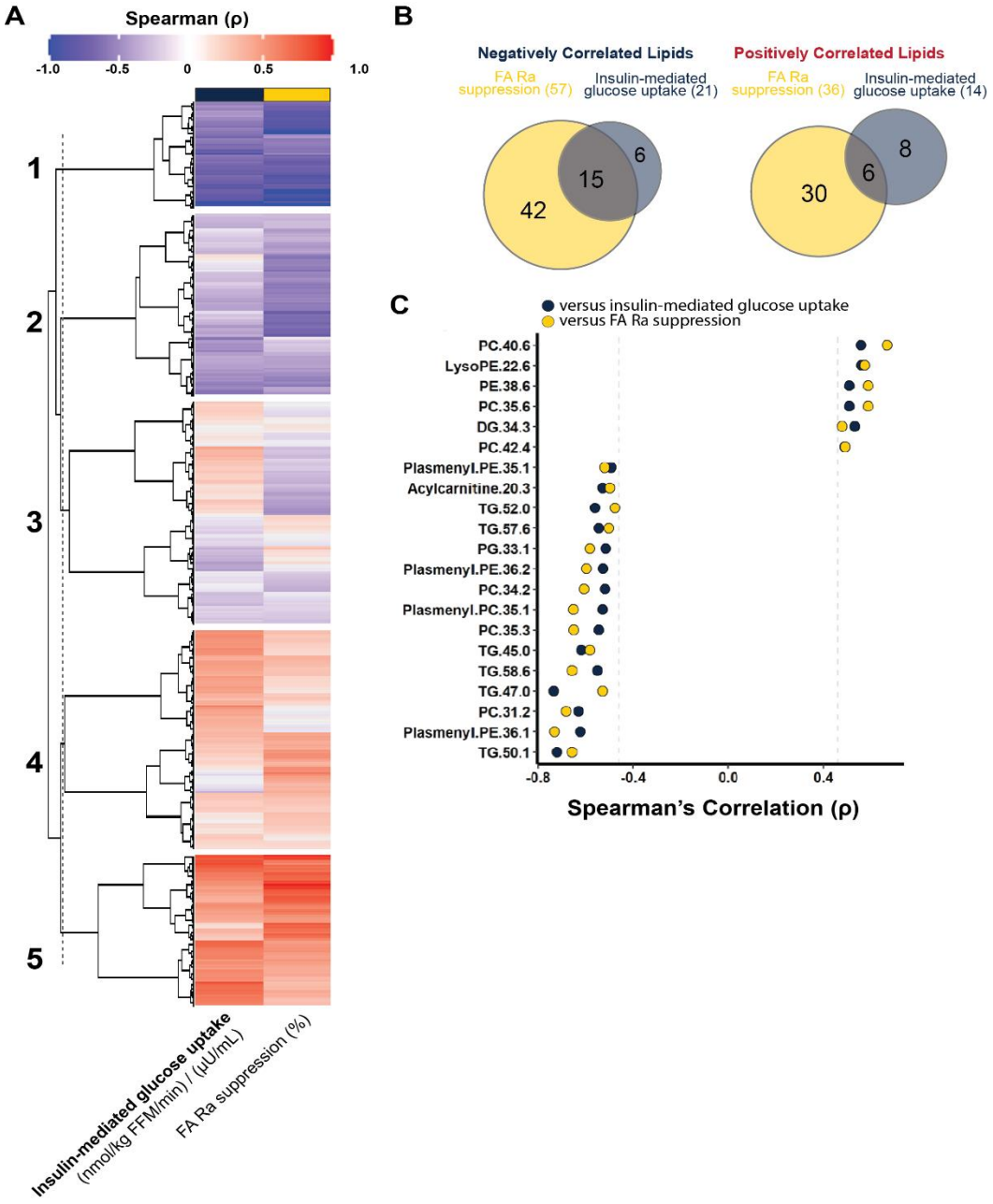

Figure III-6: Relationships between insulin sensitivity and skeletal muscle lipidomic profile.

A) Hierarchical clustering heatmap of lipids association with insulin-mediated glucose uptake and FA Ra suppression, (k=5). B) Venn-diagram of significant lipids grouped in cluster 1 - negative association with both insulin-mediated glucose uptake and FA Ra suppression, and cluster 5 - positive association with both insulin-mediated glucose uptake and FA Ra suppression. C) Significant association between individual lipid species for both insulin-mediated glucose uptake and FA Ra suppression. Significant values adjusted for multiple comparisons. n =18.

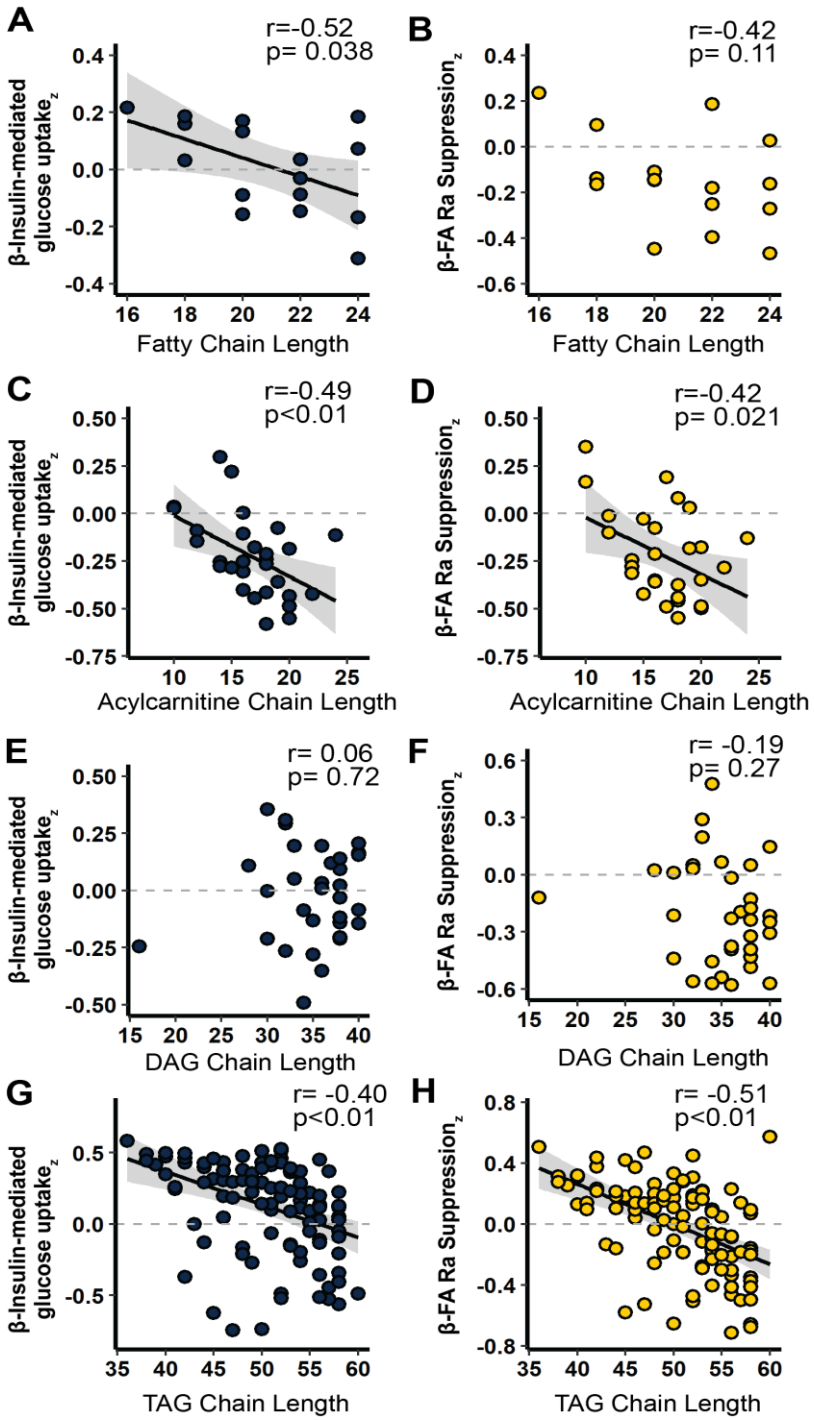

Figure III-7: Relationships between skeletal muscle free fatty acid, acylcarnitine, diacylglycerol, and triacylglycerol chain-length versus insulin-mediated glucose uptake$_z$, and FA Ra suppression$_z$.

(A-B) Relationships between beta coefficients describing models between acyl-chain lengths of skeletal muscle free fatty acids, (C-D) acylcarnitine, (E-F) diacylglycerol (DAG), and (G-H) triacylglycerol (TAG) on insulin-mediated glucose uptake$_z$ and FA Ra Suppression$_z$.

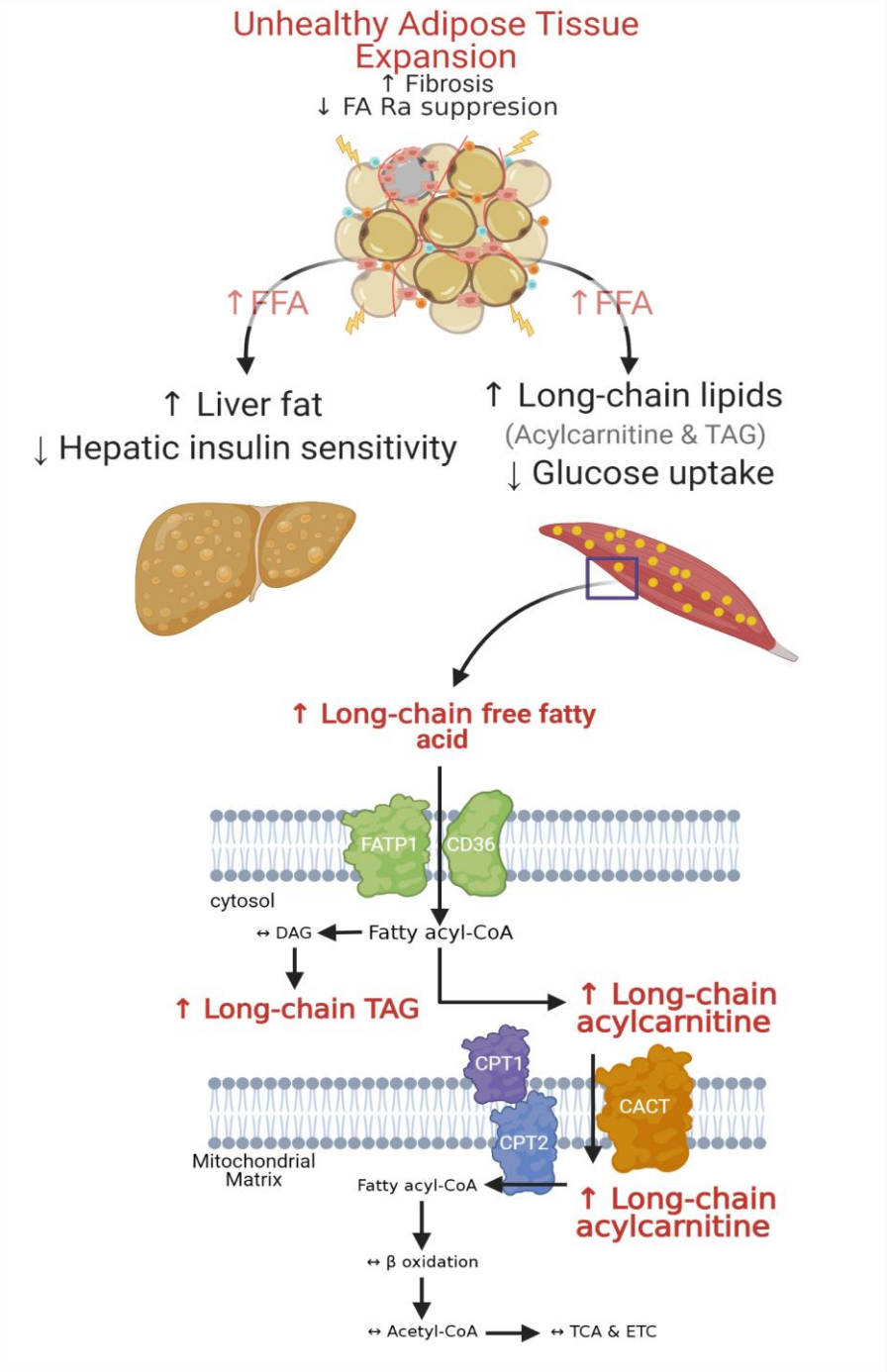

Figure III-8: Proposed tissue-specific *cross-talk* between adipose tissue fibrosis, impaired FA Ra suppression to insulin, and attenuated insulin-mediated glucose uptake in adults with obesity.

Insulin resistant adults with obesity presenting lower FA Ra suppression in adipose tissue had consequently elevated liver fat, as well as long-chain free-fatty acid, acylcarnitine, and triacylglycerol accumulation in skeletal muscle. These differences in fatty acid metabolism and/or extracellular matrix (i.e., collagen) accumulation may explain the potential mechanism contributing to the variability in whole-body and tissue-specific insulin sensitivity among adults with obesity.

TABLES

Table III-1: Participant characteristics from the entire cohort and sub-cohort analysis.

	All participants	**Sub-cohort analysis**		
	n=66	**HS** (n=8)	**LS** (n=8)	*p-value*
Sex	F=46,M=20	F=6,M=2	F=6,M=2	-
Age (yr)	31 ± 7	31 ± 6	32 ± 5	0.85
Body Weight (kg)	96.9 ± 12.2	94.7 ± 9.6	94.9 ± 8.7	0.96
Fat Mass (kg)	42.1 ± 6.7	40.7 ± 4.7	40.8 ± 5.8	0.99
Fat Free Mass (kg)	54.7 ± 9.5	53.9 ± 9.7	54.2 ± 9.1	0.96
Body Fat %	43.5 ± 5.4	43.3 ± 5.7	43.1 ± 6.1	0.95
BMI (kg/m^2)	34.0 ± 3.0	34.0 ± 2.6	33.8 ± 2.6	0.87
Fasting Glucose (mM)	4.9 ± 0.5	4.6 ± 0.4	4.8 ± 0.6	0.40
Fasting Insulin (μU/mL)	16.2 ± 9.7	7.0 ± 2.2	19.2 ± 10*	**<0.01**
HbA1c (%)	5.3 ± 0.4	5.1 ± 0.22	5.5 ± 0.6	0.13
HOMA-IR	3.6 ± 2.3	1.4 ± 0.5	4.2 ± 2.5*	**0.010**
NEFA (μM)	432 ± 169	378 ± 99	403 ± 164	0.72
Triglyceride (mM)	0.98 ± 0.6	0.6 ± 0.2	1.1 ± 0.4*	**0.015**
HDL (mg/dL)	39.4 ± 11.3	45.4 ± 15.1	36.8 ± 6.5	0.17

Values expressed as mean ± SD. Plasma concentrations were collected after an overnight fast. HS, high FA Ra suppression, LS, low FA Ra suppression, HOMA-IR, homeostatic model assessment for insulin resistance, NEFA, nonesterified fatty acids, HDL, high-density lipoprotein. * $p<0.05$ versus HS sub-cohort.

Table III-2: Multivariate regression for clinical and subclinical factors associated with insulin-mediated glucose uptake.

Model 1: Clinical Factors

variable	*β*	*SE (β)*	t	P-value
Adiponectin: HMW (ng/mL)	0.081	0.18	0.44	0.66
Adiponectin: Total (ng/mL)	0.026	0.28	0.092	0.93
Age (yrs)	0.17	0.26	0.67	0.51
BMI (kg/m^2)	-0.93	0.64	-1.44	0.16
HDL (mg/dL)	0.0045	0.0053	0.85	0.40
Liver Fat (%)	-0.13	0.10	-1.27	0.21
Sex (F=0, M=1)	-0.027	0.14	-0.19	0.85
Triglyceride (mM)	-0.24	0.23	-1.04	0.30
Visceral Fat (cm^2)	-0.041	0.15	-0.26	0.79
Residual Standard Error (df) = 0.38(58)				
Adjusted R^2 = 0.21				
F-statistic (df) = 3.41 (7,58)				
P-value = 0.004				

Model 2: Subclinical Factors

variable	*β*	*SE (β)*	t	P-value
Age (yrs)	0.033	0.18	0.18	0.86
Fatty Acid Ra: Clamp	-0.44	0.17	-2.67	0.01
Fatty acid Ra % suppression	0.070	0.018	3.87	<0.01
Fat oxidation	0.11	0.030	3.67	<0.01
Glucose Ra: Basal	0.79	0.43	1.83	0.07
Glucose Ra % suppression	0.0052	0.0038	1.38	0.17
Glycerol Ra: Clamp	0.44	0.19	2.33	0.02
Sex (F=0,M=1)	0.020	0.095	0.21	0.84
Residual Standard Error (df) = 0.29(57)				
Adjusted R^2 = 0.55				
F-statistic (df) = 13.43 (6,57)				
P-value = $2.29e^{-09}$				

Factors chosen per model were non-zero coefficients derived by LASSO Regression. Age and sex were maintained in both models as covariates.

Table III-3: Reagents

Reagents	Source	Identifier
D-Glucose (6,6-D2)	Cambridge Isotopes	DLM-349-PK
Glycerol (1,1,2,3,3-D5)	Cambridge Isotopes	DLM-1229-PK
Potassium Palmitate (1-13C, 99%)	Cambridge Isotopes	CLM-1889-PK
Glucose Oxidase	Thermo Fisher	A22189
NEFA Standard Solution	Wako Diagnostics	27676491
Triglyceride Reagent	Sigma-Aldrich	T2449
HDL-Cholesterol E	Wako Diagnostics	9059676
Total Cholesterol E	Wako Diagnostics	9138103
Human IL-6 ELISA	R&D Systems	HS600C
C-Reactive Protein ELISA	Calbiotech	CR120C
Human Leptin ELISA	Millipore Sigma	EZHL80SK
Human Total Adiponectin/Acrp30 ELISA	R&D Systems	DRP300
Human HMW Adiponectin/Acrp30 ELISA	R&D Systems	DHWAD0
Insulin For Immulite	Siemens	10381429
BCA Protein Assay Kit	Pierce Thermo-Fisher	23225

REFERENCES

1. Reaven GM. Banting lecture 1988. Role of insulin resistance in human disease. *Diabetes.* 1988;37(12):1595-607.
2. Smith GI, Mittendorfer B, and Klein S. Metabolically healthy obesity: facts and fantasies. *J Clin Invest.* 2019;129(10):3978-89.
3. Wildman RP, Muntner P, Reynolds K, McGinn AP, Rajpathak S, Wylie-Rosett J, et al. The Obese Without Cardiometabolic Risk Factor Clustering and the Normal Weight With Cardiometabolic Risk Factor Clustering: Prevalence and Correlates of 2 Phenotypes Among the US Population (NHANES 1999-2004). *Archives of Internal Medicine.* 2008;168(15):1617-24.
4. Stefan N, Kantartzis K, Machann J, Schick F, Thamer C, Rittig K, et al. Identification and characterization of metabolically benign obesity in humans. *Arch Intern Med.* 2008;168(15):1609-16.
5. Van Pelt DW, Guth LM, Wang AY, and Horowitz JF. Factors regulating subcutaneous adipose tissue storage, fibrosis, and inflammation may underlie low fatty acid mobilization in insulin-sensitive obese adults. 2017;313(4):E429-E39.
6. Van Pelt DW, Newsom SA, Schenk S, and Horowitz JF. Relatively low endogenous fatty acid mobilization and uptake helps preserve insulin sensitivity in obese women. *International Journal of Obesity.* 2015;39(1):149-55.
7. Magkos F, Fabbrini E, Conte C, Patterson BW, and Klein S. Relationship between Adipose Tissue Lipolytic Activity and Skeletal Muscle Insulin Resistance in Nondiabetic Women. *The Journal of Clinical Endocrinology & Metabolism.* 2012;97(7):E1219-E23.
8. Groop LC, Bonadonna RC, DelPrato S, Ratheiser K, Zyck K, Ferrannini E, et al. Glucose and free fatty acid metabolism in non-insulin-dependent diabetes mellitus. Evidence for multiple sites of insulin resistance. *J Clin Invest.* 1989;84(1):205-13.
9. Koh H-CE, van Vliet S, Pietka TA, Meyer GA, Razani B, Laforest R, et al. Subcutaneous adipose tissue metabolic function and insulin sensitivity in people with obesity. *Diabetes.* 2021:db210160.
10. Nielsen S, Guo Z, Johnson CM, Hensrud DD, and Jensen MD. Splanchnic lipolysis in human obesity. *J Clin Invest.* 2004;113(11):1582-8.
11. Guilherme A, Virbasius JV, Puri V, and Czech MP. Adipocyte dysfunctions linking obesity to insulin resistance and type 2 diabetes. *Nature Reviews Molecular Cell Biology.* 2008;9(5):367-77.
12. Crewe C, An YA, and Scherer PE. The ominous triad of adipose tissue dysfunction: inflammation, fibrosis, and impaired angiogenesis. *J Clin Invest.* 2017;127(1):74-82.
13. Sakers A, De Siqueira MK, Seale P, and Villanueva CJ. Adipose-tissue plasticity in health and disease. *Cell.* 2022;185(3):419-46.
14. Unger RH, Clark GO, Scherer PE, and Orci L. Lipid homeostasis, lipotoxicity and the metabolic syndrome. *Biochimica et biophysica acta.* 2010;1801(3):209-14.

15. Shulman GI. Cellular mechanisms of insulin resistance. *J Clin Invest.* 2000;106(2):171-6.

16. DeFronzo RA, Jacot E, Jequier E, Maeder E, Wahren J, and Felber JP. The Effect of Insulin on the Disposal of Intravenous Glucose: Results from Indirect Calorimetry and Hepatic and Femoral Venous Catheterization. 1981;30(12):1000-7.

17. Itani SI, Ruderman NB, Schmieder F, and Boden G. Lipid-Induced Insulin Resistance in Human Muscle Is Associated With Changes in Diacylglycerol, Protein Kinase C, and IκB-α. 2002;51(7):2005-11.

18. Adams JM, Pratipanawatr T, Berria R, Wang E, DeFronzo RA, Sullards MC, et al. Ceramide Content Is Increased in Skeletal Muscle From Obese Insulin-Resistant Humans. 2004;53(1):25-31.

19. Ellis BA, Poynten A, Lowy AJ, Furler SM, Chisholm DJ, Kraegen EW, et al. Long-chain acyl-CoA esters as indicators of lipid metabolism and insulin sensitivity in rat and human muscle. *Am J Physiol Endocrinol Metab.* 2000;279(3):E554-60.

20. Roden M, Krssak M, Stingl H, Gruber S, Hofer A, Fürnsinn C, et al. Rapid impairment of skeletal muscle glucose transport/phosphorylation by free fatty acids in humans. *Diabetes.* 1999;48(2):358-64.

21. Boden G. Role of fatty acids in the pathogenesis of insulin resistance and NIDDM. *Diabetes.* 1997;46(1):3-10.

22. Thiébaud D, DeFronzo RA, Jacot E, Golay A, Acheson K, Maeder E, et al. Effect of long chain triglyceride infusion on glucose metabolism in man. *Metabolism.* 1982;31(11):1128-36.

23. Yu C, Chen Y, Cline GW, Zhang D, Zong H, Wang Y, et al. Mechanism by which fatty acids inhibit insulin activation of insulin receptor substrate-1 (IRS-1)-associated phosphatidylinositol 3-kinase activity in muscle. *The Journal of biological chemistry.* 2002;277(52):50230-6.

24. Bajaj M, Suraamornkul S, Romanelli A, Cline GW, Mandarino LJ, Shulman GI, et al. Effect of a Sustained Reduction in Plasma Free Fatty Acid Concentration on Intramuscular Long-Chain Fatty Acyl-CoAs and Insulin Action in Type 2 Diabetic Patients. 2005;54(11):3148-53.

25. van Hees AM, Jans A, Hul GB, Roche HM, Saris WH, and Blaak EE. Skeletal muscle fatty acid handling in insulin resistant men. *Obesity (Silver Spring, Md).* 2011;19(7):1350-9.

26. DeFronzo RA, Tobin JD, and Andres R. Glucose clamp technique: a method for quantifying insulin secretion and resistance. *The American journal of physiology.* 1979;237(3):E214-23.

27. Dixon WT. Simple proton spectroscopic imaging. 1984;153(1):189-94.

28. Ryan BJ, Schleh MW, Ahn C, Ludzki AC, Gillen JB, Varshney P, et al. Moderate-intensity exercise and high-intensity interval training affect insulin sensitivity similarly in obese adults. *The Journal of clinical endocrinology and metabolism.* 2020.

29. Bligh EG, and Dyer WJ. A rapid method of total lipid extraction and purification. *Canadian journal of biochemistry and physiology.* 1959;37(8):911-7.

30. Kind T, Liu KH, Lee DY, DeFelice B, Meissen JK, and Fiehn O. LipidBlast in silico tandem mass spectrometry database for lipid identification. *Nature methods.* 2013;10(8):755-8.

31. Steele R. Influences of glucose loading and of injected insulin on hepatic glucose output. *Annals of the New York Academy of Sciences.* 1959;82:420-30.

32. Weir JBDB. New methods for calculating metabolic rate with special reference to protein metabolism. *J Physiol.* 1949;109(1-2):1-9.

33. Frayn KN. Calculation of substrate oxidation rates in vivo from gaseous exchange. *Journal of Applied Physiology.* 1983;55(2):628-34.

34. Parlee SD, Lentz SI, Mori H, and MacDougald OA. In: Macdougald OA ed. *Methods in Enzymology*. Academic Press; 2014:93-122.

35. Divoux A, Tordjman J, Lacasa D, Veyrie N, Hugol D, Aissat A, et al. Fibrosis in Human Adipose Tissue: Composition, Distribution, and Link With Lipid Metabolism and Fat Mass Loss. *Diabetes.* 2010;59(11):2817.

36. Schneider CA, Rasband WS, and Eliceiri KW. NIH Image to ImageJ: 25 years of image analysis. *Nature methods.* 2012;9(7):671-5.

37. Friedman J, Hastie T, and Tibshirani R. Regularization Paths for Generalized Linear Models via Coordinate Descent. *Journal of statistical software.* 2010;33(1):1-22.

38. Revelle W. psych: Procedures for Psychological, Psychometric, and Personality Research. *Northwestern University.* 2020.

39. Smyth GK. Linear models and empirical bayes methods for assessing differential expression in microarray experiments. *Statistical applications in genetics and molecular biology.* 2004;3:Article3.

40. Benjamini Y, and Hochberg Y. Controlling the false discovery rate: A practical and powerful approach to multiple testing. *Journal of the Royal Statistical Society.* 1995;57(1):289-300.

41. R Core Team. R: A Language and Environment for Statistical Computing. *R Foundation for Statistical Computing.* 2019.

42. Kanehisa M, and Goto S. KEGG: kyoto encyclopedia of genes and genomes. *Nucleic acids research.* 2000;28(1):27-30.

43. Khan T, Muise ES, Iyengar P, Wang ZV, Chandalia M, Abate N, et al. Metabolic Dysregulation and Adipose Tissue Fibrosis: Role of Collagen VI. 2009;29(6):1575-91.

44. Spencer M, Yao-Borengasser A, Unal R, Rasouli N, Gurley CM, Zhu B, et al. Adipose tissue macrophages in insulin-resistant subjects are associated with collagen VI and fibrosis and demonstrate alternative activation. *Am J Physiol Endocrinol Metab.* 2010;299(6):E1016-27.

45. Keophiphath M, Achard V, Henegar C, Rouault C, Clément K, and Lacasa Dl. Macrophage-Secreted Factors Promote a Profibrotic Phenotype in Human Preadipocytes. *Molecular Endocrinology.* 2009;23(1):11-24.

46. Santomauro AT, Boden G, Silva ME, Rocha DM, Santos RF, Ursich MJ, et al. Overnight lowering of free fatty acids with Acipimox improves insulin resistance and glucose tolerance in obese diabetic and nondiabetic subjects. *Diabetes.* 1999;48(9):1836-41.

47. Horowitz JF, Coppack SW, Paramore D, Cryer PE, Zhao G, and Klein S. Effect of short-term fasting on lipid kinetics in lean and obese women. *The American journal of physiology.* 1999;276(2):E278-84.

48. Wolfe BM, Klein S, Peters EJ, Schmidt BF, and Wolfe RR. Effect of elevated free fatty acids on glucose oxidation in normal humans. *Metabolism.* 1988;37(4):323-9.

49. Campbell PJ, Carlson MG, Hill JO, and Nurjhan N. Regulation of free fatty acid metabolism by insulin in humans: role of lipolysis and reesterification. *The American journal of physiology.* 1992;263(6):E1063-9.

50. Yeckel CW, Dziura J, and DiPietro L. Abdominal obesity in older women: potential role for disrupted fatty acid reesterification in insulin resistance. *The Journal of clinical endocrinology and metabolism.* 2008;93(4):1285-91.

51. Meegalla RL, Billheimer JT, and Cheng D. Concerted elevation of acyl-coenzyme A:diacylglycerol acyltransferase (DGAT) activity through independent stimulation of mRNA expression of DGAT1 and DGAT2 by carbohydrate and insulin. *Biochem Biophys Res Commun.* 2002;298(3):317-23.

52. Ali AH, Mundi M, Koutsari C, Bernlohr DA, and Jensen MD. Adipose Tissue Free Fatty Acid Storage In Vivo: Effects of Insulin Versus Niacin as a Control for Suppression of Lipolysis. *Diabetes.* 2015;64(8):2828-35.

53. Chuang S-J, Johanns M, Pyr dit Ruys S, Steinberg GR, Kemp BE, Viollet B, et al. AMPK activation by SC4 inhibits noradrenaline-induced lipolysis and insulin-stimulated lipogenesis in white adipose tissue. *Biochemical Journal.* 2021;478(21):3869-89.

54. Frayn KN, Shadid S, Hamlani R, Humphreys SM, Clark ML, Fielding BA, et al. Regulation of fatty acid movement in human adipose tissue in the postabsorptive-to-postprandial transition. *American Journal of Physiology-Endocrinology and Metabolism.* 1994;266(3):E308-E17.

55. Wueest S, Rapold RA, Rytka JM, Schoenle EJ, and Konrad D. Basal lipolysis, not the degree of insulin resistance, differentiates large from small isolated adipocytes in high-fat fed mice. *Diabetologia.* 2009;52(3):541-6.

56. Laurencikiene J, Skurk T, Kulyté A, Hedén P, Åström G, Sjölin E, et al. Regulation of Lipolysis in Small and Large Fat Cells of the Same Subject. *The Journal of Clinical Endocrinology & Metabolism.* 2011;96(12):E2045-E9.

57. Weyer C, Foley JE, Bogardus C, Tataranni PA, and Pratley RE. Enlarged subcutaneous abdominal adipocyte size, but not obesity itself, predicts type II diabetes independent of insulin resistance. *Diabetologia.* 2000;43(12):1498-506.

58. Goossens GH, Bizzarri A, Venteclef N, Essers Y, Cleutjens JP, Konings E, et al. Increased adipose tissue oxygen tension in obese compared with lean men is accompanied by insulin resistance, impaired adipose tissue capillarization, and inflammation. *Circulation.* 2011;124(1):67-76.

59. Sun K, Halberg N, Khan M, Magalang UJ, and Scherer PE. Selective Inhibition of Hypoxia-Inducible Factor 1α Ameliorates Adipose Tissue Dysfunction. *Molecular and Cellular Biology.* 2013;33(5):904.

60. Fujisaka S, Usui I, Ikutani M, Aminuddin A, Takikawa A, Tsuneyama K, et al. Adipose tissue hypoxia induces inflammatory M1 polarity of macrophages in an HIF-1α-dependent and HIF-1α-independent manner in obese mice. *Diabetologia.* 2013;56(6):1403-12.

61. Cifarelli V, Beeman SC, Smith GI, Yoshino J, Morozov D, Beals JW, et al. Decreased adipose tissue oxygenation associates with insulin resistance in individuals with obesity. *J Clin Invest.* 2020;130(12):6688-99.

62. Weisberg SP, McCann D, Desai M, Rosenbaum M, Leibel RL, and Ferrante AW, Jr. Obesity is associated with macrophage accumulation in adipose tissue. *J Clin Invest.* 2003;112(12):1796-808.

63. Murdolo G, Hammarstedt A, Sandqvist M, Schmelz M, Herder C, Smith U, et al. Monocyte chemoattractant protein-1 in subcutaneous abdominal adipose tissue: characterization of interstitial concentration and regulation of gene expression by insulin. *The Journal of clinical endocrinology and metabolism.* 2007;92(7):2688-95.

64. Pietiläinen KH, Kannisto K, Korsheninnikova E, Rissanen A, Kaprio J, Ehrenborg E, et al. Acquired obesity increases CD68 and tumor necrosis factor-alpha and decreases adiponectin gene expression in adipose tissue: a study in monozygotic twins. *The Journal of clinical endocrinology and metabolism.* 2006;91(7):2776-81.

65. Lagathu C, Yvan-Charvet L, Bastard JP, Maachi M, Quignard-Boulangé A, Capeau J, et al. Long-term treatment with interleukin-1β induces insulin resistance in murine and human adipocytes. *Diabetologia.* 2006;49(9):2162-73.

66. Hotamisligil GS, Peraldi P, Budavari A, Ellis R, White MF, and Spiegelman BM. IRS-1-mediated inhibition of insulin receptor tyrosine kinase activity in TNF-alpha- and obesity-induced insulin resistance. *Science.* 1996;271(5249):665-8.

67. Lagathu C, Bastard J-P, Auclair M, Maachi M, Capeau J, and Caron M. Chronic interleukin-6 (IL-6) treatment increased IL-6 secretion and induced insulin resistance in adipocyte: prevention by rosiglitazone. *Biochemical and Biophysical Research Communications.* 2003;311(2):372-9.

68. Marcelin G, Silveira ALM, Martins LB, Ferreira AVM, and Clément K. Deciphering the cellular interplays underlying obesity-induced adipose tissue fibrosis. *J Clin Invest.* 2019;129(10):4032-40.

69. Halberg N, Khan T, Trujillo ME, Wernstedt-Asterholm I, Attie AD, Sherwani S, et al. Hypoxia-inducible factor 1alpha induces fibrosis and insulin resistance in white adipose tissue. *Mol Cell Biol.* 2009;29(16):4467-83.

70. Marcelin G, Ferreira A, Liu Y, Atlan M, Aron-Wisnewsky J, Pelloux V, et al. A PDGFRα-Mediated Switch toward CD9(high) Adipocyte Progenitors Controls Obesity-Induced Adipose Tissue Fibrosis. *Cell Metab.* 2017;25(3):673-85.

71. Pellegrinelli V, Heuvingh J, du Roure O, Rouault C, Devulder A, Klein C, et al. Human adipocyte function is impacted by mechanical cues. *J Pathol.* 2014;233(2):183-95.

72. Scharenberg MA, Pippenger BE, Sack R, Zingg D, Ferralli J, Schenk S, et al. TGF-β-induced differentiation into myofibroblasts involves specific regulation of two MKL1 isoforms. *J Cell Sci.* 2014;127(Pt 5):1079-91.

73. Massagué J. TGFβ signalling in context. *Nature Reviews Molecular Cell Biology.* 2012;13(10):616-30.

74. Vila IK, Badin PM, Marques MA, Monbrun L, Lefort C, Mir L, et al. Immune cell Toll-like receptor 4 mediates the development of obesity- and endotoxemia-associated adipose tissue fibrosis. *Cell Rep.* 2014;7(4):1116-29.

75. Shao M, Hepler C, Zhang Q, Shan B, Vishvanath L, Henry GH, et al. Pathologic HIF1α signaling drives adipose progenitor dysfunction in obesity. *Cell Stem Cell.* 2021;28(4):685-701.e7.

76. Samuel VT, Liu Z-X, Qu X, Elder BD, Bilz S, Befroy D, et al. Mechanism of Hepatic Insulin Resistance in Non-alcoholic Fatty Liver Disease. 2004;279(31):32345-53.

77. Shulman GI. Ectopic Fat in Insulin Resistance, Dyslipidemia, and Cardiometabolic Disease. *New England Journal of Medicine.* 2014;371(12):1131-41.

78. Koves TR, Ussher JR, Noland RC, Slentz D, Mosedale M, Ilkayeva O, et al. Mitochondrial Overload and Incomplete Fatty Acid Oxidation Contribute to Skeletal Muscle Insulin Resistance. *Cell Metabolism.* 2008;7(1):45-56.

79. Bloch-Damti A, and Bashan N. Proposed mechanisms for the induction of insulin resistance by oxidative stress. *Antioxidants & redox signaling.* 2005;7(11-12):1553-67.

80. Muoio Deborah M, and Neufer PD. Lipid-Induced Mitochondrial Stress and Insulin Action in Muscle. *Cell Metabolism.* 2012;15(5):595-605.

81. Adams SH, Hoppel CL, Lok KH, Zhao L, Wong SW, Minkler PE, et al. Plasma acylcarnitine profiles suggest incomplete long-chain fatty acid beta-oxidation and altered tricarboxylic acid cycle activity in type 2 diabetic African-American women. *The Journal of nutrition.* 2009;139(6):1073-81.

82. Fisher-Wellman KH, and Neufer PD. Linking mitochondrial bioenergetics to insulin resistance via redox biology. *Trends in endocrinology and metabolism: TEM.* 2012;23(3):142-53.

83. Anderson EJ, Lustig ME, Boyle KE, Woodlief TL, Kane DA, Lin CT, et al. Mitochondrial H2O2 emission and cellular redox state link excess fat intake to insulin resistance in both rodents and humans. *J Clin Invest.* 2009;119(3):573-81.

84. Aguer C, McCoin CS, Knotts TA, Thrush AB, Ono-Moore K, McPherson R, et al. Acylcarnitines: potential implications for skeletal muscle insulin resistance. *FASEB journal : official publication of the Federation of American Societies for Experimental Biology.* 2015;29(1):336-45.

85. Özcan U, Cao Q, Yilmaz E, Lee A-H, Iwakoshi NN, Özdelen E, et al. Endoplasmic Reticulum Stress Links Obesity, Insulin Action, and Type 2 Diabetes. 2004;306(5695):457-61.

86. Malhotra JD, and Kaufman RJ. Endoplasmic reticulum stress and oxidative stress: a vicious cycle or a double-edged sword? *Antioxidants & redox signaling.* 2007;9(12):2277-93.

87. Funai K, Lodhi IJ, Spears LD, Yin L, Song H, Klein S, et al. Skeletal Muscle Phospholipid Metabolism Regulates Insulin Sensitivity and Contractile Function. 2016;65(2):358-70.

88. Borkman M, Storlien LH, Pan DA, Jenkins AB, Chisholm DJ, and Campbell LV. The relation between insulin sensitivity and the fatty-acid composition of skeletal-muscle phospholipids. *The New England journal of medicine.* 1993;328(4):238-44.

89. Heden TD, Neufer PD, and Funai K. Looking Beyond Structure: Membrane Phospholipids of Skeletal Muscle Mitochondria. *Trends in Endocrinology & Metabolism.* 2016;27(8):553-62.

90. Newsom SA, Brozinick JT, Kiseljak-Vassiliades K, Strauss AN, Bacon SD, Kerege AA, et al. Skeletal muscle phosphatidylcholine and phosphatidylethanolamine are related to insulin sensitivity and respond to acute exercise in humans. 2016;120(11):1355-63.

91. Funai K, Song H, Yin L, Lodhi IJ, Wei X, Yoshino J, et al. Muscle lipogenesis balances insulin sensitivity and strength through calcium signaling. *J Clin Invest.* 2013;123(3):1229-40.

92. Thorp AA, and Schlaich MP. Relevance of Sympathetic Nervous System Activation in Obesity and Metabolic Syndrome. *J Diabetes Res.* 2015;2015:341583.

93. Bäckdahl J, Franzén L, Massier L, Li Q, Jalkanen J, Gao H, et al. Spatial mapping reveals human adipocyte subpopulations with distinct sensitivities to insulin. *Cell Metabolism.* 2021;33(9):1869-82.e6.

94. Li Q, Hagberg CE, Silva Cascales H, Lang S, Hyvönen MT, Salehzadeh F, et al. Obesity and hyperinsulinemia drive adipocytes to activate a cell cycle program and senesce. *Nature Medicine.* 2021.

Chapter IV

Project 2
Comparison of Intramyocellular Lipid Accumulation and Skeletal Muscle Insulin Signaling in Obese Adults with High versus Low Insulin Sensitivity

ABSTRACT

The vast majority of adults with obesity are insulin resistant, but factors explaining why some obese adults remain relatively insulin sensitive are not clear. Based on previous work by our lab and others, differences in systemic fatty acid (FA) availability, intramyocellular lipid accumulation, and altered insulin signaling events in skeletal muscle are all likely candidates. The primary aims of this study were: 1) to compare the number and size of lipid droplets (LDs) within the intramyofibrillar (IMF) and subsarcolemmal (SS) regions of skeletal muscle from cohorts of obese adults with high versus low insulin sensitivity, and 2) to compare insulin signaling events within skeletal muscle from the same cohorts of obese subjects with high versus low insulin sensitivity. Seventeen adults with obesity completed a 2h hyperinsulinemic-euglycemic clamp with stable isotope tracer infusions ([6,6$^{2}H_{2}$]glucose and [1-^{13}C]palmitate) to measure glucose rate of disappearance from the circulation (Glucose Rd) and FA rate of appearance (FA Ra) into the circulation under basal and insulin-mediated conditions. Skeletal muscle biopsies were collected under fasted conditions (basal) and 30min into the hyperinsulinemic clamp. Participants were stratified into HIGH (n=7, BMI=35±3kg/m^{2}) and LOW (n=10, BMI=36±3 kg/m^{2}) insulin sensitivity sub-cohorts based on their Glucose Rd measured during the clamp (LOW: 273±54, HIGH: 817±256 nmol/kgFFM/min/[μU insulin/mL]). We found insulin-mediated suppression of FA Ra in response to insulin was attenuated in LOW versus HIGH ($p<0.01$), suggesting a relatively high systemic FA availability in LOW may contribute to their insulin resistance. Although total intramyocellular lipid content was not different between LOW and HIGH, we found significantly larger LDs in the SS region of the myocyte in LOW versus HIGH ($p<0.01$), which may contribute to their insulin resistance by interfering with key insulin signaling processes at the muscle membrane. Additionally, we also found insulin receptor (IR) interaction with the regulatory

proteins CD36 and Fyn to be suppressed in LOW vs HIGH ($p<0.01$), which aligned with attenuated insulin-mediated phosphorylation of IRβ and other key downstream proteins in LOW ($p<0.05$). Overall, our findings indicate that low insulin sensitivity to reduce FA mobilization from adipose tissue may contribute to insulin resistance via modifications in LD size and distribution within the myocyte, as well as through disruption of the IR to interact with key regulatory proteins.

INTRODUCTION

Obesity has now surpassed 40% of the United States population (1), and is a major risk factor for the development of chronic metabolic disorders such as insulin resistance (2, 3), which in turn underlies many obesity-related diseases. Although most adults with obesity are insulin resistant, some remain relatively insulin sensitive (4-8), and the factors helping protect against the development on insulin resistance in these individuals are not clear. Work from our lab (9, 10) and others (11-13) indicate the rate of fatty acid (FA) mobilization in the systemic circulation is directly linked with whole-body insulin sensitivity among adults with obesity. The vast majority of FA in the systemic circulation are derived from abdominal subcutaneous adipose tissue (aSAT) (14), and based on findings from Project 1 of my dissertation, as well as other previous work (10-13), we contend that variability in the regulation of FA release from aSAT is an important contributor to the differences in the magnitude of insulin resistance among adults with obesity.

The link between excessive systemic FA mobilization and whole-body insulin resistance has been largely attributed to high rates of FA uptake into skeletal muscle and the resultant accumulation of intramyocellular lipids (15, 16). In particular, the lipid-intermediates diacylglycerol (17) and ceramide (18), and long-chain fatty acyl CoA (19, 20) have been reported to disrupt insulin signaling – but the contribution of each of these lipid intermediates to insulin resistance remains somewhat controversial (21-23). Intramyocellular lipids are primarily stored within lipid droplets (LD), which are composed of a triacylglycerol-rich core surrounded by a phospholipid monolayer containing proteins that can regulate FA storage and release, as well as help navigate intracellular trafficking/transport of the LD (24, 25). Importantly, the role of the LDs can vary depending on their location within the myocyte. For example, LDs within the intramyofibrillar region (IMF; towards the center of the myocyte) are proposed to support mitochondrial respiration and muscle contraction (26, 27), and LDs in the subsarcolemmal region (SS; towards the periphery of the myocyte) primarily support membrane function. The

intracellular distribution of LDs within the myocyte has also been linked with insulin resistance, where LDs in the SS region have been linked with impaired insulin sensitivity (28-30), perhaps a consequence of a greater lipid intermediate release in the vicinity of the membrane where insulin signaling is initiated. Differences in the number and size of intramyocellular LDs within the IMF and SS regions may also impact insulin sensitivity, but these relationships have not been firmly established. One of the principal aims of this study was to compare the number and size of LDs within the IMF and SS regions of skeletal muscle from a cohort of adults with high versus low insulin sensitivity.

Classically, the disruption of insulin signaling induced by the intramyocellular lipids have primarily been attributed to modifications in the phosphorylation of signaling proteins downstream of the insulin receptor (e.g., insulin receptor substrate-1 (IRS-1), Akt). However, some recent evidence suggests the lipid-induced disruption of insulin receptor (IR) may also contribute to insulin resistance (31). The membrane glycoprotein, cluster of differentiation 36 (CD36) is well-known for its role in regulating long-chain FA uptake (32, 33), but it may also play a role in modifying IR phosphorylation and downstream signaling (31). The physical interaction between CD36 and the insulin receptor has been found to increase phosphorylation of the insulin receptor via CD36-mediated recruitment of the src family tyrosine kinase, Fyn (31). Conversely elevated saturated FA availability attenuated Fyn kinase recruitment to CD36 (31, 34), leading to a blunted insulin signaling (31). These previous experiments have been conducting *in vitro*, and whether differences in systemic FA availability among adults with obesity may contribute to modifications in CD36 recruitment of Fyn kinase to the insulin receptor (IR), and modify IR phosphorylation and downstream signaling in human skeletal muscle is not known. Therefore, another major aim of this study was to compare basal- and insulin-mediated interaction between CD36 and Fyn kinase with IRβ, as well as proximal insulin-stimulated signaling events in skeletal muscle from a cohort of adults with high versus low insulin sensitivity.

METHODS

Participants

Seventeen men (n=6) and women (n=11) with obesity participated in this study (BMI=30-40 kg/m^2). All participants were 'inactive' by not engaging in any planned physical aerobic or resistance exercise, and weight stable (±2 kg for the previous 6 months). Participants were not be

taking medications known to affect glucose or lipid metabolism, have a history of heart disease, or smokers. All women participating in the study were pre-menopausal with regularly occurring menses, and not pregnant, or lactating. Participants were provided written informed consent before participation. The study protocol was approved by the University of Michigan Institutional Review Board, and registered at clinicaltrials.gov (NCT02717832).

Preliminary Assessment: Body Composition, Visceral Fat Area, and Liver Fat.

Body composition was assessed by dual-energy X-ray absorptiometry (Lunar DPX DEXA Scanner, GE, Madison, WI) at the Michigan Clinical Unit (MCRU). Visceral fat area (cm^2) and hepatic fat percentage was measured by magnetic resonance imaging (MRI: Ingenia 3T MR System, Phillips, Netherlands) at the University of Michigan Medicine's Department of Radiology.

Experimental Protocol

The night before the experimental trial, participants were provided a standardized meal at 1900h (30% estimated daily energy expenditure; 55% carbohydrate, 30% fat, 15% protein) and a snack at 2200h (see Appendix G for study schematic). The following morning, participants arrived to MCRU at 0700h and quietly rested for 60min. Intravenous catheters were inserted at ~0800h into the hand vein for continuous blood sampling, and forearm vein for continuous isotope, insulin, and glucose infusion. At ~0900h, a baseline blood sample was collected for background isotope labeling, followed by a primed continuous infusion of [6,6 $^2H_2$]glucose (35 µmol/kg priming dose, and 0.41 µmol/kg/min continuous infusion; Cambridge Isotopes). At ~0915h, a skeletal muscle biopsy was collected from the vastus lateralis muscle. Upon obtaining the muscle biopsy, visible connective tissue was removed, and the first two samples were manually aligned in parallel to confirm muscle fibers were oriented, then were fixed in optimal cutting temperature (OCT) solid, and flash frozen in isopentane chilled over liquid nitrogen. The remaining samples were rinsed with saline, blotted dry, and flash frozen in liquid nitrogen for immunoblot analysis. Following the basal muscle biopsy, a continuous [1-^{13}C]palmitate bound to human albumin infusion began at ~1000h (0.04 µmol/kg/min continuous infusion; Cambridge). By ~1050h, three 'arterialized' samples collected (heated hand technique) basal glucose and FA kinetics. At ~1100h, a 2h hyperinsulinemic-euglycemic clamp procedure (40 $mU/m^2/min$) began to determine whole-body insulin sensitivity (35). Exactly 30min into the hyperinsulinemic clamp procedure, a second

muscle biopsy was obtained to identify insulin-mediated signaling events occurring after acute insulin exposure. Continuous blood glucose samples were obtained and measured every 5min (StatStrip, Nova Biomedical, Waltham MA), and dextrose infusion rate (20% dextrose in 0.9% NaCl) was adjusted accordingly to accommodate insulin-induced hypoglycemia and attain baseline glucose concertation (~5.0 mM). After the 2h clamp procedure, and when glucose was stabilized for ~20 minutes without adjusting glucose infusion rate, arterialized blood samples were collected to quantify insulin-mediated substrate kinetics, and clamp insulin concentration.

Participant stratification by glucose Rd

For paired analyses, participants were stratified into binary sub-cohorts of LOW glucose Rd (181 nmol/kg FFM/min / (μU/mL) ≤ LOW ≤ 382 nmol/kg FFM/min / (μU/mL); n=10) and HIGH glucose Rd (552 nmol/kg FFM/min / (μU/mL) ≤ HIGH ≤ 1274 nmol/kg FFM/min / (μU/mL);n=7).

Analytical Procedures

Plasma glucose and fatty acid kinetics.

The tracer-to-tracee ratio (TTR) for calculations pertaining to glucose and palmitate kinetics were determined by gas-chromatography-mass spectrometry (GC/MS) using a Mass Selective Detector 5973 system (Agilent Technologies, Santa Clara, CA), as described previously by our lab (36). FA rate of appearance (Ra) was determined by dividing palmitate Ra by the ratio of total palmitate (C16:0) to FAs within a standard. Glucose TTR was selectively analyzed and peak abundances averaged at the following m/z for ion fragments (103/105, 115/117, 127/129, and 217/219) for endogenous and isotope labeled [6,6 $^{2}H_{2}$]glucose respectively. FA Ra and Glucose Ra were calculated from their respective TTR using the Steele equation for steady state conditions (37).

Plasma glucose, lipid, and insulin concentration

Plasma glucose, non-esterified fatty acid (NEFA), triglyceride, high-density lipoproteins (HDL), and total cholesterol were measured in plasma from commercially available colorimetric assays. Plasma interleukin-6 (IL-6), C-reactive protein (CRP), leptin, total adiponectin, and high

molecular-weight (HMW) adiponectin were measured via enzyme-linked immunoassay (ELISA). Insulin was measured by radioimmunoassay (Siemens). See Table IV-2 for vendor details

Skeletal muscle histochemistry: lipid droplet analysis

Skeletal muscle from OCT embedded samples were cut into 5µm sections at -20°C and mounted onto an ethanol-cleaned glass slide. Sections were fixed in 4% paraformaldehyde for 1h, and permeabilized for 5min in 0.5% Triton X-100. Sections were then incubated with primary antibodies myosin heavy chain type 1 (MHC-1) at 1:200 for 1h at 37ºC, followed by 30min secondary antibody incubation: AlexaFluor 647, goat-anti mouse IgG2b at 1:200. Afterwards, sections were stained with Bodipy 493/503 at 1:100 for 20min, followed by 20min incubation with anti-wheat germ agglutinin (WGA) conjugated with AlexaFluor 555 to identify muscle membranes. Sections were mounted with ProLong Gold Antifade Mountant, covered with #1 coverslips (2975-245, Corning), and stored in the dark until imaging. See Table IV-2 for detailed list for histochemistry and immunohistochemistry products, and Appendix H for detailed protocol.

Fluorescence image acquisition, image processing, and analysis

LD area (% stained), LD density (# LDs/mm^2), and median LD size (µm^2) were captured on a Keyence Bz-X710 fluorescence microscope (Keyence) with a 20X N.A.=0.45 objective lens using 1440 X 1080 pixels (533 µm x 400 µm) field of view. Bodipy 493/503 was captured using GFP (470/40 nm) filter, MHC type I was captured using Cy5 (620/60 nm) filter, and WGA captured using Texas Red (560/40nm) filter. Following image capture, LD characteristics (i.e., size and density), and distribution were quantified using a custom script developed in MATLAB R2021a (Mathworks, Inc., Natick, MA). In brief, images captured at 20X were converted to grayscale and re-scaled to accommodate image variability between samples. Individual fibers were identified and labeled using a custom ridge detection algorithm, and watershed segmentation to complete non-continuous cell borders and completely identify cells. Type I fibers were identified based on positive MHC type I-positive stain, and non-stained fibers considered type II fibers. Fiber types were partitioned into type I or type II fibers dependent on signal intensity using k-means clustering (k=2). Lipid droplets identified in the SS region were contained within ~3 µm of the peripheral border of each fiber (10 pixel width), while the IMF region was all remaining area in the center of each fiber (IMF region; ~91% of total myocyte volume). Lipid droplets were detected as the mean area of puncta, and a top-hat filter was used to accommodate for image

variability and background noise within the sample. Lipid droplets identified and included for analysis for within each muscle were contained within a normal Gaussian distribution. In total, ~3 fields of view were obtained per participant, resulting in 125±57 muscle fibers analyzed per participant.

Skeletal muscle lysate preparation for immunoblot

Frozen muscle samples were weighed (~25mg) and transferred into pre-chilled microcentrifuge tubes containing 1mL ice-cold lysis buffer [RIPA Buffer: 20 mM Tris-HCl-pH 7.5, 150 mM NaCl, 1 mM Na_2EDTA, 1 mM EGTA, 1% NP-40, 1% sodium deoxycholate, 2.5 mM sodium pyrophosphate, 1 mM β-glycerophosphate, 1 mM Na_3VO_4, 1 µg/mL leupeptin (9086, Cell Signaling Technology)], 1% phosphatase inhibitor cocktail #1 & #2 (P2850, P5726, Sigma-Aldrich), 1% protease inhibitor cocktail (P8340, Sigma-Aldrich), and two steel ball bearings per sample. Samples were homogenized for 30s at 45Hz using Qiagen TissueLyser II, then solubilized for 60min by inverted end-over-end rotation at 50rpm in the cold (4°C). Afterwards, samples were centrifuged at 15,000g for 15 minutes at 4°C, discarding the pellet. Protein concentration was determined by bicinchoninic acid (BCA) assay (23225, Pierce Thermo-Fisher), and samples were diluted in 4x Laemmli buffer (1610747, Bio-Rad) to 1mg/mL concentration, and heated for 7min at 95°C. Proteins were separated by SDS-Page (8-12% acrylamide), transferred to nitrocellulose membranes, and probed for the following primary antibodies displayed in Table IV-2. To account for loading control, membranes were normalized to total protein abundance determined by Memcode reversible protein stain (24580, Pierce Thermo-Fisher), and each gel contained an internal standard sample from 8 obese individuals to account for gel-to-gel variability. Each protein was also normalized to their internal standard.

Immunoprecipitation

Frozen skeletal muscle samples were homogenized in 1% Triton-based lysis buffer [20 mM Tris-HCl (pH 7.5), 150 mM NaCl, 1 mM Na2EDTA, 1 mM EGTA, 1% Triton, 2.5 mM sodium pyrophosphate, 1 mM beta-glycerophosphate, 1 mM Na3VO4, 1 µg/ml leupeptin]; 9803, Cell Signaling Technology) using a chilled dounce homogenizer. Homogenates were then solubilized by end-over-end rotation for 60min, and centrifuged at 100,000g for 60min. The supernatant was then collected, protein concentration quantified (BCA method), and 300µg protein from the lysate was adjusted to 500 µL volume with lysis buffer. The adjusted volume was rotated

by end-over-end overnight at 4°C with 5µg IRβ antibody. The following day, 25µL protein-A magnetic beads (88845, Pierce Thermo-Fisher) were washed in wash buffer (25 mM Tris, 0.15M NaCl, 0.05% Tween-20, pH 7.5), then added to the lysate-antibody mixture, and rotated gently end-over-end for 2h at room temperature. The immunoprecipitation matrix, which includes the bead-antibody-antigen complex, was separated using a magnetic rack [DynaMag2, 12321D, Thermo-Fisher) to form the bead-complex pellet, and washed three times with lysis buffer, twice with wash buffer, and once with PBS. Antigens were eluted from the bead complex with 100 µL 2X Laemmli SDS buffer, by a combination of rotation & vortexing samples for 10min, and discarding the beads when finished. Following immunoprecipitation, protein abundance 40 µL from the elutes were loaded and analyzed by immunoblot for basal and insulin-mediated anti-CD-36, IRβ, and Fyn kinase. CD36 and Fyn interaction with IRβ was normalized to a 15µL input sample from the same participant loaded onto the same gel as the elute. See Table IV-2 for primary and secondary antibody details, and Appendix I for detailed immunoprecipitation protocol

Hepatic and visceral fat.

Fat content from MRI images were captured by the Dixon method (38), and image acquisition was described previously from our lab (39). Visceral fat area was measured from 3, 5-mm axial slices between L2-L3 vertebral region, and hepatic fat percentage was measured from 3, 5-mm axials slices of the liver.

Calculations

Insulin-mediated glucose uptake

Insulin-mediated glucose uptake was quantified by rate of glucose disappearance (Rd) at the end of the hyperinsulinemic-euglycemic clamp (glucose infusion rate (nmol/min) + glucose rate of appearance (nmol/min), and normalized to both fat-free mass and insulin during the clamp (Rd= nmol/kg FFM/min / [µU/mL]).

Statistical analysis

All measurements that were not normally distributed were log transformed in effort to achieve normality. Linear mixed models were used to examine the main effects for group (HIGH versus LOW insulin sensitivity), main effects for insulin (basal versus insulin-mediated

conditions), and group x insulin interaction for measurements including targeted protein analysis, immunoprecipitation, FA Ra, and glucose Ra. For LD histochemistry analysis, measurements of lipid content, LD number, and LD area were segregated into regional distribution (IMF and SS region). Linear mixed models were then used on the segregated outcomes to identify main effects of group (HIGH versus LOW), main effects for fiber type (type I vs type II), and group x fiber-type interaction in the IMF and SS region independently. When significant effects were observed, fisher's least significant difference post-hoc test was used to identify significant interactions between groups. Unpaired Student's t-tests were used to test for significant between-group (HIGH vs LOW) differences in all other clinical variables. Pearson's correlation was used to identify relationships between clinical outcomes and insulin sensitivity continuously with the entire study sample. Statistical analysis was completed using R version 4.1.0 (40). Data are displayed as mean ± SD, and significance set to $p < 0.05$.

RESULTS

Sub-cohort stratification based on insulin-mediated glucose uptake

As anticipated, glucose Rd during the insulin clamp (i.e., insulin-mediated glucose uptake) varied widely among our obese participants (Figure IV-1A). To conduct pairwise comparisons between sub-cohorts with relatively low versus relatively high glucose Rd during the insulin clamp, we stratified subjects into two sub-cohorts; 1) Low glucose Rd ('LOW'; glucose Rd ≤ 400 nmol/kg FFM/min / (µU/mL); n=10), and 2) High glucose Rd ('HIGH': glucose Rd > 550 nmol/kg FFM/min / (µU/mL), n=7; Figure IV-1B). The striking differences in glucose Rd were present between LOW and HIGH sub-cohorts whether or not glucose Rd was normalized to insulin concentration during the clamp (Figure IV-1B and IV-1C). Additionally, HOMA-IR for all members of the LOW sub-cohort was > 2.5 (Table IV-1), which is a recognized index of peripheral insulin resistance (41).

Insulin effects on hepatic glucose production and FA release from adipose tissue

Despite the robust difference in glucose Rd between LOW and HIGH sub-cohorts during the insulin clamp, hepatic glucose production (Glucose Ra) was similar between groups both before and during the insulin clamp (Figure IV-1D). Additionally, the insulin-mediated suppression of glucose Ra (index of hepatic insulin sensitivity) was also not statistically different

between groups (Figure IV-1E). In contrast, insulin-mediated FA Ra suppression (an index of adipose tissue insulin sensitivity to reduce FA mobilization) was greater in HIGH compared with LOW (Figure IV-1F and IV-1G). Interestingly, insulin-mediated FA Ra suppression was significantly correlated with glucose Rd across all subjects (Figure IV-1H; $r = 0.68$; $p<0.01$), indicating a relatively low adipose tissue insulin sensitivity to reduce FA mobilization was related to an impairment of insulin-mediated glucose uptake in skeletal muscle.

Skeletal muscle insulin signaling

Skeletal muscle IR interaction with CD36 and Fyn. Although the total protein abundances of both CD36 and the Src family kinase, Fyn were similar between HIGH and LOW (Figures IV-2A and 2B), the interaction (determined by co-immunoprecipitation) of the IRβ with CD36 (Figure IV-2C) and Fyn kinase (Figure IV-2D) were significantly greater in HIGH versus LOW (group main effects; $p<0.01$). Furthermore, correlational analyses across all subjects revealed significant positive correlations between CD36 interaction with IRβ during the clamp and glucose Rd (Figure IV-2F), as well as CD36 interaction with IRβ during the clamp and FA Ra suppression (Figure IV-2H), suggesting potential cross-talk between FAs released from adipose tissue and the physical interaction between CD36 and IRβ in skeletal muscle. Additionally, there was a significant positive association with glucose Rd and Fyn kinase interaction with IRβ at both baseline ($p<0.01$; Figure IV-2I) and during the clamp ($p=0.04$; Figure IV-2J). The insulin-mediated FA Ra suppression did not significantly correlate with Fyn interaction with IRβ (Figure IV-2K and IV-2L).

Canonical insulin signaling. Aligning with the greater interaction between IRβ and the tyrosine kinase, Fyn in HIGH versus LOW, we also found the insulin-mediated phosphorylation of $IR\beta^{Y1150}$ to be greater in HIGH versus LOW (Figures IV-3A and IV-3B). Similarly, insulin significantly increased Akt phosphorylation at Ser 473 and Thr 308 ($p < 0.01$; Figures IV-3C and IV-3E) in both LOW and HIGH, but LOW exhibited a blunted increase in $pAkt^{S473}$ compared with HIGH ($p < 0.01$; Figure IV-3C and IV-3D). The slightly attenuated insulin-stimulated increase in $pAkt^{T308}$ in LOW versus HIGH was not statistically significant between groups (Figure IV-3F).

Insulin significantly increased $pFOX01^{S256}$ ($p<0.01$; Figure IV-4A) and tended to increase $pGSK\alpha^{S21}$ ($p=0.06$; Figure IV-4C), both of which are downstream targets of Akt. In line with the differential pAkt response between groups, the insulin-mediated responses for $pFOX01^{S256}$ and $pGSK\alpha^{S21}$ were blunted in LOW compared with HIGH ($p<0.05$; Figures IV-4B and IV-4D).

Surprisingly, we did not detect an insulin-stimulated increase in pAS160^{T642} or pP44/42 MAPK$^{T202,\ Y204}$ (ERK 1/2) in either LOW or HIGH (Figures IV-4E and IV-4G), perhaps because activation of AS160 at Ser^{588} may be necessary for complete convergence of AS160 to promote full Rab GTPase activity, and thus, GLUT4 translocation. Interestingly, total GLUT4 abundance was greater in HIGH compared to LOW (p=0.01, Figure IV-4I).

Intramyocellular lipid droplet (LD) storage in type I and II skeletal muscle fibers

Total muscle lipid content was not different between HIGH and LOW (7.8 ± 2.0 versus 8.5 ± 2.9 % stained, respectively; p=0.6). As anticipated, total lipid content was greater in type I versus type II muscle fibers, and this was the case for both groups (type I= 9.3 ± 4.9 versus type II=6.2 ± 4.1 % stained; p<0.01; see representative Figure IV-5A). Measurements within the IMF and SS regions of the muscle fibers also revealed no difference in total lipid content between HIGH and LOW within either the IMF or SS regions. In contrast, there was a strong trend (p=0.06) for the number of LDs (per μm^2) in the IMF region to be greater in HIGH versus LOW (Figure IV-5C). This difference in LD number was not found in the SS region (Figure IV-5F), but LD size (i.e., median LD area) within the SS region was found to be larger in LOW versus HIGH (Figure IV-5G). This difference in LD size between groups was statistically significant in type II fibers (p=0.01), and trended greater in type I fibers (p=0.09). Interestingly, median LD area in type II fibers was negatively correlated with insulin-mediated glucose uptake (p=0.03; Figure IV-5H).

DISCUSSION

Although skeletal muscle insulin resistance is very common in adults with obesity (42), not all adults with obesity are insulin resistant (4, 5), and factors underlying this difference among a relatively homogeneous cohort of adults with obesity are not well understood. Here, we confirm that low adipose tissue insulin sensitivity to reduce FA mobilization was a strong predictor of impaired insulin-mediated glucose uptake. This relationship is consistent with the well described phenomenon that high rates of FA mobilization can lead to a disruption in skeletal muscle insulin signaling (12, 43-46). Studies conducted in vitro have reported elevated saturated FA availability reduced IR binding with both CD36 and Fyn kinase, which in turn can modify downstream signaling events (31). Our findings that skeletal muscle IR interaction with CD36 and Fyn kinase were attenuated in LOW suggests that the impairments in skeletal muscle insulin signaling that are

common in many obese adults, may begin further upstream in the insulin signaling cascade than commonly considered (31). Additionally, we found differences in the number, size, and location of LDs within skeletal muscle were also related to differences in insulin-mediated glucose uptake in our participants. Together, these findings support the notion that low adipose tissue insulin sensitivity to reduce FA mobilization may lead to the development of impaired insulin signaling in skeletal muscle, in part through modifications in interactions between the IR and key regulatory proteins, as well as LD distribution within skeletal muscle.

The increase in plasma insulin concentration in response to a meal markedly reduces systemic FA availability in healthy adults (47, 48). In contrast, individuals who are more resistant to the effects of insulin in adipose tissue experience persistent elevations in systemic FA availability (even after meals), which is known to be a key factor underlying impaired insulin-mediated glucose uptake in skeletal muscle (12, 45, 46, 49). Because the vast majority of FA released into the systemic circulation are derived from abdominal subcutaneous adipose tissue (aSAT), rather than gluteal/femoral or visceral adipose tissue (14), we contend the blunted response to insulin's effect of reducing FA mobilization is occurring in aSAT. Therefore, our findings that low sensitivity to insulin's effects on reducing FA mobilization was a primary predictor of impaired insulin-mediated peripheral glucose uptake, suggests insulin resistance in aSAT may precede the development of insulin resistance in skeletal muscle. However, the temporal pattern by which insulin resistance develops among different tissues are still not clear. Some previous reports in rodents support the notion that the onset of adipose tissue insulin resistance in response to high fat diets occurs before skeletal muscle insulin resistance (50, 51). Additionally, in lipodystrophy (a condition where adipose tissue cannot effectively store triglycerides, resulting the very high systemic FA concentrations), the excessive systemic FA availability precedes insulin resistance in skeletal muscle (52). In adults with obesity, abnormalities within aSAT, including inflammation, fibrosis, and hypoxia are also suggestive to contribute to the development of skeletal muscle insulin resistance (53).

The specific mechanisms within aSAT that may underlie an impaired ability of insulin to blunt FA mobilization are not completely understood. Insulin potently inhibits lipolytic rate, largely through Akt-mediated phosphorylation of phosphodiesterase 3B (PDE3B), which in turn leads to the inhibition of key lipase enzymes (54). However, based on findings from Project 1 of my dissertation, as well as other previous work (55), low sensitivity to the anti-lipolytic response

to insulin does not appear to be responsible for the blunted FA Ra suppression in response to insulin we report here. Because adipose tissue is exceptionally sensitive to the anti-lipolytic effects of insulin, it is possible that insulin-mediated anti-lipolysis may be unimpeded even if insulin signaling is modestly attenuated. A modest impairment in insulin signaling in adipocytes can impact other processes, such as the rate of FA re-esterification (56, 57), which is the most likely candidate for the blunted FA Ra suppression we report here. Local inflammation (e.g., TNFα, IL6, and IL1β) within adipose tissue has been attributed to impair insulin signaling in adipose tissue (58-60), and may contribute to impaired ability to reduce FA mobilization in response to insulin. Morphological features of aSAT such as large adipocytes may also contribute, perhaps due in part to greater pro-inflammatory profile (61). In addition, relatively low capillary density coupled with hypertrophied adipocytes can result in attenuated insulin delivery as well as induce adipocyte hypoxia, which has been linked to impaired insulin responsiveness (53, 62, 63). Excessive fibrosis within the ECM of aSAT has also been linked with an impaired response to insulin in adipose tissue (64, 65). How aSAT fibrotic content or composition induces insulin resistance within the tissue remains elusive, but potential factors include, increased pro-inflammatory cytokine abundance by mechanical stress induced by excess collagen accumulation (66), and physical constraints limiting insulin delivery and signaling (64, 67). Overall, dysfunctional insulin signaling, large adipocyte size, relatively low capillary density, and abundant fibrosis may converge to attenuate the adipose tissue insulin sensitivity to reduce FA mobilization from aSAT of insulin resistant adults with obesity.

Insulin-mediated glucose uptake in skeletal muscle is mediated by intracellular signaling events triggering GLUT4 translocation from the cytosol to the plasma membrane (68). The ~20% greater GLUT4 protein abundance we found in HIGH vs. LOW likely contributed somewhat to differences in insulin response between groups (69). However, we contend much of the difference in insulin sensitivity between our HIGH and LOW subjects was a due to differences in FA availability and lipid metabolism between groups. Insulin resistance in skeletal muscle stemming from high FA availability has been causally linked to diacylglycerol (DAG) and ceramide (17, 18), resulting in non-typical PKC isoform activation (70) and decreased AKT phosphorylation (71) respectively. However, there remains ongoing debate regarding specific lipid mediators that may disrupt canonical insulin signaling in skeletal muscle (21-23). The membrane glycoprotein CD36, is well-known for its role in FA transport, but recent evidence has demonstrated CD36 can also

modify insulin signaling (31, 72). The physical interaction between CD36 and the IR was found to enhance IR phosphorylation by facilitating the interaction between the IR and the tyrosine kinase protein, Fyn (31, 72). Our findings that the physical interaction (determined by co-immunoprecipitation) between the IR and both CD36 and Fyn were greater in HIGH versus LOW, align with the notion that a greater interaction among these proteins may help propagate intracellular insulin signaling. Importantly, elevated saturated FA availability was previously found to attenuate CD36 from recruiting Fyn to the IR (31), contributing to the blunted insulin response commonly found when FA availability is high (16, 73). Therefore, the relatively low insulin sensitivity to reduce FA mobilization in LOW may contribute to the blunted interaction between CD36 and the IR, thereby lowering Fyn recruitment and subsequent phosphorylation of the IR. Our findings that insulin-mediated phosphorylation of AKT^{S473}, as well as phosphorylation of the Akt substrates, $GSK3\alpha^{S21}$ and $FOXO1^{S256}$ were lower in LOW versus HIGH, align with the notion that interaction between the IR and Fyn may impact canonical insulin signaling downstream of the IR. Whether the CD36-mediated recruitment of Fyn to the IR involves a direct physical interaction between CD36 and Fyn is not known. However, Fyn binding sites have been identified along the cytoplasmic lipid raft domains of CD36 (74, 75), suggesting this process might involve direct binding between these proteins. Unfortunately, we did not have enough tissue for the co-immunoprecipitation assay to confirm whether CD36 interaction with Fyn was also attenuated in LOW versus HIGH. Together, these findings are the first to our knowledge in human skeletal muscle to support a previously proposed mechanism (31) by which CD36 regulates IR phosphorylation and downstream signaling, and that FA availability and uptake into skeletal muscle may modify this effect.

Lipid accumulation in lipid droplets (LDs), and their location within the myocyte have also been implicated in the regulation of insulin signaling in skeletal muscle (76). Our observation that LDs in the SS region of the myocyte were larger in LOW versus HIGH, aligns with previous reports demonstrating correlations between SS LD size and insulin resistance (28-30, 77). The mechanistic link explaining how an accumulation of larger LDs in the SS region of the myocyte induces insulin resistance is still unclear, but the proximity of these large LDs to the muscle membrane may disrupt key insulin signaling steps that occur there (28). For example, the accumulation of lipid intermediates in the SS region, which may be released from SS LDs, have been linked with insulin resistance (78). Additionally, larger LDs have a lower surface area-to-

volume ratios than small LDs, which may limit lipolytic control at the membrane of the larger LDs. In turn, this may increase the susceptibility for incomplete lipolysis (79-81), resulting in aberrant lipid accumulation within the SS region of the myocyte, in close proximity to insulin signaling events that occur at or near the plasma membrane. Our findings that the number of LDs in the IMF region tended to be greater in HIGH versus LOW suggests that a partitioning of LDs away from the SS region may be protective against impaired insulin signaling. The greater abundance of LDs in the IMF region may also help protect against the development of insulin resistance by their close proximity to more mitochondria (27, 82), which may aid in the direct lipid transfer towards oxidative metabolism, and thereby may mitigate cytosolic lipid accumulation. We contend that differences in LD size and distribution observed between LOW and HIGH, may be due in part to differences in adipose tissue insulin sensitivity to reduce FA mobilization, whereby, a chronic elevation in systemic FA availability and uptake in individuals with low FA Ra suppression in response to insulin modifies LD storage and metabolism.

Although we interpret our findings describing the relationship between insulin-mediated suppression of FA release and glucose uptake to suggest a suppressed response to insulin in adipose tissue may contribute the development of whole-body insulin resistance, we acknowledge that this interpretation was largely based on correlational analyses, which of course does not indicate causation. However, these findings are consistent with other studies (11-13), and supports the observation that insulin resistance development is a consequence of excess FA release from aSAT, resulting in greater FA uptake into skeletal muscle. We also acknowledge that our in vivo measurements aimed to identify key contributors to insulin resistance in our subjects was not exhaustive, and additional factors such as vascular dysfunction may be one of several contributors to insulin resistance in our participants (83, 84). Additionally, the phosphorylation of canonical insulin signaling can also be regulated by other intracellular responses that were not measured in this study (e.g., novel PKCs, JNK, and mTORC1/S6 kinase) – many of which are known to negatively influence activation of proximal insulin signaling components (85). It is also important to acknowledge that our LOW group had a greater proportion of male participants compared to HIGH (LOW: 5M/5F, HIGH: 6F/1M) – and men are commonly found to be more insulin resistant than women (86, 87). Therefore, we cannot exclude that sex differences are contributing to excessive FA release, and whole-body insulin sensitivity between groups.

In conclusion, our findings suggest low adipose tissue insulin sensitivity to reduce FA mobilization from aSAT is an important contributor to whole-body insulin resistance. A low sensitivity to insulin in aSAT can lead to a persistent elevation in systemic FA availability, which is a major factor underlying the development of insulin resistance in obesity. Novel findings from our study suggest this high systemic FA availability may diminish skeletal muscle insulin signaling, in part by reducing the interaction between CD36 and Fyn with the IR, and attenuating downstream insulin signaling. The insulin resistant subjects in our study also presented larger-sized LDs in the SS region of the myocyte, which may contribute to their insulin resistance by interfering with key insulin signaling processes at the muscle membrane. Overall, our findings suggest that low adipose tissue insulin sensitivity to reduce FA mobilization may contribute to an inter-organ cross-talk, whereby excess FA release from aSAT disrupts IR interaction with key regulatory proteins, and modifies LD size and distribution in the myocyte.

FIGURES

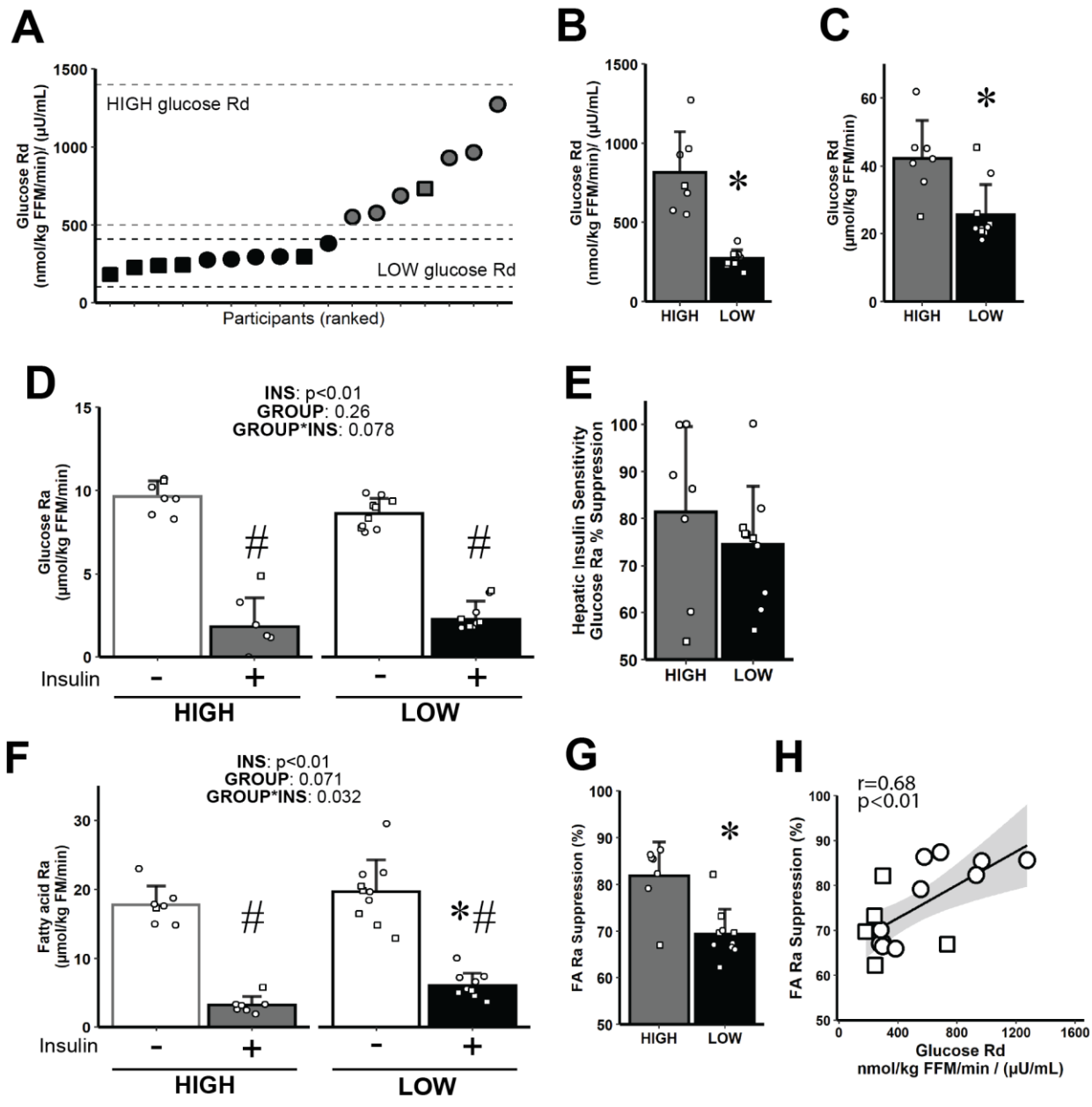

Figure IV-1: Insulin sensitivity variability across all participants, and substrate kinetics.

A) Glucose Rd variability across all participants. B-C) Stratification into HIGH (n=7) and LOW (n=10) sub-cohorts - expressed as glucose Rd normalized to insulin (nmol/kg FFM/min / (µU/mL), (B), and glucose Rd normalized only to lean body mass (µmol/kg FFM/min, (C). D) Basal and insulin-mediated glucose Ra. E) Glucose Ra % suppression. F) Basal and insulin-mediated fatty acid Ra. G) FA Ra suppression. H) Correlation between glucose Rd and FA Ra suppression in all participants. ○=Female, □=Male. # $p<0.05$ main-effect for insulin (basal versus clamp). * $p<0.05$ versus HIGH. Data are expressed mean ± SD.

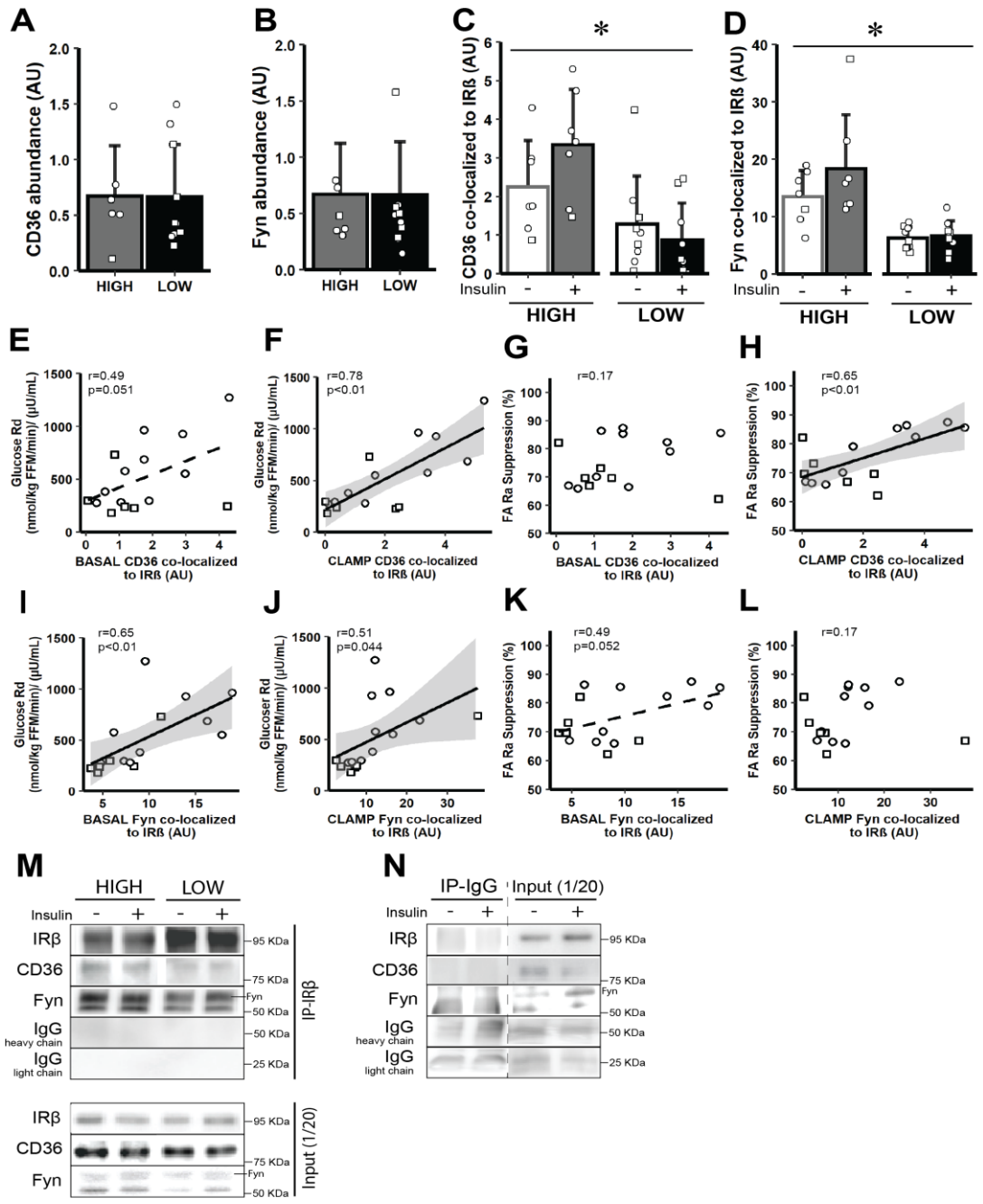

Figure IV-2: Insulin-mediated interaction between CD36 and Fyn kinase with IRβ.

A) Whole muscle CD36 abundance. B) Whole muscle Fyn kinase abundance. C) CD36 co-localized to IRβ at baseline and during the clamp. D) Fyn kinase co-localized to IRβ at baseline and during the clamp. E-F) Correlation between glucose Rd and CD36 co-localized to IRβ at baseline (E) and during the clamp (F). G-H) Correlation between FA Ra suppression and CD36 co-localized to IRβ at baseline (G) and during the clamp (H). I-J) Correlation between glucose Rd and Fyn kinase co-localized to IRβ at baseline (I) and during the clamp (J). K-L) Correlation between FA Ra suppression and Fyn kinase co-localized to IRβ at baseline (K) and during clamp (L). M) Representative immunoblots from the IRβ immunoprecipitation assay, including input controls. N) IgG immunoprecipitation negative control with dashed lines to denote breaks in lanes removed for clarity. ○=Female, □=Male;. n=7 in HIGH and n=9 in LOW. * $p<0.05$ - main effect for group, HIGH versus LOW. Data are mean±SD.

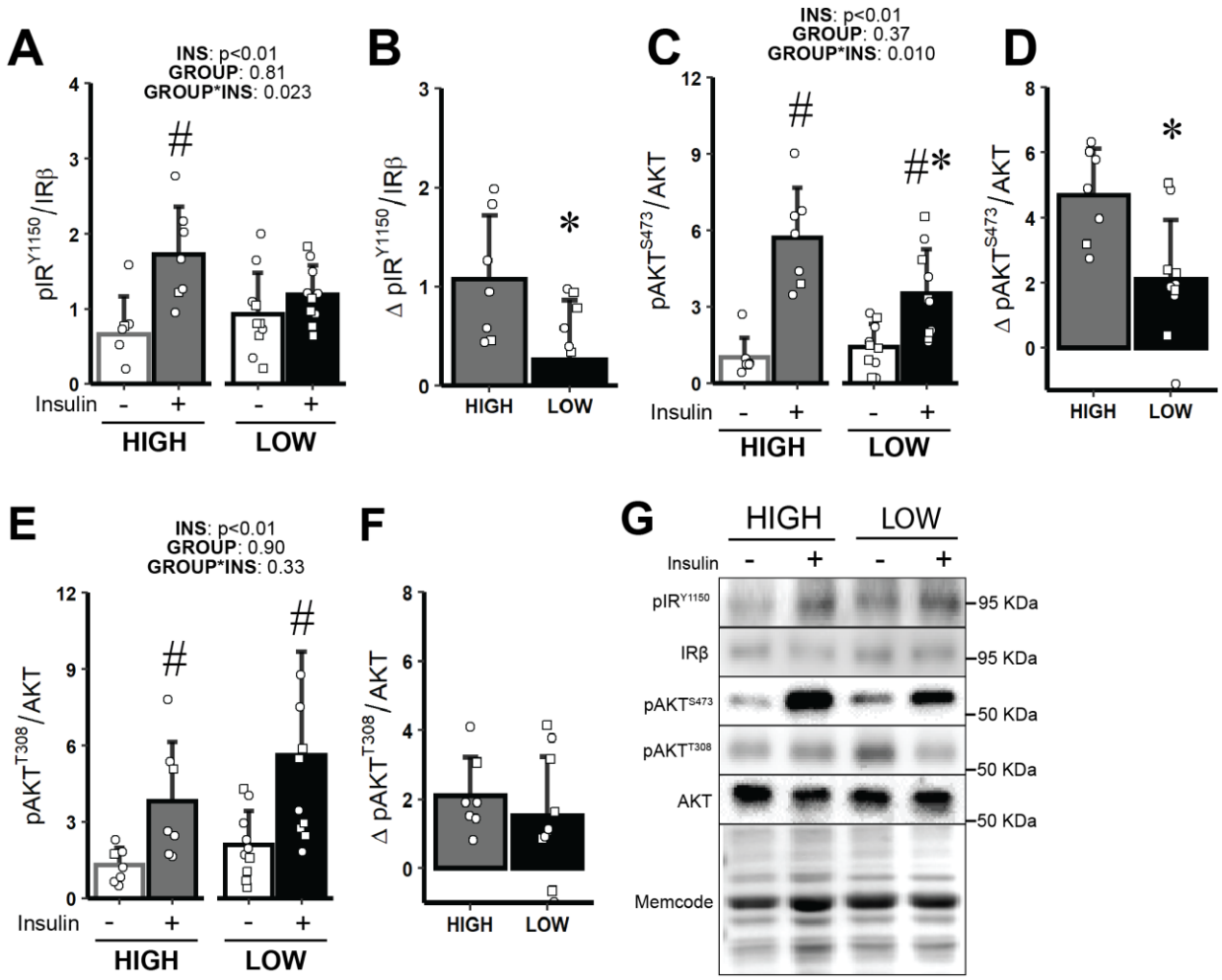

Figure IV-3: Comparison of acute insulin-mediated signaling events in skeletal muscle proximal to Akt.

A) Insulin-mediated pIRβ^{Y1150} at baseline and during the hyperinsulinemic clamp. B) Delta pIRβ^{Y1150} (difference between clamp baseline abundance). C) Insulin-mediated pAKT^{S473}. D) Delta pAKT^{S473}. E) Insulin-mediated pAKT^{T308}. F) Delta pAKT^{T308}. G) Representative immunoblots from whole muscle. ○=Female, □=Male; n=7 in HIGH and n=10 in LOW. # p<0.05 main-effect for insulin (basal versus clamp). * p<0.05 versus HIGH. Data are expressed mean ± SD.

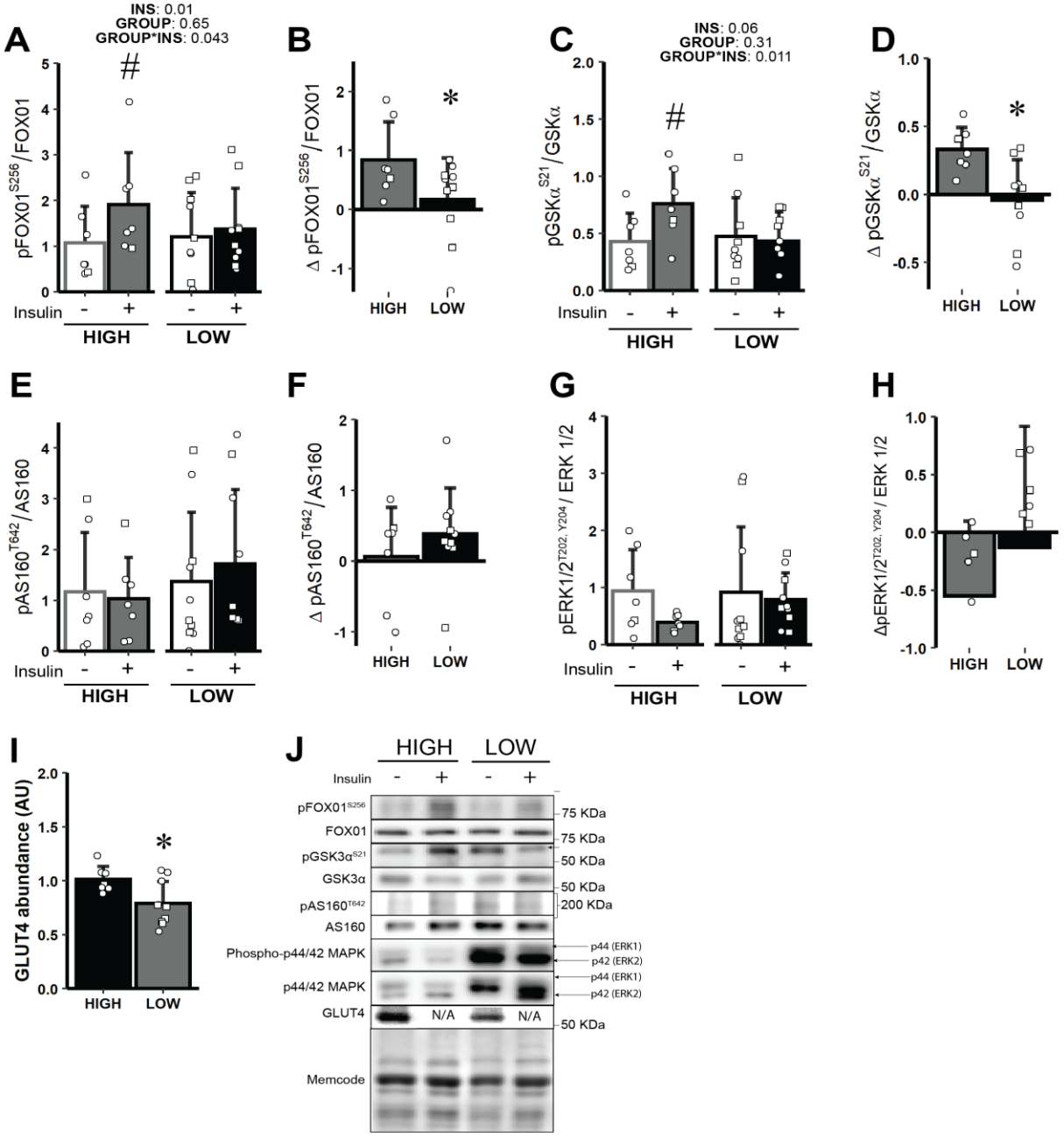

Figure IV-4: Comparison of acute insulin-mediated signaling events in skeletal muscle distal to Akt.

A) Insulin-mediated pFOXO1^{S256}. B) Delta pFOXO1^{S256} (difference between clamp baseline abundance). C) Insulin-mediated pGSKα^{S21}. D) Delta pGSKα^{S21}. E) Insulin-mediated pAS160^{T642}. F) Delta pAS160^{T642}. G) Insulin-mediated pERK1/2$^{T202/Y204}$. H) Delta pERK1/2$^{T202/Y204}$. I) Skeletal muscle GLUT4 abundance. J) Representative immunoblots from whole muscle. ○=Female, □=Male; n=7 in HIGH and n=10 in LOW. # $p<0.05$ main-effect for insulin (basal versus clamp). * $p<0.05$ versus HIGH. Data are expressed mean ± SD.

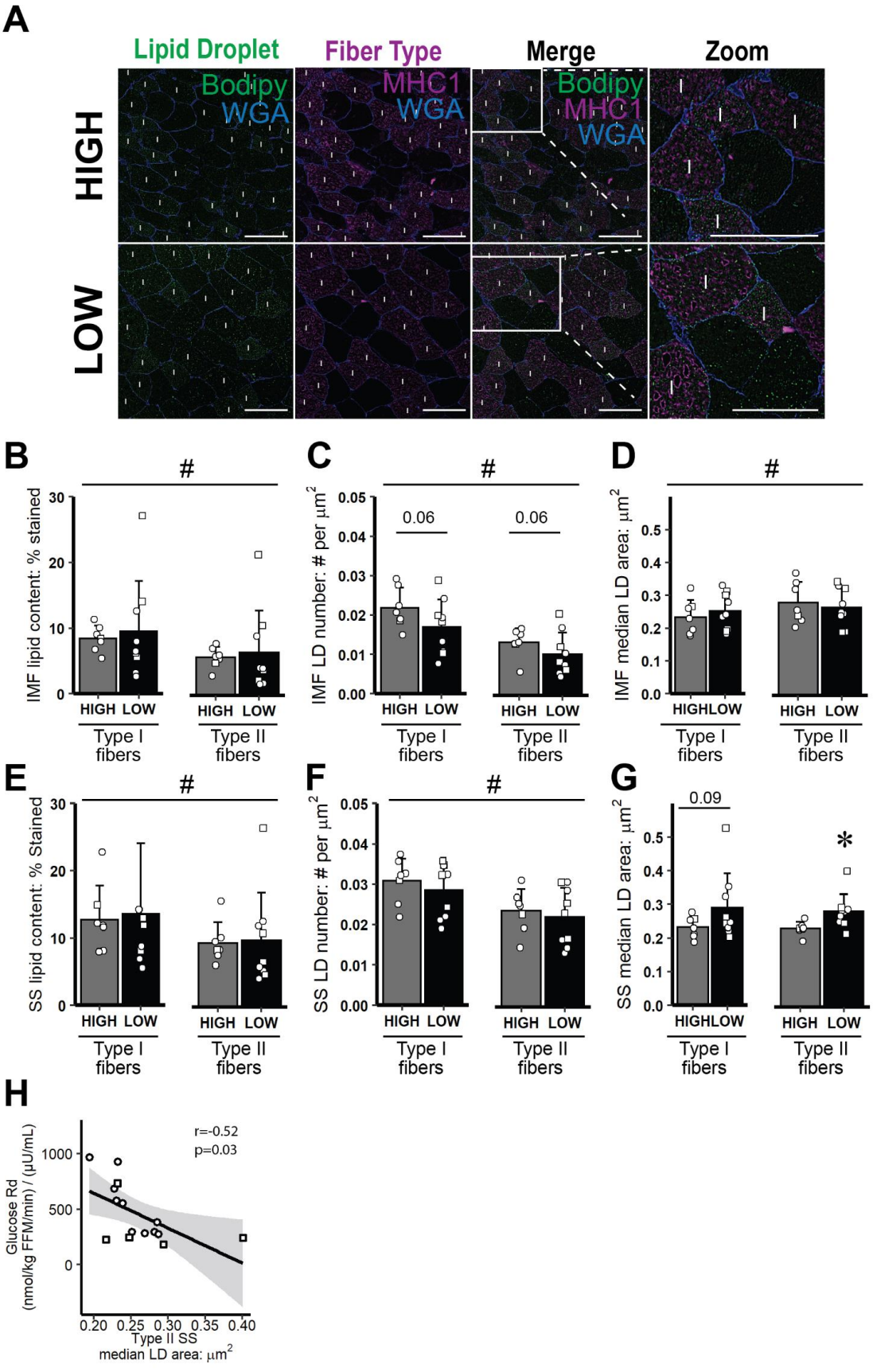
A
Lipid Droplet
Fiber Type
Merge
Zoom
Bodipy
WGA
MHC1
WGA
Bodipy
MHC1
WGA
HIGH
LOW
B
IMF lipid content: % stained
C
IMF LD number: # per µm2
0.06
0.06
D
IMF median LD area: µm2
E
SS lipid content: % Stained
F
SS LD number: # per µm2
G
SS median LD area: µm2
0.09
*
#
HIGH LOW
Type I fibers
Type II fibers
H
Glucose Rd (nmol/kg FFM/min) / (µU/mL)
r=-0.52
p=0.03
Type II SS median LD area: µm2

Figure IV-5: Intramyocellular LD characteristics and distribution in type I and II skeletal muscle fibers.

A) Representative image in skeletal muscle of type I and II fibers from HIGH and LOW. Image contains bodipy stain (LD, green), myofiber stain positive for MHC I (type I fibers, purple), and wheat germ agglutinin [WGA] (membranes, blue). The region inside the white box are enlarged for a clearer view. Magnification, 20X. Scale bar, 100μm for all images. 'I' denotes type I muscle fiber. B-G) lipid content and LD characteristics within the IMF and SS region in type I and type II fibers. B) IMF lipid content (represented as % stained). C) IMF LD number (# LDs per μm^2). D) IMF median LD area per fiber (μm^2). E) SS lipid content. F) SS LD number. G) SS LD area per muscle fiber. H) Correlation between glucose Rd and SS LD area in type II fibers. ○=Female, □=Male; n=6 in HIGH and n=10 in LOW. # $p<0.05$ main-effect for fiber type (type I versus type II). * $p<0.05$ main-effect for group (HIGH versus LOW), with post-hoc analysis identifying significant difference in HIGH versus LOW. Data are expressed mean ± SD.

TABLES

Table IV-1: Participant characteristics

	HIGH (n=7)	**LOW (n=10)**	*P-value*
Sex (m/f)	1/6	5/5	
Age (yrs)	32 ± 9	31 ± 8	0.75
BMI (kg/m^2)	35 ± 3	36 ± 3	0.18
Body mass (kg)	93 ± 9	105 ± 11*	0.02
Fat mass (kg)	43 ± 5	46 ± 5	0.22
Fat free mass (kg)	50 ± 10	60 ± 9	0.06
Body fat (%)	46 ± 6	43 ± 5	0.22
Liver Fat (%)	3.4±2.0	9.5±8.3	0.48
Visceral Fat (cm^2)	107±49	169±58	0.09
Fasting glucose (mM)	4.6 ± 0.4	4.7 ± 0.4	0.70
Fasting insulin (μU/mL)	6.3 ± 2.5	16.8 ± 4.7*	$3.4e^{-05}$
HOMA-IR	1.3 ± 0.6	3.5 ± 1.0*	$6.3e^{-05}$
HbA1c (%)	5.3 ± 0.4	5.4 ± 0.2	0.76
NEFA (mM)	438 ± 197	544 ± 176	0.27
Triglyceride, (mg/dL)	58 ± 34	80 ± 38	0.24
HDL (mg/dL)	44 ± 10	38 ± 12	0.27
Cholesterol (mg/dL)	141 ± 15	143 ± 32	0.88
Plasma CRP (mg/L)	11 ± 14	9 ± 11	0.79
Plasma IL6 (ρg/mL)	3.0 ± 1.4	3.3 ± 2.2	0.74
Plasma HMW Adiponectin (ng/mL)	2581 ± 1412	1658 ± 1261	0.08
Plasma Adiponectin (Total) (ng/mL)	5978 ± 2139	3840 ± 2017	0.06
Plasma Leptin (ng/mL)	61 ± 29	51 ± 19	0.44

Data are mean ± SD. BMI, body mass index. HOMA IR, homeostatic model for insulin resistance. NEFA, nonesterified fatty acid. HDL, high density lipoprotein. CRP, C-reactive protein, HMW adiponectin, high molecular weight adiponectin. * $p<0.05$ versus HIGH

Table IV-2: Antibodies and Reagents

Primary and secondary antibodies	Source	Identifier
Phospho-IGF-I Receptor β (Tyr1135/1136)/Insulin Receptor β (Tyr1150/1151)	CST	3024
anti-Insulin Receptor β	CST	3025
anti-pAkt^{S473}	CST	9271
anti-pAkt^{T308}	CST	9275
anti-Akt	CST	9272
pGSK3α^{S21}	CST	4337
anti-GSK3α	CST	5676
anti-pFOXO1^{S256}	CST	9461
anti-FoxO1	CST	9454
anti-pAS160^{T642}	CST	8881
anti-AS160	CST	2670
anti-human CD36	R&D Systems	AF1955
anti-Fyn	CST	4023
anti-GLUT4	Santa Cruz	sc-53566
Phospho-p44^{Thr202}/42^{Tyr204} MAPK (Erk1/2)	CST	9101
p44/42 MAPK (Erk1/2)	CST	9102
Normal Rabbit IgG	CST	2729
anti-rabbit IgG, HRP-linked Antibody	CST	7074
anti-mouse IgG, HRP-linked Antibody	CST	7076
Stable Isotope Tracers		
D-Glucose (6,6-D2)	Cambridge Isotopes	DLM-349-PK
Potassium Palmitate (1-13C, 99%)	Cambridge Isotopes	CLM-1889-PK
Histochemistry Reagents		
BODIPY 493/503	Invitrogen Thermo-Fisher	D3922
BA-D5: Myosin heavy chain Type 1	Developmental Studies Hydroma Bank	-
Alexa Fluor 647 Goat anti-Mouse IgG2b	Invitrogen Thermo-Fisher	A21242
Wheat Germ Agglutinin - Alexa Fluor 555	Invitrogen Thermo-Fisher	W32464
Triton X-100	Sigma-Aldrich	T8787
ProLong Gold Antifade Mountant	Invitrogen Thermo-Fisher	P36930
Plasma Analysis Reagents		
Glucose Oxidase	Thermo-Fisher	A22189
NEFA Standard Solution	Wako Diagnostics	27676491
Triglyceride Reagent	Sigma-Aldrich	T2449
HDL-Cholesterol E	Wako Diagnostics	9059676
Total Cholesterol E	Wako Diagnostics	9138103
Human IL-6 ELISA	R&D Systems	HS600C
C-Reactive Protein ELISA	Calbiotech	CR120C
Human Leptin ELISA	Millipore Sigma	EZHL80SK

Human Total Adiponectin/Acrp30 ELISA	R&D Systems	DRP300
Human HMW Adiponectin/Acrp30 ELISA	R&D Systems	DHWAD0
Insulin For Immulite	Siemens	10381429

Abbreviations: CST, cell signaling technology

REFERENCES

1. Hales CM, Carroll MD, Fryar CD, and Ogden CL. Prevalence of obesity and severe obesity among adults: United States, 2017–2018. 2020.
2. Reaven GM. Banting lecture 1988. Role of insulin resistance in human disease. *Diabetes.* 1988;37(12):1595-607.
3. Farin HM, Abbasi F, and Reaven GM. Body mass index and waist circumference both contribute to differences in insulin-mediated glucose disposal in nondiabetic adults. *Am J Clin Nutr.* 2006;83(1):47-51.
4. Smith GI, Mittendorfer B, and Klein S. Metabolically healthy obesity: facts and fantasies. *J Clin Invest.* 2019;129(10):3978-89.
5. Wildman RP, Muntner P, Reynolds K, McGinn AP, Rajpathak S, Wylie-Rosett J, et al. The Obese Without Cardiometabolic Risk Factor Clustering and the Normal Weight With Cardiometabolic Risk Factor Clustering: Prevalence and Correlates of 2 Phenotypes Among the US Population (NHANES 1999-2004). *Archives of Internal Medicine.* 2008;168(15):1617-24.
6. Dvorak RV, DeNino WF, Ades PA, and Poehlman ET. Phenotypic characteristics associated with insulin resistance in metabolically obese but normal-weight young women. *Diabetes.* 1999;48(11):2210-4.
7. Stefan N, Kantartzis K, Machann J, Schick F, Thamer C, Rittig K, et al. Identification and characterization of metabolically benign obesity in humans. *Arch Intern Med.* 2008;168(15):1609-16.
8. Calori G, Lattuada G, Piemonti L, Garancini MP, Ragogna F, Villa M, et al. Prevalence, metabolic features, and prognosis of metabolically healthy obese Italian individuals: the Cremona Study. *Diabetes Care.* 2011;34(1):210-5.
9. Van Pelt DW, Guth LM, Wang AY, and Horowitz JF. Factors regulating subcutaneous adipose tissue storage, fibrosis, and inflammation may underlie low fatty acid mobilization in insulin-sensitive obese adults. 2017;313(4):E429-E39.
10. Van Pelt DW, Newsom SA, Schenk S, and Horowitz JF. Relatively low endogenous fatty acid mobilization and uptake helps preserve insulin sensitivity in obese women. *International Journal of Obesity.* 2015;39(1):149-55.
11. Magkos F, Fabbrini E, Conte C, Patterson BW, and Klein S. Relationship between Adipose Tissue Lipolytic Activity and Skeletal Muscle Insulin Resistance in Nondiabetic Women. *The Journal of Clinical Endocrinology & Metabolism.* 2012;97(7):E1219-E23.
12. Groop LC, Bonadonna RC, DelPrato S, Ratheiser K, Zyck K, Ferrannini E, et al. Glucose and free fatty acid metabolism in non-insulin-dependent diabetes mellitus. Evidence for multiple sites of insulin resistance. *J Clin Invest.* 1989;84(1):205-13.
13. Koh H-CE, van Vliet S, Pietka TA, Meyer GA, Razani B, Laforest R, et al. Subcutaneous adipose tissue metabolic function and insulin sensitivity in people with obesity. *Diabetes.* 2021:db210160.

14. Nielsen S, Guo Z, Johnson CM, Hensrud DD, and Jensen MD. Splanchnic lipolysis in human obesity. *J Clin Invest.* 2004;113(11):1582-8.

15. Krssak M, Falk Petersen K, Dresner A, DiPietro L, Vogel SM, Rothman DL, et al. Intramyocellular lipid concentrations are correlated with insulin sensitivity in humans: a 1H NMR spectroscopy study. *Diabetologia.* 1999;42(1):113-6.

16. Dresner A, Laurent D, Marcucci M, Griffin ME, Dufour S, Cline GW, et al. Effects of free fatty acids on glucose transport and IRS-1-associated phosphatidylinositol 3-kinase activity. *J Clin Invest.* 1999;103(2):253-9.

17. Itani SI, Ruderman NB, Schmieder F, and Boden G. Lipid-Induced Insulin Resistance in Human Muscle Is Associated With Changes in Diacylglycerol, Protein Kinase C, and IκB-α. 2002;51(7):2005-11.

18. Adams JM, Pratipanawatr T, Berria R, Wang E, DeFronzo RA, Sullards MC, et al. Ceramide Content Is Increased in Skeletal Muscle From Obese Insulin-Resistant Humans. 2004;53(1):25-31.

19. Koves TR, Ussher JR, Noland RC, Slentz D, Mosedale M, Ilkayeva O, et al. Mitochondrial Overload and Incomplete Fatty Acid Oxidation Contribute to Skeletal Muscle Insulin Resistance. *Cell Metabolism.* 2008;7(1):45-56.

20. Houmard JA, Tanner CJ, Yu C, Cunningham PG, Pories WJ, MacDonald KG, et al. Effect of weight loss on insulin sensitivity and intramuscular long-chain fatty acyl-CoAs in morbidly obese subjects. *Diabetes.* 2002;51(10):2959-63.

21. Hoy AJ, Brandon AE, Turner N, Watt MJ, Bruce CR, Cooney GJ, et al. Lipid and insulin infusion-induced skeletal muscle insulin resistance is likely due to metabolic feedback and not changes in IRS-1, Akt, or AS160 phosphorylation. *American Journal of Physiology-Endocrinology and Metabolism.* 2009;297(1):E67-E75.

22. Skovbro M, Baranowski M, Skov-Jensen C, Flint A, Dela F, Gorski J, et al. Human skeletal muscle ceramide content is not a major factor in muscle insulin sensitivity. *Diabetologia.* 2008;51(7):1253-60.

23. Timmers S, Nabben M, Bosma M, van Bree B, Lenaers E, van Beurden D, et al. Augmenting muscle diacylglycerol and triacylglycerol content by blocking fatty acid oxidation does not impede insulin sensitivity. *Proceedings of the National Academy of Sciences of the United States of America.* 2012;109(29):11711-6.

24. Walther TC, and Farese RV, Jr. Lipid droplets and cellular lipid metabolism. *Annual review of biochemistry.* 2012;81:687-714.

25. Olzmann JA, and Carvalho P. Dynamics and functions of lipid droplets. *Nature reviews Molecular cell biology.* 2019;20(3):137-55.

26. Ferreira R, Vitorino R, Alves RM, Appell HJ, Powers SK, Duarte JA, et al. Subsarcolemmal and intermyofibrillar mitochondria proteome differences disclose functional specializations in skeletal muscle. *Proteomics.* 2010;10(17):3142-54.

27. Shaw CS, Jones DA, and Wagenmakers AJM. Network distribution of mitochondria and lipid droplets in human muscle fibres. *Histochemistry and Cell Biology.* 2008;129(1):65-72.

28. Daemen S, Gemmink A, Brouwers B, Meex RCR, Huntjens PR, Schaart G, et al. Distinct lipid droplet characteristics and distribution unmask the apparent contradiction of the athlete's paradox. *Molecular Metabolism.* 2018;17:71-81.

29. Nielsen J, Christensen AE, Nellemann B, and Christensen B. Lipid droplet size and location in human skeletal muscle fibers are associated with insulin sensitivity. 2017;313(6):E721-E30.

30. Nielsen J, Mogensen M, Vind BF, Sahlin K, Højlund K, Schrøder HD, et al. Increased subsarcolemmal lipids in type 2 diabetes: effect of training on localization of lipids, mitochondria, and glycogen in sedentary human skeletal muscle. *Am J Physiol Endocrinol Metab.* 2010;298(3):E706-13.

31. Samovski D, Dhule P, Pietka T, Jacome-Sosa M, Penrose E, Son N-H, et al. Regulation of Insulin Receptor Pathway and Glucose Metabolism by CD36 Signaling. 2018;67(7):1272-84.

32. Pepino MY, Kuda O, Samovski D, and Abumrad NA. Structure-function of CD36 and importance of fatty acid signal transduction in fat metabolism. *Annual review of nutrition.* 2014;34:281-303.

33. Su X, and Abumrad NA. Cellular fatty acid uptake: a pathway under construction. *Trends in endocrinology and metabolism: TEM.* 2009;20(2):72-7.

34. Samovski D, Sun J, Pietka T, Gross RW, Eckel RH, Su X, et al. Regulation of AMPK Activation by CD36 Links Fatty Acid Uptake to β-Oxidation. 2015;64(2):353-9.

35. DeFronzo RA, Tobin JD, and Andres R. Glucose clamp technique: a method for quantifying insulin secretion and resistance. *The American journal of physiology.* 1979;237(3):E214-23.

36. Newsom SA, Schenk S, Thomas KM, Harber MP, Knuth ND, Goldenberg N, et al. Energy deficit after exercise augments lipid mobilization but does not contribute to the exercise-induced increase in insulin sensitivity. 2010;108(3):554-60.

37. Steele R. Influences of glucose loading and of injected insulin on hepatic glucose output. *Annals of the New York Academy of Sciences.* 1959;82:420-30.

38. Dixon WT. Simple proton spectroscopic imaging. 1984;153(1):189-94.

39. Ryan BJ, Schleh MW, Ahn C, Ludzki AC, Gillen JB, Varshney P, et al. Moderate-intensity exercise and high-intensity interval training affect insulin sensitivity similarly in obese adults. *The Journal of clinical endocrinology and metabolism.* 2020.

40. R Core Team. R: A Language and Environment for Statistical Computing. *R Foundation for Statistical Computing.* 2019.

41. Ascaso JF, Pardo S, Real JT, Lorente RI, Priego A, and Carmena R. Diagnosing Insulin Resistance by Simple Quantitative Methods in Subjects With Normal Glucose Metabolism. *Diabetes Care.* 2003;26(12):3320-5.

42. DeFronzo RA, and Ferrannini E. Insulin Resistance: A Multifaceted Syndrome Responsible for NIDDM, Obesity, Hypertension, Dyslipidemia, and Atherosclerotic Cardiovascular Disease. *Diabetes Care.* 1991;14(3):173-94.

43. Roden M, Price TB, Perseghin G, Petersen KF, Rothman DL, Cline GW, et al. Mechanism of free fatty acid-induced insulin resistance in humans. *J Clin Invest.* 1996;97(12):2859-65.

44. Roden M, Stingl H, Chandramouli V, Schumann WC, Hofer A, Landau BR, et al. Effects of free fatty acid elevation on postabsorptive endogenous glucose production and gluconeogenesis in humans. *Diabetes.* 2000;49(5):701-7.

45. Boden G. Role of fatty acids in the pathogenesis of insulin resistance and NIDDM. *Diabetes.* 1997;46(1):3-10.

46. Thiébaud D, DeFronzo RA, Jacot E, Golay A, Acheson K, Maeder E, et al. Effect of long chain triglyceride infusion on glucose metabolism in man. *Metabolism.* 1982;31(11):1128-36.

47. Coppack SW, Fisher RM, Gibbons GF, Humphreys SM, McDonough MJ, Potts JL, et al. Postprandial substrate deposition in human forearm and adipose tissues in vivo. *Clin Sci (Lond).* 1990;79(4):339-48.

48. Frayn KN. Adipose tissue as a buffer for daily lipid flux. *Diabetologia.* 2002;45(9):1201-10.

49. Roden M, Krssak M, Stingl H, Gruber S, Hofer A, Fürnsinn C, et al. Rapid impairment of skeletal muscle glucose transport/phosphorylation by free fatty acids in humans. *Diabetes.* 1999;48(2):358-64.

50. Turner N, Kowalski GM, Leslie SJ, Risis S, Yang C, Lee-Young RS, et al. Distinct patterns of tissue-specific lipid accumulation during the induction of insulin resistance in mice by high-fat feeding. *Diabetologia.* 2013;56(7):1638-48.

51. Burchfield JG, Kebede MA, Meoli CC, Stöckli J, Whitworth PT, Wright AL, et al. High dietary fat and sucrose result in an extensive and time-dependent deterioration in health of multiple physiological systems in mice. *Journal of Biological Chemistry.* 2018;293(15):5731-45.

52. Mann JP, and Savage DB. What lipodystrophies teach us about the metabolic syndrome. *J Clin Invest.* 2019;129(10):4009-21.

53. Cifarelli V, Beeman SC, Smith GI, Yoshino J, Morozov D, Beals JW, et al. Decreased adipose tissue oxygenation associates with insulin resistance in individuals with obesity. *J Clin Invest.* 2020;130(12):6688-99.

54. DiPilato LM, Ahmad F, Harms M, Seale P, Manganiello V, and Birnbaum MJ. The Role of PDE3B Phosphorylation in the Inhibition of Lipolysis by Insulin. *Mol Cell Biol.* 2015;35(16):2752-60.

55. Yeckel CW, Dziura J, and DiPietro L. Abdominal obesity in older women: potential role for disrupted fatty acid reesterification in insulin resistance. *The Journal of clinical endocrinology and metabolism.* 2008;93(4):1285-91.

56. Meegalla RL, Billheimer JT, and Cheng D. Concerted elevation of acyl-coenzyme A:diacylglycerol acyltransferase (DGAT) activity through independent stimulation of mRNA expression of DGAT1 and DGAT2 by carbohydrate and insulin. *Biochem Biophys Res Commun.* 2002;298(3):317-23.

57. Ali AH, Mundi M, Koutsari C, Bernlohr DA, and Jensen MD. Adipose Tissue Free Fatty Acid Storage In Vivo: Effects of Insulin Versus Niacin as a Control for Suppression of Lipolysis. *Diabetes.* 2015;64(8):2828-35.

58. Lagathu C, Yvan-Charvet L, Bastard JP, Maachi M, Quignard-Boulangé A, Capeau J, et al. Long-term treatment with interleukin-1β induces insulin resistance in murine and human adipocytes. *Diabetologia.* 2006;49(9):2162-73.

59. Hotamisligil GS, Peraldi P, Budavari A, Ellis R, White MF, and Spiegelman BM. IRS-1-mediated inhibition of insulin receptor tyrosine kinase activity in TNF-alpha- and obesity-induced insulin resistance. *Science.* 1996;271(5249):665-8.

60. Lagathu C, Bastard J-P, Auclair M, Maachi M, Capeau J, and Caron M. Chronic interleukin-6 (IL-6) treatment increased IL-6 secretion and induced insulin resistance in adipocyte: prevention by rosiglitazone. *Biochemical and Biophysical Research Communications.* 2003;311(2):372-9.

61. Guilherme A, Virbasius JV, Puri V, and Czech MP. Adipocyte dysfunctions linking obesity to insulin resistance and type 2 diabetes. *Nature Reviews Molecular Cell Biology.* 2008;9(5):367-77.

62. Crewe C, An YA, and Scherer PE. The ominous triad of adipose tissue dysfunction: inflammation, fibrosis, and impaired angiogenesis. *J Clin Invest.* 2017;127(1):74-82.

63. Pasarica M, Rood J, Ravussin E, Schwarz J-M, Smith SR, and Redman LM. Reduced Oxygenation in Human Obese Adipose Tissue Is Associated with Impaired Insulin Suppression of Lipolysis. *The Journal of Clinical Endocrinology & Metabolism.* 2010;95(8):4052-5.

64. Marcelin G, Ferreira A, Liu Y, Atlan M, Aron-Wisnewsky J, Pelloux V, et al. A PDGFRα-Mediated Switch toward CD9(high) Adipocyte Progenitors Controls Obesity-Induced Adipose Tissue Fibrosis. *Cell Metab.* 2017;25(3):673-85.

65. Khan T, Muise ES, Iyengar P, Wang ZV, Chandalia M, Abate N, et al. Metabolic Dysregulation and Adipose Tissue Fibrosis: Role of Collagen VI. 2009;29(6):1575-91.

66. Pellegrinelli V, Heuvingh J, du Roure O, Rouault C, Devulder A, Klein C, et al. Human adipocyte function is impacted by mechanical cues. *J Pathol.* 2014;233(2):183-95.

67. Marcelin G, Silveira ALM, Martins LB, Ferreira AVM, and Clément K. Deciphering the cellular interplays underlying obesity-induced adipose tissue fibrosis. *J Clin Invest.* 2019;129(10):4032-40.

68. Klip A, Sun Y, Chiu TT, and Foley KP. Signal transduction meets vesicle traffic: the software and hardware of GLUT4 translocation. 2014;306(10):C879-C86.

69. Zisman A, Peroni OD, Abel ED, Michael MD, Mauvais-Jarvis F, Lowell BB, et al. Targeted disruption of the glucose transporter 4 selectively in muscle causes insulin resistance and glucose intolerance. *Nat Med.* 2000;6(8):924-8.

70. Itani SI, Zhou Q, Pories WJ, MacDonald KG, and Dohm GL. Involvement of protein kinase C in human skeletal muscle insulin resistance and obesity. *Diabetes.* 2000;49(8):1353-8.

71. Dobrowsky RT, Kamibayashi C, Mumby MC, and Hannun YA. Ceramide activates heterotrimeric protein phosphatase 2A. *The Journal of biological chemistry.* 1993;268(21):15523-30.

72. Sun S, Tan P, Huang X, Zhang W, Kong C, Ren F, et al. Ubiquitinated CD36 sustains insulin-stimulated Akt activation by stabilizing insulin receptor substrate 1 in myotubes. *Journal of Biological Chemistry.* 2018;293(7):2383-94.

73. Yu C, Chen Y, Cline GW, Zhang D, Zong H, Wang Y, et al. Mechanism by which fatty acids inhibit insulin activation of insulin receptor substrate-1 (IRS-1)-associated phosphatidylinositol 3-kinase activity in muscle. *The Journal of biological chemistry.* 2002;277(52):50230-6.

74. Huang MM, Bolen JB, Barnwell JW, Shattil SJ, and Brugge JS. Membrane glycoprotein IV (CD36) is physically associated with the Fyn, Lyn, and Yes protein-tyrosine kinases in human platelets. *Proceedings of the National Academy of Sciences of the United States of America.* 1991;88(17):7844-8.

75. Bull HA, Brickell PM, and Dowd PM. Src-related protein tyrosine kinases are physically associated with the surface antigen CD36 in human dermal microvascular endothelial cells. *FEBS letters.* 1994;351(1):41-4.

76. Gemmink A, Goodpaster BH, Schrauwen P, and Hesselink MKC. Intramyocellular lipid droplets and insulin sensitivity, the human perspective. *Biochimica et Biophysica Acta (BBA) - Molecular and Cell Biology of Lipids.* 2017;1862(10, Part B):1242-9.

77. Chee C, Shannon CE, Burns A, Selby AL, Wilkinson D, Smith K, et al. Relative Contribution of Intramyocellular Lipid to Whole-Body Fat Oxidation Is Reduced With Age but Subsarcolemmal Lipid Accumulation and Insulin Resistance Are Only Associated With Overweight Individuals. *Diabetes.* 2016;65(4):840-50.

78. Perreault L, Newsom SA, Strauss A, Kerege A, Kahn DE, Harrison KA, et al. Intracellular localization of diacylglycerols and sphingolipids influences insulin sensitivity and mitochondrial function in human skeletal muscle. *JCI Insight.* 2018;3(3):e96805.

79. Thiam AR, and Beller M. The why, when and how of lipid droplet diversity. *J Cell Sci.* 2017;130(2):315-24.

80. Murphy DJ. The dynamic roles of intracellular lipid droplets: from archaea to mammals. *Protoplasma.* 2012;249(3):541-85.

81. Hesselink MK, Mensink M, and Schrauwen P. Intramyocellular lipids and insulin sensitivity: does size really matter? *Obes Res.* 2004;12(5):741-2.

82. Vock R, Hoppeler H, Claassen H, Wu DX, Billeter R, Weber JM, et al. Design of the oxygen and substrate pathways. VI. structural basis of intracellular substrate supply to mitochondria in muscle cells. *J Exp Biol.* 1996;199(Pt 8):1689-97.

83. Clerk LH, Vincent MA, Jahn LA, Liu Z, Lindner JR, and Barrett EJ. Obesity blunts insulin-mediated microvascular recruitment in human forearm muscle. *Diabetes.* 2006;55(5):1436-42.

84. McClatchey PM, Williams IM, Xu Z, Mignemi NA, Hughey CC, McGuinness OP, et al. Perfusion controls muscle glucose uptake by altering the rate of glucose dispersion in vivo. *Am J Physiol Endocrinol Metab.* 2019;317(6):E1022-e36.

85. Fazakerley DJ, Krycer JR, Kearney AL, Hocking SL, and James DE. Muscle and adipose tissue insulin resistance: malady without mechanism? *Journal of lipid research.* 2019;60(10):1720-32.

86. Nuutila P, Knuuti MJ, Mäki M, Laine H, Ruotsalainen U, Teräs M, et al. Gender and insulin sensitivity in the heart and in skeletal muscles. Studies using positron emission tomography. *Diabetes.* 1995;44(1):31-6.

87. Tramunt B, Smati S, Grandgeorge N, Lenfant F, Arnal J-F, Montagner A, et al. Sex differences in metabolic regulation and diabetes susceptibility. *Diabetologia.* 2020;63(3):453-61.

Chapter V

Project 3
Effects of Exercise Training on Intramyocellular Lipid Droplet Abundance, Size, Cellular Distribution, and Turnover in Adults with Obesity

ABSTRACT

Exercise training modifies lipid metabolism in skeletal muscle, but the effect of exercise training on intramyocellular lipid droplet (LD) abundance, size, and intracellular distribution in adults with obesity are still not completely understood. The primary aims of this study were to compare high-intensity interval training (HIIT) versus more conventional moderate-intensity continuous training (MICT) in adults with obesity on intramyocellular lipid content, as well as LD characteristics (size and number) and abundance within the intramyofibrillar (IMF) and subsarcolemmal (SS) regions of type I and type II muscle fibers. Thirty-six adults with obesity (BMI=33±3 kg/m^2) completed 12 weeks (4d/week) of either HIIT (10 x 1min, 90%HRmax + 1min active recovery; n=19) or MICT (45min steady-state exercise, 70% HRmax; n=17). Subjects were on a weight-maintaining diet throughout training. Skeletal muscle samples were collected from the vastus lateralis before and after training, and intramyocellular lipid content and distribution were measured by immunofluorescence microscopy. Exercise training (both MICT and HIIT) increased total intramyocellular lipid content by ~1.5 fold ($p<0.01$), and this increase was attributed to a greater number of LDs per μm^2 in the IMF region of both type I and type II muscle fibers (both $p<0.01$). Our findings also suggest that LD lipophagy may be upregulated when measured the day after the last exercise training session ($p<0.02$ for both MICT and HIIT). But this response appeared to be transient because the increase in these measures were no longer apparent when assessed 4 days after the last exercise training session. Interestingly, despite the robust difference in exercise stimulus between MICT and HIIT, the effects of these exercise programs on intramyocellular LDs were remarkably similar. In summary, exercise programs for adults with obesity involving either MICT or HIIT lead to modifications in LD abundance and cellular distribution that are favorable for providing more lipid to support oxidative metabolism during exercise.

INTRODUCTION

Intramyocellular lipids provide an energy dense fuel to support muscle contraction during exercise (1, 2). Intramyocellular lipid content is often found to be high in endurance trained athletes (3, 4), representing a favorable exercise training adaptation. This adaptive response may be largely explained by an exercise-induced increase in skeletal muscle triacylglycerol synthesis within the hours after each exercise session (5), which in turn will increase the local energy supply to help sustain prolonged exercise. Somewhat paradoxically, sedentary adults with obesity are also often found to have elevated skeletal muscle lipid content compared with lean counterparts (6, 7). But in contrast to endurance athletes, this high muscle lipid content in obesity largely stems from chronically elevated lipolytic rates and excessive systemic fatty acid availability (8), providing abundant substrate for muscle lipid synthesis. Unfortunately, excessive intramyocellular lipid accumulation in sedentary adults with obesity are causally linked with the development of insulin resistance (9-11). Findings from previous studies examining the effects of exercise training on muscle lipid content in adults with obesity are equivocal, most reporting either an increase (12-17), while others reporting no change in total muscle lipid content (18-21). However, the response to exercise training on muscle lipid content in obese subjects have been confounded by several factors, including weight loss during training, differences in the mode and intensity of exercise, and limited dietary control - all of which can impact interpretations of the effects of exercise training on regulation of muscle lipid storage.

Intramyocellular lipids are largely stored within lipid droplets (LDs), which are dynamic organelles composed of a triacylglycerol-rich core surrounded by a phospholipid monolayer. Lipid droplet abundance is largely regulated by nascent LD biogenesis from the endoplasmic reticulum (ER), where triacylglycerol accumulation and growth within the ER bilayer promotes the budding of LDs towards the cytosol (22). Conversely, LDs are selectively degraded by a form of autophagy, called lipophagy, involving recruitment of the autophagasome specifically to the LD, and transport to the lysosome for degradation (23, 24). Muscle LDs help regulate local lipid availability within the myocyte (25), and the size of the LDs can impact this function. This is due in part to the surface area-to-volume ratio of the LD, where a relatively high surface area-to-volume ratio from small LDs can increase lipase accessibility at the LD surface, increasing fatty acid availability for cellular metabolism (26). The location of the LD also has important impact on its cellular function. For example, LDs localized to the intramyofibrillar (IMF) region of the

myocyte are recognized to support energy requirements for skeletal muscle contraction (27, 28), whereas LDs localized to the subsarcolemmal (SS) region support cell membrane biosynthesis and metabolism. Interestingly, endurance training has been found to increase LD contact with the mitochondria in the IMF region, in effort to support fatty acid availability for the contracting muscle (16, 18). Perhaps not surprisingly, LDs are more abundant in type I versus type II muscle fibers, which aligns with the high oxidative capacity of type I fibers to support prolonged and relatively low-intensity muscle activation (29). Although exercise training may favorably modify intramyocellular lipid storage and distribution (12-21), *how* exercise modifies LD storage is still not completely understood.

High-intensity interval training (HIIT) has garnered considerable attention as a time-efficient exercise prescription to increase aerobic capacity (30, 31), and improve metabolic health in obesity (32). However, the effects of HIIT versus more conventional, moderate-intensity continuous training (MICT) on intramyocellular lipid content and LD distribution in adults with obesity remains unclear. The primary aim of this study was to compare the effects of 12 weeks MICT versus HIIT on the size, number, and cellular distribution of LDs within skeletal muscle in adults with obesity. Additionally, we aimed to explore the effects of training on the regulation LD turnover by assessing LD co-localization with proteins specific to the ER (index of LD biogenesis) and proteins specific to the autophagasome (index of lipophagy). We hypothesized that the high-intensity stimulus during HIIT will increase muscle lipid content to a greater extent than MICT, primarily via increased number and size of LDs within the IMF region of the type II muscle fibers.

METHODS

Participants

Thirty-six adults with obesity (BMI=30-40 kg/m^2) participated in this study. Participants enrolled into this clinical trial were sedentary and not participating in any aerobic or resistance-training programs, and weight stable (±2 kg for the previous 6 months). Participants were not taking medications known to affect glucose or lipid metabolism, have a history of heart disease, or smoking. All females were pre-menopausal with regularly occurring menses, and not pregnant, or lactating. Participants in this study were also enrolled in a previously published study from our laboratory, focusing on the effect of 12 weeks MICT and HIIT on whole-body insulin sensitivity

(hyperinsulinemic-euglycemic clamp) and clinical biomarkers (33). The outcomes in the present study complement, but do not overlap with our previous publication. Participants were provided written informed consent before participation. The study protocol was approved by the University of Michigan Institutional Review Board, and registered at clinicaltrials.gov (NCT02706093).

Preliminary assessment

Participants arrived to the Michigan Clinical Research Unit (MCRU) for a body composition assessment using dual-energy x-ray absorptiometry (Lunar DPX DECA scanner, GE, WI), then complete a graded exercise test to determine aerobic capacity (VO_2peak) on a cycle ergometer (Corvival, Lode, Netherlands). Details regarding VO_2peak protocol were previously described by Ryan et al. (33).

Study design

Enrolled participants were randomly assigned to either MICT (n=17) or HIIT (n=19) in a counterbalanced design, with a homogenous subset of individuals matched for BMI, fat mass, and sex in each group (Table V-1). Before training, participants completed their pre-training clinical trial, which included the collection of a skeletal muscle biopsy sample. Subjects then completed 12 weeks (4 sessions/week, 48 total) of their assigned exercise training program (MICT or HIIT; details of these training programs provided below). After completing the 12-week training programs, participants completed two more clinical trials, the first of these post-training clinical trials was completed the day after the last exercise session (1d PostEx). The other post-training clinical trial was conducted four days after the last exercise session (4d PostEx), in order to examine the chronic adaptive responses to exercise training without the potent confounding effects of a recent session of exercise (34, 35). See Figure V-1 for study design. Importantly, subjects were required to maintain their body weight throughout the study trial.

Training interventions

Participants in both groups exercised 4 days per week for 12 weeks. The exercise sessions for MICT consisted of 45 minutes continuous exercise at 70% HR_{max}. For the HIIT group, each training session consisted of 3 minutes warm up (65% HR_{max}), followed by 10 x 1 minute intervals at 90% HR_{max}, with 1 minute active recover between intervals. Participants self-selected their mode of exercise (e.g., stationary bike, treadmill, elliptical, or rowing machines). HIIT sessions

were considerably shorter than MICT (25 versus 45 minutes), and energy expenditure for HIIT was less than MICT (~150 versus ~250 kcals). Despite considerably different exercise duration and energy expenditure, we aimed to compare HIIT and MICT program commonly prescribed for improving fitness and health (36).

Training familiarization and adherence monitoring

Details describing training familiarization and adherence monitoring have been previously reported (33). Briefly, during the first two weeks of the exercise familiarization period subjects were exposed to a progressive increase in exercise intensity and duration. By the beginning of week three, participants were able to complete the prescribed exercise programs for MICT (45 minutes continuous exercise at 70% HR_{max}) and HIIT (10 x 1 minute intervals at 90% HR_{max}, with 1 minute active recover between intervals). During the two-week familiarization period, research staff monitored all training sessions (4 sessions per week). After completing the exercise familiarization, participants were still required to complete four exercise sessions per week, but only two of these sessions were required to be supervised directly by research staff. For the unsupervised session, participants wore downloadable telemetry heart rate devices (Polar) that were monitored remotely by research staff to confirm exercise adherence and compliance. Body weight was also closely monitored throughout the training intervention and participants were required to maintain their weight throughout the training intervention. Our research dietician consulted participants for weight management if their weight deviated ~1-2% pre-training weight.

Clinical Trials and Skeletal Muscle Biopsy Collection

During each of the three clinical trials, subjects arrived to the MCRU at 1730h the evening before the clinical trial (see Appendix J for clinical trial schematic). The protocol for all three clinical trials were identical, with the exception of the 1d PostEx visit, during which participants completed their prescribed exercise sessions at 1800h and then consumed a nutritional supplement (BoostPlus, Nestle; 50% carbohydrate, 35% fat, 15% protein) to match the estimated energy expended during exercise session. For all three trials, participants consumed a standardized meal at 1900h (30% estimated daily energy expenditure) and a snack (10% estimated daily energy expenditure) at 2200h, and slept in MCRU overnight.

The next morning, a fasting blood sample was obtained at 0730h, and a skeletal muscle sample was collected from the vastus lateralis muscle at 0815h. For the portion of the muscle

sample to be used for immunofluorescence microscopy, visible connective tissue was removed under magnification, muscle fibers were oriented in parallel, the sample was fixed in optimal cutting temperature (OCT), and flash frozen in isopentane chilled over liquid nitrogen. The remaining muscle samples were rinsed with saline, blotted dry, and flash frozen in liquid nitrogen for immunoblot analysis.

After collecting the skeletal muscle sample during the clinical trials, we also collected abdominal subcutaneous adipose tissue samples, performed stable isotope infusions to calculate, fatty acid, glycerol, and glucose kinetics, and we also conducted a hyperinsulinemic-euglycemic clamp. Outcomes from these ancillary measures are not included in the present study, and because these methods were initiated after completion of the muscle biopsy, they would not impact the skeletal muscle outcomes presented here. Therefore, the details for these methods are not described here. See Ryan, et al (33) for detailed description of all methods conducted during these clinical trials.

Analytical Procedures

Immunofluorescence microscopy: lipid droplet analysis

Skeletal muscle samples from OCT samples were cut into 5µm sections at -20°C and mounted onto an ethanol-cleaned glass slide. Sections were fixed in 4% paraformaldehyde for 1h, and permeabilized for 5min in 0.5% Triton X-100. Sections were then incubated with primary antibodies myosin heavy chain type 1 (MHC-1) at 1:200 for 1h at 37ºC, followed by 30min secondary antibody incubation: AlexaFluor 647, goat-anti mouse IgG2b at 1:200. Afterwards, sections were stained with Bodipy 493/503 at 1:100 for 20min, followed by 20min incubation with anti-wheat germ agglutinin (WGA) conjugated with AlexaFluor 555 at 1:200 to identify muscle fiber borders. Sections were mounted with ProLong Gold Antifade Mountant**,** covered with #1 coverslips (2975-245, Corning), and stored in the dark until imaging. See Table V-2 for reagent list, and Appendix H for detailed protocol.

Immunofluorescence microscopy: co-localization analysis

Skeletal muscle samples from OCT fixed muscle were cut into 5µm sections at -20°C onto an ethanol-cleaned glass slide, then fixed in 4% paraformaldehyde for 30min, followed by 5min permeabilization in 0.3% Triton X-100, and blocked for 1h in 5% normal goat serum to prevent

nonspecific background and cross-reactivity between antibodies. For each muscle sample, one section was situated onto a glass slide incubated for primary antibodies to measure de novo LD biogenesis activity, which was quantified by PLIN2 (LD marker; 1:100 in 0.1% BSA, 0.1% Triton X-100, PBS) co-localization with KDEL (ER marker; 1:100 in 0.1% BSA, 0.1% Triton X-100, PBS) at 4ºC overnight. Additionally, one separate section from the same muscle sample was situated onto a separate glass slide, and incubated for primary antibodies to measure lipophagy, and quantified by PLIN2 co-localization with Light Chain 3 (LC3; autophagasome marker; 1:50 in 0.1% BSA, 0.3% Triton X-100, PBS) in 4ºC overnight. The following day, samples were incubated with secondary antibodies Alexa Fluor 647, goat anti-mouse IgG1 (specificity to PLIN2) at 1:200 and Alexa Fluor 488, goat anti-rabbit IgG (specificity to KDEL and LC3) at 1:200 for 1h. Samples were then incubated with anti-WGA conjugated with AlexaFluor 555 at 1:200 for 20min, mounted with ProLong Gold Antifade Mountant, and covered with #1 coverslips (Corning), and stored in the dark until imaging. See Appendix K for immunohistochemistry protocol.

Fluorescence image acquisition, image processing, and analysis

Total lipid content (% stained), LD number (# LDs per μm^2), and median LD area per muscle fiber (μm^2) were captured on a Keyence BZ-X710 fluorescence microscope (Keyence) with a 20X N.A.=0.45 objective lens using 1440 X 1080 pixels (533 µm x 400 µm) field of view. Lipid droplets stained by bodipy 493/503 were captured using GFP (470/40 nm) filter, MHC type I was captured using Cy5 (620/60 nm) filter, and WGA captured using Texas Red (560/40nm) filter. Following image capture, LD characteristics and distribution were calculated using MATLAB R2021a (Mathworks, Inc., Natick, MA). In brief, 20X images were converted to grayscale and re-scaled to accommodate for image variability between samples. Individual fibers were identified and labeled using a custom ridge detection algorithm, and watershed segmentation to complete non-continuous cell borders and completely identify cells. Type I fibers were identified based on positive MHC type I-positive stain, and non-stained fibers considered type II fibers. Fiber types were partitioned into type I or type II fibers dependent on signal intensity by k-means clustering (k=2). Lipid droplets identified in the SS region were contained within ~3 µm of the peripheral border of each fiber (10 pixel width), while LDs in the IMF region were all remaining LDs in the center of each fiber (~91% of cross-sectional myocyte area). Lipid droplets were detected as the mean area of puncta, and a top-hat filter was used to accommodate for image variability and background noise within the sample. Lipid droplets identified and included for

analysis for each muscle fiber were within a normal Gaussian distribution. In total, ~3 fields of view were obtained per participant, resulting in the analysis of 165±71 (median=147) muscle fibers per participant.

Co-localization analysis was performed separately by PLIN2 co-localization with KDEL (de novo LD biogenesis) and PLIN2 co-localization with LC3 (lipophagy). Images were captured using Keyence BZ-710X with a 40X N.A. = 0.60 objective lens using 1440 X 1080 pixels (362 µm x 273 µm). PLIN2 was captured using the Cy5 filter (620/60 nm), WGA captured using the Texas Red filter (560/40nm), and KDEL and LC3 were captured using the GFP (470/40 nm) filter to quantify de novo LD biogenesis and lipophagy respectively. Following image acquisition, an intensity threshold was selected uniformly for each target of interest in order to identify positive signals and remove background intensities. Quality control for nonspecific secondary antibody binding were completed and verified before co-localization analysis was conducted. Co-localization between PLIN2-KDEL and PLIN2-LC3 were quantified by Pearson's and Mander's (M1) overlap coefficient using Coloc2 plug-in with FIJI (NIH Image J) (37).

Skeletal muscle lysate preparation and immunoblot

Frozen muscle samples were weighed (~25mg) and transferred into pre-chilled microcentrifuge tubes containing 1mL ice-cold lysis buffer [RIPA Buffer: 20 mM Tris-HCl-pH 7.5, 150 mM NaCl, 1 mM Na_2EDTA, 1 mM EGTA, 1% NP-40, 1% sodium deoxycholate, 2.5 mM sodium pyrophosphate, 1 mM β-glycerophosphate, 1 mM Na_3VO_4, 1 µg/mL leupeptin (9086, cell signaling technology)], 1% phosphatase inhibitor cocktail #1 & #2 (P2850, P5726, Sigma-Aldrich), 1% protease inhibitor cocktail (P8340, Sigma-Aldrich), and two steel ball bearings per sample. Samples were homogenized for 30sec at 45Hz using a Qiagen TissueLyser II, then solubilized for 60min by inverted end-over-end rotation at 50rpm in the cold (4°C). Afterwards, samples were centrifuged at 15,000g for 15min at 4°C, and the pellet was discarded. Protein concentration was determined by bicinchoninic acid assay method (BCA; 23225, Pierce Thermo-Fisher), and samples diluted in 4x Laemmli buffer and RIPA buffer to achieve 1µg/µL concentration, and heated for 7min at 95°C. Proteins were separated by SDS-Page (8-15% acrylamide gels), then transferred to nitrocellulose membranes, and probed by the following primary antibodies listed in Table V-2. To account for loading variability, membranes were stained and normalized to total protein abundance by Memcode reversible protein stain (24580, Pierce Thermo-Fisher). Additionally, each gel contained an internal standard sample from 8 obese

individuals to account for gel-to-gel variability, and each protein normalized to the internal standard.

Statistical Analysis

Normality was tested using Shapiro-Wilk test, and data not normally distributed were log transformed before analysis. When missing data for a specific measurement was present and unavoidable (e.g., poor frozen section or unable to obtain sample), data for the specific measurement was excluded for all trials for the subject, and the specific sample size was reported for the given outcome in which missing data was present. For immunoblot and LD co-localization analysis; linear mixed models were used to determine the main effect of group (MICT versus HIIT), visit (pre, 1d PostEx, and 4d PostEx), and group x visit interaction. For LD histochemistry analysis, measurements of LD area, LD density, and LD size were segregated by fiber type (type I and type II fibers) and regional distribution (IMF versus SS region). Linear mixed models were then used on the segregated outcomes with the same main effects as previously described (group and visit). Data are displayed mean±SD and $p \leq 0.05$ was considered statistically significant. Statistical analysis and figure generation was completed using R version 4.1.0 (38).

RESULTS

Participant characteristics at baseline and in response to training

Table V-1 provides the physical characteristics and clinical measurements before and after training in the 36 subjects who completed the 12-week exercise training intervention (MICT=17, HIIT=19). MICT and HIIT both significantly increased aerobic capacity ($p<0.01$). The trend for a greater increase in VO_2peak after MICT versus HIIT did not reach statistical significance ($p=0.1$; Table 1). Body weight did not change after the 12 week training interventions in either groups, but the very slight reduction in fat mass after training (~0.5kg) was found to be statistically significant ($p=0.02$).

Training effects on muscle lipid content and LD regional distribution within type I and type II muscle fibers

Twelve weeks of training significantly increased total muscle lipid content, with no significant difference between MICT and HIIT (Figure V-2B). The increase in muscle lipid content

was found in both type I (Figure V-2C) and type II (Figure V-2D) muscle fibers ($p \leq 0.01$ for both). Moreover, the increase in muscle lipid content after training was specific to the IMF region of both type I and type II fibers ($p < 0.01$), and again, the responses were similar between MICT and HIIT (Figure V-3A). In contrast, lipid content in the SS region was not affected by training (Figure V-3B). The greater lipid content in the IMF region after training was attributed to an increase in the number of intramyocellular LDs (LD # per μm^2) in both type I and type II fibers (both $p \leq 0.02$; Figure V-3C), but not an increase in LD area (Figure V-3E). There were no training-induced changes observed in LD number or area in the SS region of the muscle samples (Figures V-3D and V-3F).

Training effects on mitochondrial proteins, factors regulating fatty acid transport, triglyceride esterification, lipogenesis, and ER Stress.

Training significantly increased the protein abundance of all five mitochondrial respiratory chain complexes in both MICT and HIIT ($p < 0.01$ for all measures; Figure V-4A). Data for these mitochondrial proteins were similarly reported from a sub-cohort of the same participants as the current study from Ryan et al. (33). MICT and HIIT also increased CPT1b abundance, but this increase did not reach statistical significance until four days after the last exercise session ($p = 0.03$: Figure V-4B). The protein abundance of glycerol-3-phosphate acyltransferase 1 (GPAT1), a protein responsible for acyl-CoA esterification at the mitochondria and the abundance of cleaved (i.e., activated) sterol regulatory element-binding protein 1 (SREBP-1c), a transcription factor responsible for inducing the expression of genes involved in fatty acid synthesis from glucose substrates were both increased after training (both $p < 0.01$), with no differences between MICT and HIIT (Figure V-4C and V-4D). In contrast, training did not increase protein abundance of fatty acid synthase (FASN) or the ER Stress related proteins ATF4 and CHOP in skeletal muscle (Figures V-4D and V-4E).

Training effects on de novo LD biogenesis

Both MICT and HIIT significantly increased PLIN2 abundance ($p < 0.01$), a protein highly expressed on LD membranes, which is involved in lipolytic regulation (39) (Figure V-5A). However, neither MICT nor HIIT altered the abundance of Seipin (BSCL2) or FIT1M (Figure V-5B), which are ER proteins responsible for LD stabilization and budding (40). We measured the co-localization of PLIN2 (LD marker) with the ER marker, KDEL, as a crude index of de novo

LD biogenesis from the ER (Figure V-5D provides a representative image of the co-localization experiment). We found no effect of training on the co-localization of PLIN2 and KDEL, measured by both Pearson's and Mander's co-localization coefficients (Figure V-5E).

Training effects on autophagy-mediated LD degradation

The abundance of p62, a marker of protein ubiquination was increased after training, and there were no differences between MICT and HIIT. However, p62 was only significantly increased one day after the last exercise session ($p<0.01$), and was no longer significantly greater than pre-training abundance four days after the last exercise session (Figure V-6A). LC3-II is a marker of autophagasome activation by phosphatidylethanolamine lipidation, and we found the total protein abundance of LC3-II increased only after MICT ($p=0.02$; Figure V-6A). However, the ratio of LC3-II to LC3-I, which is more reflective of LC3 activation within muscle, was found to be significantly elevated after both MICT and HIIT one day after the last exercise session ($p=0.03$; Figure V-6A), but appeared to return toward pre-training levels 4 days after the last exercise session (Figure V-6A). We measured the co-localization of PLIN2 with LC3 as a crude index of lipophagy in skeletal muscle. Here we found both MICT and HIIT increased LC3 co-localization with PLIN2 measured by both Pearson's (main-effect for visit, $p=0.04$) and Mander's (main-effect for visit, $p<0.01$) coefficients, with no significant difference in response between MICT and HIIT. Interestingly, LC3-PLIN2 co-localization was only significantly elevated one day after the last exercise session (Pearson's, $p=0.03$; Mander's, $p=0.01$), and returned towards pre-training levels four days after the last exercise session.

DISCUSSION

Endurance exercise training is often found to increase muscle lipid content (12-17), and here, we found that 12 weeks of both MICT and HIIT increased intramyocellular lipid content in previously sedentary adults with obesity. One of the important findings from this study was that the increase in total lipid content in skeletal muscle after training was due to an increased number of intramyocellular LDs, but not their size. Furthermore, the increased number of LDs was specific to the IMF region of muscle fibers, suggestive of an adaptive response to increase energy supply in close proximity to the site of high energy expenditure during muscle contraction. The mechanisms underlying the increased LD number within the IMF region are not clear, but de novo

LD biogenesis from the ER, fission of pre-existing LDs, and LD turnover by lipophagy are likely candidates. Another key finding from our study was that despite the robust differences in training intensity and energy expenditure between MICT and HIIT, their effects on our measures of lipid abundance and metabolism in skeletal muscle were remarkably similar.

Endurance exercise training is consistently found to increase muscle lipid content in lean subjects (12, 13) but this is not always the case in adults with overweight and obesity (18-20, 41-43). The absence of a measurable increase in muscle lipid content after training in some studies may be a consequence of a very high muscle lipid abundance found in some sedentary obese adults (44), which may make it challenging to detect a relatively small increase in muscle lipid content in these patients. Additionally, when an exercise training intervention is accompanied by weight loss, a training-induced increase in muscle lipid storage capacity may be countered by a reduction in lipid availability due to weight loss (6, 15, 45, 46). The observed increase in muscle lipid content in our study may be a result of the study population having relatively modest obesity (class 1 obesity), and the strict requirement for weight-maintenance during the training intervention. The effects of exercise on muscle lipid accumulation may largely be a consequence of the most recent session, or sessions of exercise, rather than an adaptive response to long-term training. Previous work from our lab demonstrated increased muscle lipid content the day after a single session of exercise was accompanied by an increase in key proteins involved in muscle triacylglycerol synthesis (i.e., mGPAT1 and DGAT1) (5). The greater muscle lipid content after training in the current study was accompanied by increased protein abundance of mGPAT1 and SREBP-1c, also supporting the notion that exercise augmented mechanisms to enhance muscle lipid synthesis. Additionally, the effects of exercise on muscle lipid availability from adipose tissue lipolysis are often elevated during the recovery period after exercise (47, 48), and increased provision of available substrate may also help augment muscle lipid synthesis after a session of exercise. This increase in muscle lipid synthesis and storage after exercise can help support the metabolic demand of the working muscle during subsequent exercise sessions.

Muscle lipids are largely stored within LDs, which are intramyocellular organelles composed of a hydrophobic core surrounded by a phospholipid monolayer (25). Assessments of the number, size and cellular distribution of LDs enhances our interpretation of intramyocellular lipid metabolism and storage after endurance training. Our finding that an increase in muscle lipid content after training was largely attributed to more LDs within muscle fibers, and not their size,

agrees with some previous studies (4, 13, 16). This adaptation to increase muscle lipid content, via a greater number of LD after training, permits total lipid content expansion without accumulating larger-sized LDs. For this reason, larger LDs may not be metabolically favorable due to their relatively low surface area-to-volume ratio, which can compromise lipolytic control of the lipids within the LD (26, 49). Interestingly, the accumulation of larger-sized LDs have been shown to inversely relate with insulin sensitivity (21, 50), and the decrease in LD size after training has been proposed to contribute to the insulin sensitizing effect of exercise training (18-20, 50). Moreover, increasing muscle lipid content by increasing the number of LDs has been found to increase the physical interaction between the LDs and the mitochondria (16, 18, 42), which can further enhance coordination between fatty acid availability for muscle lipid oxidation during exercise.

The increase in lipid content specifically in the IMF region of the muscle fiber after training, as reported here by us and by others (18-20, 51), is also favorable for coordinating energy supply and demand during exercise. Skeletal muscle fibers are highly specialized, and different subcellular regions of the myocyte support different processes. The peripheral SS region is adjacent to the cell membrane, and components of the SS are largely involved in membrane function, signaling, and maintenance (27). In contrast, the centrally-located IMF region of the muscle fiber houses the contractile proteins, and is the site of greatest energy demand during exercise (27). Therefore, an increase in LDs in the IMF region after training will likely support energy required for muscle contraction (28). Some previous reports suggest exercise training may lead to a redistribution of LDs from the SS and into the IMF region of the muscle fiber (18-20, 51). However, this was not apparent after either MICT or HIIT in our study, because the increase in LDs in the IMF region was not accompanied by a reduction in SS LDs.

Other proposed mechanisms that may contribute to increased LD number within the IMF region after training include de novo LD biogenesis from the ER (40), and fragmentation (i.e., fission) of pre-existing LDs (52, 53). De novo LD biogenesis involves fatty acid esterification into triacylglycerol within the ER leaflets, contributing to nascent LD budding towards the cytosol (40). Here, immunofluorescence microscopy was used to quantify LD co-localization with the ER as an index of de novo LD biogenesis, and we found exercise training did not affect our measure of LD co-localization with the ER. However, based on the somewhat limited resolution of the fluorescence co-localization approach we used to assess LD budding from the ER, we cannot rule

out the possibility that exercise may impact LD biogenesis. Additionally, it is possible our sampling timeline (samples collected ~14 hours after the last exercise session) was not optimal to capture an increase in de novo LD biogenesis. LD fission of pre-existing LDs is also difficult to detect, but the observed increase in the number of LDs without a reduction in LD size could reflect LD fission coupled with increased intramyocellular triacylglycerol synthesis that is known to increase after exercise (5). Mechanisms contributing to LD fission are still unclear (40), but it is intriguing to consider that an increase triacylglycerol synthesis in the hours after a session of exercise may increase tension within the hydrophobic core of LDs, facilitating LD fission (52).

Lipophagy is a specialized form of autophagy, and is an essential for the degradation of intracellular LDs by the lysosome (23). In skeletal muscle, lipophagy has been reported to help control LD turnover (54). Lipophagy appears to be regulated, at least in part, by the energy status within the cell, increasing in response to an energy deficit (23, 55). Our findings suggest muscle lipophagy may increase the day after the most recent exercise training session but may return to pre-training levels after abstaining from exercise for 4 days. The transient nature of this response may reflect the changes in intracellular energy flux occurring during the several hours of recovery after exercise, in effort to increase fatty acid availability as local lipid and carbohydrate (i.e., glycogen) stores are being replenished. Although it is reasonable to surmise that an increase in lipophagy in skeletal muscle after exercise may coincide with a *reduction* in the number of LDs, our findings suggest the opposite (i.e., the number of muscle LDs increased). In agreement with our findings, it has been reported that an increase in lipophagy in response to energy deficit was accompanied by an increase in the number of LDs, especially an increase in LDs adjacent to the mitochondria (55). Therefore, perhaps an exercise-induced increase in lipophagy may serve as an adaptive response to increase LD turnover and redistribution within the IMF region of the muscle fiber, in effort to support fatty acid availability and oxidation for the working muscle, which has been shown to occur after exercise training (16, 18).

Excessive accumulation of lipid in skeletal muscle is commonly associated with insulin resistance (9, 11). In particular, the accumulation of lipid intermediates and metabolites (e.g., diacylglycerol, ceramides and acylcarnitine) have been causally linked to impaired insulin signaling (56-58). The subcellular distribution of these lipids also appears to be important, whereby their accumulation specifically in the SS region of the myocyte have been primarily linked with insulin resistance (20, 21, 50, 59, 60). The insulin de-sensitizing effects of an

accumulation of these lipids specific to the SS region may be due largely to their proximity to the plasma membrane, the site of important insulin signaling events. It has been proposed that exercise training may help alleviate insulin resistance in obesity, in part by decreasing SS lipid content or SS LD size (18-21, 50). In contrast, however, we did not observe a reduction in SS lipid content or LD size in our subjects after 12 weeks of MICT or HIIT. Moreover, in recently published work from this same study (33) we also found 12 weeks of training did not improve insulin sensitivity .change after training in our study, perhaps this was a consequence of our strict requirement for weight maintenance in all subjects, but based on our findings, it is intriguing to consider that a reduction in SS lipid content after an exercise/lifestyle intervention may be very important for improving insulin sensitivity. Our findings that exercise training increased muscle lipid content specifically in the IMF region, suggests the exercise-induced muscle lipid adaptations to MICT and HIIT in our subject may have occurred primarily to support oxidative metabolism, without compromising insulin sensitivity.

Surprisingly, the exercise-induced adaptations in muscle lipid outcomes measured in this study were very similar between MICT and HIIT, despite marked differences in exercise intensity, duration and energy expenditure during each training session. Although this finding was contrary to our hypothesis, it does align with previous work (13) in which similar increases in muscle lipid content were found in response to MICT versus sprint interval training (SIT), which represents an even greater disparity in intensity, duration, and energy expenditure than our MICT vs HIIT comparison. Reasons to explain the similar adaptive responses between these distinct exercise stimuli are not clear. It is possible that the adaptive response to the high intensity stimuli of HIIT may have been quantitatively matched by the longer duration of muscle contraction and/or the higher energy requirements of MICT. It is also possible that exercise during each session of both MICT and HIIT surpass some "threshold" stimuli required for the observed adaptations in lipid abundance and localization. Alternatively, similar increases in the number of LDs in muscle after MICT and HIIT could derive from very different mechanisms; one training program may increase the rate of LD biogenesis while the other training program may reduce the rate of LD degradation. But this possibility seems unlikely, and is not supported by our assessments of LD biogenesis and lipophagy in this study. Regardless of the mechanisms involved to explain the similar responses between MICT and HIIT, the observation that these two exercise programs, with very distinct exercise stimuli, both increased the number of LDs in the IMF region of the muscle fibers, suggests

prioritization for adaptive responses to exercise training to provide energy rich energy substrate near the site of highest energy requirements in the cell.

Overall, our findings shed new light on the effects of MICT and HIIT on muscle lipid accumulation, however we acknowledge there are some important limitations that can impact interpretation. First, although participants were instructed to maintain their habitual dietary behaviors during the intervention, we did not control for dietary composition, changes in macronutrient composition, as well as macronutrients ingested after exercise, which can affect muscle lipids (48). In addition, regarding the comparisons between MICT and HIIT, our study was designed to address an applied comparison between these two commonly implemented training prescriptions. As a result, each session of MICT was longer than HIIT (45 versus 25 minutes) and estimated energy expenditure was also higher in MICT than HIIT (~250 versus ~150 kcals/session), so we were not able to distinguish the effects of exercise intensity, duration, or energy expenditure. However, an important outcome from our study was how remarkably similar the training adaptations were to MICT and HIIT despite the very meaningful differences in intensity, duration, and energy expended during each exercise session. It is also important to acknowledge that our study was not powered to assess sex differences, and while we did not observe any obvious trends for different responses in our male and female participants, sex differences in skeletal muscle lipid content and metabolism have been reported previously (16, 64). Finally, our measures of LD co-localization with the ER and the autophagasome using immunofluorescence microscopy provides only a very crude index of the biogenesis and degradation of LDs. Future studies using alternative analytical techniques, such as transmission electron microscopy, can better identify LD interaction with key organelles regulating LD turnover.

In summary, 12 weeks of exercise training (both MICT and HIIT) in adults with obesity increased muscle lipid abundance via an increase in the number of LD in the IMF region of the myocyte. This adaptation to exercise training results in an enhanced energy supply for mitochondrial respiration in the region of highest energy requirements during muscle contraction. Our findings also suggest an exercise-induced increase in lipophagy may underlie changes in LD turnover and redistribution within the myocyte. Interestingly, the adaptive responses to MICT and HIIT were surprisingly similar despite the considerable differences in exercise intensity, duration, and energy expenditure between these exercise programs. Overall, our findings indicate that

exercise programs for adults with obesity involving either MICT or HIIT lead to modifications in LD turnover and storage that provide more LDs to support oxidative metabolism during exercise.

ACKNOWLEDGEMENTS

We thank the study participants for their efforts; Dr. Benjamin Carr, Dr. Jacob Haus, Jeffrey Wysocki, RN; the staff at the Michigan Clinical Research Unit; Dr. Kathryn E. Luker, University of Michigan Department of Radiology for assistance with lipid droplet analysis; and all the members of the Substrate Metabolism Lab for study assistance.

FIGURES

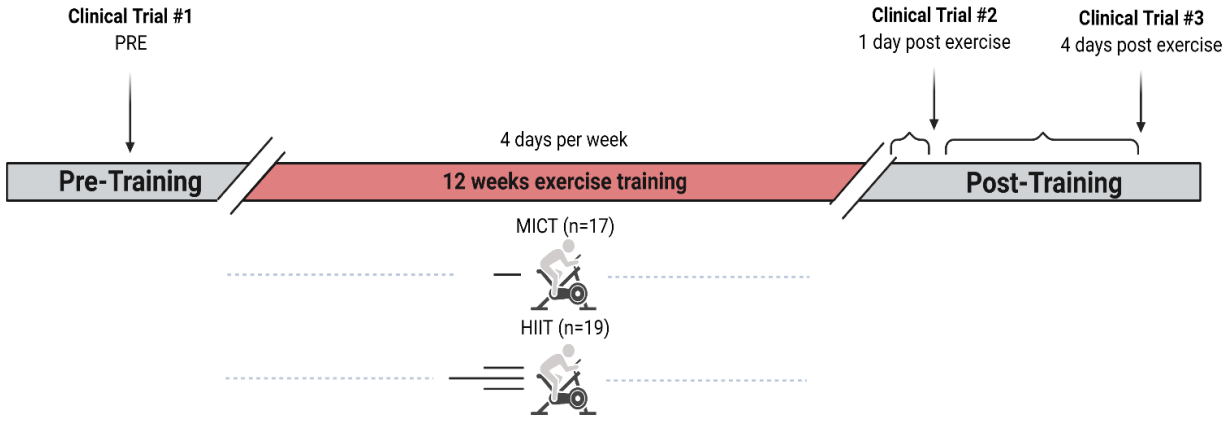

Figure V-1: Overall study design

Clinical trials were completed once pre-training, and twice post-training design (1d PostEx and 4d PostEx).

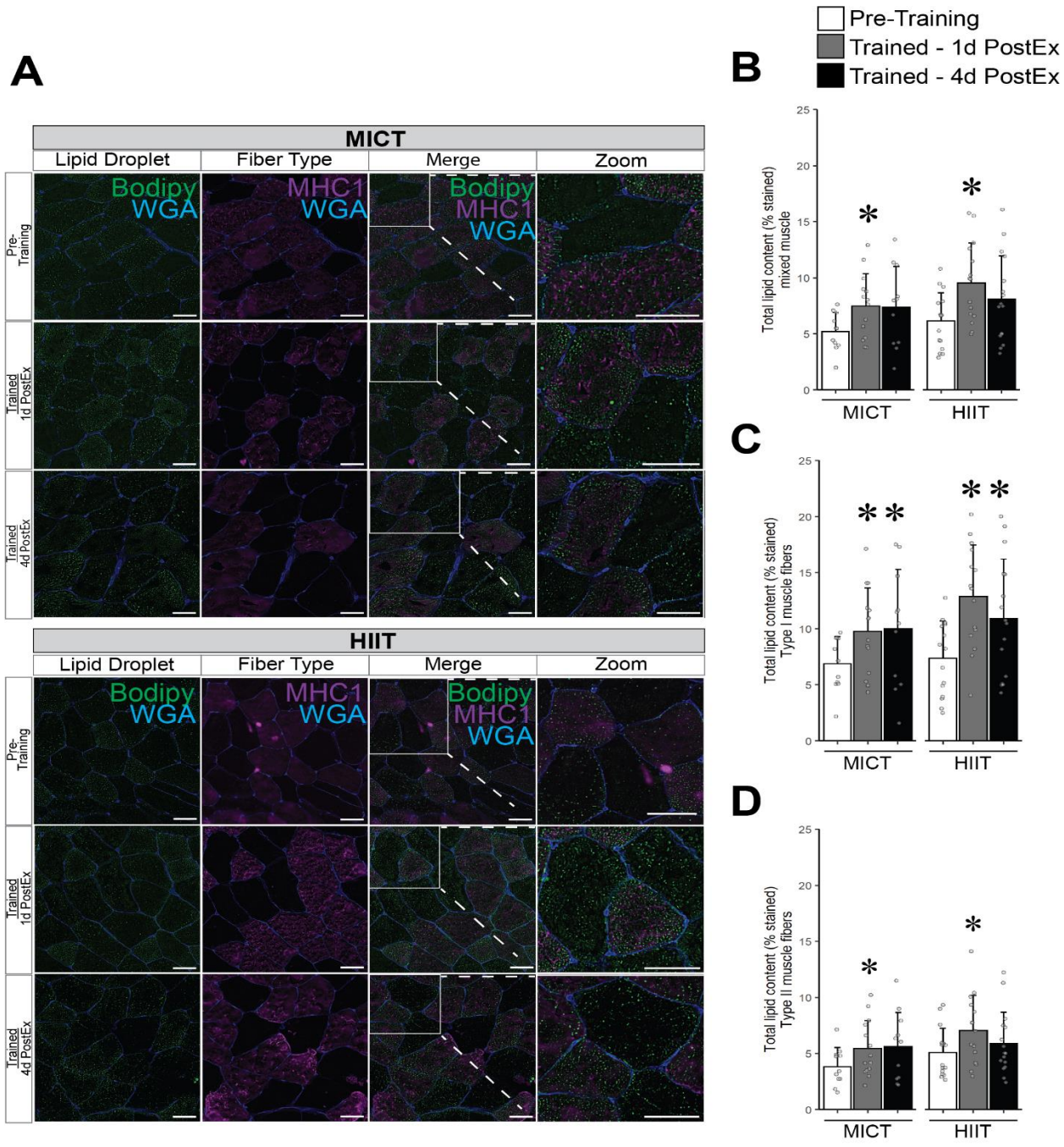

Figure V-2: Lipid content in mixed skeletal muscle, type I, and II muscle fibers in response to training.

A) Representative image: samples were stained with bodipy 493/503 (LD, green), myofiber stain for myosin heavy chain I (MHC1; type I fibers, purple), and wheat germ agglutinin (WGA; membranes, blue). The region inside the white box are enlarged for a clearer view. Representative images for each time are obtained from the same subject in each group. Magnification, 20X. Scale bar, 100µm for all images. B) Lipid content represented as % stained in mixed skeletal muscle (type I and II fibers). C) Lipid content in type I muscle fibers (MHC 1+). D) Lipid content in type II muscle fibers (MHC1-). * Main effect for visit ($p < 0.05$), and post hoc analysis identifying significant difference from pre-training. Data are expressed mean±SD.

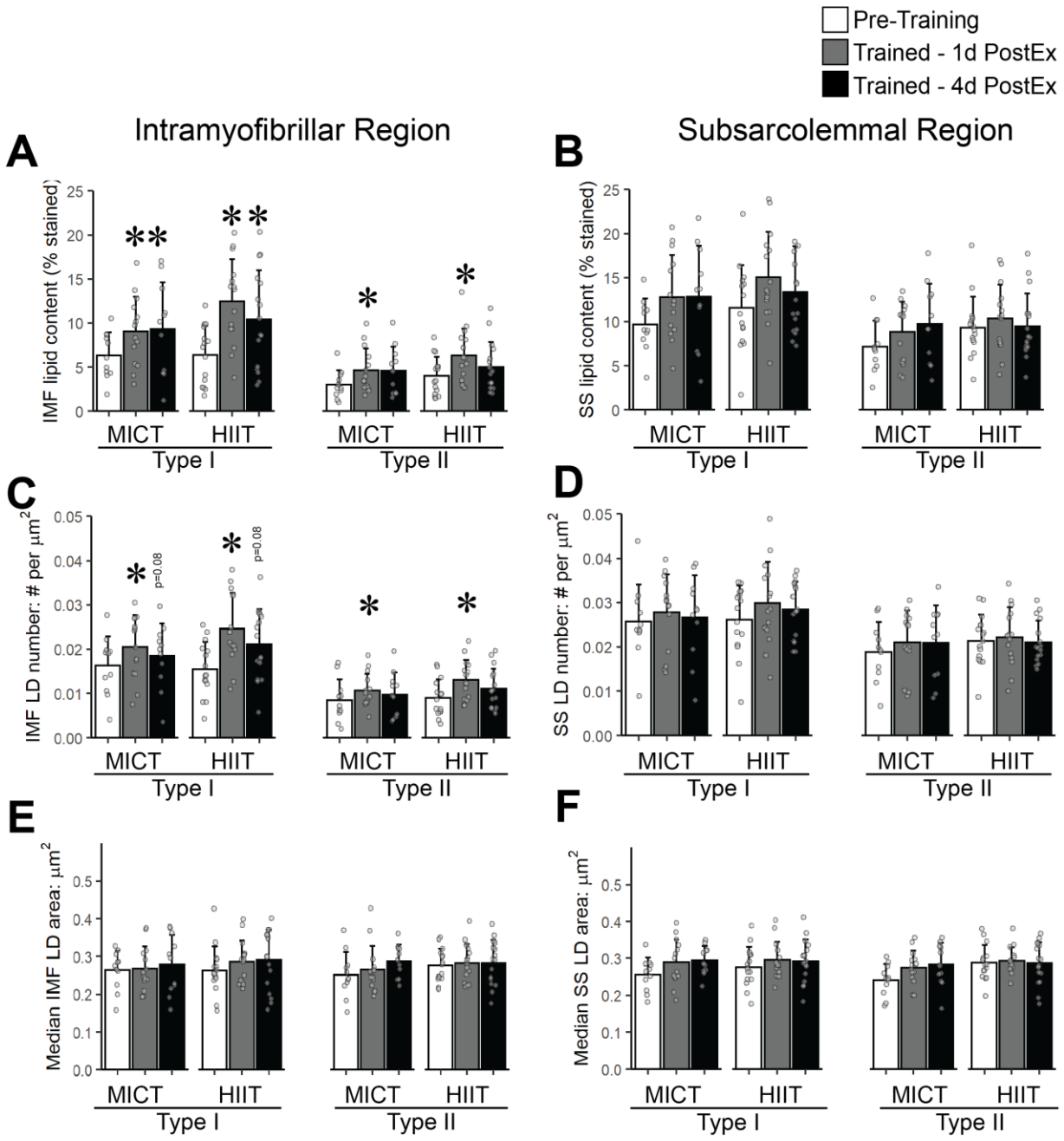

Figure V-3: LD characteristics within the IMF and SS region of type I and II muscle fibers in response to training.

A) Lipid content (% stained) in the IMF region of type I and II muscle fibers, and B) Lipid content in the SS region of type I and II muscle fibers. C) LD number (# LDs per μm^2) in the IMF region of type I and II muscle fibers, and D) LD number in the SS region of type I and II muscle fibers. E) LD median area (μm^2) per fiber in the IMF region of type I and II muscle fibers, and F) LD median area per fiber in the SS region of type I and II muscle fibers. * Main effect for visit ($p < 0.05$), and post hoc analysis identifying significant difference from pre-training. Data are expressed mean±SD.

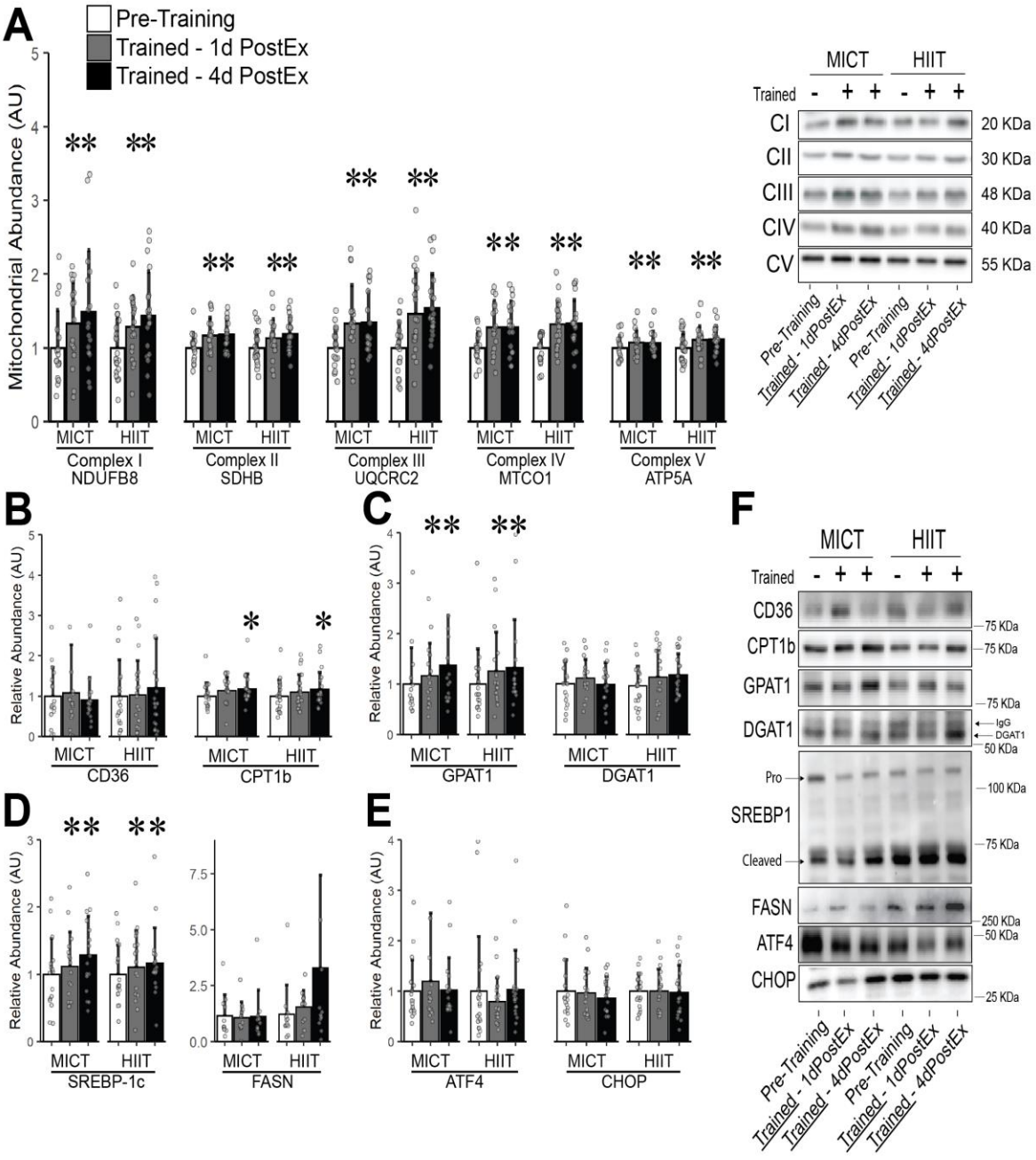

Figure V-4: Skeletal muscle adaptations to training in response to mitochondrial abundance, regulation of fatty acid transport and esterification, lipogenesis, and ER Stress.

Immunoblot abundance for proteins corresponding to: A) Respiratory chain subunits, B) cellular and mitochondrial fatty acid transport (CD36 and CPT1b), C) triacylglycerol esterification (GPAT1 and DGAT1), D) lipogenesis (SREBP1c and FASN), and E) ER stress (ATF4 and CHOP). F) Representative image for immunoblots from panels B-E. * Main effect for visit ($p<0.05$), and post hoc analysis identifying significant difference from pre-training. Data are expressed mean±SD.

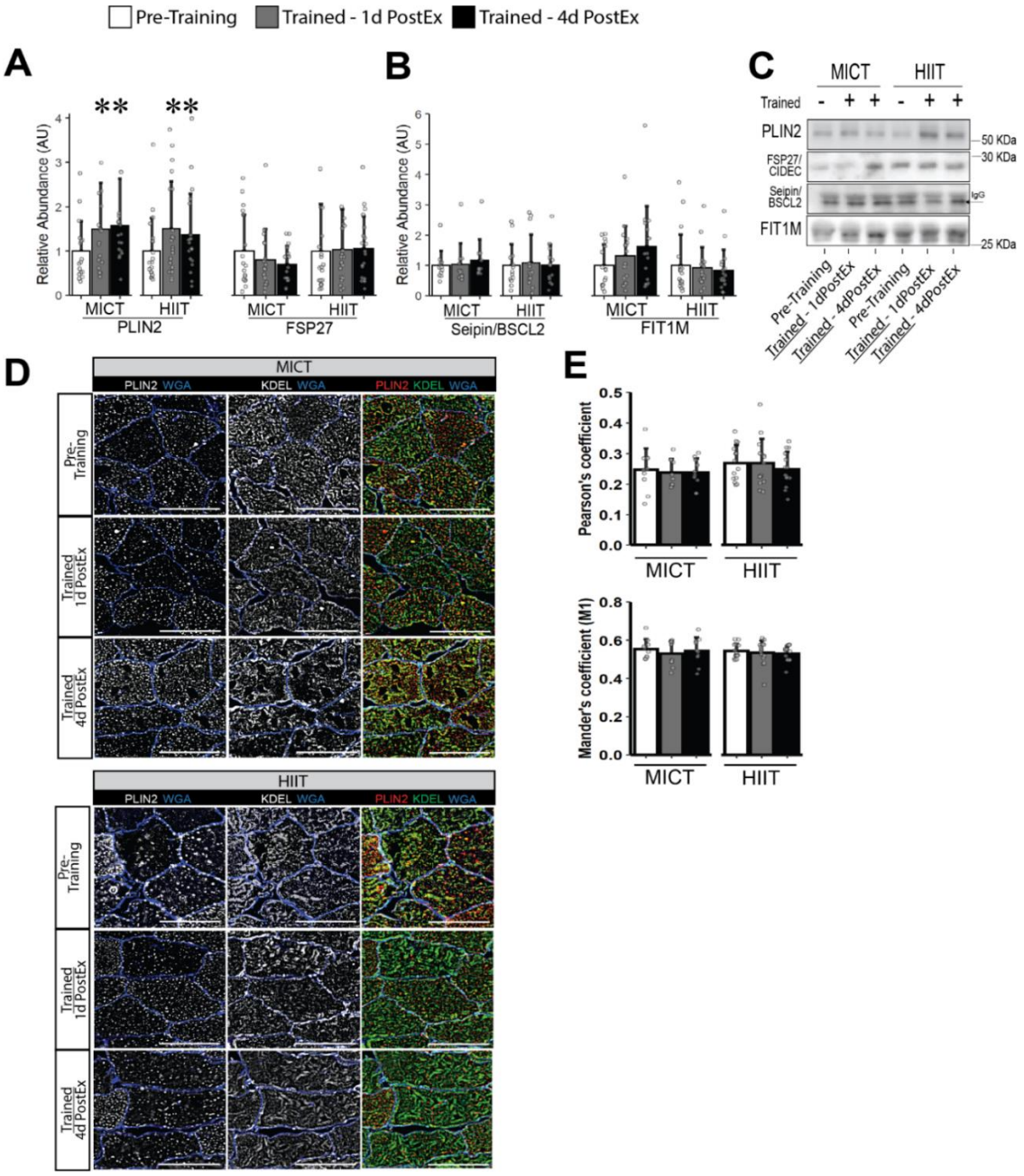

Figure V-5: Skeletal muscle LD abundance and de-novo LD biogenesis activity in response to training.

Immunoblots for proteins corresponding to A) triacylglycerol storage and release localized to the LD membrane (PLIN2 and FSP27), and B) LD stabilization localized to the ER (Seipin/BSCL2 and FIT1M). C) Representative images for immunoblots in A-B. D) Representative immunofluorescence images for LD (PLIN2, red) co-localization with the ER (KDEL, green) as a measure of de novo LD biogenesis from the ER. Membranes are stained blue. Magnification, 40X. Scale bar = 100µm. E) LD-ER co-localization measured by Pearson's and Mander's (M1) coefficient. * Main effect for visit ($p<0.05$), and post hoc analysis identifying significant difference from pre-training. Data are expressed mean±SD.

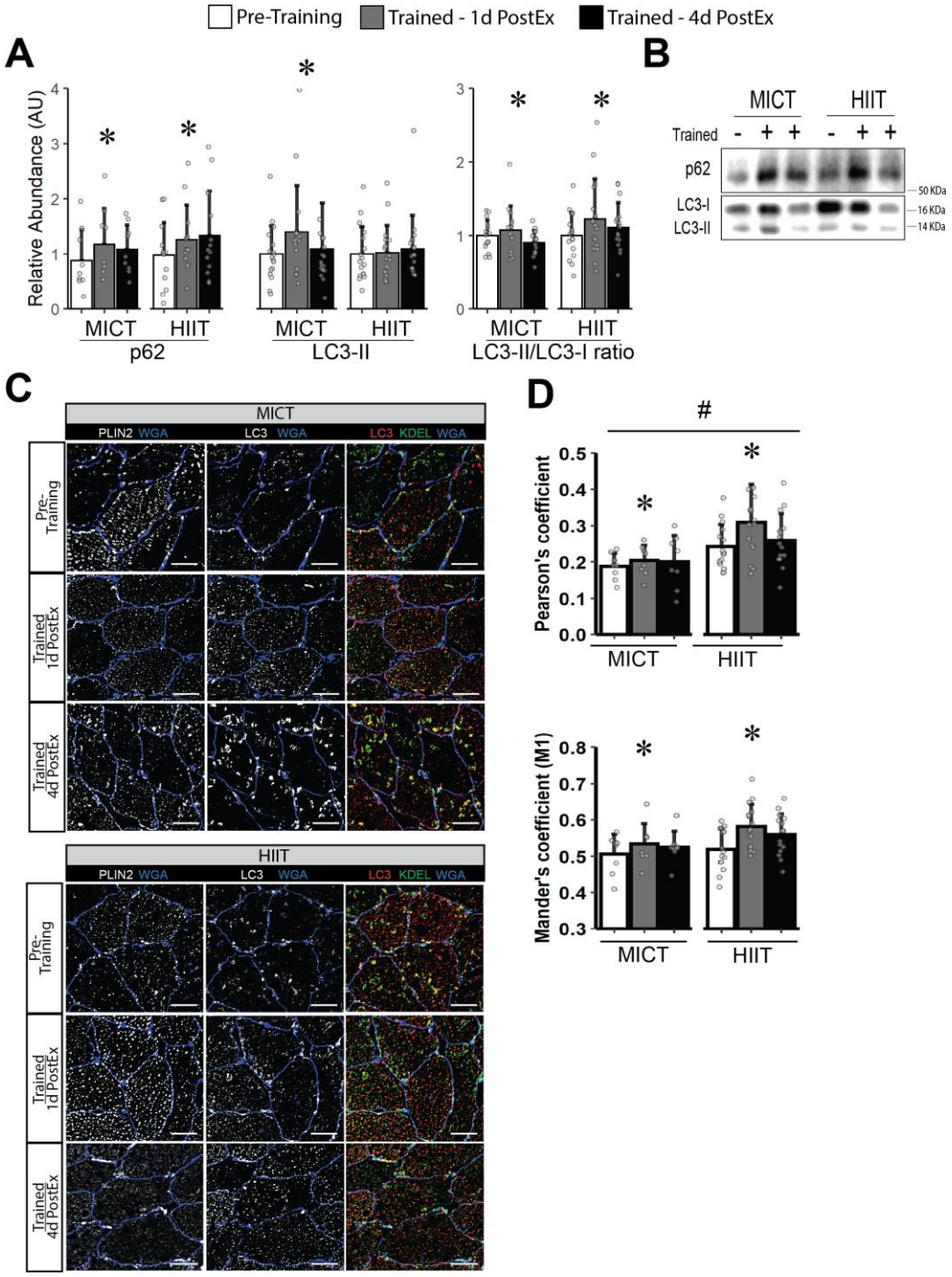

Figure V-6: Skeletal muscle autophagy induction and LD-targeted autophagy in response to training.

A) Immunoblot abundance for proteins corresponding to A) autophagy induction (p62), autophagasome activation (LC3-II), and LC3-II:LC3-I ratio - an index of active (LC3-II) to inactive (LC3-I) autophagasome abundance. B) Representative images for immunoblots. C) Representative immunofluorescence image for LD (PLIN2, red) co-localization with the autophagasome (LC3, green) as a measure of selective LD degradation (lipophagy). Membranes are stained blue. Magnification, 40X. Scale bar = 100µm. D) LD-LC3 co-localization measured by Pearson's and Mander's (M1) coefficient. * Main effect for visit ($p<0.05$), and post hoc analysis identifying significant difference from pre-training. # Main effect for group (HIIT versus MICT; $p<0.05$) Data are expressed mean±SD.

TABLES

Table V-1: Participant characteristics and metabolic biomarkers before and after exercise training.

	MICT (n=17)			HIIT (n=19)		
Sex (m/f)	12/5			12/7		
Age (years)	30 ± 6			31 ± 7		
Height (m)	1.7 ± 0.08			1.71 ± 0.09		
	Pre-Training	**Trained** 1d PostEx	**Trained** 4d PostEx	Pre-Training	**Trained** 1d PostEx	**Trained** 4d PostEx
Body Mass (kg)	98.0 ± 11.7	97.3 ± 11.5	97.6 ± 11.7	96.4 ± 13.7	96.6 ± 13.7	96.6 ± 13.6
Fat Mass (kg)	42.5 ± 7.7	41.8 ± 7.7*	42.0 ± 7.7*	40.5 ± 7.1	40.0 ± 7.1*	40.1 ± 7.2*
Fat Free Mass (kg)	55.5 ± 9.3	55.5 ± 9.5	55.7 ± 9.6	55.9 ± 10.5	56.5 ± 10.4	56.5 ± 10.3
BMI (kg/m^2)	34.0 ± 3.2	33.7 ± 3.0	33.8 ± 2.9	32.9 ± 2.9	32.9 ± 3.0	33.0 ± 3.0
Body fat %	43.4 ± 6.0	-	43.1 ± 6.4*	42.1 ± 5.4	-	41.6 ± 5.4*
VO_2 peak (ml/min)	2322 ± 544	-	2498 ± 589*	2452 ± 600	-	2750 ± 638*
Glucose (mM)	5.0 ± 0.4	4.9 ± 0.4	5.0 ± 0.5	4.8 ± 0.4	5.0 ± 0.4	4.9 ± 0.4
Insulin (µU/ml)	18.0 ± 9.0	17.5 ± 6.3	18.8 ± 7.8	16.0 ± 10.0	15.4 ± 14.6	15.3 ± 7.6
NEFA (µM)	391 ± 159	440 ± 125	408 ± 118	433 ± 156	413 ± 123	387 ± 122
Triglyceride (mM)	1.25 ± 0.7	0.99 ± 0.4	1.10 ± 0.6	0.95 ± 0.64	0.96 ± 0.6	0.91 ± 0.69

*Significant main effect of training status ($p<0.05$). BMI = Body Mass Index, VO2peak = peak oxygen uptake rate, NEFA = non-esterified fatty acid. Data are mean ± SD.

Table V-2: Antibodies and reagents

Primary and secondary antibodies (immunoblot)	Source	Identifier
anti-p62	Abcam	109012
Microtubule-associated protein light chain 3 (LC3)	CST	2775
anti-PLIN2	R&D systems	MAB7634
Anti-CIDEC Antibody/FSP27	Sigma-Aldrich	ABC300
anti-Seipin/BSCL2	CST	23846
anti-FIT1M	Sigma	HPA019842
anti-Mitochondrial OXPHOS	Abcam	110411
anti-CD36	R&D systems	AF1955
anti-CPT1b	Abcam	ab134988
anti-GPAT1	Thermo-Fisher	PA5-20524
anti-DGAT1	Novus Biologicals	110-41487
anti-SREBP-1c	Thermo-Fisher	MA5-11685
anti-FASN	CST	3180
anti-ATF4	CST	11815
anti-CHOP	CST	2895
anti-LC3A/B	CST	4108
anti-rabbit IgG, HRP-linked Antibody	CST	7074
anti-mouse IgG, HRP-linked Antibody	CST	7076
Histochemistry and Immunohistochemistry antibodies and reagents		
BODIPY 493/503	Thermo-Fisher	D3922
BA-D5: Myosin heavy chain Type 1	Developmental Studies Hydroma Bank	-
anti-Perilipin-2 Antibody (PLLIN 2)	R&D systems	MAB7634
anti-KDEL	Invitrogen-Thermo Fisher	PA1-013
anti-LC3A/B	CST	4108
Alexa Fluor 647 Goat anti-Mouse IgG2b	Invitrogen-Thermo Fisher	A-21242
Alexa Fluor 647 Goat anti-Mouse IgG1	Invitrogen-Thermo Fisher	A-21240
Alexa Fluor 488 Goat anti-Rabbit IgG	Invitrogen-Thermo Fisher	A-11034
Wheat Germ Agglutinin - Alexa Fluor 555	Invitrogen-Thermo Fisher	W32464
Triton X-100	Sigma-Aldrich	93443
Normal Goat Serum	Invitrogen-Thermo Fisher	PI31872
ProLong Gold Antifade Mountant	Invitrogen-Thermo Fisher	P36930
Plasma Reagents		
NEFA Standard Solution	Wako Diagnostics	27676491
Triglyceride Reagent	Sigma-Aldrich	T2449
HDL-Cholesterol E	Wako Diagnostics	9059676
Total Cholesterol E	Wako Diagnostics	9138103

Abbreviations: CST, cell signaling technology

REFERENCES

1. Romijn JA, Coyle EF, Sidossis LS, Gastaldelli A, Horowitz JF, Endert E, et al. Regulation of endogenous fat and carbohydrate metabolism in relation to exercise intensity and duration. 1993;265(3):E380-E91.
2. van Loon LJ, Koopman R, Stegen JH, Wagenmakers AJ, Keizer HA, and Saris WH. Intramyocellular lipids form an important substrate source during moderate intensity exercise in endurance-trained males in a fasted state. *J Physiol.* 2003;553(Pt 2):611-25.
3. Goodpaster BH, He J, Watkins S, and Kelley DE. Skeletal Muscle Lipid Content and Insulin Resistance: Evidence for a Paradox in Endurance-Trained Athletes. *The Journal of Clinical Endocrinology & Metabolism.* 2001;86(12):5755-61.
4. van Loon LJ, Koopman R, Manders R, van der Weegen W, van Kranenburg GP, and Keizer HA. Intramyocellular lipid content in type 2 diabetes patients compared with overweight sedentary men and highly trained endurance athletes. *Am J Physiol Endocrinol Metab.* 2004;287(3):E558-65.
5. Schenk S, and Horowitz JF. Acute exercise increases triglyceride synthesis in skeletal muscle and prevents fatty acid–induced insulin resistance. *J Clin Invest.* 2007;117(6):1690-8.
6. Goodpaster BH, Theriault R, Watkins SC, and Kelley DE. Intramuscular lipid content is increased in obesity and decreased by weight loss. *Metabolism.* 2000;49(4):467-72.
7. Bonen A, Parolin ML, Steinberg GR, Calles-Escandon J, Tandon NN, Glatz JF, et al. Triacylglycerol accumulation in human obesity and type 2 diabetes is associated with increased rates of skeletal muscle fatty acid transport and increased sarcolemmal FAT/CD36. *FASEB journal : official publication of the Federation of American Societies for Experimental Biology.* 2004;18(10):1144-6.
8. Horowitz JF, Coppack SW, Paramore D, Cryer PE, Zhao G, and Klein S. Effect of short-term fasting on lipid kinetics in lean and obese women. *The American journal of physiology.* 1999;276(2):E278-84.
9. Krssak M, Falk Petersen K, Dresner A, DiPietro L, Vogel SM, Rothman DL, et al. Intramyocellular lipid concentrations are correlated with insulin sensitivity in humans: a 1H NMR spectroscopy study. *Diabetologia.* 1999;42(1):113-6.
10. Perseghin G, Scifo P, De Cobelli F, Pagliato E, Battezzati A, Arcelloni C, et al. Intramyocellular triglyceride content is a determinant of in vivo insulin resistance in humans: a 1H-13C nuclear magnetic resonance spectroscopy assessment in offspring of type 2 diabetic parents. 1999;48(8):1600-6.
11. Pan DA, Lillioja S, Kriketos AD, Milner MR, Baur LA, Bogardus C, et al. Skeletal muscle triglyceride levels are inversely related to insulin action. *Diabetes.* 1997;46(6):983-8.
12. Schrauwen-Hinderling VB, Schrauwen P, Hesselink MK, van Engelshoven JM, Nicolay K, Saris WH, et al. The increase in intramyocellular lipid content is a very early response to training. *The Journal of clinical endocrinology and metabolism.* 2003;88(4):1610-6.

13. Shepherd SO, Cocks M, Tipton KD, Ranasinghe AM, Barker TA, Burniston JG, et al. Sprint interval and traditional endurance training increase net intramuscular triglyceride breakdown and expression of perilipin 2 and 5. *J Physiol.* 2013;591(3):657-75.

14. Haus JM, Solomon TPJ, Lu L, Jesberger JA, Barkoukis H, Flask CA, et al. Intramyocellular lipid content and insulin sensitivity are increased following a short-term low-glycemic index diet and exercise intervention. *Am J Physiol Endocrinol Metab.* 2011;301(3):E511-E6.

15. Dubé JJ, Amati F, Toledo FGS, Stefanovic-Racic M, Rossi A, Coen P, et al. Effects of weight loss and exercise on insulin resistance, and intramyocellular triacylglycerol, diacylglycerol and ceramide. *Diabetologia.* 2011;54(5):1147-56.

16. Tarnopolsky MA, Rennie CD, Robertshaw HA, Fedak-Tarnopolsky SN, Devries MC, and Hamadeh MJ. Influence of endurance exercise training and sex on intramyocellular lipid and mitochondrial ultrastructure, substrate use, and mitochondrial enzyme activity. *American journal of physiology Regulatory, integrative and comparative physiology.* 2007;292(3):R1271-8.

17. Pruchnic R, Katsiaras A, He J, Kelley DE, Winters C, and Goodpaster BH. Exercise training increases intramyocellular lipid and oxidative capacity in older adults. *Am J Physiol Endocrinol Metab.* 2004;287(5):E857-62.

18. Devries MC, Samjoo IA, Hamadeh MJ, McCready C, Raha S, Watt MJ, et al. Endurance Training Modulates Intramyocellular Lipid Compartmentalization and Morphology in Skeletal Muscle of Lean and Obese Women. *The Journal of Clinical Endocrinology & Metabolism.* 2013;98(12):4852-62.

19. Koh H-CE, Ørtenblad N, Winding KM, Hellsten Y, Mortensen SP, and Nielsen J. High-intensity interval, but not endurance, training induces muscle fiber type-specific subsarcolemmal lipid droplet size reduction in type 2 diabetic patients. 2018;315(5):E872-E84.

20. Nielsen J, Mogensen M, Vind BF, Sahlin K, Højlund K, Schrøder HD, et al. Increased subsarcolemmal lipids in type 2 diabetes: effect of training on localization of lipids, mitochondria, and glycogen in sedentary human skeletal muscle. *Am J Physiol Endocrinol Metab.* 2010;298(3):E706-13.

21. Nielsen J, Christensen AE, Nellemann B, and Christensen B. Lipid droplet size and location in human skeletal muscle fibers are associated with insulin sensitivity. 2017;313(6):E721-E30.

22. Walther TC, Chung J, and Jr. RVF. Lipid Droplet Biogenesis. *Annual Review of Cell and Developmental Biology.* 2017;33(1):491-510.

23. Singh R, Kaushik S, Wang Y, Xiang Y, Novak I, Komatsu M, et al. Autophagy regulates lipid metabolism. *Nature.* 2009;458(7242):1131-5.

24. Singh R, and Cuervo AM. Lipophagy: connecting autophagy and lipid metabolism. *Int J Cell Biol.* 2012;2012:282041.

25. Walther TC, and Farese RV, Jr. Lipid droplets and cellular lipid metabolism. *Annual review of biochemistry.* 2012;81:687-714.

26. Thiam AR, and Beller M. The why, when and how of lipid droplet diversity. *J Cell Sci.* 2017;130(2):315-24.

27. Ferreira R, Vitorino R, Alves RM, Appell HJ, Powers SK, Duarte JA, et al. Subsarcolemmal and intermyofibrillar mitochondria proteome differences disclose functional specializations in skeletal muscle. *Proteomics.* 2010;10(17):3142-54.

28. Shaw CS, Jones DA, and Wagenmakers AJM. Network distribution of mitochondria and lipid droplets in human muscle fibres. *Histochemistry and Cell Biology.* 2008;129(1):65-72.

29. Shaw CS, Swinton C, Morales-Scholz MG, McRae N, Erftemeyer T, Aldous A, et al. Impact of exercise training status on the fiber type-specific abundance of proteins regulating intramuscular lipid metabolism. *Journal of Applied Physiology.* 2020;128(2):379-89.

30. Burgomaster KA, Hughes SC, Heigenhauser GJ, Bradwell SN, and Gibala MJ. Six sessions of sprint interval training increases muscle oxidative potential and cycle endurance capacity in humans. *J Appl Physiol (1985).* 2005;98(6):1985-90.

31. Gillen JB, Percival ME, Ludzki A, Tarnopolsky MA, and Gibala MJ. Interval training in the fed or fasted state improves body composition and muscle oxidative capacity in overweight women. *Obesity (Silver Spring, Md).* 2013;21(11):2249-55.

32. Little JP, Gillen JB, Percival ME, Safdar A, Tarnopolsky MA, Punthakee Z, et al. Low-volume high-intensity interval training reduces hyperglycemia and increases muscle mitochondrial capacity in patients with type 2 diabetes. 2011;111(6):1554-60.

33. Ryan BJ, Schleh MW, Ahn C, Ludzki AC, Gillen JB, Varshney P, et al. Moderate-intensity exercise and high-intensity interval training affect insulin sensitivity similarly in obese adults. *The Journal of clinical endocrinology and metabolism.* 2020.

34. Heath GW, Gavin JR, Hinderliter JM, Hagberg JM, Bloomfield SA, and Holloszy JO. Effects of exercise and lack of exercise on glucose tolerance and insulin sensitivity. *Journal of Applied Physiology.* 1983;55(2):512-7.

35. King DS, Dalsky GP, Clutter WE, Young DA, Staten MA, Cryer PE, et al. Effects of exercise and lack of exercise on insulin sensitivity and responsiveness. 1988;64(5):1942-6.

36. Gibala MJ. Interval Training for Cardiometabolic Health: Why Such A HIIT? *Curr Sports Med Rep.* 2018;17(5):148-50.

37. Schneider CA, Rasband WS, and Eliceiri KW. NIH Image to ImageJ: 25 years of image analysis. *Nature methods.* 2012;9(7):671-5.

38. R Core Team. R: A Language and Environment for Statistical Computing. *R Foundation for Statistical Computing.* 2019.

39. Brasaemle DL, Barber T, Wolins NE, Serrero G, Blanchette-Mackie EJ, and Londos C. Adipose differentiation-related protein is an ubiquitously expressed lipid storage droplet-associated protein. *Journal of lipid research.* 1997;38(11):2249-63.

40. Olzmann JA, and Carvalho P. Dynamics and functions of lipid droplets. *Nature reviews Molecular cell biology.* 2019;20(3):137-55.

41. Meex RC, Schrauwen-Hinderling VB, Moonen-Kornips E, Schaart G, Mensink M, Phielix E, et al. Restoration of muscle mitochondrial function and metabolic flexibility in type 2 diabetes by exercise training is paralleled by increased myocellular fat storage and improved insulin sensitivity. *Diabetes.* 2010;59(3):572-9.

42. Shepherd SO, Cocks M, Meikle PJ, Mellett NA, Ranasinghe AM, Barker TA, et al. Lipid droplet remodelling and reduced muscle ceramides following sprint interval and moderate-intensity continuous exercise training in obese males. *Int J Obes (Lond).* 2017;41(12):1745-54.

43. He J, Goodpaster BH, and Kelley DE. Effects of weight loss and physical activity on muscle lipid content and droplet size. *Obes Res.* 2004;12(5):761-9.

44. Hulver MW, Berggren JR, Cortright RN, Dudek RW, Thompson RP, Pories WJ, et al. Skeletal muscle lipid metabolism with obesity. *Am J Physiol Endocrinol Metab.* 2003;284(4):E741-7.

45. Schenk S, Harber MP, Shrivastava CR, Burant CF, and Horowitz JF. Improved insulin sensitivity after weight loss and exercise training is mediated by a reduction in plasma fatty acid mobilization, not enhanced oxidative capacity. 2009;587(20):4949-61.

46. Helge JW, Stallknecht B, Drachmann T, Hellgren LI, Jiménez-Jiménez R, Andersen JL, et al. Improved glucose tolerance after intensive life style intervention occurs without changes in muscle ceramide or triacylglycerol in morbidly obese subjects. *Acta Physiologica.* 2011;201(3):357-64.

47. Mulla NA, Simonsen L, and Bülow J. Post-exercise adipose tissue and skeletal muscle lipid metabolism in humans: the effects of exercise intensity. *J Physiol.* 2000;524 Pt 3(Pt 3):919-28.

48. Daemen S, Polanen Nv, Bilet L, Phielix E, Moonen-Kornips E, Schrauwen-Hinderling VB, et al. Postexercise changes in myocellular lipid droplet characteristics of young lean individuals are affected by circulatory nonesterified fatty acids. *American Journal of Physiology-Endocrinology and Metabolism.* 2021;321(4):E453-E63.

49. Hesselink MK, Mensink M, and Schrauwen P. Intramyocellular lipids and insulin sensitivity: does size really matter? *Obes Res.* 2004;12(5):741-2.

50. Daemen S, Gemmink A, Brouwers B, Meex RCR, Huntjens PR, Schaart G, et al. Distinct lipid droplet characteristics and distribution unmask the apparent contradiction of the athlete's paradox. *Molecular Metabolism.* 2018;17:71-81.

51. Li Y, Lee S, Langleite T, Norheim F, Pourteymour S, Jensen J, et al. Subsarcolemmal lipid droplet responses to a combined endurance and strength exercise intervention. *Physiol Rep.* 2014;2(11).

52. Long AP, Manneschmidt AK, VerBrugge B, Dortch MR, Minkin SC, Prater KE, et al. Lipid droplet de novo formation and fission are linked to the cell cycle in fission yeast. *Traffic.* 2012;13(5):705-14.

53. Marcinkiewicz A, Gauthier D, Garcia A, and Brasaemle DL. The Phosphorylation of Serine 492 of Perilipin A Directs Lipid Droplet Fragmentation and Dispersion*. *Journal of Biological Chemistry.* 2006;281(17):11901-9.

54. Lam T, Harmancey R, Vasquez H, Gilbert B, Patel N, Hariharan V, et al. Reversal of intramyocellular lipid accumulation by lipophagy and a p62-mediated pathway. *Cell Death Discovery.* 2016;2(1):16061.

55. Rambold AS, Cohen S, and Lippincott-Schwartz J. Fatty acid trafficking in starved cells: regulation by lipid droplet lipolysis, autophagy, and mitochondrial fusion dynamics. *Developmental cell.* 2015;32(6):678-92.

56. Itani SI, Zhou Q, Pories WJ, MacDonald KG, and Dohm GL. Involvement of protein kinase C in human skeletal muscle insulin resistance and obesity. *Diabetes.* 2000;49(8):1353-8.

57. Adams JM, Pratipanawatr T, Berria R, Wang E, DeFronzo RA, Sullards MC, et al. Ceramide Content Is Increased in Skeletal Muscle From Obese Insulin-Resistant Humans. 2004;53(1):25-31.

58. Koves TR, Ussher JR, Noland RC, Slentz D, Mosedale M, Ilkayeva O, et al. Mitochondrial Overload and Incomplete Fatty Acid Oxidation Contribute to Skeletal Muscle Insulin Resistance. *Cell Metabolism.* 2008;7(1):45-56.

59. Chee C, Shannon CE, Burns A, Selby AL, Wilkinson D, Smith K, et al. Relative Contribution of Intramyocellular Lipid to Whole-Body Fat Oxidation Is Reduced With Age but Subsarcolemmal Lipid Accumulation and Insulin Resistance Are Only Associated With Overweight Individuals. *Diabetes.* 2016;65(4):840-50.

60. Perreault L, Newsom SA, Strauss A, Kerege A, Kahn DE, Harrison KA, et al. Intracellular localization of diacylglycerols and sphingolipids influences insulin sensitivity and mitochondrial function in human skeletal muscle. *JCI Insight.* 2018;3(3):e96805.

61. Burgomaster KA, Howarth KR, Phillips SM, Rakobowchuk M, Macdonald MJ, McGee SL, et al. Similar metabolic adaptations during exercise after low volume sprint interval and traditional endurance training in humans. *J Physiol.* 2008;586(1):151-60.

62. Gollnick PD, Armstrong RB, Sembrowich WL, Shepherd RE, and Saltin B. Glycogen depletion pattern in human skeletal muscle fibers after heavy exercise. *Journal of Applied Physiology.* 1973;34(5):615-8.

63. Vøllestad NK, and Blom PC. Effect of varying exercise intensity on glycogen depletion in human muscle fibres. *Acta Physiol Scand.* 1985;125(3):395-405.

64. Devries MC, Lowther SA, Glover AW, Hamadeh MJ, and Tarnopolsky MA. IMCL area density, but not IMCL utilization, is higher in women during moderate-intensity endurance exercise, compared with men. *American journal of physiology Regulatory, integrative and comparative physiology.* 2007;293(6):R2336-42.

Chapter VI

Overall Discussion

INTRODUCTION

Obesity is a major risk factor for cardiovascular diseases (1, 2) and type 2 diabetes (3). With obesity prevalence now surpassing more than 40% of the United States population (4), it is important to identify therapies aimed to limit obesity-related metabolic complications. Although a large portion of adults with obesity are insulin resistant, there remains a small population of adults (~10-30%) that are still insulin sensitive despite presenting excess fat mass (5-7). Abdominal subcutaneous adipose tissue (aSAT) dysfunction is common in obesity, resulting in excessive fatty acid (FA) release, and consequently results in ectopic lipid deposition (8, 9). Findings from this dissertation proposed factors such as fibrosis within the extracellular matrix (ECM) of aSAT may be contributing to excessive FA rate of appearance (FA Ra) into the circulation, which may explain the variability in whole-body insulin sensitivity found among adults with obesity. Furthermore, the integrative component from these projects links impairments in insulin-mediated FA Ra (i.e., low FA Ra suppression) with modifications in skeletal muscle lipid composition, which may affect insulin-mediated signaling events. Moreover, exercise is often prescribed as a first-line approach to alleviate metabolic dysfunction common in obesity (10, 11). However, the effects of exercise *intensity*, *duration,* and *timing post-exercise* (e.g., 1 day versus 4 days after the most recent exercise session) on intramyocellular lipid handling and lipid droplet (LD) storage are still unclear.

The overall findings from this dissertation identified the contribution of aSAT metabolic health towards the variability in whole-body insulin resistance in adults with obesity. Additionally, this dissertation identified the effect of endurance training to modify intramyocellular lipid handling and LD storage. In this chapter, I will summarize the key findings from all three dissertation projects, and integrate these clinical findings to improve our understanding of aSAT contribution to metabolic health, and the influence of exercise on lipid handling. To conclude the discussion of major findings, I will address key questions to consider for follow-up studies.

SUMMARY OF KEY FINDINGS

Project 1: *Assessment of factors underlying whole-body insulin resistance in adults with obesity.*

In Project 1, a combination of stable isotope dilution methods coupled with clinical and subclinical measurements were completed, in effort to identify a cluster of factors that may best 'predict' insulin-mediated glucose uptake among a relatively homogenous cohort of adults with obesity. Based on findings from this correlational analysis, aSAT proteomic profile was compared between two sub-cohorts of participants presenting largely dissimilar insulin-mediated response to FA release (i.e., FA Ra suppression), but nearly identical body composition. Additionally, a series of regression analyses were completed to link the contribution of FA release from aSAT with the accumulation of skeletal muscle lipids, and the composition of these lipids with respect to acyl-chain length and unsaturation. Furthermore, the relationship between lipid composition and whole-body insulin sensitivity was compared, in effort to identify skeletal muscle lipids that are accumulating as a result of excessive FA release from aSAT and are contributing to whole-body insulin resistance.

Key findings:

- Insulin-mediated FA Ra suppression was the strongest 'predictor' of whole-body insulin sensitivity from all the clinical and subclinical outcomes.
- Extracellular matrix (ECM) fibrosis in aSAT (e.g., collagen and integrin accumulation) was greater in adults with obesity presenting Low FA Ra suppression (LS sub-cohort).
- Fatty acid Ra suppression inversely associated with skeletal muscle acyl-chain length from acylcarnitine and triacylglycerol lipid classes.
- Whole-body insulin sensitivity inversely associated with skeletal muscle acyl-chain length from fatty acid, acylcarnitine, and triacylglycerol lipid classes.

Overall, findings from Project 1 supports the concept that limiting aSAT fibrosis will permit insulin-mediated suppression of FA Ra to remain high, which may limit long-chain lipid accumulation in skeletal muscle, and maintain insulin sensitivity in obesity.

Project 2: *Comparison of intramyocellular lipid accumulation and skeletal muscle insulin signaling in obese adults with high versus low insulin sensitivity.*

In Project 2, a combination of stable isotope dilution methods during the hyperinsulinemic-euglycemic clamp were completed similar to Project 1, and confirmed the rate of insulin-mediated FA release from aSAT (FA Ra suppression) strongly associated with insulin-mediated glucose uptake in adults with obesity. In this study, two sub-cohorts presenting HIGH insulin-mediated glucose uptake and LOW insulin-mediated glucose uptake (defined as HIGH and LOW for the rest of chapter VI) were stratified to identify insulin-mediated signaling events in skeletal muscle that may diverge between these groups presenting strikingly different insulin sensitivity. To measure insulin-mediated signaling events, skeletal muscle biopsies were collected at baseline (fasted) and 30 minutes into the hyperinsulinemic-euglycemic clamp.

Key findings:

- Insulin-mediated FA Ra suppression directly associated with whole-body insulin sensitivity, and was attenuated in LOW.
- Insulin-mediated insulin receptor phosphorylation was attenuated in LOW, and may be partly attributed to lower CD36 and Fyn co-localization with the insulin receptor at baseline and during the clamp.
- Insulin-mediated phosphorylation of Akt^{S473}, and distal Akt substrates, $GSK\alpha^{S21}$ and $FOXO1^{S256}$ were attenuated in LOW.
- LD size within the subsarcolemmal (SS) region of type II muscle fibers was larger in LOW, implying atypical lipid storage within LDs near the membrane of type II muscle fibers may contribute to impaired insulin signaling.

Overall, this project proposed a tissue-specific *cross-talk* relationship, by which excess FA release from aSAT and uptake into skeletal muscle modifies insulin receptor signaling through its interaction with CD36 and Fyn kinase, and further impacts phosphorylation of key regulatory proteins at Akt and its distal substrates. Additionally, LD morphology and distribution may also contribute to the variability in insulin-mediated signaling events observed among adults with obesity.

Project 3: *Effects of exercise training on intramyocellular lipid droplet abundance, size, cellular distribution, and turnover in adults with obesity.*

In Project 3, skeletal muscle samples were collected before and after 12 weeks moderate-intensity continuous training (MICT) or high-intensity interval training (HIIT). Lipid content and LD characteristics (e.g., LD size and number of LDs per μm^2), distribution within the intramyofibrillar (IMF) and SS region, and LD abundance between type I and type II muscle fibers were measured by immunofluorescence microscopy. Additionally, an index of de novo LD biogenesis from the endoplasmic reticulum (ER), and selective LD degradation by the autophagasome (lipophagy) was measured by immunofluorescence co-localization before and after training.

Key findings:

- Training increased total lipid content (% stained) in skeletal muscle, and was increased similarly after training in MICT and HIIT groups.
- The increase in lipid content after training was a result of a greater number of LDs (per μm^2), and not an increase in their size.
- The increase in the number of LDs after training occurred specifically in the IMF region of the myocyte, and not the SS region.
- Training did not influence de novo LD biogenesis from the ER.
- Training influenced lipophagy induction, in which LC3 co-localization with PLIN2 was increased only one day after the last exercise session.

Overall, findings from this project identified the impact of HIIT and MICT to modify intramyocellular LD turnover and storage, in effort to enhance FA availability for oxidative metabolism during exercise.

INTEGRATED INTERPRETATION OF RESULTS

Adipose tissue as a central node for tissue-specific *cross-talk*.

Together, Projects 1 and 2 from this dissertation provide evidence linking the insulin-mediated suppression FA Ra with whole-body insulin sensitivity. More specifically, these findings demonstrate that impaired FA Ra suppression contributes to insulin resistance in multiple

organ systems, including; 1) impaired insulin-mediated glucose uptake into skeletal muscle (Projects 1 and 2), and 2) impaired insulin-mediated suppression of glucose release from liver (Project 1). Our findings support the notion that an inability to regulate FA release after the most recent meal or snack is a key contributor to ectopic lipid accumulation and whole-body insulin resistance in obesity (8, 9).

Impaired insulin-mediated suppression of FA release modifies the skeletal muscle lipid composition.

High rates of FA availability and uptake into skeletal muscle is a key mediator of insulin resistance (12-14). Project 1 of this dissertation connected the relationship between FA release from aSAT with the accumulation of long-chain lipids in skeletal muscle. Furthermore, Project 1 also linked the relationship between long-chain lipid accumulation in skeletal muscle with whole-body insulin resistance - in effort to connect metabolic health of aSAT as a contributor to skeletal muscle insulin resistance. From our lipidomic findings, no considerable cluster of lipid classes (e.g., phosphatidylcholine, sphingomyelin, triacylglycerol) directly related with both FA Ra suppression and whole-body insulin sensitivity. Rather, the acyl-chain length for fatty acid, acylcarnitine, and triacylglycerol inversely related with whole-body insulin sensitivity. Interestingly, acyl-chain lengths of acylcarnitine and triacylglycerol also inversely related with FA Ra suppression. These findings are the first to our knowledge, to integrate the contribution of FA availability from aSAT with the accumulation of long-chain lipids in skeletal muscle, and their contribution with whole-body insulin resistance. These findings propose a tissue-specific relationship, by which greater FA release from aSAT, and subsequent uptake into skeletal muscle is occurring without a compensatory increase in tricarboxylic acid cycle flux. Thus, creating a 'mismatch' between FA availability and oxidation in skeletal muscle, which contributes to the observed increase in long-chain lipids and lipid metabolites in skeletal muscle. These findings align with previous reports by Koves et al., who proposed an 'incomplete' fat oxidation contributed to insulin resistance in skeletal muscle - due to greater rates of mitochondrial β-oxidation, but inability to subsequently increase tricarboxylic acid cycle flux (15). Therefore, we propose the increase in acyl-chain length of acylcarnitines may relate with insulin resistance, as a consequence of increased mitochondrial FA import that exceeds the metabolic demand of sedentary muscle. The implications by which these long-chain lipids directly contribute to skeletal muscle insulin

resistance is unresolved and require further mechanistic follow-up studies, and the proposed mechanisms include; 1) increased inflammatory response (16-18), 2) mitochondrial-derived oxidative stress (19-21), and 3) ER stress (22, 23). Moreover, Project 1 identified the contribution of excessive FA release from aSAT to modify skeletal muscle lipid composition and whole-body insulin resistance. However, these findings were concluded from whole-muscle homogenate samples that do not link the contribution of these lipids with respect to spatial localization in the muscle fiber, which has been found to significantly contribute to skeletal muscle insulin resistance (24-27). Therefore, Project 2 warranted further investigations to identify the effect of subcellular lipid deposition (within the IMF and SS region of myocytes) to modify whole-body insulin sensitivity.

Impaired insulin-mediated suppression of FA release modifies intramyocellular lipid distribution.

Results from Projects 1 and 2 confirmed that impaired FA Ra suppression inversely related with whole-body insulin sensitivity. Project 1 proposed insulin resistance is associated with the accumulation of long-chain fatty acids, acylcarnitines, and triacylglycerol in skeletal muscle. Project 2 expanded these findings to suggest that intramyocellular lipid distribution within the SS region (i.e., towards the periphery of the myocyte) inversely related with whole-body insulin sensitivity. More specifically, the size of SS LDs within type II muscle fibers inversely related with whole-body insulin sensitivity. Although it remains elusive, we speculate the lower surface area-to-volume ratios from larger-sized LDs limits lipolysis control at the LD membrane (28-30), and subsequently induces lipotoxic effects near the muscle membrane. Interestingly, because these larger-sized LDs were observed within the SS region of muscle fibers, their proximity to the membrane may also contribute insulin signaling defects (26, 27, 31). These findings are in agreement with Perreault et al., who showed the subcellular localization of lipid intermediates (e.g., diacylglycerol and ceramides) within the membrane region of muscle fibers, but not within the cytosol, were inversely related with insulin sensitivity (24). However, these findings did not consider the relationship between acyl-chain length and insulin sensitivity, which may underscore the complexity of these lipids in cellular metabolism and signaling. Therefore, future studies aimed to identify skeletal muscle lipidomic contributions to insulin resistance are challenged to look beyond individual lipid species in whole-muscle, and identify the contribution of subcellular lipid distribution and lipid morphology to modify insulin sensitivity. Altogether, Projects 1 and 2

identified that the acyl-chain lengths of lipids, and lipid distribution within the SS region of the myocyte are implicated to modify whole-body insulin sensitivity in adults with obesity.

Impaired insulin-mediated suppression of FA release modifies skeletal muscle insulin signaling

Intramyocellular lipid accumulation in obesity is commonly associated with insulin resistance (13, 32). Insulin-mediated signaling defects caused by excess lipid accumulation are proposed to be a cause of by serine/threonine phosphorylation of IRS-1 (33), and lower Akt phosphorylation (34). Therefore, a follow-up aim from Project 2 proposed an alternative insulin signaling response that may be mediated by defective lipid storage in skeletal muscle (and/or greater FA availability). Project 2 found insulin receptor phosphorylation was attenuated in LOW, which may be attributed to blunted CD36 and Fyn kinase interaction with the insulin receptor caused by excess FA availability. Although unconfirmed, this project speculates CD36 may be limiting its interaction with the insulin receptor when FA availability is high in effort to increase cellular FA uptake into skeletal muscle in preference over glucose uptake. Consequently, limited CD36 interaction with the insulin receptor decreased Fyn kinase interaction with the insulin receptor, and limited insulin receptor phosphorylation, which suggests that insulin receptor phosphorylation may be partly regulated by the ability for CD36 to recruit Fyn kinase to the insulin receptor. Furthermore, this relationship may modify insulin-mediated phosphorylation of downstream regulatory proteins, including AKT^{S473}, $GSK3\alpha^{S21}$ and $FOXO1^{S256}$.

Findings from Project 1 and Project 2 propose a series of tissue-specific *cross-talk* events between aSAT and skeletal muscle. Whereby, impaired FA Ra suppression strongly associated with whole-body insulin resistance. The proposed consequence of this relationship resulted in the accumulation of long-chain fatty acids, acylcarnitines, and triacylglycerols in skeletal muscle. Furthermore, the accumulation of large-sized LDs distributed in the SS region of the type II fibers suggests these long-chain lipids may accumulate towards the membrane where insulin signaling occurs, and attenuate CD36 and Fyn kinase interaction with the insulin receptor, limiting downstream insulin signaling.

Adiponectin release from adipose tissue relates with whole-body insulin sensitivity.

Adiponectin is an endocrine hormone secreted by adipocytes (35), and has been noted to inversely relate with body fat percentage (36). However, circulating adiponectin is also directly associated with whole-body insulin sensitivity independently of body composition, and has been noted to be an insulin sensitizing adipokine (37-39). In agreement with previous reports, Project 1 found circulating total adiponectin (Figure VI-IA) and high molecular weight (HMW) adiponectin (biologically active isoform of adiponectin; Figure VI-1B) directly associated with whole-body insulin sensitivity in our obese cohort. Although these findings were not discussed in detail from Project 1, it is appropriate to consider circulating adiponectin released from aSAT may contribute to a *tissue-specific cross-talk* relationship. Despite great interest in adiponectin as an anti-diabetic therapy, the mechanism by which adiponectin contributes to improved metabolic health are still unconfirmed. Studies attempting to identify the insulin sensitizing mechanism of action have proposed adiponectin to; 1) increase ceramidase activity to enhance ceramide catabolism (40), 2) increase AMPK activation to stimulate fat oxidation and limit lipid intermediate accumulation (41, 42), and 3) influence the paracrine effects of adiponectin to increase triacylglycerol esterification in adipose tissue (41). Altogether, adiponectin may act in both endocrine and paracrine fashion, where the tissue-specific *cross-talk* may be explained by a feed-forward mechanism to increase FA uptake into aSAT, and resulting in the reduction of lipid intermediates within skeletal muscle. Future studies are warranted to identify whether adiponectin limits long-chain lipid accumulation in skeletal muscle by modifying FA availability, tricarboxylic acid cycle flux, and/or subcellular lipid distribution in the myocyte. All of which were implicated in Project 1 and Project 2 of this dissertation.

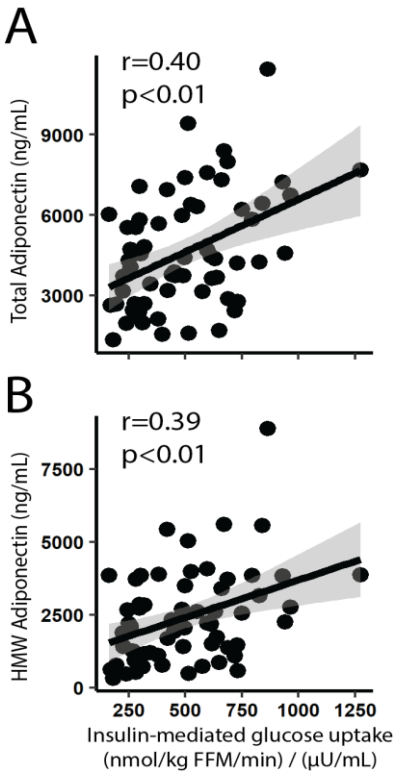

Figure VI-1: Adiponectin and insulin sensitivity

Relationship between A) Total adiponectin and B) HMW adiponectin with whole-body insulin sensitivity. n=66

Local factors within aSAT contributing to greater FA availability

Contribution of aSAT extracellular matrix accumulation towards impaired insulin-mediated suppression of FA release

The extracellular matrix (ECM) is an important component of aSAT, providing structural support and signaling networks for adipocytes within adipose tissue (43). In obesity, chronic low grade inflammation associates with inadequate tissue remodeling, contributing to a feed-forward mechanism resulting in ECM accumulation (44). If left unresolved, adipose tissue plasticity becomes compromised, and the ability for adipose tissue to control systemic FA uptake and release becomes impaired. The proteomic analysis from Project 1 revealed obese adults with low FA Ra suppression from aSAT (e.g., LS sub-cohort from Project 1) presented greater ECM collagen and integrin protein abundance compared to the high FA Ra suppression sub-cohort (HS sub-cohort). More specifically, several highly abundant collagen proteins (e.g., COLIA, COLIIIA, COLVI) were enriched in the LS versus HS. Interestingly, TGFβ1 concentration was greater in LS, and suggests fibrosis development may be occurring by chronic inflammation (45, 46). Follow-up measurements from these proteomic findings found collagen accumulation (determined by picrosirius red staining) inversely associated with whole-body insulin sensitivity, but not the anti-lipolytic response to insulin from aSAT (Appendix D).

Findings from our lab have linked basal FA mobilization with aSAT ECM fibrosis genes (47), while others have also found aSAT fibrosis inversely relates with whole-body insulin sensitivity (48, 49). Interestingly, others have proposed adipose tissue fibrosis directly impairs insulin signaling within the adipose tissue itself (50, 51). Therefore, we speculate fibrosis development contributes whole-body insulin resistance by; 1) increasing adipose stiffness and impeding aSAT expansion, 2) disrupting hormone delivery to the adipocyte (e.g., insulin) (50, 52), and 3) increased mechanical stress, which contributes to excess lipolysis (53). Whether intracellular insulin signaling is modified by the fibrotic adipose tissue milieu, or whether extracellular insulin delivery to the adipocyte is modified remains unknown. Findings from this study are warranted to identify whether insulin signaling is directly perturbed in adipose tissue when fibrosis is high, or whether fibrosis is secondary to other factors such as hypoxia and inflammation. Altogether, Project 1 identified a relationship between ECM fibrosis and impaired FA Ra suppression, which likely contributes to the development of insulin resistance.

Contribution of inflammation towards impaired insulin-mediated suppression of FA release from aSAT.

Obesity is associated with chronic low-grade inflammation (54, 55), where local immune cell and pro-inflammatory cytokine abundance in aSAT are implicated to contribute to insulin resistance in obesity (54, 56). Inflammatory cytokines (e.g., IL6, TNFα, and IL1β) have been shown to directly attenuate insulin signaling in aSAT (57-59), and may likely explain the contribution of inflammation towards the impaired FA Ra suppression in response to insulin, which was found in Project 1 and Project 2. Unfortunately, an in-depth assessments of the immune cell and cytokine profile in adipose tissue were not within the scope of these projects, but we acknowledge local inflammation in aSAT may likely contribute to our findings. Fortunately, single cell RNA sequencing (scRNA-seq) has become more cost-effective and feasible, and future studies profiling immune cell population (e.g., $CD8^+$ T cells, B cells, and natural killer cells) towards the anti-lipolytic response to insulin from aSAT are warranted.

Exercise training modifies intramyocellular lipid content and LD distribution.

Findings from Project 1 and Project 2 both identified a direct relationship between the rate of insulin-mediated FA Ra suppression with whole-body insulin sensitivity. Therefore, Project 3 aimed to identify *how* exercise influences lipid storage in skeletal muscle from adults with obesity – in effort to alleviate whole-body insulin resistance caused by excess FA availability. Project 3 measured the effect of exercise training on intramyocellular lipid content and LD distribution, independently of body weight modifications during training. Additionally, this project compared MICT and HIIT interventions on muscle lipid content and LD distribution, as well as timing post-exercise to identify both acute effects and chronic responses to exercise training. Project 3 showed that training increased the number of intramyocellular LDs within the IMF region of both type I and type II muscle fibers. The partitioning of lipids towards the IMF region after training are proposed to be an adaptive response in effort to improve intramyocellular FA availability for oxidative metabolism during exercise. Project 3 did not find an effect of training on to modify LD size in the SS region of either type I or type II muscle fibers. Therefore, we cannot confirm the insulin sensitizing effects of exercise are attributed to modifications in SS LD size, which was

shown to inversely relate with insulin sensitivity in Project 2. Unfortunately, we do not present skeletal muscle lipidomic data from this study, and cannot show the effect of training on acyl-chain length to be modified, which were found to inversely relate with insulin sensitivity in Project 1.

The mechanisms contributing towards the increase in the number of LDs within IMF region still remains elusive. Project 3 showed this affect may be partly attributed to a selective form of autophagy called lipophagy, which was increased the day after exercise. We propose autophagy mediates LD catabolism in effort to provide bulk FA availability to the mitochondria for oxidation, and also redistributes FAs and LD membrane proteins to more preferential locations within the cytosol in effort to adaptively increase energy availability for the contracting muscle (e.g., LD-mitochondrial contact). Interestingly, the response for lipophagy to degrade LDs was also attributed to increased number of LDs, which may improve FA trafficking towards the mitochondria, which has been shown in previous reports in response to energy deficit (60), and after exercise training (61, 62). Altogether, findings from Project 3 support a role for MICT and HIIT to remodel lipid content by increasing the number of LDs, and LD distribution to the IMF region in effort to support oxidative metabolism.

DIRECTIONS FOR FUTURE RESEARCH

Future direction study 1: *Identification of aSAT cellular heterogeneity between metabolically healthy versus insulin resistant adults with obesity using single cell RNA sequencing.*

Project 1 linked aSAT fibrosis with impaired FA Ra suppression in response to insulin, which may contribute to whole-body insulin resistance. However, these findings were supported by proteomic analysis collected from whole aSAT biopsies. Although the use of proteomic as an analytical tool are important to identify cellular markers influential for biological function, this measurement does not provide detailed assessments of the cellular population within whole adipose tissue niche. Adipose tissue is composed of an adipocyte and non-adipocyte stromal vascular fraction (SVF). Although adipocytes contain ~90% of adipose tissue volume, they reflect only 20-40% of the total adipose tissue cellular population (63-65), where the SVF contains distinct populations of fibroblasts, endothelial cells, and immune cells. Therefore, identifying different cell types within the adipose tissue niche that are differentially populated between insulin

resistant versus insulin sensitive adults with obesity are an important first step to link the contribution of specific cell types with metabolic health. The development of single cell RNA sequencing (scRNA-seq) is influential for clinical and biological scientists to identify tissue-specific cellular heterogeneity and complexity (66). Recently, scRNA-seq studies have compared cellular profiles in aSAT between lean versus obese populations (67, 68), and healthy versus type II diabetic populations (69). To my knowledge, no studies have compared the cellular population of aSAT from metabolically healthy versus insulin resistant adults with obesity using scRNA-seq, and doing so will remove the confounding effects of body composition on the cellular population within adipose tissue.

The cellular origins associated with fibrosis development in humans are still unclear. Marcelin et al., identified a subset of pro-fibrotic precursor cells expressing platelet-derived growth factor receptor-α-positive (PDGFRα^{+}) that were CD9^{high} (50). Additionally, Hepler et al., also identified a progenitor cell population that is LY6C^{+}, PDGFRβ^{+}, and CD9^{+} that are pro-fibrogenic, and differentiated by inflammation (70). Therefore, identifying the transcriptional program of PDGFRα^{+} and/or PDGFRβ^{+} progenitor cells in humans between metabolically healthy (i.e., insulin sensitive) versus insulin resistant aSAT phenotypes will help identify specific cell populations contributing to excess ECM deposition, that may explain findings from Project 1 of this dissertation.

Future Direction 1 Aim: To compare adipose tissue cellular populations, and transcriptomic profile of PDGFRα^{+} and PDGFRβ^{+} progenitor cells between insulin sensitive versus insulin resistant adults with obesity using single nucleus RNA sequencing (sNuc-seq).

Approach: Thirty adults with obesity will be recruited for this study, and will complete a hyperinsulinemic-euglycemic clamp (40 mU/m^2/min) to measure insulin sensitivity. Afterwards, participants will be stratified into tertiles and grouped into the most insulin sensitive sub-cohort (n=10), and the least insulin sensitive cohort (i.e., insulin resistant; n=10). Adipose tissue biopsies will be collected before the clamp and snap-frozen. Therefore, sNuc-seq will be preferable analytical method for whole aSAT biopsies, because; 1) mature adipocytes are noted to be too fragile to withstand single cell sorting, 2) and analysis and sNuc-seq can be measured from frozen tissue samples (71).

Anticipated results and interpretation: We expect insulin resistant adults with obesity to present higher CD9 gene expression within the PDGFRα^{+} progenitor cell cluster, because CD9 has been described as a marker of fibrogenic cells (50). Additionally, we will identify unique 'sub-clusters' of PDGFRα^{+} and PDGFRβ^{+} progenitor cells expressing CD9 as a signature marker that will inversely relate with insulin sensitivity, and be differentially expressed between groups. Therefore, sNuC-seq will identify clusters of progenitor cells contributing to fibrosis development and whole-body insulin resistance. Beyond fibrosis development, insulin resistant obese adults will present greater abundance of immune cell populations; CD8^{+} T cells, dendritic cells, and B cells, NK cells within aSAT. Findings from this study will be critical to identify transcriptional reprogramming in obesity, and will identify novel cellular populations contributing to fibrosis development from progenitor cells, and whole-body insulin resistance.

Future direction study 2: *Effects of acute exercise on skeletal muscle LD biogenesis and LD turnover by transmission electron microscopy.*

In Project 3 of this dissertation, exercise training increased the number of LDs only in the IMF region of muscle fibers. However, the mechanisms contributing to increased number of LDs after training, or a session of exercise, are not completely known. One proposed mechanism from Project 3 was the selective degradation of LDs by lipophagy may contribute to increased LD turnover and recycling, and thus, increase nascent LD biogenesis. However, these findings were proposed from immunofluorescence co-localization methods, whereby the fluorescence overlap of the autophagasome (LC3) with the LD (PLIN2) presented an index of lipophagy. However, fluorescence co-localization can only suggest molecular interaction based on their overlap, where transmission electron microscopy (TEM) provides the cellular resolution to visually confirm cellular interaction.

The mechanism by which the number of LDs increased after training was originally hypothesized to be attributed to de novo LD biogenesis from the ER. TEM provides the resolution to visually identify neutral lipid accumulation between the ER leaflets, and nascent LD budding towards the cytosol (72, 73). In addition, LD turnover can be attributed to; 1) macroautophagy, described as the 'engulfment' of LDs by the autophagasome and delivery to the lysosome for degradation, and 2) microautophagy, involving partial LD engulfment by the lysosome for

degradation (74). To my knowledge, no studies have identified the effect of a single exercise session of LD biogenesis and LD turnover using TEM.

Future Direction 2 Aim 1: To identify the effect of a single exercise session on LD growth within the ER leaflet and LD biogenesis from the ER by TEM.

Future Direction 2 Aim 2: To identify the effect of a single exercise session on LD turnover by co-localization with the autophagasome (LC3) and LD co-localization with the lysosome by TEM.

Approach: Twenty participants with obesity will be recruited to complete this study. Skeletal muscle biopsies will be collected before the exercise session (Pre-exercise), and 4h after a moderate-intensity exercise session (45minutes at 70% HR_{max}; Post-exercise). For TEM analysis, immuno-gold labeling of LC3 will identify LC3-positive autophagasomes in contact with LDs as described previously (75). After immunolabeling, samples will be fixed, dehydrated, and embedded in a hydrophobic resin medium. De novo LD biogenesis will be quantified by the number of LDs localized within the ER leaflet, and the number of LDs budding towards the cytosol as explained previously (76). Lipophagy will be quantified by the number of LDs in contact with LC3-positive autophagasomes, and the lysosome, as explained previously (77). All analyses will be quantified by a trained pathologist in TEM

Anticipated results and interpretation: We anticipate a single session of exercise to increase LD turnover and biogenesis in skeletal muscle. Therefore, exercise will increase LD degradation, whereby a greater number of LDs will be in contact with both LC3-positive autophagasomes and the lysosome within a respective area in skeletal muscle. Additionally, a single session of exercise will increase LD biogenesis, and increase the number of LDs localized within the ER leaflet, and number of LDs budding from the ER. These findings will support a role for exercise to increase LD turnover in skeletal muscle, in effort to remodel LD distribution for greater FA availability to support mitochondrial respiration. Importantly, TEM analysis will provide proper identification for LD turnover occurring in skeletal muscle, and explain adaptations occurring to improve lipid handling and lipid metabolism.

OVERALL CONCLUSION

Adipose tissue dysfunction is implicated to contribute to whole-body insulin resistance in obesity. Importantly, several factors within aSAT are likely to contribute to aSAT dysfunction (i.e., inflammation, hypoxia, and fibrosis), resulting in excessive FA availability and uptake into ectopic tissues. Projects 1 and 2 of this dissertation demonstrated insulin-mediated FA Ra suppression directly associated with whole-body insulin sensitivity. Importantly, Project 1 proposed the development of fibrosis is implicated with impaired FA Ra suppression, contributing to greater FA availability into the circulation and whole-body insulin resistance. These findings shed light onto follow-up studies, where future work is suggested to identify whether fibrosis directly perturbs adipose tissue insulin signaling, or if fibrosis development is secondary to other mediators of adipose tissue insulin resistance (e.g., inflammation and hypoxia).

Excessive FA release and uptake into skeletal muscle contributes to whole-body insulin resistance. Projects 1 and 2 both addressed the implications by which aSAT dysfunction modifies skeletal muscle lipid composition, and insulin signaling. Project 1 demonstrated long-chain acylcarnitines and triacylglycerol accumulate as a consequence of impaired FA Ra suppression in response to insulin, and in turn, these lipids were also linked with whole-body insulin resistance. Additionally, Project 2 found LD size in the SS region of type II fibers were related to insulin resistance. Therefore, these findings suggest the subcellular distribution and lipid chain-lengths within skeletal muscle may be a consequence of excess FA release and uptake into skeletal muscle, contributing to insulin resistance. Furthermore, excess FA availability in LOW was suggested to limit CD36 and Fyn kinase interaction with the insulin receptor. Altogether, Project 1 and 2 propose that excessive FA release from aSAT mediates a tissue-specific *cross-talk* relationship affecting skeletal muscle metabolism.

Project 3 addressed the therapeutic effect of exercise training on skeletal muscle LD storage. Training may help 'prime' skeletal muscle to improve FA availability for mitochondrial oxidation, and the acute induction of lipophagy may contribute to greater LD turnover and remodeling after an exercise session. Findings from my dissertation provide an integrative approach identifying the contribution of aSAT towards whole-body insulin resistance, and proposes potential mechanisms by which exercise may modify LD storage, contributing to the prevention of obesity-related metabolic conditions such as insulin resistance.

REFERENCES

1. Poirier P, Giles TD, Bray GA, Hong Y, Stern JS, Pi-Sunyer FX, et al. Obesity and cardiovascular disease: pathophysiology, evaluation, and effect of weight loss: an update of the 1997 American Heart Association Scientific Statement on Obesity and Heart Disease from the Obesity Committee of the Council on Nutrition, Physical Activity, and Metabolism. *Circulation.* 2006;113(6):898-918.
2. Eckel RH, and Krauss RM. American Heart Association Call to Action: Obesity as a Major Risk Factor for Coronary Heart Disease. 1998;97(21):2099-100.
3. Nguyen NT, Nguyen X-MT, Lane J, and Wang P. Relationship between obesity and diabetes in a US adult population: findings from the National Health and Nutrition Examination Survey, 1999-2006. *Obes Surg.* 2011;21(3):351-5.
4. Hales CM, Carroll MD, Fryar CD, and Ogden CL. Prevalence of obesity and severe obesity among adults: United States, 2017–2018. 2020.
5. Smith GI, Mittendorfer B, and Klein S. Metabolically healthy obesity: facts and fantasies. *J Clin Invest.* 2019;129(10):3978-89.
6. Wildman RP, Muntner P, Reynolds K, McGinn AP, Rajpathak S, Wylie-Rosett J, et al. The Obese Without Cardiometabolic Risk Factor Clustering and the Normal Weight With Cardiometabolic Risk Factor Clustering: Prevalence and Correlates of 2 Phenotypes Among the US Population (NHANES 1999-2004). *Archives of Internal Medicine.* 2008;168(15):1617-24.
7. Stefan N, Kantartzis K, Machann J, Schick F, Thamer C, Rittig K, et al. Identification and characterization of metabolically benign obesity in humans. *Arch Intern Med.* 2008;168(15):1609-16.
8. Unger RH, Clark GO, Scherer PE, and Orci L. Lipid homeostasis, lipotoxicity and the metabolic syndrome. *Biochimica et biophysica acta.* 2010;1801(3):209-14.
9. Virtue S, and Vidal-Puig A. Adipose tissue expandability, lipotoxicity and the Metabolic Syndrome — An allostatic perspective. *Biochimica et Biophysica Acta (BBA) - Molecular and Cell Biology of Lipids.* 2010;1801(3):338-49.
10. Colberg SR, Sigal RJ, Yardley JE, Riddell MC, Dunstan DW, Dempsey PC, et al. Physical Activity/Exercise and Diabetes: A Position Statement of the American Diabetes Association. *Diabetes Care.* 2016;39(11):2065.
11. Garber CE, Blissmer B, Deschenes MR, Franklin BA, Lamonte MJ, Lee IM, et al. American College of Sports Medicine position stand. Quantity and quality of exercise for developing and maintaining cardiorespiratory, musculoskeletal, and neuromotor fitness in apparently healthy adults: guidance for prescribing exercise. *Medicine and science in sports and exercise.* 2011;43(7):1334-59.
12. Boden G. Role of fatty acids in the pathogenesis of insulin resistance and NIDDM. *Diabetes.* 1997;46(1):3-10.

13. Krssak M, Falk Petersen K, Dresner A, DiPietro L, Vogel SM, Rothman DL, et al. Intramyocellular lipid concentrations are correlated with insulin sensitivity in humans: a 1H NMR spectroscopy study. *Diabetologia.* 1999;42(1):113-6.

14. Dresner A, Laurent D, Marcucci M, Griffin ME, Dufour S, Cline GW, et al. Effects of free fatty acids on glucose transport and IRS-1-associated phosphatidylinositol 3-kinase activity. *J Clin Invest.* 1999;103(2):253-9.

15. Koves TR, Ussher JR, Noland RC, Slentz D, Mosedale M, Ilkayeva O, et al. Mitochondrial Overload and Incomplete Fatty Acid Oxidation Contribute to Skeletal Muscle Insulin Resistance. *Cell Metabolism.* 2008;7(1):45-56.

16. Bloch-Damti A, and Bashan N. Proposed mechanisms for the induction of insulin resistance by oxidative stress. *Antioxidants & redox signaling.* 2005;7(11-12):1553-67.

17. Muoio Deborah M, and Neufer PD. Lipid-Induced Mitochondrial Stress and Insulin Action in Muscle. *Cell Metabolism.* 2012;15(5):595-605.

18. Adams SH, Hoppel CL, Lok KH, Zhao L, Wong SW, Minkler PE, et al. Plasma acylcarnitine profiles suggest incomplete long-chain fatty acid beta-oxidation and altered tricarboxylic acid cycle activity in type 2 diabetic African-American women. *The Journal of nutrition.* 2009;139(6):1073-81.

19. Fisher-Wellman KH, and Neufer PD. Linking mitochondrial bioenergetics to insulin resistance via redox biology. *Trends in endocrinology and metabolism: TEM.* 2012;23(3):142-53.

20. Anderson EJ, Lustig ME, Boyle KE, Woodlief TL, Kane DA, Lin CT, et al. Mitochondrial H2O2 emission and cellular redox state link excess fat intake to insulin resistance in both rodents and humans. *J Clin Invest.* 2009;119(3):573-81.

21. Aguer C, McCoin CS, Knotts TA, Thrush AB, Ono-Moore K, McPherson R, et al. Acylcarnitines: potential implications for skeletal muscle insulin resistance. *FASEB journal : official publication of the Federation of American Societies for Experimental Biology.* 2015;29(1):336-45.

22. Özcan U, Cao Q, Yilmaz E, Lee A-H, Iwakoshi NN, Özdelen E, et al. Endoplasmic Reticulum Stress Links Obesity, Insulin Action, and Type 2 Diabetes. 2004;306(5695):457-61.

23. Malhotra JD, and Kaufman RJ. Endoplasmic reticulum stress and oxidative stress: a vicious cycle or a double-edged sword? *Antioxidants & redox signaling.* 2007;9(12):2277-93.

24. Perreault L, Newsom SA, Strauss A, Kerege A, Kahn DE, Harrison KA, et al. Intracellular localization of diacylglycerols and sphingolipids influences insulin sensitivity and mitochondrial function in human skeletal muscle. *JCI Insight.* 2018;3(3):e96805.

25. Nielsen J, Christensen AE, Nellemann B, and Christensen B. Lipid droplet size and location in human skeletal muscle fibers are associated with insulin sensitivity. 2017;313(6):E721-E30.

26. Nielsen J, Mogensen M, Vind BF, Sahlin K, Højlund K, Schrøder HD, et al. Increased subsarcolemmal lipids in type 2 diabetes: effect of training on localization of lipids,

mitochondria, and glycogen in sedentary human skeletal muscle. *Am J Physiol Endocrinol Metab.* 2010;298(3):E706-13.

27. Daemen S, Gemmink A, Brouwers B, Meex RCR, Huntjens PR, Schaart G, et al. Distinct lipid droplet characteristics and distribution unmask the apparent contradiction of the athlete's paradox. *Molecular Metabolism.* 2018;17:71-81.

28. Thiam AR, and Beller M. The why, when and how of lipid droplet diversity. *J Cell Sci.* 2017;130(2):315-24.

29. Murphy DJ. The dynamic roles of intracellular lipid droplets: from archaea to mammals. *Protoplasma.* 2012;249(3):541-85.

30. Hesselink MK, Mensink M, and Schrauwen P. Intramyocellular lipids and insulin sensitivity: does size really matter? *Obes Res.* 2004;12(5):741-2.

31. Chee C, Shannon CE, Burns A, Selby AL, Wilkinson D, Smith K, et al. Relative Contribution of Intramyocellular Lipid to Whole-Body Fat Oxidation Is Reduced With Age but Subsarcolemmal Lipid Accumulation and Insulin Resistance Are Only Associated With Overweight Individuals. *Diabetes.* 2016;65(4):840-50.

32. Perseghin G, Scifo P, De Cobelli F, Pagliato E, Battezzati A, Arcelloni C, et al. Intramyocellular triglyceride content is a determinant of in vivo insulin resistance in humans: a 1H-13C nuclear magnetic resonance spectroscopy assessment in offspring of type 2 diabetic parents. 1999;48(8):1600-6.

33. Morino K, Neschen S, Bilz S, Sono S, Tsirigotis D, Reznick RM, et al. Muscle-Specific IRS-1 Ser→Ala Transgenic Mice Are Protected From Fat-Induced Insulin Resistance in Skeletal Muscle. 2008;57(10):2644-51.

34. Adams JM, Pratipanawatr T, Berria R, Wang E, DeFronzo RA, Sullards MC, et al. Ceramide Content Is Increased in Skeletal Muscle From Obese Insulin-Resistant Humans. 2004;53(1):25-31.

35. Scherer PE, Williams S, Fogliano M, Baldini G, and Lodish HF. A Novel Serum Protein Similar to C1q, Produced Exclusively in Adipocytes (*). *Journal of Biological Chemistry.* 1995;270(45):26746-9.

36. Arita Y, Kihara S, Ouchi N, Takahashi M, Maeda K, Miyagawa J, et al. Paradoxical decrease of an adipose-specific protein, adiponectin, in obesity. *Biochem Biophys Res Commun.* 1999;257(1):79-83.

37. Aguilar-Salinas CA, García EG, Robles L, Riaño D, Ruiz-Gomez DG, García-Ulloa AC, et al. High adiponectin concentrations are associated with the metabolically healthy obese phenotype. *The Journal of clinical endocrinology and metabolism.* 2008;93(10):4075-9.

38. Ahl S, Guenther M, Zhao S, James R, Marks J, Szabo A, et al. Adiponectin Levels Differentiate Metabolically Healthy vs Unhealthy Among Obese and Nonobese White Individuals. *The Journal of Clinical Endocrinology & Metabolism.* 2015;100(11):4172-80.

39. Doumatey AP, Bentley AR, Zhou J, Huang H, Adeyemo A, and Rotimi CN. Paradoxical Hyperadiponectinemia is Associated With the Metabolically Healthy Obese (MHO) Phenotype in African Americans. *Journal of endocrinology and metabolism.* 2012;2(2):51-65.

40. Holland WL, Miller RA, Wang ZV, Sun K, Barth BM, Bui HH, et al. Receptor-mediated activation of ceramidase activity initiates the pleiotropic actions of adiponectin. *Nature Medicine.* 2011;17(1):55-63.

41. Li X, Zhang D, Vatner DF, Goedeke L, Hirabara SM, Zhang Y, et al. Mechanisms by which adiponectin reverses high fat diet-induced insulin resistance in mice. *Proceedings of the National Academy of Sciences.* 2020;117(51):32584.

42. Yamauchi T, Kamon J, Minokoshi Y, Ito Y, Waki H, Uchida S, et al. Adiponectin stimulates glucose utilization and fatty-acid oxidation by activating AMP-activated protein kinase. *Nature Medicine.* 2002;8(11):1288-95.

43. Frantz C, Stewart KM, and Weaver VM. The extracellular matrix at a glance. *Journal of Cell Science.* 2010;123(24):4195-200.

44. Crewe C, An YA, and Scherer PE. The ominous triad of adipose tissue dysfunction: inflammation, fibrosis, and impaired angiogenesis. *J Clin Invest.* 2017;127(1):74-82.

45. Scharenberg MA, Pippenger BE, Sack R, Zingg D, Ferralli J, Schenk S, et al. TGF-β-induced differentiation into myofibroblasts involves specific regulation of two MKL1 isoforms. *J Cell Sci.* 2014;127(Pt 5):1079-91.

46. Massagué J. TGFβ signalling in context. *Nature Reviews Molecular Cell Biology.* 2012;13(10):616-30.

47. Van Pelt DW, Guth LM, Wang AY, and Horowitz JF. Factors regulating subcutaneous adipose tissue storage, fibrosis, and inflammation may underlie low fatty acid mobilization in insulin-sensitive obese adults. 2017;313(4):E429-E39.

48. Divoux A, Tordjman J, Lacasa D, Veyrie N, Hugol D, Aissat A, et al. Fibrosis in Human Adipose Tissue: Composition, Distribution, and Link With Lipid Metabolism and Fat Mass Loss. *Diabetes.* 2010;59(11):2817.

49. Henegar C, Tordjman J, Achard V, Lacasa D, Cremer I, Guerre-Millo M, et al. Adipose tissue transcriptomic signature highlights the pathological relevance of extracellular matrix in human obesity. *Genome Biology.* 2008;9(1):R14.

50. Marcelin G, Ferreira A, Liu Y, Atlan M, Aron-Wisnewsky J, Pelloux V, et al. A PDGFRα-Mediated Switch toward CD9(high) Adipocyte Progenitors Controls Obesity-Induced Adipose Tissue Fibrosis. *Cell Metab.* 2017;25(3):673-85.

51. Khan T, Muise ES, Iyengar P, Wang ZV, Chandalia M, Abate N, et al. Metabolic Dysregulation and Adipose Tissue Fibrosis: Role of Collagen VI. 2009;29(6):1575-91.

52. Marcelin G, Silveira ALM, Martins LB, Ferreira AVM, and Clément K. Deciphering the cellular interplays underlying obesity-induced adipose tissue fibrosis. *J Clin Invest.* 2019;129(10):4032-40.

53. Pellegrinelli V, Heuvingh J, du Roure O, Rouault C, Devulder A, Klein C, et al. Human adipocyte function is impacted by mechanical cues. *J Pathol.* 2014;233(2):183-95.

54. Xu H, Barnes GT, Yang Q, Tan G, Yang D, Chou CJ, et al. Chronic inflammation in fat plays a crucial role in the development of obesity-related insulin resistance. *J Clin Invest.* 2003;112(12):1821-30.

55. Hotamisligil GS, Shargill NS, and Spiegelman BM. Adipose expression of tumor necrosis factor-alpha: direct role in obesity-linked insulin resistance. *Science.* 1993;259(5091):87-91.

56. Weisberg SP, McCann D, Desai M, Rosenbaum M, Leibel RL, and Ferrante AW, Jr. Obesity is associated with macrophage accumulation in adipose tissue. *J Clin Invest.* 2003;112(12):1796-808.

57. Lagathu C, Yvan-Charvet L, Bastard JP, Maachi M, Quignard-Boulangé A, Capeau J, et al. Long-term treatment with interleukin-1β induces insulin resistance in murine and human adipocytes. *Diabetologia.* 2006;49(9):2162-73.

58. Hotamisligil GS, Peraldi P, Budavari A, Ellis R, White MF, and Spiegelman BM. IRS-1-mediated inhibition of insulin receptor tyrosine kinase activity in TNF-alpha- and obesity-induced insulin resistance. *Science.* 1996;271(5249):665-8.

59. Lagathu C, Bastard J-P, Auclair M, Maachi M, Capeau J, and Caron M. Chronic interleukin-6 (IL-6) treatment increased IL-6 secretion and induced insulin resistance in adipocyte: prevention by rosiglitazone. *Biochemical and Biophysical Research Communications.* 2003;311(2):372-9.

60. Rambold AS, Cohen S, and Lippincott-Schwartz J. Fatty acid trafficking in starved cells: regulation by lipid droplet lipolysis, autophagy, and mitochondrial fusion dynamics. *Developmental cell.* 2015;32(6):678-92.

61. Devries MC, Samjoo IA, Hamadeh MJ, McCready C, Raha S, Watt MJ, et al. Endurance Training Modulates Intramyocellular Lipid Compartmentalization and Morphology in Skeletal Muscle of Lean and Obese Women. *The Journal of Clinical Endocrinology & Metabolism.* 2013;98(12):4852-62.

62. Tarnopolsky MA, Rennie CD, Robertshaw HA, Fedak-Tarnopolsky SN, Devries MC, and Hamadeh MJ. Influence of endurance exercise training and sex on intramyocellular lipid and mitochondrial ultrastructure, substrate use, and mitochondrial enzyme activity. *American journal of physiology Regulatory, integrative and comparative physiology.* 2007;292(3):R1271-8.

63. Lee MJ, Wu Y, and Fried SK. Adipose tissue heterogeneity: implication of depot differences in adipose tissue for obesity complications. *Mol Aspects Med.* 2013;34(1):1-11.

64. Corvera S. Cellular Heterogeneity in Adipose Tissues. *Annual Review of Physiology.* 2021;83(1):257-78.

65. Eto H, Suga H, Matsumoto D, Inoue K, Aoi N, Kato H, et al. Characterization of structure and cellular components of aspirated and excised adipose tissue. *Plast Reconstr Surg.* 2009;124(4):1087-97.

66. Tang F, Barbacioru C, Wang Y, Nordman E, Lee C, Xu N, et al. mRNA-Seq whole-transcriptome analysis of a single cell. *Nature methods.* 2009;6(5):377-82.

67. Jaitin DA, Adlung L, Thaiss CA, Weiner A, Li B, Descamps H, et al. Lipid-Associated Macrophages Control Metabolic Homeostasis in a Trem2-Dependent Manner. *Cell.* 2019;178(3):686-98.e14.

68. Hildreth AD, Ma F, Wong YY, Sun R, Pellegrini M, and O'Sullivan TE. Single-cell sequencing of human white adipose tissue identifies new cell states in health and obesity. *Nature Immunology.* 2021;22(5):639-53.

69. Vijay J, Gauthier MF, Biswell RL, Louiselle DA, Johnston JJ, Cheung WA, et al. Single-cell analysis of human adipose tissue identifies depot and disease specific cell types. *Nat Metab.* 2020;2(1):97-109.

70. Hepler C, Shan B, Zhang Q, Henry GH, Shao M, Vishvanath L, et al. Identification of functionally distinct fibro-inflammatory and adipogenic stromal subpopulations in visceral adipose tissue of adult mice. *eLife.* 2018;7:e39636.

71. Emont MP, Jacobs C, Essene AL, Pant D, Tenen D, Colleluori G, et al. A single-cell atlas of human and mouse white adipose tissue. *Nature.* 2022;603(7903):926-33.

72. Czabany T, Athenstaedt K, and Daum G. Synthesis, storage and degradation of neutral lipids in yeast. *Biochimica et Biophysica Acta (BBA) - Molecular and Cell Biology of Lipids.* 2007;1771(3):299-309.

73. Jacquier N, Choudhary V, Mari M, Toulmay A, Reggiori F, and Schneiter R. Lipid droplets are functionally connected to the endoplasmic reticulum in Saccharomyces cerevisiae. *J Cell Sci.* 2011;124(Pt 14):2424-37.

74. De Duve C, and Wattiaux R. Functions of lysosomes. *Annu Rev Physiol.* 1966;28:435-92.

75. Mattoscio D, Raimondi A, Tacchetti C, and Chiocca S. Immunogold Electron Microscopy of the Autophagosome Marker LC3. *Bio Protoc.* 2017;7(24):e2648-e.

76. Choudhary V, Ojha N, Golden A, and Prinz WA. A conserved family of proteins facilitates nascent lipid droplet budding from the ER. *Journal of Cell Biology.* 2015;211(2):261-71.

77. Schott MB, Weller SG, Schulze RJ, Krueger EW, Drizyte-Miller K, Casey CA, et al. Lipid droplet size directs lipolysis and lipophagy catabolism in hepatocytes. *Journal of Cell Biology.* 2019;218(10):3320-35.

Appendices

Appendix A: Timeline of events for Project 1

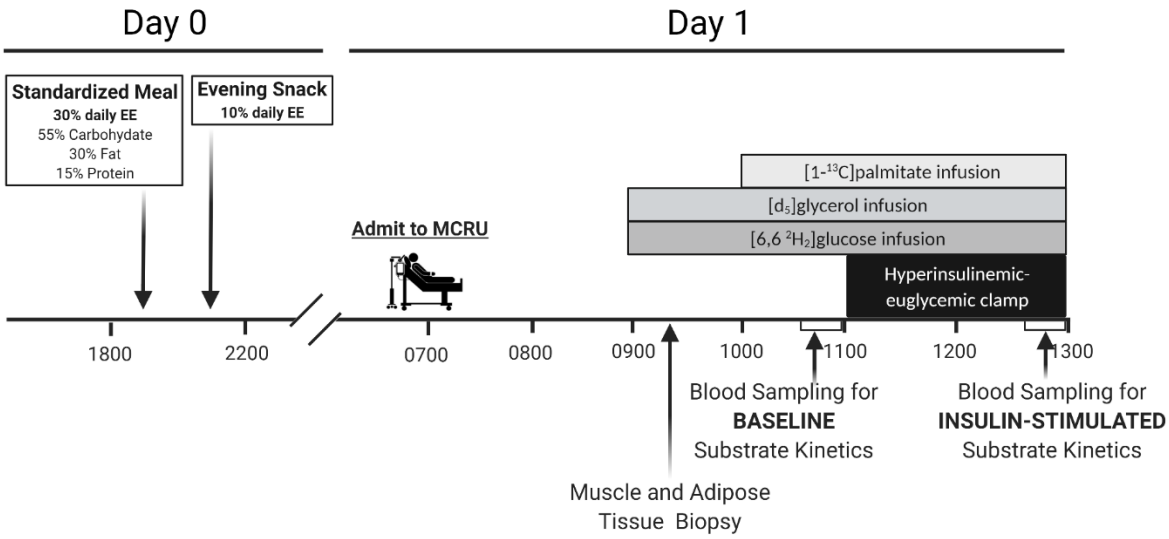

Figure A-1: Timeline of events for Project I

Appendix B: Adipose Tissue Proteomics; Protein extraction, TMT labeling procedure, LC-MS/MS analysis/quantification

Protein Extraction and Tandem Mass Tag (TMT) labeling procedure

TMT labeling will be performed for mass spectrometry (MS) using 16-plex isobaric labeling kit (A44521, Thermo Fisher). Fifty μg protein from each sample will be reduced in 5mM Dithiothreitol (DTT) for 60 minutes at 45°C, followed by alkylation with 2-chloroacetamide (15 mM) at room temperature (RT) for 30 minutes. Proteins will then be precipitated by adding ice cold acetone, and incubated overnight at -20°C. The following day, samples will be thawed on ice and centrifuged at 8,000g for 10 minutes at 4°C. The pellet will be retrieved and resuspended in 100 μL of 100 mM TEAB. Proteins will then be digested overnight at 37°C by adding 1.1 μg of porcine trypsin (#650279, Sigma Aldrich). TMT reagents will then be constituted in 40μL of anhydrous acetonitrile and digested peptides transferred to the TMT reagent vial, and incubated for 60 minutes at RT. The reaction will be quenched by adding 8 μL of 5% hydroxylamine and incubating for 15 minutes. Samples will then be combined, dried, and separated by 2D separation using high pH reverse phase fractionation kit according the manufacturers protocols (#84868, Thermo Fisher). Fractions will then be dried and reconstituted in 10 μL of loading buffer, 0.1% formic acid and 2% acetonitrile.

Liquid Chromatography-MS/MS analysis

An Orbitrap Fusion mass spectrometer (Thermo-Fisher) and RSLC Ultimate 3000 nano-ultra performance liquid chromatographer (Dionex/Thermo-Fisher) will obtain raw spectra. Two microliters from each fraction will be resolved in 2D on a nanocapillary reverse phase column as described previously, and directly sprayed onto Orbitrap Fusion with EasySpray (Thermo-Fisher); Spray voltage (positive ion) = 1900 V, Spray voltage (negative ion) = 600 V, method duration = 180 min, ion source type = NSI). The mass spectrometer will be set to collect the MS1 scan (Orbitrap; 120 K resolution; AGC target 2 × 105; max IT 100 ms), and then data-dependent Top Speed (3s) MS2 scans (collision induced dissociation; ion trap; NCD 35; AGC 5 × 103; max IT 100 ms). For multinotch-MS3, the top 10 precursor ions from each MS2 scan will be fragmented by HCD followed by Orbitrap analysis (NCE 55; 60 K resolution; AGC 5 × 104; max IT 120 ms; 100-500 m/z scan range).

Protein Quantification

Protein groups will be filtered to 1% false discovery rate (FDR) using the target-decoy strategy and the best peptide approach (1), with FDR adjustment (2). The individual peptide spectrum matches (PSM) lists for each TMT 16-plex we assembled, with peptides assigned either as a unique peptide to a particular protein group or assigned as a razor peptide to a single protein group that had the most peptide evidence, and additionally filtered to 1% PSM-level FDR. For PSMs passing these filters, MS1 intensity of the

corresponding precursor-ion was extracted using the Philosopher label-free quantification module based on the moFF method (10 ppm mass tolerance and 0.4 min retention time for extracted ion chromatogram peak tracing) (3). For all PSMs corresponding to a TMT-labeled peptide, 16 TMT reporter ion intensities will be extracted from the corresponding MS3 scans (using 0.002 Da window) and precursor-ion purity scores will be calculated using the intensity of the sequenced precursor ion and that of other interfering ions observed in MS1 data (within 0.7 Da isolation window). Before normalization, proteins detected that will be foreign to adipose tissue (i.e. hemoglobin-specific proteins) will be removed from the protein set. Peak areas will then be $\log_2$ transformed and normalize relative to total peptide abundance for each sample.

References

1. Nesvizhskii AI, Keller A, Kolker E, and Aebersold R. A statistical model for identifying proteins by tandem mass spectrometry. *Analytical chemistry.* 2003;75(17):4646-58.
2. Savitski MM, Wilhelm M, Hahne H, Kuster B, and Bantscheff M. A Scalable Approach for Protein False Discovery Rate Estimation in Large Proteomic Data Sets. *Molecular & cellular proteomics : MCP.* 2015;14(9):2394-404.
3. da Veiga Leprevost F, Haynes SE, Avtonomov DM, Chang H-Y, Shanmugam AK, Mellacheruvu D, et al. Philosopher: a versatile toolkit for shotgun proteomics data analysis. *Nature methods.* 2020;17(9):869-70.

Appendix C: Multivariate analysis index in Project I - Net Elastic Regression (LASSO)

Response Variable: Insulin-mediated glucose uptake [(nmol/kg FFM/min) / (μU/mL)]

Clinical Factors	Subclinical Factors
Sex (0=F, 1=M)	Sex (0=F, 1=M)
Age (yrs)	Age (yrs)
BMI (Kg/m^2)	Respiratory Exchange Ratio (VCO_2/VO_2)
Fat Mass (Kg)	Carbohydrate oxidation [μmol/(min•FFM)]
Liver Fat (%)	Fat oxidation [μmol/(min•FFM)]
Visceral Fat (cm^2)	Basal FA Ra [μmol/(KgFM•min)]
HbA1c (%)	Clamp FA Ra (μmol/[KgFM•min])
Fasting Glucose (mM)	FA Ra Suppression (%)
Plasma Non-esterified Fatty Acid (mM)	Basal Glucose Ra (μmol/[KgFFM•min])
Plasma HDL (mg/dL)	Clamp Glucose Ra (μmol/[KgFFM•min])
Plasma Triglyceride (mM)	Glucose Ra Suppression (%)
Plasma Cholesterol (mg/dL)	Glycerol Ra (μmol/[KgFFM•min])
Plasma CRP (ng/mL)	Glycerol Ra (μmol/[KgFFM•min])
Plasma IL6 (ρg/mL)	Glycerol Ra Suppression (%)
Plasma Total Adiponectin (ng/mL)	
Plasma HMW Adiponectin (ng/mL)	

Table A-1: Clinical and subclinical explanatory variables predicting insulin-mediated glucose uptake

Appendix D: Relationship between fibrosis whole-body insulin sensitivity

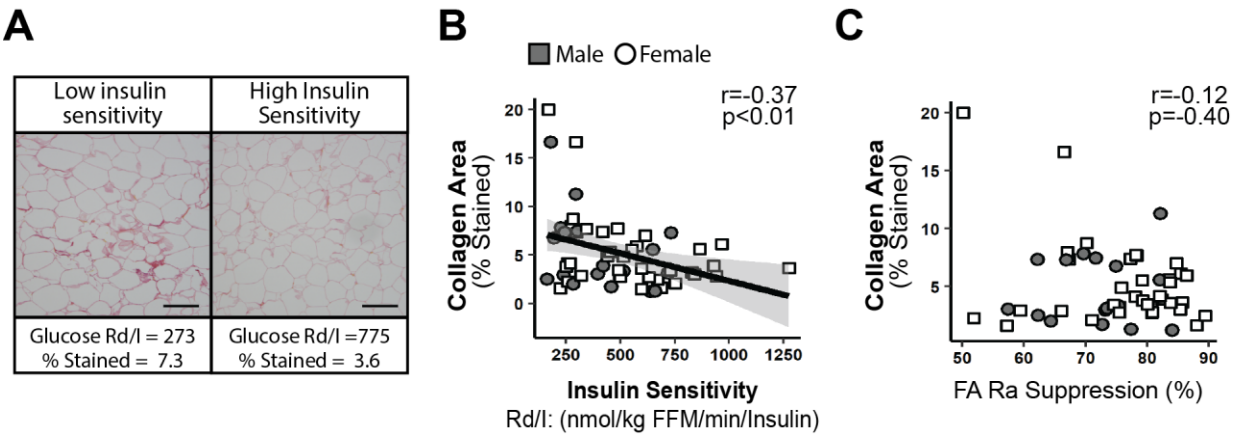

Figure A-1: Relationship between fibrosis whole-body insulin sensitivity

A) Representative image from participant with low and high insulin-mediated glucose uptake. Scale bar = 100µm. B) Relationship between fibrosis (% stained) and insulin-mediated glucose uptake, and C) and FA Ra suppression. n=57.

Appendix E: Skeletal muscle free fatty acid, acylcarnitine, diacylglycerol, and triacylglycerol unsaturation relationship with insulin-mediated glucose uptake$_z$, and FA Ra suppression$_z$.

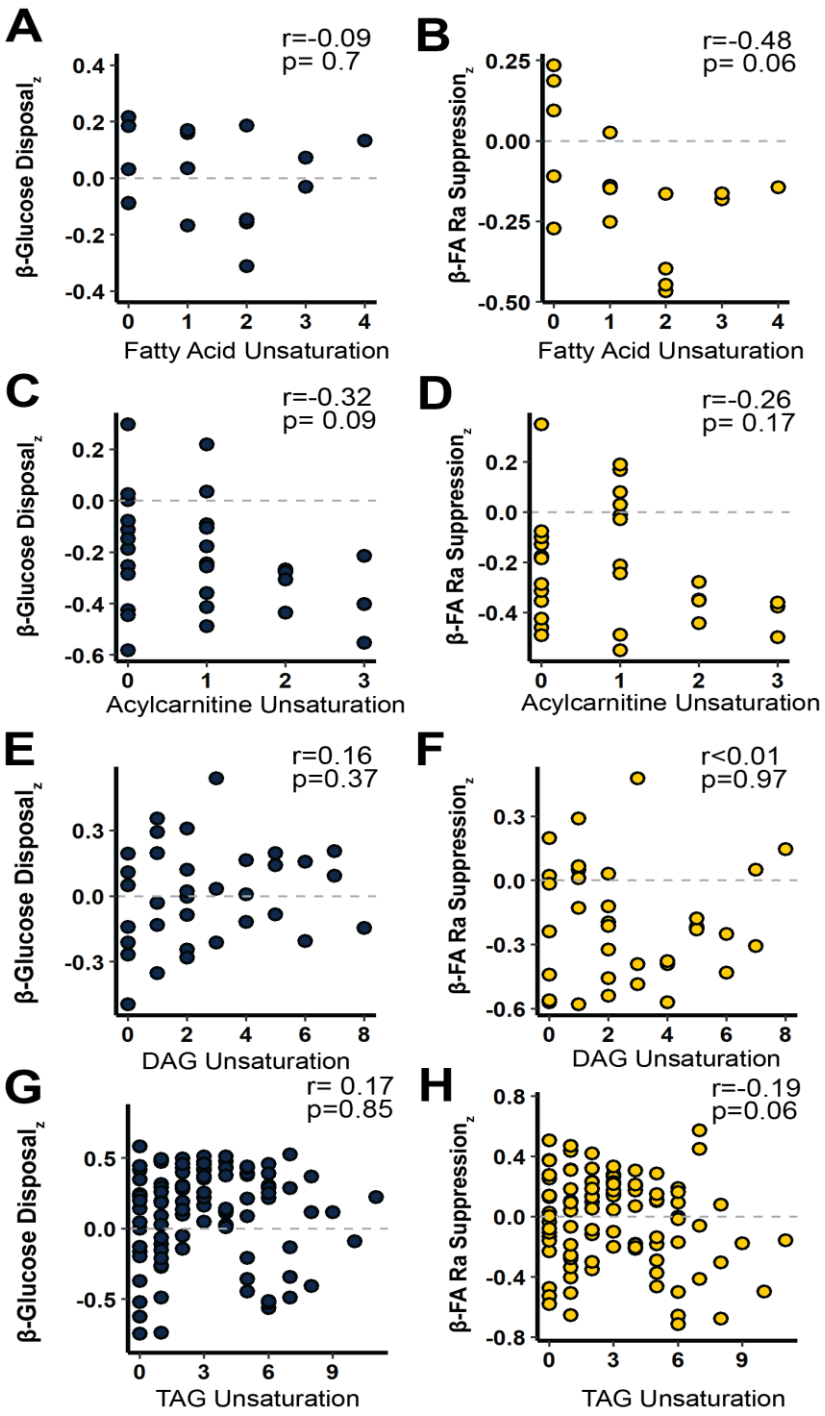

Figure A-2: Relationships between skeletal muscle free fatty acid, acylcarnitine, diacylglycerol, and triacylglycerol unsaturation versus insulin-mediated glucose uptake$_z$, and FA Ra suppression$_z$.

Appendix F: Association between skeletal muscle phospholipid abundance with insulin-mediated glucose uptake$_z$ and FA Ra Suppression$_z$.

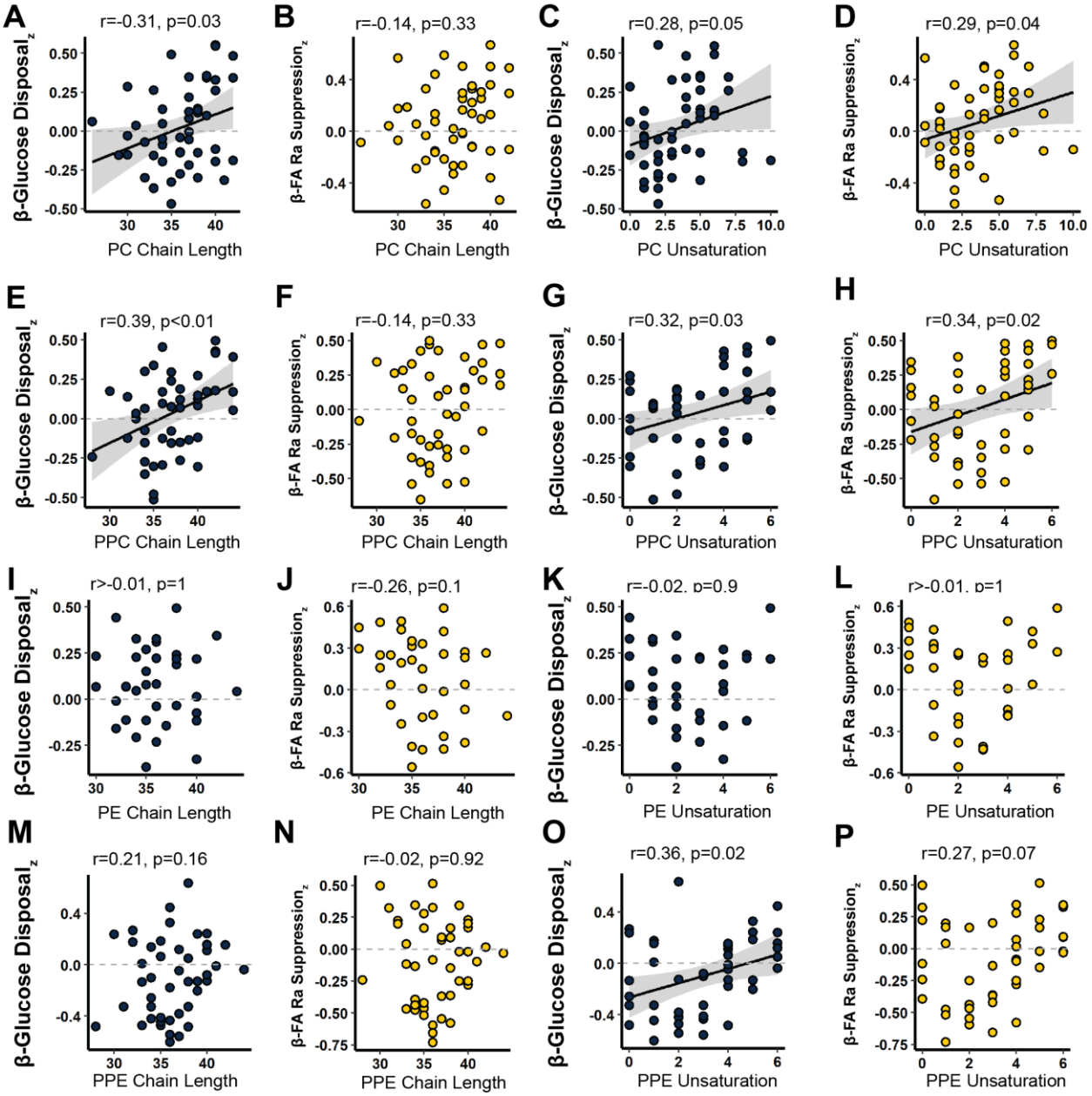

Figure A-3: Relationships between skeletal muscle phospholipid classes; phosphatidylcholine (PC), plasmenyl phosphatidylcholine (PPC), Phosphatidylethanolamine (PE), and plasmenyl-phosphatidylethanolamine (PPE) chain length and unsaturation versus insulin-mediated glucose uptake$_z$, and FA Ra suppression$_z$.

Appendix G: Timeline of Events for Project II

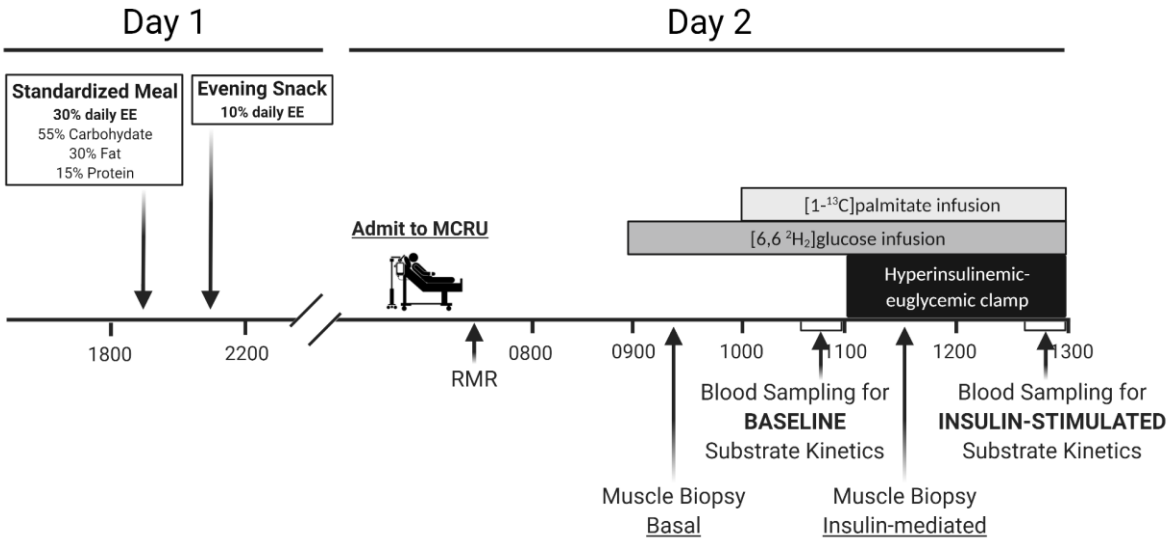

Figure A-4: Timeline of events for Project I

Appendix H: Histochemistry Protocol - Lipid Droplet Staining

1. Retrieve samples from -80C and place into -20C cryostat for ~10-20min
2. Section 2 samples per slide into 5µm sections
    - Confirm samples are in cross-section and not freeze-fractured by imaging in Brightfield
3. **Fix** for 1h in 4% Paraformaldehyde in PBS
4. Wash with 1x PBS 3 x 30s
5. **Permeabilize** for 5min in 0.5% Triton-X100 in PBS -> Dilute from the 2% TX-100 stock
6. Wash in 1x PBS 3x5min
7. **Primary Antibody Stain - MHC1**: Incubate BA-D5 at 1:200 for 1h at 37˚C
8. Wash in 1X PBS 3x5min
9. **Secondary Antibody Stain:** Incubate in AF 647 goat anti-mouse IgG2 at 1:200 for 30min @ room temperature in the dark
10. Wash 1x PBS 3x5min
11. **Bodipy (493/503) Stain for Lipid Droplets:** Incubate 1:100 for 20min in the dark
12. Wash 1x PBS 3x5min
13. **Lectin Stain**: Incubate WGA 555 1:200 in for 20min in the dark
14. Wash 1x PBS 3x5min
15. Add **<u>one drop</u>** Prolong Gold Anti-fade Mountant per sample
16. Cover with Corning #1 coverslip and store in the dark.
17. Samples will be ready to image ~24 hours after mounting

*** ALL diluted antibodies and reagents are in 1X PBS**

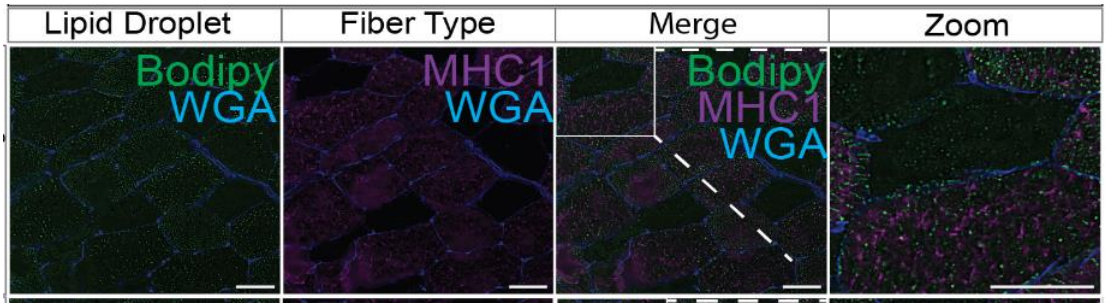

EXAMPLE IMAGE: Scale bar = 100µm

Appendix I: Immunoprecipitation Protocol

Reagents and antibodies

- **Protein A Magnetic Beads** (Pierce, 88846)
- **Lysis Buffer:** Cell Signaling Lysis Buffer #9803
    - 20 mM Tris-HCl (pH 7.5), 150 mM NaCl, 1 mM Na2EDTA, 1 mM EGTA, 1% Triton, 2.5 mM sodium pyrophosphate, 1 mM beta-glycerophosphate, 1 mM Na3VO4, 1 µg/ml leupeptin.
- 1% protease and phosphatase inhibitor cocktail (Sigma)
- **Wash Buffer:** 25 mM Tris, 0.15M NaCl, 0.05% Tween-20, pH 7.5
- **Primary Antibodies:**
    - **IRβ:** CST#3025 (Rabbit IgG**)**
    - **CD36**: R&D sytems AF1955 (Polyclonal Goat IgG)
    - **IRS1**, sc8038 (mouse monoclonal)
    - **Fyn:** CST #4023 (Rabbit IgG)

1) Skeletal Muscle Sample Preparation

1. Chip 15-30mg muscle on dry ice platform + frozen weigh boat. Place the chipped samples into pre-chilled labelled tubes on dry ice. Return tubes to -80 when done chipping or proceed with homogenization.
2. Prepare the required volume of 1x buffer from frozen 10X stock: **CELL SIGNALING LYSIS BUFFER #9803.**
3. **Add 30uL buffer/mg wet weight per sample.** Make sure to make extra buffer so there is enough room for all samples.
4. Homogenize tissue by hand using DOUNCE homogenizer (~20 strokes).
5. Solubilize samples by rotating end-over-end (~50rpm) at 4°C.
6. Centrifuge at 100,000g for 1 hour at 4°C.
7. Retrieve the supernatant and proceed to BCA assay and freeze at -80C or proceed to Immunoprecipitation.

2) Immunoprecipitation Method

DAY 1

1. Combine 300ug homogenate with 5ug Insulin Receptor β antibody.
2. Adjust the reaction volume to 500 uL by adding 1X Lysis Buffer.
3. rotate end-over-end overnight at 4ºC.

DAY 2

Bead Preparation

- In a separate 1.5mL microcentrifuge tube, add 25uL Protein A magnetic beads into a 1.5mL microcentrifuge tube containing 175uL wash buffer.
- Gently vortex to mix sample (#2 on the vortex mixer).
- Place the tube into a magnetic stand, and discard the supernatant.
- Add 1mL of Wash Buffer to the tube. Invert the tube several times or gently vortex to mix for 1 minute. Collect beads with magnetic stand & discard supernatant.

Mix beads with sample

- Add the antigen sample/antibody mixture to a 1.5mL microcentrifuge tube containing pre-washed magnetic beads and incubate at room temperature for 2 hours with mixing.
- Collect the beads with a magnetic stand and then remove the flow-through and save for analysis.

Wash beads

- Add 500µL of Lysis Buffer to the tube and gently mix. Collect the beads and discard the supernatant. Repeat wash for a total of three times.
- Add 500uL wash buffer and gently mix.
- Add 500µL of PBS to the tube and gently mix. Collect the beads on a magnetic stand and discard the supernatant.

Elution

- Add 100µL of SDS-PAGE reducing sample buffer (2X Laemmli buffer) to the washed beads and incubate at room temperature for 10 minutes with mixing. Magnetically separate the beads and save the supernatant containing the target antigen.
- ***Note: If you will be performing a Western blot using rabbit antibodies (primary or secondary) do not heat the samples. Incubate at room temperature for 10 minutes with mixing.***

Appendix J: Clinical trial schematic for Project III.

*nutritional supplement kcals were estimated to match energy expenditure from the previous exercise session.

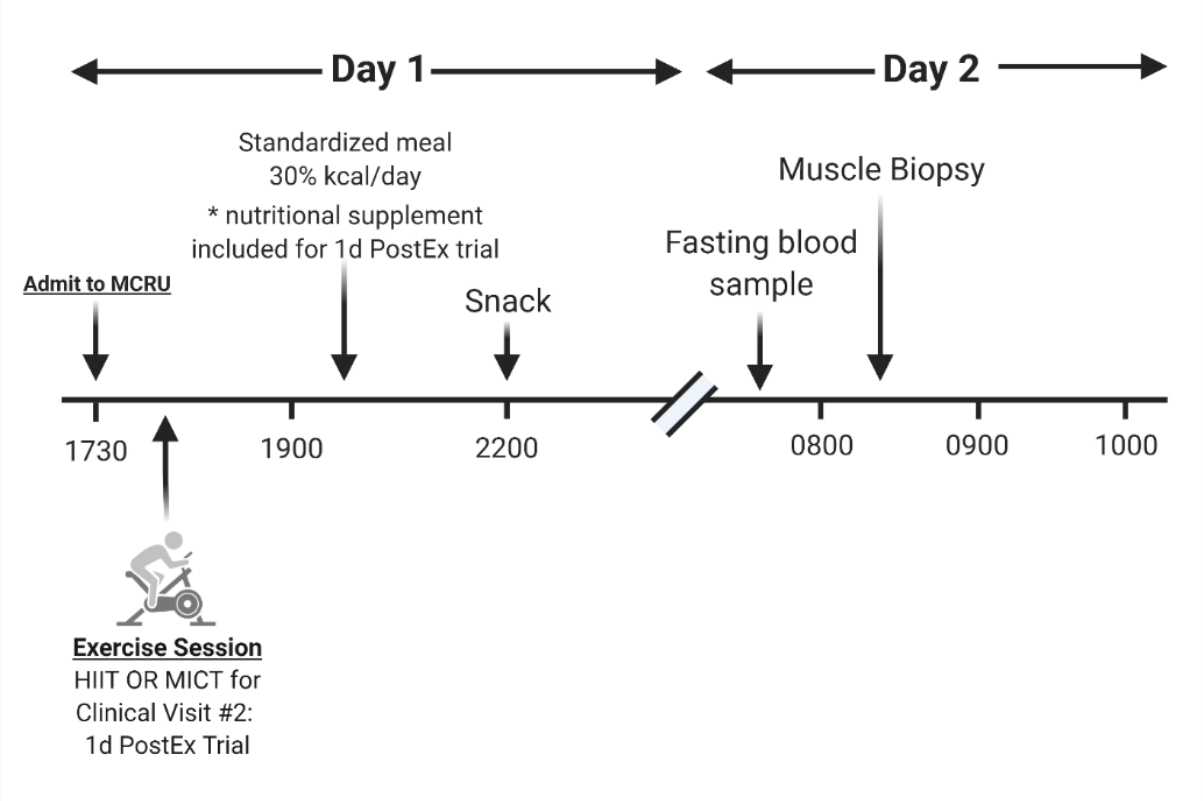

Figure A-5: Clinical trial schematic for Project III.

Appendix K: Immunohistochemistry Protocol for PLIN2-KDEL co-localization, and PLIN2-LC3 co-localization

DAY1

- Section two samples per slide at 5µm
- **FIX** - 4% PFA for 30 minutes
- **Wash** - 3x5 minute wash in 1X PBS
- **Permeabilize** - 0.3% Triton-X for 5 minutes
- **Wash** - 3x5 minute wash in 1x PBS
- **Block** - 5% Goat Serum for 60 minutes
- **Wash** - 3x5 minute wash in 1x PBS

Primary Antibody incubation

Incubate Primary Antibody overnight at 4°C

PRIMARY CONCENTRATIONS

- PLIN2 = 1:100 in PBS with 1%BSA, 0.1% Triton-X100
- KDEL = 1:100 in PBS with 1%BSA, 0.1% Triton-X100
- LC3AB = 1:50 in PBS with 1%BSA, 0.3% Triton-X100

DAY2

- **Wash** 3x5 min in PBS
- Incubate in **Secondary Antibody** for 60 minutes at RT

SECONDARY ANTIBODY/CONCENTRATIONS

- PLIN2 = 1:200, Goat-anti-mouse IgG1 AF 647
- KDEL AND LC3AB = 1:200, Goat in anti-rabbit IgG AF 488

- **Wash** 3x5 minutes in 1X PBS
- **Lectin WGA 555** for 1 hour at 1:200 in PBS
- **Wash** 3x5 minutes
- **Mount** in Prolong Gold Anti-fade mountant